

INTERNATIONAL JOURNAL OF BIOPRINTING



WHIOCE PUBLISHING PTE. LTD.
PROVIDING
FIRST-CLASS SCIENTIFIC INFORMATION
FOR TOP SCHOLARS

Volume 6 Issue 3 • 2020
ISSN 2424-7723 (print) ISSN 2424-8002 (online)

INTERNATIONAL JOURNAL OF BIOPRINTING

Editor-in-Chief

Chee Kai Chua

*Singapore University of Technology and Design,
Singapore*



CONTENTS

1	Bioprinting in the Russian Federation: Can Russians Compete? <i>Peter Timashev, Vladimir Mironov</i>	COMMENTARY
7	Bioethical and Legal Issues in 3D Bioprinting <i>Anastasia Kirillova, Stanislav Bushev, Aydar Abubakirov, Gennady Sukikh</i>	PERSPECTIVE ARTICLE
17	Collagen as Bioink for Bioprinting: A Comprehensive Review <i>Egor Olegovich Osidak, Vadim Igorevich Kozhukhov, Mariya Sergeevna Osidak, Sergey Petrovich Domogatsky</i>	REVIEW ARTICLE
27	Fibrin-based Bioinks: New Tricks from an Old Dog <i>Anastasia Shpichka, Daria Osipova, Yuri Efremov, Polina Bikmulina, Nastasia Kosheleva, Marina Lipina, Evgeny A. Bezrukov, Roman B. Sukhanov, Anna B. Solovieva, Massoud Vosough, Peter Timashev</i>	REVIEW ARTICLE
41	Software for Bioprinting <i>Catherine Pakhomova, Dmitry Popov, Eugenii Maltsev, Iskander Akhatov, Alexander Pasko</i>	REVIEW ARTICLE
62	3D Bioprinting: The Roller Coaster Ride to Commercialization <i>Anton Elemoso, Grigoriy Shalunov, Yakov M. Balakhovsky, Alexander Yu. Ostrovskiy, Yusef D. Khesuani</i>	REVIEW ARTICLE
77	Laser-induced Forward Transfer Hydrogel Printing: A Defined Route for Highly Controlled Process <i>Vladimir Yusupov, Semyon Churbanov, Ekaterina Churbanova, Ksenia Bardakova, Artem Antoshin, Stanislav Evlashin, Peter Timashev, Nikita Minaev</i>	ORIGINAL ARTICLE
93	3D Printed Gene-activated Octacalcium Phosphate Implants for Large Bone Defects Engineering <i>Ilya Y. Bozo, Roman V. Deev, Igor V. Smirnov, Alexander Yu. Fedotov, Vladimir K. Popov, Anton V. Mironov, Olga A. Mironova, Alexander Yu. Gerasimenko, Vladimir S. Komlev</i>	ORIGINAL ARTICLE
110	Scaffold-free, Label-free, and Nozzle-free Magnetic Levitational Bioassembler for Rapid Formative Biofabrication of 3D Tissues and Organs <i>Vladislav A. Parfenov, Stanislav V. Petrov, Frederico D. A. S. Pereira, Aleksandr A. Levin, Elizaveta V. Koudan, Elizaveta K. Nezhurina, Pavel A. Karalkin, Mikhail M. Vasiliev, Oleg F. Petrov, Vladimir S. Komlev, Yusef D. Khesuani, Vladimir A. Mironov</i>	ORIGINAL ARTICLE

COMMENTARY

Bioprinting in the Russian Federation: Can Russians Compete?

Peter Timashev^{1,2,3}, Vladimir Mironov^{1,4*}

¹Institute for Regenerative Medicine, Sechenov University, Moscow, Russia

²Department of Chemistry, Lomonosov Moscow State University, Moscow, Russia

³Department of Polymers and Composites, N.N. Semenov Institute of Chemical Physics, Moscow, Russia

⁴3D Bioprinting Solutions, Moscow, Russia

Abstract: Bioprinting is a rapidly emerging biomedical research field. Three-dimensional bioprinting is defined as a robotic additive, layer-by-layer biofabrication of functional tissues and organs from living cells, and biomaterials according to a digital model. Bioprinting can revolutionize medicine by automated robotic production of human tissues and organs suitable for transplantation. Bioprinting is based on sophisticated high technology, and it is obvious that only technologically advanced countries can make a real contribution to this rapidly evolving multidisciplinary field. In this paper, we present main Russia's achievements in bioprinting. Here, we also discuss challenges and perspectives of bioprinting research and development in Russia. Russian researchers already made some impressive contributions with long-lasting impact and they have capacities, potential, and ambitions to continue contribute to the advancements of bioprinting.

Keywords: Russia, Three-dimensional bioprinting, Bioinks, Tissue engineering, Laser-induced forward transfer

*Corresponding Author: Vladimir Mironov, The Laboratory of Biotechnological Research, 3D Bioprinting Solutions, Kashirskoe Roadway, 68/2, Moscow, Russian Federation; vladimir.mironov54@gmail.com

Received: June 20, 2020; **Accepted:** July 01, 2020; **Published Online:** July 24, 2020

(This article belongs to the *Special Section: Bioprinting in Russia*)

Citation: Timashev P, Mironov V, 2020, Bioprinting in the Russian Federation: Can Russians Compete? *Int J Bioprint*, 6(3): 303. DOI: 10.18063/ijb.v6i3.303.

1 Introduction

Bioprinting is defined as an additive biofabrication of three-dimensional (3D) tissues and organs from living cells and biomaterials according to digital design. Bioprinting is a rapidly emerging biomedical technology which promises to solve the urgent and yet unsolved problem of the shortage of human organ for transplantation, once and for all. In the past two decades, many research groups around the world became involved in systematical research in this multidisciplinary field. There are a lot of original papers, influential reviews^[1-3], and even textbooks^[4-6] which have already been

published. There are several new societies (such as International Society for Biofabrication) and new journals (such as Biofabrication, Bioprinting, and International Journal of Bioprinting) with impressive impact factors. The commercialization of bioprinting technology is also under way. There are more than 100 bioprinting companies in the world. Thus, bioprinting is already a global phenomenon. In this context, it will be extremely interesting and even potentially useful to investigate comparative landscape of bioprinting research and development in different countries around the world, to identify specific directions in research as well as strength and weakness in

dominated approaches, and to outline potential perspectives. In this review, we focus our attention on bioprinting research and development in Russia. To date, Russia still represents a sufficiently big player with strong research infrastructure, traditions, research schools, and impressive educational and training system. Thus, the focus of this paper is to illustrate how Russian research community can address new research challenges and explore a perspective in high technology areas such as 3D bioprinting and to estimate how competitive is bioprinting research in Russia now and the potential of Russian contribution to this new field in the future.

2 Four Russian bioprinting success stories

Conventionally, to show contribution of specific country to the development of emerging research field, quantitative scientometric analysis was used. However, we believe that it is a basically formal approach and that the presentation of so-called success stories sometimes provides much more valuable qualitative information about competitive potential of the analyzed research community. Here, we will present four most impressive Russian bioprinting success stories which reflect a strong creative and competitive potential of Russian bioprinting research community.

2.1 Development of the first Russian original commercial 3D bioprinter

A 3D bioprinter is a robotic device that carries out layer-by-layer biofabrication of 3D human tissues and organs from living cells and hydrogels according to a digital model^[7]. Development of commercial 3D bioprinters certifiable for clinical use will enable bioprinting 3D human tissues and organs that are suitable for implantation. The capacity to develop an original 3D bioprinter is also a direct evidence of the competitiveness of a particular country on a global level. Fabion is the first Russian original commercial multifunctional 3D bioprinter of extrusion type that is suitable for robotic biofabrication of 3D human tissues and organs and potentially certifiable for clinical use. The development of Fabion is not only an

important milestone but also a manifestation of competitiveness of Russian bioprintists.

Multifunctional commercial clinical 3D bioprinter “Fabion” of extrusion type has been not only designed and developed, but some of its most essential functionalities have been also tested^[7]. The main principle constructive feature of a 3D bioprinter is a separation of a cell printing process from hydrogel spraying, which allows the use of photosensitive hydrogel with ultraviolet-induced polymerization without cell damage. The 3D bioprinter enables extrusion and precision placing of (i) hydrogel filaments with or without living cells, (ii) continuous cellular rods, and (iii) separated tissue spheroids as well as (iv) independent spraying of biocompatible hydrogels based on different principles of induced polymerization. The “built-in” multifunctionality of the Russian 3D bioprinter allows the layer-by-layer additive biofabrication of complex 3D human organ constructs using tissue spheroids as building blocks. The use of only disposable and sterilized components in the multinozzle system made the 3D bioprinter Fabion suitable and certifiable for clinical use^[7].

According to independent rating, bioprinter Fabion is one of the top 5 world best commercial bioprinters. The development of an original certifiable clinical multifunctional 3D bioprinter is an important step toward practical implementation of desirable organ printing technology in Russia.

2.2 Development of the first Russian laser-assisted 3D bioprinter

To date, laser-assisted bioprinting is one of the actively developing techniques in bioprinting and developed based on a nozzle-free laser-induced forward gel microdroplet transfer helping to remove nozzle-associated side effects^[8]. One of the pioneers who introduced this technique was Boris Chichkov. However, it was mostly exploited outside Russia (mainly in Germany and France) for a long period of time. In 2019, the research team from Institute for Regenerative Medicine (Sechenov University) and Institute of Photon Technologies (Federal Research Center Crystallography and Photonics) announced that they had constructed

the first Russian laser-assisted bioprinter BioDrop and initiated studies on fabrication of tissue-engineered constructs using it for their further clinical applications. This bioprinter has the same advantages as foreign setups. Taking into account that there is only one commercial laser-assisted bioprinter on the global market, it can become a good alternative after its commercialization.

2.3 Bioprinting of functional and vascularized animal organ

The best possible demonstration of functionality of a 3D bioprinter is its capacity to bioprint functional and vascularized 3D tissues and organs. We define bioprinting in more narrow sense as an additive biofabrication of 3D tissues and organ constructs using tissue spheroids as building blocks. In this approach, the self-assembling properties of tissue spheroids have been explored. The endocrine organs such as the thyroid gland, a relatively simple endocrine organ without complicated ductal system is more suitable for testing using the proposed bioprinting technology. The 3D bioprinting of a functional vascularized mouse thyroid gland construct from embryonic tissue spheroids as a proof of concept has been recently reported^[9]. The thyroid tissue has been generated from thyroid spheroids and allantoic spheroids as a source of thyrocytes and endothelial cells. The closely placed embryonic tissue spheroids fused into a single vascularized tissue construct. Radiatively ablated mice were used as an animal model of thyroid gland hypofunction. The cultured bioprinted construct was functional as it could normalize blood thyroxine levels and body temperature after grafting under the kidney capsule of hypothyroid mice^[9]. Bioprinting of the functional vascularized mouse thyroid gland construct represents an important milestone and impressive advance in the development of bioprinting technology.

2.4 Bioprinting in space

Magnetic levitational bioassembly of 3D tissue constructs represents a novel rapidly emerging scaffold-free and label-free approach as well as

alternative conceptual and experimental advance in tissue engineering. However, implementation of magnetic levitation on Earth requires the use of relatively toxic paramagnetic medium that, in most cases, contains gadolinium salts. The magnetic levitational bioassembly under the conditions of space microgravity can be implemented at low non-toxic concentrations of gadolinium salts. A new magnetic bioassembler has been designed, developed, and certified for life space research. To the best of our knowledge, 3D tissue constructs have been biofabricated for the 1st time in space under microgravity from tissue spheroids consisted of human chondrocytes using magnetic levitational bioassembly at low non-toxic concentrations of paramagnetic medium^[10]. Bioassembled 3D tissue constructs demonstrated good viability and advanced stages of tissue spheroid fusion processes. These data strongly suggest that scaffold-free, label-free, and nozzle-free formative biofabrication using magnetic fields is a feasible alternative to traditional scaffold-based approaches. It opens a new perspective avenue of research which could significantly advance tissue engineering. Magnetic levitational bioassembly of 3D tissue constructs in space can also advance space life science and space regenerative medicine^[10]. It is another impressive example of important contribution of Russian bioprinting research community which capitalized on strong existing Russian expertise in space research^[11].

3 Education and training bioprintists in Russia

However, as bioprinting is developing and there is an increasing demand for specialists with multidisciplinary background, new educational and training programs focused on bioprinting and related fields have been appearing. This mostly becomes possible after the foundation of first two institutes for regenerative medicine in two biggest and recognized universities (Sechenov University and Lomonosov Moscow State University) in 2016. For instance, Institute for Regenerative Medicine of the Sechenov University launched a new discipline called the “Introduction to Regenerative Medicine” for medical students in

2017 and introduced a training program called “Tissue Engineer,” first of its kind in Russia, for the final year students majoring in General Medicine and Pharmacy in 2018. The first Russian textbook “3D Printing in Medicine” has recently been published^[10].

To date, there is an increasing number of both national and international student exchange programs supported by the government, universities, and national and international foundations. Most of such programs are developed to increase international academic mobility and cover almost all expenses, giving a unique chance for students to broaden their background in top research teams from all around the world. Since the frequencies of international student exchanges are constantly increasing, young Russian researchers can also attend established training courses on bioprinting and biofabrication in the USA, The Netherlands, Australia, etc.

Moreover, 3D Bioprinting Solutions, a private Russian company, offers 3-week training courses on bioprinting for young Russian students and researchers. Comics “Adventure in Bioprinting Laboratory” has also been developed.

Thus, there are real possibilities to get education and training in bioprinting in Russia. There are also certain undeniable advantages of carrying out research in Russia on which the emerging community of Russian bioprintists can capitalize: (i) There are new grant schemes and funding organizations; (ii) Russian scientists can participate in conferences, workshops, meetings, and congresses abroad without any restrictions; (iii) young Russian researchers can now receive training in foreign countries; (iv) access to foreign literature and patent databases is not a problem anymore; and (v) foreign researchers are welcomed to Russia to build a research laboratory.

4 Can Russian bioprintists compete?

Russian scientists can indeed compete and be very successful. Breakthrough pioneering works of Prof. Boris Chichkov who is a Russian scientist in laser-based bioprinting technologies

(Hannover, Germany) is the best evidence. In addition, Vladimir Mironov, one of the authors of this paper, was awarded the prestigious Senior Investigator Award from the International Society of Biofabrication for his pioneering contribution to the development of bioprinting technology in 2018.

The bioprinting success in Russia depends on not only the scientist *per se* but also many other factors. We believe that to guarantee success and optimize competitiveness of Russian bioprintists community, several highly desirable aspects require our utmost attention; they include: (i) Organization of center(s) of excellence and/or National Bioprinting Research Center or Institute; (ii) training of young scientists in the best bioprinting research centers around the world; (iii) recruitment of foreign scientists to work in Russia; (iv) increasing collaborations with the world’s best bioprinting research scientists, research groups, and bioprinting research centers; (v) increasing publications in top journals; (vi) increasing application for patents; (vii) developing start-up companies in bioprinting; and (viii) clinical translation.

Today, Russia’s successes are also proven by the increase in bioprinting activity and the establishment of the society on regenerative medicine in 2013 (President Prof. Vsevolod Tkachuk; Honorary President Prof. Gennadiy Sukhikh). It is also noteworthy that Russia was invited by the International Society on Tissue Engineering and Regenerative Medicine to be a Guest Nation on TERMIS-EU Chapter 2019 (May 27–31, 2019). The increasing visibility of Russia on the world TERM map is also due to the organization of world class events such as Sechenov International Biomedical Summit (<https://sechenov-sibs.confreg.org/>) and National Congress on Regenerative Medicine (<https://congress.regenerative-med.ru/>) where leading scientists (Anthony Atala, James Yoo, William Wagner, etc.) from the USA, Italy, Germany, France, Iran, the Netherlands, China, Ireland, etc., present their recent achievements.

In view of the bioprinting success stories such as the creation of the world’s first animal organ

in Russia and the establishment of bioprinting research infrastructure in several Russian universities and research organizations, it is logical to assume that Russia may take the lead to bioprint the world's first human organ and also achieve the first successful clinical transplantation of bioprinted human organ in Russia. Hence, Russian researchers and engineers can compete and compete successfully.

5 Conclusion and outlook

3D bioprinting is a rapidly emerging biomedical technology that promises to transform the landscape of organ transplantation. Russian contribution to global development of this technology cannot be understated; at least five main achievements of Russian bioprintists deserve the attention of the global research community: (i) Development of new software for bioprinting based on function representation (see paper in this issue); (ii) development of natural bioinks (see papers in this issue); (iii) development of original 3D bioprinters (see papers in this issue); (iv) bioprinting of the world's first functional and vascularized organ construct – mouse thyroid glands^[9]; and (v) magnetic levitational bioassembly of 3D tissue constructs in the condition of microgravity in space (accepted for publication in *Science Advances*).

For the next decade, it is logical to expect further contribution of Russian researchers in traditional areas of Russian expertise. First, bioprinting in space at the Russian segment of the International Space Station will continue to advance^[12]. Second, new type of bioprinters especially laser-based bioprinters will be developed in Russia due to the traditional strong expertise in laser research. Third, Russian bioprintists can capitalize on their initial success with bioprinting the world's first functional and vascularized animal organ and have chances to bioprint and test *in vivo* the world's first functional and vascularized human organ. There are attempts to advance education and training young generations of specialists in the field of bioprinting. The first Russian textbook in 3D printing in medicine and bioprinting has been already

published^[10], and several universities introduced programs on 3D bioprinting technology. Recently, Russian bioprintists also contributed to one of the most comprehensive textbooks on 3D printing and biofabrication^[13]. Moreover, the commercialization and clinical translation of 3D bioprinting will need to be supported. It remains to be seen how competitive will Russian bioprintists be and how successfully established Russian research potential, expertise and infrastructure in bioprinting field will be commercialized and clinically translated.

The special issue “**Bioprinting in Russia**” published in the *International Journal of Bioprinting* demonstrates the broad potential of Russian bioprintists research community which includes the development of novel software based on principle of function representation, novel bioinks based on natural polymers such as fibrin and collagen, new types of 3D bioprinters, laser-based bioprinting and magnetic levitational bioprinting in space, as well as ethical aspects of bioprinting and emerging business models in bioprinting. We believe that the selected papers will demonstrate quality and perspectives of bioprinting research in Russia and will support our opinion that Russia will continue to be an important and highly competitive player in the advancements of bioprinting technology.

Acknowledgment

This work was supported by the Russian Foundation for Basic Research grant # 18-29-17050 and by Russian academic excellence project "5-100".

Conflict of interest

The authors declare no conflict of interest.

References

1. Murphy SV, Atala A, 2014, 3D Bioprinting of Tissues and Organs. *Nat Biotechnol*, 32:773–85. DOI: 10.1038/nbt.2958.
2. Ng WL, Chua CK, Shen YF, 2019, Print me an Organ! Why we are not there yet. *Prog Polym Sci*, 97:101145. DOI: 10.1016/j.progpolymsci.2019.101145.
3. Matai I, Kaur G, Seyedsalehi A, *et al.*, 2020, Progress in 3D Bioprinting Technology for Tissue/Organ Regenerative

- Engineering. *Biomaterials*, 226:119536. DOI: 10.1016/j.biomaterials.2019.119536.
4. Chua CK, Yeong WY, 2015, *Bioprinting: Principles and Applications*. World Scientific Publishing Co. Ltd, Singapore.
 5. Ozbolat IT, 2016, *3D Bioprinting: Fundamentals, Principles and Applications*. Engineering Science and Mechanics Materials Research Institute (MRI), Texas.
 6. Khademhosseini A, Camci-Unal G, 2018, *3D Bioprinting in Regenerative Engineering: Principles and Applications*. CRC Press, Boca Raton, Florida.
 7. Hesvani YD, Pereira FD, Parfenov VA, *et al.*, 2016, Design and Implementation of Novel Multifunctional 3D Bioprinter. *3D Print Addit Manuf*, 3:65–8.
 8. Antoshin AA, Churbanov SN, Minaev NV, *et al.*, 2019, LIFT-Bioprinting, is it Worth it? *Bioprinting*, 15:e00052. DOI: 10.1016/j.bprint.2019.e00052.
 9. Bulanova EA, Koudan EV, Degosserie J, *et al.*, 2017, Bioprinting of a Functional Vascularized Mouse Thyroid Gland Construct. *Biofabrication*, 9(3):034105. DOI: 10.1088/1758-5090/aa7fdd.
 10. Koryakin NN, Gorbatov PO, 2019, 3D-Bioprinting in Medicine. GEOTAP-Media, Moscow, p. 240. DOI: 10.33029/9704-5163-2-PRI-2019-1-240.
 11. Sun W, Starly B, Daly AC, *et al.*, 2020, The bioprinting roadmap. *Biofabrication*, 12(2):022002.
 12. Ghidini T, 2018, Regenerative Medicine and 3D Bioprinting for Human Space Exploration and Planet Colonisation. *J Thorac Dis*, 10:S2363–75. DOI: 10.21037/jtd.2018.03.19.
 13. Ovsianikov A, Yoo J, Mironov V, editors, 2018, *3D Printing and Biofabrication*. Springer, Berlin, Germany.

Bioethical and Legal Issues in 3D Bioprinting

Anastasia Kirillova^{1,†,*}, Stanislav Bushev^{2,†}, Aydar Abubakirov¹, Gennady Sukikh¹

¹National Medical Research Center for Obstetrics, Gynecology and Perinatology Named After Academician V.I. Kulakov of the Ministry of Healthcare of Russian Federation, Moscow, 117513, Russia

²Department of Philosophy, Lomonosov Moscow State University, Moscow, 119991, Russia

[†]These authors contributed equally to this work.

Abstract: Bioethical and legal issues of three-dimensional (3D) bioprinting as the emerging field of biotechnology have not yet been widely discussed among bioethicists around the world, including Russia. The scope of 3D bioprinting includes not only the issues of the advanced technologies of human tissues and organs printing but also raises a whole layer of interdisciplinary problems of modern science, technology, bioethics, and philosophy. This article addresses the ethical and legal issues of bioprinting of artificial human organs.

Keywords: Three-dimensional printing, Bioethics, Ethical issues, Regulatory concerns, Artificial ovary, Oncofertility

***Corresponding Author:** Anastasia Kirillova, National Medical Research Center for Obstetrics, Gynecology and Perinatology Named After Academician V.I. Kulakov of the Ministry of Healthcare of Russian Federation, Moscow, 117513, Russia; stasia.kozyreva@gmail.com

Received: February 16, 2020; **Accepted:** March 16, 2020; **Published Online:** April 28, 2020

(This article belongs to the *Special Section: Bioprinting in Russia*)

Citation: Kirillova A, Bushev S, Abubakirov A, *et al.*, 2020, Bioethical and Legal Issues in 3D Bioprinting, *Int J Bioprint*, 6(3): 272. DOI: 10.18063/ijb.v6i3.272.

1 Introduction

Three-dimensional (3D) bioprinting of tissue-engineered constructs and prototype organs for regenerative medicine is one of the most rapidly developing and promising areas of biotechnology. There are already more than a dozen leading companies in medical bioprinting: EnvisionTEC (Germany), RegenHu (Switzerland), Poetis (France), Organovo (USA), Sciperio/nScript (USA), Cellink (Sweden/USA), Allevi (formerly BioBots) (USA), BioDevices (USA), three Dynamics systems (USA), Aspect Biosystems (Canada), Rokit (South Korea), 3D Bioprinting Solutions (Russia), etc.^[1]. The development of 3D bioprinting technologies has even been called the megatrend of the fourth industrial revolution^[2].

To date, the development of bioprinting technology completed the first stage, which can

be called the stage of “apologetics,” when doubts about the possibility of implementing bioprinting have been dispelled, successes of using the technology for bioprinting tissues and organs have been demonstrated, basic techniques and methods have been worked out, and a number of technical restrictions for implementing the technology have been overcome. The latest advances in bioprinting technologies and biofabrication approaches are indeed impressive. Since the pioneering work of organ printing^[3], the scientific community of biofabrication has been developed, uniting biologists, medical doctors, physicists, chemists, and computer scientists^[4]. Although the technology progressed very fast, on the onset of its development the possibility of functional human organ bioprinting seemed like a highly desirable, yet a long-term, and goal^[4]. Now, decades later with the successes in

human^[5-7] and animal models^[8-10] bioprinting, we became much closer to the ultimate goal.

Now comes the next stage, which can be called the stage of “evangelism” which is the demonstration of the possibilities of bioprinting application for solving a number of problems in medicine. The bioprinting approach has already been used to address problems in transplantology, regenerative medicine, and even in the field of reproduction. Printed tissues are used in experimental pharmacology research for drugs and toxicity testing and in cosmetology^[11,12]. Naturally, the prospect of replacing diseased organs with healthy ones can be interpreted as a weal. It can not only solve the issue of organ and tissue shortage for transplantation but can also overcome a number of ethical problems related to transplantation. The bioprinting technologies can also contribute to the emergence of a new paradigm in medicine – personalized medicine^[13], including personalized drug delivery^[14]. Successes in the field of bioprinting announce the promising possibility for replacing bones, cartilage, blood vessels, and internal organs (heart, kidneys, liver, etc.) in humans. Research is underway in the field of reproductive medicine using bioprinting technologies, in particular, the biofabrication of artificial ovaries^[15-18].

However, as for every new technology, the ethical and legal norms of 3D bioprinting will have a long way until they establish. In this work, we will address the ethical and legal problems of human organ 3D bioprinting. We will highlight the issues of artificial ovary biofabrication, as this unique technology concerns not only patients’ health but also the health and well-being of future offspring. In the end, we will formulate a number of recommendations for the regulation of this field of scientific research and medical practice in the future.

2 Bioethical and legal issues of 3D bioprinting

2.1 Current and possible directions of bioethical discussions related to the emergence and development of 3D-bioprinting

The development of bioprinting technologies raises deep questions related to the very human nature, biotechnological projects

of “human enhancement”^[19], the issues of “technological design”^[20] youth extension, and even “technological immortality” of a human being. “Technological immortality” programs can be divided into two groups: Rejuvenation technologies (stopping the aging program) and consciousness transfer technology (unloading of the human personality). New organs bioprinting and replacing the old organs with them belongs to the rejuvenation technologies^[21] which raises the question of indications and limits of application of bioprinting technologies.

One of the first issues related to the development of organs and tissues bioprinting is the question of the feasibility of developing these technologies and the moral validity of it. Why and for what purpose are we ready to print organs? The answer seems obvious, based on the need for organ transplantation, the shortage of organ donation around the world. The development of technology can help save the lives of a very large number of people. The majority of governmental and international organizations now see this technology as morally justified if it has a therapeutic effect. As G. B. Yudin observes: “The main platform for justifying the widespread use of biotechnology is provided by the utilitarian philosophy.” Undoubtedly, there are gradations here – from radical transhumanism, which recognizes no limits for technological improvement of a human being (human enhancement), to more cautious versions, which recognize the social risks of human change. In general, however, the utilitarian framework of ethical thought is more inclined to protect human modification projects as they are driven by the individual’s desire for self-improvement and a better life^[22]. The scope of medical biotechnologies is becoming wider and increasingly blurred, and it is already difficult to distinguish between therapy and human improvement^[23]. It is also very important to pay attention to the speed at which these technologies develop to identify and study ethical problems before a therapeutic 3D bioprinting is ready for widespread use in patients^[24].

3D bioprinting deserves special attention as the utilization of viable cells in the printing process creates particular ethical and regulatory

problems^[24,25]. The “cell” is the most important component of bioprinting. The type of cells used plays a key role in determining the characteristics of the bioprinted tissue. In the case of allogeneic cell transplantation, we face classical ethical problems associated with donation: (1) The donor confidentiality, (2) the informed donor consent, (3) the possible invasive cell production procedure, and (4) donor cell ownership. There is still no verdict among clinicians and researchers regarding one of the basic rules of medical ethics – *Primum non nocere* (First, do no harm). The principle of misuse takes into account the moral nature of the action, the intention of the agent, the means of action, the possible adverse effects, and the proportionality between good and bad effects.

Stem cells are often used as “building blocks” for human tissue and organ biofabrication. The main ethical issue with regard to stem cells is its “source.” The use of human embryonic stem cells (ESCs) has been heavily criticized and has relevant limitations, both legal^[26,27] and moral^[28,29]. The main source of these cells are embryos or fetuses, so the problem of obtaining ESC is at the intersection of bioethical problems of determining the moral status of an embryo, legal pregnancy termination, and human participation in the experiments. In addition to the ethical and legal issues associated with the use of ESCs, other factors may influence the ethical acceptability of using bioinks from allogeneic cells. For instance, the issues of obtaining stem cells from donors who have been pressured, coerced, or have not given informed consent should be taken into consideration. Moreover, there are barriers for commercialization and therefore, the application of 3D printing technology on the basis of ESC as “use of human embryos in industrial and commercial purposes cannot be the objects for patent rights” according to the subclause 3 of Clause 4 of Article 1349 of the Civil Code of the Russian Federation.

Another option for the cell source for bioprinting is xenogeneic cells. In this case, it is necessary to take into consideration the social and religious aspects of animal cell utilization. Patients with xenotransplantation might experience psychosocial problems associated with their personal identity^[30]. Moreover, patients with

religious beliefs may disagree with the use of cells of certain animal species.

The emerging possibilities of reprogramming differentiated cells and producing induced pluripotent stem cells (iPSCs) eliminate the ethical issues of using ESCs or xenogeneic cells. iPSCs can be purposefully differentiated into any specific adult body cell types, ranging from skin cells to cardiac cells and neurons. However, we believe that the technology of 3D printing of human organs using autologous iPSC in bioink is not ethically neutral. It also has a number of problematic aspects, even if the bioinks are derived from the patient’s own cells. The technology of cell reprogramming is also very far from perfect. Today, one of the main challenges is to develop the methods that will ensure correct differentiation of all stem cells before transplantation. The risk of tumorigenicity is a major problem when using iPSC^[31-33]. To provide safety of iPSC-based therapies, genetic testing of stem cell lines potentially suitable for clinical application has to be performed^[34-36]. However, it brings additional ethical and legal issues related to the personal genetic information collection, storage, and use.

Data exchange for research purposes increases the number of individuals who can access personal genomic data which, in turn, increases the likelihood of data leakage and its malicious use, including for the purpose of committing a crime. In 2012, The Presidential Commission for the Study of Bioethical Issues published “Privacy and Progress in Whole Genome sequencing” report in the United States^[37]. This report gives recommendations for individual’s privacy protection while allowing exchanging genetic data. The Russian legislation does not regulate the organization and conducts of research related to human genome data and activities of the relevant genetic companies. Requirements for obtaining consent from a donor for participation in research, as well as requirements for the processing and transfer of genetic information as a special category of personal data, are not defined in the existing legislation. Additionally, current legislation does not regulate the circulation of biological materials seized from donors for the purpose of conducting scientific research, does not provide guarantees of

protection rights of donors, and does not stipulate the mandatory procedure for the preliminary approval of research by ethical committees^[38,39].

Another aspect that needs to be taken into consideration while evaluating the ethics of bioprinting is that the technology is set by a digital model. A number of authors note that the development of 3D bioprinting technology leads to the “digitalization” of objects of the material world, the boundaries between the physical world and the digital space erase, and bioprinting starts to digitize the person himself^[40,41]. The printed organs which are biofabricated on the basis of digital models will replace the natural ones, and thus, models will replace nature. Therefore, a question of responsibility for the development and evaluation of the 3D models arises: who and to which extent shall be responsible for the translation of the anatomical image into digital - «designers», biologists, or programmers? Who will have the legal rights for the model? Will it be possible to use the model without a patient’s consent? Is it possible to apply the models commercially? The questions of confidentiality and privacy arise regarding human digitization. In the case of bioprinting technology, the digital 3D model will represent personalized human data. Such information needs to be considered private, and special rules regulating the receipt, storage, handling, processing, and application of such information are required.

The two fundamental principles of human rights protection in the field of biomedical research are the principle of informed consent and the principle of confidentiality. The principle of confidentiality is closely related to the notion of “medical secrecy” and implies that the circumstances of treatment and the patient’s characteristics are kept confidential with the respect to the patient’s life. Confidentiality helps to build trust relationships that are essential for effective and timely medical care. The principle of informed consent is also one of the main in the system of ethical and legal support of medical activity^[42,43]. It derives from the concept of general human rights and is, therefore, generally accepted and allocated in a number of international and national documentations. For example, the Nuremberg

Code provides for absolute voluntary consent for human participation in medical trials including knowledge of the nature, duration, and purpose of the experiment, its methods, and associated risks. According to the Convention for the protection of Human Rights and Dignity of the Human Being with regard to the Application of Biology and Medicine: Convention on Human Rights and Biomedicine (ETS No. 164), medical intervention can be performed only after the person gives his/her voluntary written consent based on the information received on the purpose and nature of the intervention, as well as its consequences and risk. In 3D bioprinting, problems might arise in case of obtaining informed consent in emergency situations where a patient is unable to express informed consent. Obtaining informed consent can also be challenged in situations where a participant does not have the full ability to make a donation decision (e.g., some patients may be in intensive care units)^[24].

To introduce the 3D bioprinting technology into clinical practice and eliminate the associated risks, clinical trials are required. Along with the known ethical rules and standards for conducting experimental procedures involving humans, in the case of 3D bioprinting of human tissues and organs, specific issues arise regarding the design of human clinical trials^[24]. As 3D bioprinting technology develops within the personalized medicine paradigm^[13,20], each biofabricated product is individually tailored for a particular person and might require additional modifications to the experiment design in each case. Thus, standard approaches for clinical trials such as double-blind randomized control studies cannot be applied to 3D bioprinting technology. Each 3D bioprinted treatment is unique and adapted to a specific individual taking into consideration only his or her conditions, and therefore, results of each case cannot be fully extrapolated into future treatments. Nevertheless, while the biomaterials are personalized, criteria and protocols for the procedures can be standardized based on the first clinical trials. The organization of the experimental studies on human organ 3D bioprinting is a challenging task. The study has to be ethically

acceptable and safe for the patients. The efficiency and safety of the custom-made organs cannot be tested on other individuals; therefore, in this respect; each patient becomes the first examinee. Consequently, the question arises of the ratio of risks to benefits, criteria of inclusion, for instance, the participation of terminally ill patients in experiments.

Another issue concerning clinical studies of 3D bioprinting-assisted treatments is the question of study termination by a participant. Unlike standard clinical trials, for example, when drug dosage can be gradually adjusted, patients involved in a 3D printing trial may have difficulties with exercising their right to withdraw from the trial after implantation of an artificial organ. Interventions in 3D bioprinting treatments might be limited in terms of procedure reversibility (removal of the implant and all cells that have grown out of it) and the attempts of reverse implantation might lead to further harm to patients. Most importantly, a patient might lose a chance for an alternative treatment due to participation in a bioprinting trial^[24].

2.2 Legal issues of 3D bioprinting and introduction into clinical practice

Legal and government institutions around the world define the legal regulation of 3D bioprinting as a complex problem with no generally accepted satisfactory solutions for addressing the potential and uncertain risks of harm. The issues become even more exacerbated as numerous participants are involved in the production chain of bioprinting. Expertise from 3D model designers, medical professionals, lawyers, engineers, biologists, members of the ethical committee, and insurance companies are necessary for multi-stakeholder collaboration to form an acceptable path for the bioprinting technology development and introduction into clinical practice. There is currently no *sui generis* regulatory regime governing the entire bioprinting process, but there is partial legislation concerning tissue engineering and regenerative medicine.

According to the European Commission (EC) and European Medicines Agency gene therapies,

somatic cell therapies and tissue engineered products are called advanced therapy medicinal products (ATMPs)^[44]. The principles developed in the ATMPs Regulations of the EC might be applied to different stages of 3D bioprinting production. The key aspects of bioprinting management include the risks regulation and responsibility for product quality^[45]. In this regard, the following issues may be very important: Who is primarily responsible for the quality of bioprinted products – the 3D bioprinting providers or medical organizations; who should be responsible for quality control; who should be liable in case of bioprinted organ quality claims from the recipient; etc.

Legal problems of creation and use of bioprinting human organs, discussion of a possible model of legal regulation of bioprinting technologies received special consideration in Russia^[41,46,47]. The absence of norms in Russian legislation that regulates in the area of creation and implantation of bioprinted human organs is proposed to be a deterrent factor of 3D bioprinting technologies development^[41]. Current revision of the Federal law dated 23.06.2016 No. 180-FZ “On biomedical cellular products” for the time being cannot regulate the utilization of biofabricated human organ, as this law does not govern organ transplantation issues. At the same time, the Law of the Russian Federation dated 22.12.1992 No. 4180-1 “On human organs and (or) tissue transplantation” can neither regulate the use of 3D printed organs, as 3D bioprinted products are artificial^[41,48].

At present, the relations between 3D bioprinting providers, medical organizations, and patients can be settled down in the contract for works or medical services contract^[46]. Such types of contracts can be used in case of personalized biofabrication of organs or tissues for an individual order. However, if bioprinted organs are depersonalized, then the sale-purchase agreement can be applied^[46].

It also seems permissible for some specialists to “commercialize” the products in the field of bioprinting, as the final product of tissue engineering is so far from its original source (human biomaterial), that is, why the turnover of such products cannot be considered as

commercialization of the human body or its individual parts^[41]. Bioprinted human organs have objective features that distinguish them from human organs. Biofabricated organs are created artificially, and the creative process is purposeful and controlled. They are formed outside of the human body and there are no significant risks to life and health of the cell donor during the biofabrication of artificial organs. Moreover, the informed consent concerns only the production of biological material, but not biofabrication of the organ itself^[47]. These particular traits of 3D bioprinted organs before their transplantation to the human body might allow them to relate to objects of civil rights. As a result, the assumption of limited commercialization of the creation and utilization of biofabricated organs might be permitted^[47]. However, after implantation of organs and tissues, they should be recognized as an integral part of a human body. Therefore, it is necessary to recognize the legal death of this organ as an object with the termination of the title of ownership and with the corresponding prohibitions and restrictions on their removal and subsequent sale, which exist with regard to the human biomaterial today^[46].

The scope of legal regulation of 3D bioprinting action also includes a wide range of intellectual property rights, including patents, copyrights, design rights, and trademarks. Government intervention in research and new technologies development is essential because it will determine the future of technology. The political resolutions must be determined and corresponded normative issues must be addressed at the earliest stages of technological development. 3D bioprinting technology can save lives and revolutionize the medical sphere. Therefore, it deserves special attention and development of an appropriate legal framework^[49].

2.3 Ethical issues of artificial ovary 3D bioprinting and introduction into clinical practice

Among organ bioprinting, biofabrication of reproductive organs stay apart as the need for transplantation of artificial ovaries, testes, and

uteruses is not directly related to the threat of life, but to perceptions of the quality of life. Gonadotoxic oncological treatment can result in primary ovarian insufficiency in women of reproductive age. Therefore, different methods of fertility preservation (such as oocytes, embryos, and ovarian tissue cryopreservation) have been developed^[50]. Unfortunately, there are currently no options for fertility restoration after remission for the group of patients with ovarian cancer or types of cancer metastasizing into the ovaries (such as leukemia, neuroblastoma, and Burkitt lymphoma)^[16]. After the ovariectomy or the gonadotoxic oncological treatment, these patients suffer from irretrievable loss of reproductive and ovarian endocrine function. The development of artificial ovary technology gives hope to this group of patients for fertility preservation and the birth of genetically-related children. Such technology is currently under development, and the first successful animal experiments are known^[9]. Human clinical trials are still far away, however at this stage of technology development, it is of high importance to identify and solve several important ethical and regulatory issues associated with artificial ovary 3D bioprinting.

Along with the ethical and legal issues of 3D bioprinting technologies discussed above, the bioprinted ovary project addresses issues related to human reproduction. First and foremost, the major ethical issue related to the development of a 3D bioprinted ovary project is the question of the risk-benefit ratio. Ovariectomy and gonadotoxic chemo- and radio-therapies, as oncological treatments are necessary procedures for patient's life preservation and therefore can be considered as the good. However, loss of reproductive function is a harm, and if there is an opportunity to correct it following the principle of *primum non nocere* and restore reproductive function, then it will be possible to compensate for the caused harm. It is a strong argument in favor of developing artificial ovary technology, but a number of profound conditions should be taken into consideration.

The risks associated with transplantation of 3D printed artificial ovaries should be clinically assessed as minimal. Therefore, all the possible

risks should be evaluated at each step of technology: Starting with bioinks creation and ending with organ transplantation. The particular and highly important feature of the artificial ovary technology is that the risks concern not only the patient herself but also the future offspring. The major concern is that *ex vivo* manipulations with ovarian follicles might lead to genetic and epigenetic changes in the egg cells which will directly affect the offspring's health. Moreover, quite often malignant diseases are hereditary. Thus, the artificial ovary technology would contribute to the transmission of genetic variants, associated with cancer to the next generations and therefore will artificially increase the percentage of patients with cancer. Another question that may arise with the artificial ovary technology implementation is the right to receive information about the birth of children. Can the information of conception with the assistance of artificial ovary 3D printing technology be traumatic to a child? Can it lead to a new form of stigmatization in society in the future?

Another important aspect of development and introduction into the clinical practice the ovary bioprinting technology is that several years have to pass from the moment of ovary removal to the moment of the possibility of artificial ovary transplantation due to oncological treatment. A patient might refuse transplantation when the organ is printed, but the use of such an expensive technology might emotionally pressure and oblige a patient to motherhood. The problem of voluntary rejection of transplantation in the case when an artificial organ is already printed raises both ethical and legal questions of ownership of printed organs. The same question is relevant in case of a patient's death. Can an artificial ovary be donated for scientific research or pharmaceutical drug testing?

The next equally important issue involved in the development of bioprinted ovary is the aspect of technology commercialization and the associated moral issue. The legislation of Russia allows commercial relations in assisted reproductive technologies. For instance, *in vitro* fertilization (IVF) can be provided in clinics on a paid basis. However, commercial relations in transplantation are prohibited by law in Russia. For example, the

prohibition of organ sale is in conformity with the basic law of moral relations between people. The trend toward the commercialization of organ transplantation has its own objective reasons. One of the main reasons is the shortage of organs for transplantation, which forces patients to find extraordinary sources of donor organs. With the help of 3D printing technology, the problem of donor organ shortage can be solved, but an issue of the accessibility of technology to the entire population will arise. It is clear that the rich will be able to take advantage of 3D bioprinting, which will further widen the gap between the possessing classes and the indigent in our society. In the case of commercial creation and transplantation of artificial ovaries, this expensive scientific and technical solution can benefit only few members of a certain group, bringing an ethical problem of social stratification of bioprinting^[51].

A number of questions arise regarding the inclusion criteria for artificial ovary technology implementation. Should there be an age limit for the use of technology? If a patient already has children, should artificial ovary transplantation be allowed? Can a woman with artificial ovaries participate in IVF programs? How can the presence of an artificial ovary affect the physical and mental integrity of a patient? If the ultimate goal of live birth is not achieved, how the responsibility will be distributed among programmers, engineers, biologists, and doctors? Should the state finance the production and transplantation of artificial ovary to its underprivileged, low-income citizens?

3 Conclusions and perspectives

As it is easy to see, there are more questions than answers in the area of bioethical and legal issues of 3D bioprinting. The lack of answers is due to the fact that the speed of development of research and the increase of technological capabilities largely outstrips the speed of our understanding of the moral and legal consequences of their development. Currently in Russia and globally, there is neither suitable statutory framework nor special regulatory guidelines governing 3D bioprinting of tissues and organs and their further

transplantation. The problem of ethical evaluation and legal regulation of 3D bioprinting are that this technology cannot be thoroughly evaluated using standard clinical trials or taking into account the current regulatory requirements.

However, before the 3D bioprinting technology spreads and becomes clinically available, several regulations of scientific research and medical practice should be adopted. First of all, there is a need to develop informed consents for donation, material manipulation, storage, and its further use, including for commercial and research purposes. Moreover, it is necessary to develop requirements for safety, quality, and efficiency of technological procedures and the end products obtained by 3D bioprinting taking into account the human rights and dignity. Furthermore, it is of great importance to establish committees for creation and regulation of national guidelines on technical, legal, and ethical issues related to the development and application of 3D bioprinting technologies. All patients including minors and incapable people need to be legally protected. Last but not least, it is essential to establish regulations of turnover and limits of commercialization for 3D bioprinting technologies of human organs and tissues, as well as possible sanctions for illegal trafficking of artificial organs.

Authors' contributions

Conception and design: AK and GS; Collection and assembly of data: AK, SB, and AA; Data analysis and interpretation: SB, AK, and AA; Manuscript writing: SB and AK; Final approval of manuscript: All authors.

Acknowledgments

AK was supported by the Grant of the President of the Russian Federation – for state support of young Russian scientists – K-3244.2019.7. The authors thank Nelli Mamaiusupova for her critical reading of the manuscript.

Conflicts of interest

No conflicts of interest are reported by the authors.

References

1. Pereira FD, Parfenov V, Khesuani YD, *et al.*, 2018, Commercial 3D Bioprinters. In: 3D Printing and Biofabrication. Springer International Publishing, Cham, Switzerland, pp. 535–549. DOI: 10.1007/978-3-319-45444-3_12.
2. Schwab K, 2017, The Fourth Industrial Revolution, Crown Business. Crown Business Group, New York.
3. Mironov V, 2003, Printing Technology to Produce Living Tissue. *Expert Opin Biol Ther*, 3:701–704.
4. Guillemot F, Mironov V, Nakamura M, 2010, Bioprinting is coming of age: Report from the international conference on bioprinting and biofabrication in Bordeaux (3B'09). *Biofabrication*, 2:010201. DOI: 10.1088/1758-5082/2/1/010201.
5. Zopf DA, Hollister SJ, Nelson ME, *et al.*, 2013, Bioresorbable Airway Splint Created with a Three-Dimensional Printer. *N Engl J Med*, 368:2043–2045. DOI: 10.1056/nejmc1206319.
6. Grigoryan B, Paulsen SJ, Corbett DC, *et al.*, 2019, Multivascular Networks and Functional Intravascular Topologies within Biocompatible Hydrogels. *Science*, 364:458–464. DOI: 10.1126/science.aav9750.
7. Crowley C, Birchall M, Seifalian AM, 2015, Trachea Transplantation: From Laboratory to Patient: Trachea Transplantation. *J Tissue Eng Regen Med*, 9:357–367. DOI: 10.1002/term.1847.
8. Zhong C, Xie HY, Zhou L, *et al.*, 2016, Human Hepatocytes Loaded in 3D Bioprinting Generate Mini-liver. *Hepatobiliary Pancreat Dis Int*, 15:512–518. doi.org/10.1016/s1499-3872(16)60119-4. DOI: 10.1016/s1499-3872(16)60119-4.
9. Laronda MM, Rutz AL, Xiao S, *et al.*, 2017, A Bioprosthetic Ovary Created Using 3D Printed Microporous Scaffolds Restores Ovarian Function in Sterilized Mice. *Nat Commun*, 8:15261. DOI: 10.1038/ncomms15261.
10. Bulanova EA, Koudan EV, Degosserie J, *et al.*, 2017, Bioprinting of a Functional Vascularized Mouse Thyroid Gland Construct. *Biofabrication*, 9:034105. DOI: 10.1088/1758-5090/aa7fdd.
11. Arslan-Yildiz A, Assal RE, Chen P, *et al.*, 2016, Towards Artificial Tissue Models: Past, Present, and Future of 3D Bioprinting. *Biofabrication*, 8:014103. DOI: 10.1088/1758-5090/8/1/014103.
12. Murphy SV, Atala A, 2014, 3D Bioprinting of Tissues and Organs. *Nat Biotechnol*, 32:773–785. DOI: 10.1038/nbt.2958.
13. Radenkovic D, Solouk A, Seifalian A, 2016, Personalized Development of Human Organs Using 3D Printing Technology. *Med Hypotheses*, 87:30–33. DOI: 10.1016/j.mehy.2015.12.017.

14. Afsana, Jain V, Haider N, et al. 2019, 3D Printing in Personalized Drug Delivery. *Curr Pharm Des*, 24:5062–5071. DOI: 10.2174/1381612825666190215122208.
15. Amorim CA, 2011, Artificial ovary. In: Practice of Fertility Preservation. Cambridge University Press, Cambridge, pp. 448–458.
16. Amorim CA, Shikanov A, 2016, The Artificial Ovary: Current Status and Future Perspectives. *Future Oncol*, 12:2323–2332. DOI: 10.2217/fon-2016-0202.
17. Krotz SP, Robins JC, Ferruccio TM, et al., 2010, In Vitro Maturation of Oocytes Via the Pre-fabricated Self-assembled Artificial Human Ovary. *J Assist Reprod Gen*, 27:743–750. DOI: 10.1007/s10815-010-9468-6.
18. Cho E, Kim YY, Noh K, et al., 2019, A New Possibility in Fertility Preservation: The Artificial Ovary. *J Tissue Eng Regen Med*, 13:1294–1315. DOI: 10.1002/term.2870.
19. Yudin BG, 2016, Institutionalization of Bioethics and Human Enhancement. *Workbooks Bioeth*, 23:5–11.
20. Tishchenko PD, 2015, Designing of the Person: Ideals and Technologies. *Workbooks Bioeth*, 24:36–64.
21. Bushev S, 2018, The Philosophical and Natural-science Aspects of the Study of the Problem of Aging and Technological Immortality. *Soc Poli Nauki*, 3:198-200.
22. Yudin GA, 2019, Communitarian Approach for Bioethics, *Ethical Thought*, 19(1):36-48.
23. Yudin B, 2016, Technoscience and “Human Enhancement”. *Epistemol Philos Sci*, 48(2):18-27.
24. Gilbert F, O’Connell CD, Mladenovska T, et al., 2018, Print Me an Organ? Ethical and Regulatory Issues Emerging from 3D Bioprinting in Medicine. *Sci Eng Ethics*, 24(1):73–91. DOI: 10.1007/s11948-017-9874-6.
25. Gilbert F, Víaña JNM, O’Connell CD, et al., 2018, Enthusiastic Portrayal of 3D Bioprinting in the Media: Ethical Side Effects. *Bioethics*, 32(2):94–102. DOI: 10.1111/bioe.12414.
26. Directive 2004/23/EC of the European parliament and of the council of 31 March 2004 on setting standards of quality and safety for the donation, procurement, testing, processing, preservation, storage and distribution of human tissues and cells 2004. *Off J Eur Union*, 102:48–58.
27. Russian Federation. Federal Law dated 23.06.2016 No. 180-FZ “on Biomedical Cellular Products”. Russian Federation, Moscow.
28. Lo B, Parham L, 2009, Ethical Issues in Stem Cell Research. *Endocr Rev*, 30:204–213.
29. Volarevic V, Markovic BS, Gazdic M, et al., 2018, Ethical and Safety Issues of Stem Cell-Based Therapy. *Int J Med Sci*, 15:36–45. DOI: 10.7150/ijms.21666.
30. Gulyaev VA, Khubutiya MS, Novruzbekov MS, et al., 2019, Xenotransplantation: History, Problems and Development Prospects. *Transplantol Russ J Transplant*, 11:37–54.
31. Blum B, Benvenisty N, 2009, The Tumorigenicity of Diploid and Aneuploid Human Pluripotent Stem Cells. *Cell Cycle*, 8:3822–3830. DOI: 10.4161/cc.8.23.10067.
32. Nori S, Okada Y, Nishimura S, et al., 2015, Long-Term Safety Issues of iPSC-Based Cell Therapy in a Spinal Cord Injury Model: Oncogenic Transformation with Epithelial-Mesenchymal Transition. *Stem Cell Rep*, 4:360–373. DOI: 10.1016/j.stemcr.2015.01.006.
33. Tang W, 2019, Challenges and Advances in Stem Cell Therapy. *BioScience Trends*, 13:286–286.
34. Andrews PW, Ben-David U, Benvenisty N, et al., 2017, Assessing the Safety of Human Pluripotent Stem Cells and Their Derivatives for Clinical Applications. *Stem Cell Rep*, 9:1–4. DOI: 10.1016/j.stemcr.2017.05.029.
35. Sullivan S, Stacey GN, Akazawa C, et al., 2018, Quality Control Guidelines for Clinical-grade Human Induced Pluripotent Stem Cell Lines. *Regen Med*, 13:859–866.
36. Jo HY, Han HW, Jung I, et al., 2020, Development of Genetic Quality Tests for Good Manufacturing Practice-compliant Induced Pluripotent Stem Cells and their Derivatives. *Sci Rep*, 10(1):3939. DOI: 10.1038/s41598-020-60466-9.
37. The Presidential Commission for the Study of Bioethical Issues, 2016, Privacy and Progress in whole Genome Sequencing. Available from: <https://www.bioethicsarchive.georgetown.edu/pcsbi/sites/default/files/6%20Privacy%20-%20Privacy%20and%20Progress%209.30.16.pdf>.
38. Vasiliev SA, Osavelyuk AM, Burtcev AK, et al., 2019, Problems of Legal Regulation of Diagnostics and Human Genome Editing in the Russian Federation. *Lex Russica*, 6:71–79. DOI: 10.17803/1729-5920.2019.151.6.071-079.
39. Stambolsky DV, Bryzgalina EV, Efimenko AY, et al., 2018, Informed Consent to the Receipt and use of Human Cellular Material: Juristic and Ethical Regulation. *Russ J Cardiol*, 12:84–90. DOI: 10.15829/1560-4071-2018-12-84-91.
40. Osborn LS, 2014, Regulating Three-Dimensional Printing: The Converging Worlds of Bits and Atoms. Vol. 51. Campbell University School of Law, San Diego Law Review, pp. 553-622.
41. Bogdanov DE, 2019, Bioprinting Technology as a Legal Challenge: Determining the Model of Legal Regulation. *Lex Russica*, 6:80-91. DOI: 10.17803/1729-5920.2019.151.6.080-091.
42. Degtyarev YG, Fomin OY, Soltanovich AV, et al., 2014, Informed Consent for Medical Interference: Medical and

- Legal Aspects. *Zdravookhranenie*, 2:27-38.
43. Povarov YS, 2019, Requirements for Consent to Conduct Research, Treatment or Diagnostics in the Area of Human Genome. *Jurid J Samara Univ*, 5:23. DOI: 10.18287/2542-047x-2019-5-2-23-28.
 44. European Commission, 2017, European Commission-DG Health and Food Safety and European Medicines Agency Action Plan on ATMPs. Available from: https://www.ema.europa.eu/en/documents/other/european-commission-dg-health-food-safety-european-medicines-agency-action-plan-advanced-therapy_en.pdf. DOI: 10.1211/pj.2014.11137703.
 45. Li P, 2018, 3D Bioprinting: Regulation, innovation, and patents. In: *3D Bioprinting for Reconstructive Surgery*. Elsevier, Berlin, 217–231. DOI: 10.1016/b978-0-08-101103-4.00020-x.
 46. Ayusheeva IZ, 2019, Problems of Legal Regulation of Contractual Relations in the Process of Creating Bio-Print Human Organs. *Lex Russica*, 6:92–99. DOI: 10.17803/1729-5920.2019.151.6.092-099.
 47. Ksenofontova DS, 2019, Legal Issues of Creation and Use of Bioprinted Human Organs. *Lex Russica*, 1:109–118. DOI: 10.17803/1729-5920.2019.154.9.109-118.
 48. Kelly E, 2018, FDA Regulation of 3D-Printed Organs and Associated Ethical Challenges. *Univ Pa Law Rev*, 166:515–546.
 49. Vijayavenkataraman S, Lu WF, Fuh JY, 2016, 3D Bioprinting an Ethical, Legal and Social Aspects (ELSA) Framework. *Bioprinting*, 1–2:11–21. DOI: 10.1016/j.bprint.2016.08.001.
 50. Medrano JV, Andrés M, García S, *et al.*, 2018, Basic and Clinical Approaches for Fertility Preservation and Restoration in Cancer Patients. *Trends Biotechnol*, 36:199–215.
 51. Vermeulen N, Haddow G, Seymour T, *et al.*, 2017, 3D Bioprint me: A Socioethical View of Bioprinting Human Organs and Tissues. *J Med Ethics*, 43:618–624. DOI: 10.1136/medethics-2015-103347.

Collagen as Bioink for Bioprinting: A Comprehensive Review

Egor Olegovich Osidak^{1,2*}, Vadim Igorevich Kozhukhov^{2,3}, Mariya Sergeevna Osidak¹,
Sergey Petrovich Domogatsky^{2,3}

¹Imtek Ltd., 3rd Cherepkovskaya 15A, Moscow, Russia

²Gamaleya Research Institute of Epidemiology and Microbiology Federal State Budgetary Institution, Ministry of Health of the Russian Federation, Gamalei 18, Moscow, Russia

³Russian Cardiology Research and Production Center Federal State Budgetary Institution, Ministry of Health of the Russian Federation, 3 Cherepkovskaya 15A, Moscow, Russia

Abstract: Biomaterials made using collagen are successfully used as a three-dimensional (3D) substrate for cell culture and considered to be promising scaffolds for creating artificial tissues. An important task that arises for engineering such materials is the simulation of physical and morphological properties of tissues, which must be restored or replaced. Modern additive technologies, including 3D bioprinting, can be applied to successfully solve this task. This review provides the latest evidence on advances of 3D bioprinting with collagen in the field of tissue engineering. It contains modern approaches for printing pure collagen bioinks consisting only of collagen and cells, as well as the obtained results from the use of pure collagen bioinks in different fields of tissue engineering.

Keywords: Collagen, Three-dimensional bioprinting, Tissue engineering, Cell-laden hydrogels

***Corresponding Author:** Egor Olegovich Osidak, Gamaleya Research Institute of Epidemiology and Microbiology Federal State Budgetary Institution, Ministry of Health of the Russian Federation, Gamalei 18, Moscow, Russia; OsidakEgor_egorosidak@gmail.com

Received: March 02, 2020; **Accepted:** March 16, 2020; **Published Online:** April 21, 2020

(This article belongs to the *Special Section: Bioprinting in Russia*)

Citation: Osidak EO, Kozhukhov VI, Osidak MS, *et al.*, 2020, Collagen as Bioink for Bioprinting: A Comprehensive Review. *Int J Bioprint*, 6(3): 270. DOI: 10.18063/ijb.v6i3.270.

1 Introduction

For the past few years, additive technologies, including the technology of three-dimensional (3D) bioprinting, have emerged into a rapidly developing tissue engineering sphere^[1]. These technologies allow creating layer-by-layer assembled structures with a specific pore size and porosity that promotes the restoration of defects of soft or hard tissues. Another indisputable advantage of the 3D bioprinting is that it allows creating personalized implants for the specific needs of a patient, taking the individual features of the

patient into account at the same time^[2]. Moreover, the use of this technology allows building complex structures that are already colonized with cells at the moment of bioprinting. Cell-laden hydrogels, which are also called bioinks, are used to create such structures^[3].

Synthetic polymers, such as poly(ethylene glycol), as well as native proteins, such as collagen, can be used as a structural basis for such hydrogels^[3,4]. Collagen-containing hydrogels are currently the most popular cell scaffold and material for tissue engineering, especially if working with cells is

intended^[5]. Nevertheless, the most important thing here is that materials created using 3D bioprinting and collagen have very high chances of clinical success in the future, because collagen biomaterials have been already been actively and successfully used in clinical practice for a long time. This is possible due to the unique properties of collagen – biocompatibility and low immunogenicity^[6,7]. However, low immunogenicity of 3D constructs can be achieved only with the use of high purity collagen solutions without potential immunogenic admixtures^[6]. Thus, in this review, “collagen” will be meant as a purified protein obtained through extraction from collagen-containing tissues and not a decellularized extracellular matrix of any tissue or organ containing a large amount of collagen^[8]. The main barrier that prevents the use of decellularized materials is immunological rejection, which significantly limits the possibility of clinical use of such materials.

Therefore, the purpose of this review is to conduct a comprehensive study of the use of collagen-based bioinks for 3D bioprinting in various fields of tissue engineering. The review covers topics such as general limitations and advantages of collagen and collagen-based bioinks used in different areas and the main approaches for collagen-based bioinks 3D printing.

2 Pure collagen bioink: Printability aspects

As it was already noted before, soft biomaterials loaded with living cells are called bioinks^[3]. The basis of collagen bioink is a collagen hydrogel, physical properties of which represent its printability. The majority of collagen hydrogels are produced from type I collagen, which makes up around 90% of the protein mass in the connective tissues of mammals^[9]. Type I collagen belongs to the group of fibril-forming collagens and consists of three alpha-helices that form a triple-helical structure^[9,10]. Under physiological conditions (neutral pH and 37°C), collagen molecules start to self-organize into fibrils, and collagen solution forms a hydrogel. The printability of collagen bioink depends on the kinetics of this process – the higher the speed, the higher is printing accuracy.

The majority of existing studies on 3D printing and bioprinting using collagen specify the main problem with collagen bioink – its low mechanical properties^[3,11]. All these studies were carried out using collagen solutions of low concentration – usually, not more than 5 mg/ml and rarely, 10 mg/ml^[12]. This problem refers to not only in 3D bioprinting but also other sections of tissue engineering. More than 90% of known studies were carried out using collagen hydrogels prepared from solutions with not more than 10 mg/ml collagen^[5].

One of the possible approaches to overcome this limitation is the use of supportive hydrogels. When using a supportive hydrogel for 3D bioprinting with a collagen bioink, the whole process occurs inside of the secondary hydrogel (e.g., gelatin slurry), which in turn acts as temporary thermo-reversible support (FRESH technique – freeform reversible embedding of suspended hydrogels)^[13-15]. On the one hand, this method allows printing complex structures using collagen solutions of low concentrations with a polymerization period of 40 – 60 min. On the other hand, gelatin from the supportive hydrogel can diffuse inside the bioink during the polymerization period. This, in turn, will lead to a final construct that potentially contains gelatin. The effect of the remaining FRESH gelatin in a final construct at *in vivo* implantation is not fully studied.

Another approach to compensate for the low mechanical properties of collagen hydrogels was proposed by Diamantides *et al.*^[16]. According to their study, the best way to improve the printability of collagen bioinks is to increase the storage modulus of the ink before extrusion. This strategy was described more accurately by Osidak *et al.*^[17], it was shown that collagen bioinks with a much greater storage modulus than loss modulus are suitable for direct extrusion bioprinting.

The storage modulus of collagen solution depends on the concentration of NaCl in the solution^[18], its temperature^[19], and on collagen concentration^[17,19,20]. The most effective method to increase the storage modulus is to increase the collagen concentration in a solution^[17]. Such highly concentrated collagen solutions of 80 mg/ml named Viscoll Bioink (viscous collagen

bioink solution) are available on the market. When mixed with a mammal cell suspension in a cultural medium and then heated to 37°C, Viscoll bioink quickly forms a stable cell-laden hydrogel. The survival rate of NIH 3T3 cells as a part of rigid collagen hydrogels was approximately 90% after printing and after a week of *in vitro* cultivation. Unfortunately, this is the only data on the behavior of cells during cultivation inside rigid 3D collagen hydrogels that are currently available.

3 Tissue engineering applications of collagen-based bioinks

Due to the prevalence of collagen-based bioinks with a low protein concentration usage in various fields of tissue engineering, collagen is mixed with various materials to improve the manufacturing process and the final characteristics of the printed construct^[21,22]. There are only few studies, where collagen bioinks were used as a pure substance without any additives. These works are listed below.

Currently, there are two general methods for creating tissue-engineering designs – *in vitro* bioprinting and *in situ* bioprinting. In the case of *in vitro* bioprinting, the printing of design is carried out in the laboratory environment. After printing, the design is either implanted into a laboratory animal or cultivated for a specific period for cell behavior study. In the case of *in situ* bioprinting, printing is carried out directly onto the defective area of a laboratory animal.

3.1 Skin

Koch *et al.*^[23] in their work have printed a construct with the use of laser-assisted bioprinter onto the surface of a supportive scaffold – decellularized dermal matrix (Matrigel). The printing process was carried out in two stages – 20 layers of fibroblast (murine NIH 3T3) were applied onto the surface, which was followed by 20 layers of keratinocyte (human HaCaT), embedded into collagen hydrogel (3 mg/ml). As a result, it was shown that a bi-layered construct that generates dermis and epidermis has been successfully created. After 10 days of cell cultivation inside of the construct, the presence of Connexin 43 in the epidermis, which showed

the ability to form gap junctions, was detected. In another study of Koch *et al.*^[24], similar bi-layered constructs were created in *in vitro* conditions and then implanted *in vivo*, employing the dorsal skin-fold chamber in nude mice. It was found that fibroblasts can migrate into a supportive scaffold. Moreover, it was noted that the presence of several blood vessels in the wound bed could be observed after 11 days of transplantation.

Shi *et al.*^[25] have printed six-layered cellular structures using extrusion-based bioprinter. They used three types of cells: Human melanocytes (HEM), HaCat, and human dermal fibroblasts (HDF). As a material for bioink, they used a mixture of GeIMA and collagen. In addition, I-2959 photoinitiator and tyrosinases were added to the obtained mixture. The biocompatibility of created designs was evaluated *in vitro* and *in vivo* through implantation of these structures without cells into a full-thickness wound model of Sprague-Dawley rat. The viability of these three cell lines during 14 days of cultivation was above 90%. *In vivo* tests have shown that healing rates of the wound can be accelerated when treated with the tyrosinase doped bioinks.

Another study worth noting was made up by Yoon *et al.*^[12]. To create 3D skin substitutes, they used pure (single-component) collagen bioinks. Primary human epidermal keratinocytes (HEK) and HDF were used to fabricate cell-laden 3D scaffolds. Cell-laden 3D scaffolds were created through extrusion bioprinting and were composed of four layers. The top-level contained keratinocytes and the other three layers had fibroblasts. According to the results of the study, cell-laden 3D scaffolds in a 1 × 1 cm² full-thickness excision mouse model have successfully demonstrated their efficiency. After 1 week, the damaged skin almost completely and clearly regenerated. The hair follicles on the wound bed also regenerated almost perfectly.

In the work of Skardal *et al.*^[26], amniotic fluid-derived stem cells (AFSC) and mesenchymal stem cells (MSC) were separately suspended in the fibrinogen/collagen solution. They used a bioprinter to directly print two layers of a fibrin-collagen gel by depositing a layer of thrombin, a layer of fibrinogen/collagen, another layer of thrombin, another layer of fibrinogen/collagen,

and the final layer of thrombin onto a full-thickness skin wound ($2 \times 2 \text{ cm}^2$). In 2 weeks, AFS-treated mice showed an average of 3% of unclosed wounds, whereas MSC-treated wounds showed an average of 2%. These values were significantly lower than those of mice treated with gel only, which had an average of 13% of unclosed wounds.

Further development of this result was continued by Albanna *et al.*^[27], where excisional wounds were bioprinted with layered autologous dermal fibroblasts and epidermal keratinocytes in a fibrinogen/collagen carrier (25 mg/ml fibrinogen, and 1.1 mg/ml collagen) in two different models: Murine full-thickness wound model ($3 \times 2.5 \text{ cm}$) and porcine full-thickness wound model ($10 \times 10 \text{ cm}$). The obtained results showed a rapid wound closure, reduced contraction, and accelerated re-epithelialization.

3.2 Bone and cartilage

Native bone tissues can withstand heavy loads. Therefore, 3D printed structures, ideally must possess the same characteristics. In this case, to strengthen 3D bioprinted structures, composite materials are being actively used nowadays, for example, a mixture of collagen with various types of bioceramics^[28-31].

Kim *et al.*^[29] have introduced bioceramic-based cell-printing technique and a cell-laden ceramic structure. Using 3D bioprinting technology, they created a cell-laden scaffold using α -tricalcium phosphate (α -TCP) type I collagen and MC3T3-E1 cells. First, they have printed a porous layer consisting of micro-sized α -TCP/collagen struts without cells, and then a cell-laden collagen bioink was printed onto it. This procedure was repeated several times to form a 3D porous cell-laden ceramic scaffold. The elastic modulus of the α -TCP/collagen scaffold was 550 kPa. However, this value is much lower than the elastic modulus of a real trabecular bone (around 20 MPa)^[32]. Nevertheless, it was shown that the designed scaffold demonstrated good cellular activities, including metabolic activity and mineralization.

In the other work of Kim and Kim^[28], β -TCP, type I collagen and MC3T3-E1 cells were used as a bioink, and Genipin was used as a crosslinking

agent. With new materials, the elastic modulus of printed structures was 5.94 MPa. The *in vitro* evaluation of cellular responses (viability and proliferation) was comparable to results obtained in the pure cell-laden collagen.

One of the earliest studies on cartilage bioprinting using pure collagen bioinks was carried out in 2016 when primary meniscal fibrochondrocytes and high-density collagen hydrogels (from 10 to 20 mg/ml) were bioprinted^[20]. In that study, the influence of collagen on several parameters, including geometric fidelity, cell viability, and mechanical properties of printed constructs, was evaluated. The concentration of collagen gel had no impact on cell viability, whereas the compressive modulus of printed gels increased linearly with an increase in collagen concentration. With the highest printable concentration, the elastic modulus of the printed structure reached 30 kPa. These structures maintained cell viability and their geometric fidelity for 10 days while being stored in a culture medium. The geometric accuracy of structures, printed with 15 mg/ml and 17.5 mg/ml collagen solutions, was at 74 – 78%.

Shim *et al.*^[33] have printed a construct for osteochondral tissue regeneration in the rabbit knee joint. Pure collagen bio-ink that consisted of atelocollagen, human turbinat-derived mesenchymal stromal cells (hTMSCs), and recombinant human bone morphogenetic protein-2 (rhBMP-2), was printed into a preprinted polycaprolactone (PCL) scaffold. The prepared cylinder-shaped construct was 5 mm in diameter and 5 mm in height, with a “subchondral bone layer” (PCL, atelocollagen, hTMSCs, and rhBMP-2) of 4 mm in thickness, and “superficial cartilage layer” (Cucurbit[6]uril, hTMSCs, and TGF- β) of 1 mm in thickness. This construct was *in vivo* implanted onto the defective part of the rabbit knee joint. Eight weeks later, it was shown that the construct possessed a capability for osteochondral regeneration. The adjacent native cartilage maintained its structure without any signs of degeneration. The newly regenerated cartilage tissues smoothly integrated themselves with ends of the host cartilage tissue. The immunohistochemical analysis for collagen type

II (COL-II) and COL-X expression indicated that zonal cartilage regeneration was reached.

An alternative approach was proposed by Yang *et al.*^[34]. In this work, to prepare the bioink, collagen (15 mg/ml) was mixed with alginate (sodium alginate SA/COL). Then, primary chondrocytes isolated from articular cartilage of new-born rats were added to the mixture. As a comparison, two types of other bioinks were used: Bioink made from agarose (AG) and bioink made from a mixture of alginate and AG (SA/AG). When comparing SA/COL with SA/AG and SA, the proliferation and survival of chondrocytes were significantly promoted in the case of SA/COL bioinks. The expression of specific gene markers of cartilage, including Sox9, Acan, and Col2a1, was also significantly higher in SA/COL group.

3.3 Cardiovascular tissues

In general, the research work on bioprinting for cardiovascular tissue regeneration is focused on myocardium, heart valves, and vasculature^[35].

Maxson *et al.*^[14] have demonstrated the potential of the use of the highly concentrated type I collagen hydrogel for the heart valve bioprinting. In addition to collagen, the bioink contained rat MSCs. With this bioink, Maxson *et al.* managed to print collagen disks of 1 mm in thickness and 28 mm in diameter onto a FRESH slurry. After slurry removal, the printed structures were subcutaneously implanted into rats. The implanted samples were extracted at 2, 4, 8, and 12 months with the subsequent study on their mechanical properties, evaluation of cell infiltration, and determination of levels of specific inflammation markers expression. The profile of stress-strain curves of the bioprinted aortic heart valve scaffolds indicated that scaffolds have transitioned through phases of resorption, synthesis, stabilization, ultimately, and remodeling.

At the resorption stage (2 – 4 weeks), the mechanical properties of implanted scaffolds were reduced. Moreover, the increased expression of CD3 biomarker from acute inflammation was also noted during this period.

At the synthesis stage (4 – 8 weeks), the mechanical properties of implanted scaffolds

began to increase. Gross encapsulation of the implanted scaffold, which additionally indicates an inflammatory reaction, was also noted. The concentration of CD3 biomarker (that is an indication of an inflammatory process) was reduced compared with the first stage. However, the gross encapsulation of the implanted scaffold shows that the inflammation process is still presented.

At the stabilizing stage (8 – 12 weeks), peak values of elastin, vimentin, and alpha-SMA production were noted. This indicates the active deposition of collagen by infiltrated cells and the strengthening of the extracellular matrix in the bioprinted scaffold. However, compared with the previous stage, there was no significant increase in the mechanical properties of the implanted material.

This work of Maxson *et al.* is of particular interest due to the demonstrated recellularization potential of a bioprinted aortic heart valve scaffold from a highly concentrated type I collagen hydrogel. Furthermore, an increased level of the CD3 marker expression in experimental animals may be associated with the presence of residual gelatin from FRESH slurry and allogeneic rat cells in the construct.

Despite concerns of inducing a systemic immune response, it is worth noting that the indisputable advantage of FRESH technology is the ability to 3D print the human heart components at various scales from capillaries to the full organ with a high degree of accuracy. For example, Lee *et al.*^[15] have printed a simplified model of a small coronary artery-scale linear tube from COL for perfusion with a custom-designed pulsatile perfusion system. The linear tube had an inner diameter of 1.4 mm and a wall thickness of ~300 µm. C2C12 cells within a collagen gel were cast around the printed collagen tube. Only in case of active perfusion through the collagen structure, cells remained alive in their entirety. Next, they printed the left ventricle of the heart using human stem cell-derived cardiomyocytes. The ventricle was designed as an ellipsoidal shell with inner and outer walls of collagen and a central core region which contained cells. Cardiac ventricles printed with human cardiomyocytes showed synchronized contractions, directional action

potential propagation, and wall thickening of up to 14% during peak systole.

Summarizing the above, the data^[14,15] have demonstrated the effectiveness of the use of highly concentrated type I collagen hydrogel as a main material of bioinks for cardiovascular tissue regeneration.

3.4 Liver

A variety of 3D printing techniques are used for liver tissue engineering^[36]. The general purpose of such works, along with a recreation of a complex microarchitecture and cell diversity, is a development of sustainable *in vitro* models of the liver for drug testing and pathology study.

As an example, Shim *et al.*^[37] have successfully developed a hybrid scaffold consisting of PCL and MC3T3-E1-laden collagen hydrogel. The scaffold was prepared using a multi-head deposition system, followed by primary hepatocyte seeding to create a patterned 3D coculture. In the proposed method, a tough supporting PCL construct was used to maintain the specific 3D form of the printed structure. However, it should be noted that the mechanical properties of such structures differ from the mechanical properties of the liver tissues significantly, and the problem of the printed structure stabilization for a long-term *in vitro* cell cultivation remains open. To solve this problem, Mazzocchi *et al.*^[38] have proposed to use a mixture of methacrylated type-I collagen and hyaluronic acid as a structural basis for bioink. Into this mixture, they introduced primary human hepatocytes. After that, the resulting structure was crosslinked using UV irradiation. The printed cell-laden constructs were incubated in a culture medium for 15 days. The functionality of hepatocytes was evaluated on the 6th day of cultivation by exposure constructs to acetaminophen (APAP) and hepatic toxicant. Levels of cell expression of albumin, urea, and lactic acid dehydrogenase (LDH) into the culture medium were also evaluated. A pronounced decrease in the levels of albumin and urea expression was found on the 9th day of cultivation in the APAP treated group. This reduction continued until day 15. In contrast with the untreated group, these parameters were

stable during the whole period of cultivation. Levels of alpha-glutathione S-transferases and detoxification protein increased at day 9 (3 days after APAP addition) but subsequently decreased by day 12, which was more likely due to cell death. APAP treated constructs demonstrated decreasing LDH activity, again, likely due to toxicity related cell death. Untreated conditions maintained steady LDH levels.

3.5 Nervous system models and regeneration

Collagen, as a material, is widely used in nerve regeneration^[39,40]. The neurite growth is more pronounced in collagen hydrogels, prepared using mildly concentrated collagen solutions^[41,42]. Therefore, such collagen solutions are used for 3D printing more often^[43,44] in this field of tissue engineering, whereas there are only few studies that report the use of highly concentrated collagen solution^[45].

In 2009, Lee *et al.*^[43] have proposed a direct cell printing technique to pattern neural cells in a 3D multilayered collagen hydrogel. First, they printed a layer of collagen hydrogel to create a scaffold for cells. Next, rat embryonic neurons and astrocytes were printed onto the existing layer. The process was repeated layer-by-layer to create 3D cell hydrogel composites. This study demonstrated the ability of microvalve printing to create a pattern of various cells in a single construct.

In another work^[44], microvalve printing was used to create a layered 3D neural stem cell (NSC)-laden hydrogel collagen construct. Next to collagen hydrogel, a thrombin crosslinked fibrin gel was printed. The fibrin gel acted as a depot releasing the vascular endothelial growth factor (VEGF) for 3 days. Cells in the collagen construct migrated to the VEGF-releasing fibrin gel. During the experiment, the increased proliferation and increased branched morphology with neurite projections were observed. In control samples, cells did not show any signs of proliferation or migration (where fibrin without VEGF or VEGF was printed directly into collagen).

Chen *et al.*^[45] have created 3D bioprinted collagen-heparin sulfate scaffolds. To promote axonal regeneration and functional recovery

Table 1. Collagen-based bioinks for different tissue-engineering applications.

Bioink		Cross-link	Supportive Scaffold	<i>In vitro</i> / <i>In vivo</i>	Bioprinting technology	Ref.
Materials	Cells					
Skin						
Collagen I type	HEK and HDF	pH and temperature	-	Both	Extrusion-based bioprinting	[12]
Collagen I type	NIH 3T3 and HaCaT	pH and temperature	Matriderm	<i>In vitro</i>	Laser-assisted bioprinting	[23]
Collagen I type	NIH 3T3 and HaCaT	pH and temperature	Matriderm	Both	Laser-assisted bioprinting	[24]
Collagen I type and GelMa	HEM, HaCaT, and HDF	pH and temperature	-	Both	Extrusion-based bioprinting	[25]
Collagen I type and fibrin	AFSCs and MSCs	Thrombin	-	<i>In vivo</i>	Ink-jet in situ bioprinting	[26]
Collagen I type and fibrin	dermal fibroblasts and epidermal keratinocytes	Thrombin	-	<i>In vivo</i>	Ink-jet in situ bioprinting	[27]
Bone and cartilage						
Collagen I type and β -TCP	MC3T3-E1 and hASCs	Genipin	-	<i>In vitro</i>	Extrusion-based bioprinting	[28]
Collagen I type	MC3T3-E1	Tannic acid	α -TCP/collagen	<i>In vitro</i>	Extrusion-based bioprinting	[29]
Collagen I type	fibrochondrocytes	pH and temperature	-	<i>In vitro</i>	Extrusion-based bioprinting	[20]
Collagen I type	hTMSCs	pH and temperature	PCL	Both	Extrusion-based bioprinting	[33]
Collagen I type and alginate	chondrocytes	CaCl ₂	-	<i>In vitro</i>	Extrusion-based bioprinting	[34]
Cardiovascular tissues						
Collagen I type	MSCs	pH and temperature	FRESH	<i>In vivo</i>	Extrusion-based bioprinting	[14]
Collagen I type	C2C12 and hESC-CMs	pH and temperature	FRESH	<i>In vitro</i>	Extrusion-based bioprinting	[15]
Liver tissues						
Collagen I type	MC3T3-E1	pH and temperature	PCL	<i>In vitro</i>	Extrusion-based bioprinting	[37]
Methacrylated collagen type I and hyaluronic acid	hepatocytes	UV light	-	<i>In vitro</i>	Extrusion-based bioprinting	[38]
Nervous system						
Collagen I type	neurons and astrocytes*	pH and temperature	-	<i>In vitro</i>	Microvalve printing	[43]
Collagen I type	C17.2*	pH and temperature	-	<i>In vitro</i>	Microvalve printing	[44]
Collagen I type and heparin sulfate	NSCs*	UV light	-	Both	Extrusion-based bioprinting	[45]
Cornea						
Methacrylated collagen type I and alginate	hCSKs	CaCl ₂	FRESH	<i>In vitro</i>	Extrusion-based bioprinting	[47]
Collagen I type and agarose	hCSKs	pH and temperature	-	<i>In vitro</i>	Electromagnetic microvalve bioprinting	[48]

*In this study, cells were not a part of a bioink—they were seeded onto the surface of the 3D printed scaffold. HEK: Human epidermal keratinocytes; HDF: Human dermal fibroblasts; AFSC: Amniotic fluid-derived stem cells; MSCs: Mesenchymal stromal cells; hTMSCs: Human turbinate-derived mesenchymal stromal cells; NSC: Neural stem cell; UV: Ultraviolet; α -TCP: α -tricalcium phosphate; PCL: Polycaprolactone; FRESH: Freeform reversible embedding of suspended hydrogels

from spinal cord injury, they cultivated NSC on the surface of scaffolds. Next, scaffolds were implanted into transection lesions in T10 of the spinal cord in rats. Two months after, a significant recovery of locomotor functions was observed.

3.6 Cornea

Cornea bioprinting is one of the new approaches in tissue engineering^[46]. The extracellular matrix of the native cornea consists of almost 90% of I type collagen. This is why bioinks for artificial cornea also must contain collagen. The bioprinting of cornea through the extrusion method allows controlling the thickness and geometrical properties of a printed structure. For example, Isaacson *et al.*^[47] have printed a corneal like cell-laden structure. As a bioink, they used a mixture of SA and methacrylated type I collagen with encapsulated corneal keratocytes. Cell survival in the printed structures during 7-day cultivation was at a high level. Similar results on cell survival were obtained in AG, collagen, and corneal stromal keratocytes bioinks^[48].

These studies show that it will be possible to create an artificial cornea in the future. However, *in vitro* experiments do not give sufficient information for it. For this case, more studies that imply 3D bioprinting of different versions of the artificial cornea will have to be tested *in vivo*.

4 Concluding remarks and future perspectives

For the last few years, there was significant progress in 3D bioprinting and adaptation of collagen solutions to the needs of this technology. Without any doubt, the combination of collagen-based bioink and 3D bioprinting has great potential in the manufacture of artificial organs and tissues for tissue engineering and regenerative medicine. **Table 1** provides a list of existing variants of collagen-based bioinks that could be used for such purposes. However, the development in this direction is very slow. It is mostly connected with the absence of easily-accessible collagen bioinks which would correspond to requirements of the “perfect” bioink. The applicability of collagen for

3D bioprinting depends on collagen concentration in a solution. Only high concentrations of collagen (more than 20 mg/ml) in single-component collagen bioinks allow increasing the accuracy of printing. At present, there are only a few commercially available concentrated collagen bioinks – Lifeink® (35 mg/ml, Advanced Biomatrix, USA) and Viscoll® (80 mg/ml, Imtek, Russia). One of the distinctive characteristics of these bioinks is the possibility to add not only cells but also any components of the extracellular matrix to their composition. This allows to bioprint an artificial cell-laden matrix, which can be required by a researcher to solve a specific problem.

Despite the absence of sufficient data on the behavior of mammalian cells in dense collagen hydrogels, a large number of scientists are concerned that cells will inevitably collapse in dense collagen hydrogels during cultivation. However, primary tests^[17] have debunked those concerns. It was found that fibroblasts retain their high viability in high-density collagen gels (up to 40 mg/ml). These results lead the way to some new studies devoted to the behavior of cells in high-density collagen hydrogels, their proliferation and migration activity, differentiation, functionality retention, as well as the creation of various scaffolds using 3D printing technology with their subsequent colonization with cells in various fields of tissue engineering.

Acknowledgments

This work was funded by the Foundation for Assistance to Small Innovative Enterprises (FASIE), Project no. 44700.

Conflicts of interest

The authors declare that they have no conflicts of interest.

References

1. Xia Z, Jin S, Ye K, 2018, Tissue and organ 3D bioprinting. *SLAS Technol*, 23:301–314. DOI: 10.1177/2472630318760515.
2. Nagarajan N, Dupret-Bories A, Karabulut E, *et al.*, 2018, Enabling personalized implant and controllable biosystem development through 3D printing. *Biotechnol Adv*, 36:521–

533. DOI: 10.1016/j.biotechadv.2018.02.004.
3. Hospodiuk M, Dey M, Sosnoski D, *et al.*, 2017, The bioink: A comprehensive review on bioprintable materials. *Biotechnol Adv*, 35:217-239. DOI: 10.1016/j.biotechadv.2016.12.006.
 4. Kloxin AM, Kloxin CJ, Bowman CN, *et al.*, 2010, Mechanical properties of cellularly responsive hydrogels and their experimental determination. *Adv Mater*, 22:3484–94. DOI: 10.1002/adma.200904179.
 5. Antoine EE, Vlachos PP, Rylander MN, 2014, Review of collagen I hydrogels for bioengineered tissue microenvironments: Characterization of mechanics, structure, and transport. *Tissue Eng Part B Rev*, 20:683–96. DOI: 10.1089/ten.teb.2014.0086.
 6. Lynn AK, Yannas IV, Bonfield W, 2004, Antigenicity and immunogenicity of collagen. *J Biomed Mater Res B App Biomater*, 71:343–54. DOI: 10.1002/jbm.b.30096.
 7. Parenteau-Bareil R, Gauvin R, Berthod F, 2010, Collagen-based biomaterials for tissue engineering applications. *Materials (Basel)*, 3:1863–87. DOI: 10.3390/ma3031863.
 8. Sriya Y, Shibu C, Ashis KB, *et al.*, 2019, Tissue-Specific Bioink from Xenogeneic Sources for 3D Bioprinting of Tissue Constructs, in *Xenotransplantation-comprehensive Study*, Shuji Miyagawa, IntechOpen, Available from: <https://www.intechopen.com/books/xenotransplantation-comprehensive-study/tissue-specific-bioink-from-xenogeneic-sources-for-3d-bioprinting-of-tissue-constructs>. DOI: 10.5772/intechopen.89695.
 9. Gelse K, Pöschl E, Aigner T, 2003, Collagens--structure, function, and biosynthesis. *Adv Drug Deliv Rev*, 55:1531–46. DOI: 10.1016/j.addr.2003.08.002.
 10. Ricard-Blum S, 2011, The collagen family. *Cold Spring Harb Perspect Biol*, 3:a004978. DOI: 10.1101/cshperspect.a004978.
 11. Włodarczyk-Biegun MK, Del Campo A, 2017, 3D bioprinting of structural proteins. *Biomaterials*, 134:180–201. DOI: 10.1016/j.biomaterials.2017.04.019.
 12. Yoon H, Lee JS, Yim H, *et al.*, 2016, Development of cell-laden 3D scaffolds for efficient engineered skin substitutes by collagen gelation. *RSC Adv*, 6:21439–47. DOI: 10.1039/c5ra19532b.
 13. Hinton TJ, Jallerat Q, Palchesko RN, *et al.*, 2015, Three-dimensional printing of complex biological structures by freeform reversible embedding of suspended hydrogels. *Sci Adv*, 1:e1500758. DOI: 10.1126/sciadv.1500758.
 14. Maxson EL, Young MD, Noble C, *et al.*, 2019, *In vivo* remodeling of a 3D-bioprinted tissue engineered heart valve scaffold. *Bioprinting*, 16:e00059. DOI: 10.1016/j.bprint.2019.e00059.
 15. Lee A, Hudson AR, Shiwardski DJ, *et al.*, 2019, 3D bioprinting of collagen to rebuild components of the human heart. *Science*, 365:482–87. DOI: 10.1126/science.aav9051.
 16. Diamantides N, Wang L, Pruiksma T, *et al.*, 2017, Correlating rheological properties and printability of collagen bioinks: The effects of riboflavin photocrosslinking and pH. *Biofabrication*, 9:034102. DOI: 10.1088/1758-5090/aa780f.
 17. Osidak EO, Karalkin PA, Osidak MS, *et al.*, 2019, Viscoll collagen solution as a novel bioink for direct 3D bioprinting. *J Mater Sci Mater Med*, 30:31. DOI: 10.1007/s10856-019-6233-y.
 18. Lian D, Jiheng L, Conghu L, *et al.*, 2013, Effects of NaCl on the rheological behavior of collagen solution, *Korea-Aust Rheol J*, 25:137–144. DOI: 10.1007/s13367-013-0014-9.
 19. Lai G, Li Y, Li G, 2008, Effect of concentration and temperature on the rheological behavior of collagen solution. *Int J Biol Macromol*, 42:285–91.
 20. Rhee S, Putzer JL, Mason BN, *et al.*, 2016, 3D Bioprinting of spatially heterogeneous collagen constructs for cartilage tissue engineering. *ACS Biomater Sci Eng*, 2:1800–1805. DOI: 10.1021/acsbiomaterials.6b00288.
 21. Lee H, Yang GH, Kim M, *et al.*, 2018, Fabrication of micro/nanoporous collagen/dECM/silk-fibroin biocomposite scaffolds using a low temperature 3D printing process for bone tissue regeneration. *Mater Sci Eng C Mater Biol Appl*, 84:140-147. DOI: 10.1016/j.msec.2017.11.013.
 22. Moncal KK, Ozbolat V, Datta P, *et al.*, 2019, Thermally-controlled extrusion-based bioprinting of collagen. *J Mater Sci: Mater Med*, 30:55. DOI: 10.1007/s10856-019-6258-2.
 23. Koch L, Deiwick A, Schlie S, *et al.*, 2012, Skin tissue generation by laser cell printing. *Biotechnol Bioeng*, 109:1855–63.
 24. Michael S, Sorg H, Peck CT, *et al.*, 2013, Tissue engineered skin substitutes created by laser-assisted bioprinting form skin-like structures in the dorsal skin fold chamber in mice. *PLoS One*, 8:e57741. DOI: 10.1371/journal.pone.0057741.
 25. Shi Y, Xing TL, Zhang HB, *et al.*, 2018, Tyrosinase-doped bioink for 3D bioprinting of living skin constructs. *Biomed Mater*, 13:035008. DOI: 10.1088/1748-605x/aaa5b6.
 26. Skardal A, Mack D, Kapetanovic E, *et al.*, 2012, Bioprinted amniotic fluid-derived stem cells accelerate healing of large skin wounds. *Stem Cells Transl Med*, 11:792–802. DOI: 10.5966/sctm.2012-0088.
 27. Albanna M, Binder KW, Murphy SV, *et al.*, 2019, *In Situ* bioprinting of autologous skin cells accelerates wound healing of extensive excisional full-thickness wounds. *Sci*

- Rep*, 9:1856. DOI: 10.1038/s41598-018-38366-w.
28. Kim W, Kim G, 2019, Collagen/bioceramic-based composite bioink to fabricate a porous 3D hASCs-laden structure for bone tissue regeneration. *Biofabrication*, 12:015007. DOI: 10.1088/1758-5090/ab436d.
 29. Kim WJ, Yun HS, Kim GH, 2017, An innovative cell-laden α -TCP/collagen scaffold fabricated using a two-step printing process for potential application in regenerating hard tissues. *Sci Rep*, 7:3181. DOI: 10.1038/s41598-017-03455-9.
 30. Lin KF, He S, Song Y, *et al.*, 2016, Low-temperature additive manufacturing of biomimic three-dimensional hydroxyapatite/collagen scaffolds for bone regeneration. *ACS Appl Mater Interfaces*, 8:6905–16.
 31. Marques CF, Diogo GS, Pina S, *et al.*, 2019, Collagen-based bioinks for hard tissue engineering applications: A comprehensive review. *J Mater Sci Mater Med*, 30:32. DOI: 10.1007/s10856-019-6234-x.
 32. Mishra R, Basu B, Kumar A, 2019, Physical and cytocompatibility properties of bioactive glass-polyvinyl alcohol-sodium alginate biocomposite foams prepared via sol-gel processing for trabecular bone regeneration. *J Mater Sci: Mater Med*, 20:2493–500. DOI: 10.1007/s10856-009-3814-1.
 33. Shim JH, Jang KM, Hahn SK, *et al.*, 2016, Three-dimensional bioprinting of multilayered constructs containing human mesenchymal stromal cells for osteochondral tissue regeneration in the rabbit knee joint. *Biofabrication*, 8:014102. DOI: 10.1088/1758-5090/8/1/014102.
 34. Yang X, Lu Z, Wu H, *et al.*, 2018, Collagen-alginate as bioink for three-dimensional (3D) cell printing based cartilage tissue engineering. *Mater Sci Eng C Mater Biol Appl*, 83:195–201. DOI: 10.1016/j.msec.2017.09.002.
 35. Cui H, Miao S, Esworthy T, *et al.*, 2018, 3D bioprinting for cardiovascular regeneration and pharmacology. *Adv Drug Del Rev*, 132:252–269.
 36. Lewis PL, Shah RN, 2016, 3D Printing for liver tissue engineering: Current approaches and future challenges. *Curr Transpl Rep*, 3:100–108. DOI: 10.1007/s40472-016-0084-y.
 37. Shim JH, Kim JY, Park M, *et al.*, 2011, Development of a hybrid scaffold with synthetic biomaterials and hydrogel using solid freeform fabrication technology. *Biofabrication*, 3:034102. DOI: 10.1088/1758-5082/3/3/034102.
 38. Mazzocchi A, Devarasetty M, Huntwork R, *et al.*, 2018, Optimization of collagen Type I-hyaluronan hybrid bioink for 3D bioprinted liver microenvironments. *Biofabrication*, 11:015003. DOI: 10.1088/1758-5090/aae543.
 39. Klein S, Vykoukal J, Felthaus O, *et al.*, 2016, Collagen Type I conduits for the regeneration of nerve defects. *Materials (Basel)*, 9:219. DOI: 10.3390/ma9040219.
 40. Madduri S, Feldman K, Tervoort T, *et al.*, 2010, Collagen nerve conduits releasing the neurotrophic factors GDNF and NGF. *J Control Release*, 143:168–74. DOI: 10.1016/j.jconrel.2009.12.017.
 41. O'Connor SM, Stenger DA, Shaffer KM, *et al.*, 2000, Primary neural precursor cell expansion, differentiation and cytosolic Ca(2+) response in three-dimensional collagen gel. *J Neurosci Methods*, 102:187–95. DOI: 10.1016/s0165-0270(00)00303-4.
 42. Labour MN, Vigier S, Lerner D, *et al.*, 2016, 3D compartmented model to study the neurite-related toxicity of A β aggregates included in collagen gels of adaptable porosity. *Acta Biomater*, 37:38–49. DOI: 10.1016/j.actbio.2016.04.001.
 43. Lee W, Pinckney J, Lee V, *et al.*, 2009, Three-dimensional bioprinting of rat embryonic neural cells. *Neuroreport*, 20:798–803. <https://doi.org/10.1097/wnr.0b013e32832b8be4>.
 44. Lee YB, Polio S, Lee W, *et al.*, 2010, Bio-printing of collagen and VEGF-releasing fibrin gel scaffolds for neural stem cell culture. *Exp Neurol*, 223:645–52. DOI: 10.1016/j.expneurol.2010.02.014.
 45. Chen C, Zhao ML, Zhang RK, *et al.*, 2017, Collagen/heparin sulfate scaffolds fabricated by a 3D bioprinter improved mechanical properties and neurological function after spinal cord injury in rats. *J Biomed Mater Res A*, 105:1324–32. DOI: 10.1002/jbm.a.36011.
 46. Zhang B, Xue Q, Li J, *et al.*, 2019, 3D bioprinting for artificial cornea: Challenges and perspectives. *Med Eng Phys*, 71:68–78.
 47. Isaacson A, Swioklo S, Connon CJ, 2018, 3D bioprinting of a corneal stroma equivalent. *Exp Eye Res*, 173:188–193. DOI: 10.1016/j.exer.2018.05.010.
 48. Campos DD, Rohde M, Ross M, *et al.*, 2019, Corneal bioprinting utilizing collagen-based bioinks and primary human keratocytes. *J Biomed Mater Res Part A*, 107:1945–53. DOI: 10.1002/jbm.a.36702.

Fibrin-based Bioinks: New Tricks from an Old Dog

Anastasia Shpichka^{1,2*}, Daria Osipova¹, Yuri Efremov¹, Polina Bikmulina¹,
Nastasia Kosheleva^{3,4}, Marina Lipina⁵, Evgeny A. Bezrukov⁶, Roman
B. Sukhanov⁶, Anna B. Solovieva⁷, Massoud Vosough⁸, Peter Timashev^{1,2,7,9}

¹Department of Advanced Biomaterials, Institute for Regenerative Medicine, Sechenov First Moscow State Medical University, Moscow, Russia

²Department of Chemistry, Lomonosov Moscow State University, Moscow, Russia

³Department of Molecular and Cell Pathophysiology, FSBSI Institute of General Pathology and Pathophysiology, Moscow, Russia

⁴Department of Embryology, Lomonosov Moscow State University, Faculty of Biology, Moscow, Russia

⁵Department of Traumatology, Orthopedics and Disaster Surgery, Sechenov First Moscow State Medical University, Moscow, Russia

⁶Department of Urology, Sechenov First Moscow State Medical University, Moscow, Russia

⁷Department of Polymers and Composites, NN Semenov Institute of Chemical Physics, Moscow, Russia

⁸Department of Regenerative Medicine, Cell Science Research Centre, Royan Institute for Stem Cell Biology and Technology, ACECR, Tehran, Iran

⁹Institute of Photon Technologies, Federal Research Center Crystallography and Photonics RAS, Moscow, Russia

Abstract: For the past 10 years, the main efforts of most bioprinting research teams have focused on creating new bioink formulations, rather than inventing new printing set-up concepts. New tissue-specific bioinks with good printability, shape fidelity, and biocompatibility are based on “old” (well-known) biomaterials, particularly fibrin. While the interest in fibrin-based bioinks is constantly growing, it is essential to provide a framework of material’s properties and trends. This review aims to describe the fibrin properties and application in three-dimensional bioprinting and provide a view on further development of fibrin-based bioinks.

Keywords: Fibrin, Bioink, Tissue engineering, Regenerative medicine, Bioprinting, Biofabrication

*Corresponding Author: Anastasia Shpichka, Department of Advanced Biomaterials, Institute for Regenerative Medicine, Sechenov First Moscow State Medical University, Moscow, Russia; ana-shpichka@yandex.ru

Received: February 28, 2020; **Accepted:** March 15, 2020; **Published Online:** April 29, 2020

(This article belongs to the *Special Section: Bioprinting in Russia*)

Citation: Shpichka A, Osipova D, Efremov Y, *et al.*, 2020, Fibrin-based Bioinks: New Tricks from an Old Dog. *Int J Bioprint*, 6(3): 269. Doi: 10.18063/ijb.v6i3.269.

1 Introduction

Tissue engineering, particularly three-dimensional (3D) bioprinting, is one of the most rapidly developing fields in biomedicine. As any cutting-edge technology, 3D bioprinting requires both complex equipment and novel materials. Hence, its development can be divided into at least two steps: Technical and material.

To date, the technical step has almost passed, and the main approaches in printing set-ups have been already presented and are based on extrusion, droplet deposition, stereolithography, and laser-induced forward transfer^[1-4]. However, the material step involving bioinks is in progress.

Bioinks consisting of cells (or spheroids) and biomaterials are an essential element of 3D

bioprinting, and their development should ensure both precise deposition and tissue specificity. For the last decade, there is a bioink boom, and the efforts of many research teams focus on not inventing new set-ups, but creating new bioink formulations. New tissue-specific bioinks with good printability, shape fidelity, and biocompatibility can be based on “old” biomaterials. Among their huge variety, fibrin is of particular interest.

Despite its long history of use, fibrin is still highly in demand that is ensured by its unique properties. Except its biocompatibility, it is biodegradable, and the degradation products are not toxic. Moreover, compared to other biomaterials, fibrin properties (fiber morphology, stability, mechanics, etc.) can be simply tuned by varying component concentrations, buffers, etc.^[5-9] While the interest in fibrin-based bioinks is constantly growing, it is essential to provide a framework of material properties and trends. This review focuses on describing the fibrin properties and application in 3D bioprinting and providing a view on further development of fibrin-based bioinks.

2 Fibrin overview

2.1 Classification and structure

Fibrin is a fibrillar protein formed from fibrinogen circulating in blood. It may have different origin and can be derived from salmon, bovine, porcine, and human blood plasma. Fibrinogen is an elongated dimeric glycoprotein (inactive fibrin monomer) which consists of two-dimensional domains bound by a coiled-coil segment to the central E domain. The fibrinogen molecule is formed by three polypeptide chains $A\alpha$, $B\beta$, and γ connected to each other in the N-terminal E domain by disulfide bridges^[10,11]. It is synthesized by hepatocytes^[12] that makes the liver to be the main source of fibrinogen. Fibrinogen is mostly distributed in circulating blood plasma; however, it can also be found in platelets, lymph, and interstitial fluid. Fibrinogen synthesis can be stimulated by injury and/or inflammation which causes a ten-fold increase in concentration^[7]. Such activation is induced by interleukin-6 (IL-6) which triggers intercellular signaling pathways

in hepatocytes and modulates gene expression through various transcription factors^[13].

2.2 Fibrinogenesis

Fibrin formation from fibrinogen is one of the essential steps in the enzymatic cascade of blood coagulation pathway to stop bleeding. This process can be divided into two stages: Enzymatic and non-enzymatic. In the first stage, thrombin (Factor II) induces proteolytic cleavage and fibrinopeptide release from $A\alpha$ and $B\beta$ chains. Hence, two polymerization regions, α and β , are formed and spontaneously interact with complementary polymerization centers a- and b- in γC and βC regions on the D knot of another fibrin monomer. This leads to the gradual formation of protofibrils. Protofibrils' aggregation in lateral and longitudinal directions ensures the formation of fibers, which branch and form a fibrin network providing structural stability^[12,14]. Transglutaminase (Factor XIIIa) stabilizes this fibrillar network.

2.3 Fibrinolysis

Fibrinolysis is controlled by various cofactors, inhibitors, and receptors^[15]. The main enzyme which lyses fibrin to fragments known as D-dimers is plasmin activated by plasminogen^[16]. Plasminogen is a physiological substrate for two serine proteases, tissue-type plasminogen activator (tPA) and urokinase-type plasminogen activator (uPA). The first one is synthesized and released by endothelial cells; the second one by monocytes, macrophages, and urothelial cells^[17]. Both activators have a short half-life period (4 – 8 min) because of high concentrations of inhibitors (e.g. plasminogen activator inhibitor-1 (PAI-1)) in blood plasma. Compared to tPA, uPA has low affinity to plasminogen and does not require fibrin as a cofactor; normally, it functions in extravascular regions^[17]. Both tPA and uPA are eliminated by the liver after the formation of a complex with low density lipoprotein (LDL)-receptor-like protein^[18]. Moreover, fibrin can be easily lysed by other proteolytic enzymes, for example, proteinase K, collagenase, trypsin, accutase, and metalloproteinases.

2.4 Mechanical properties

Pure fibrinogen solutions show a nonlinear increase in viscosity with increasing concentration, with the values ranging from ones to hundreds of cP^[19]. Moreover, the concentration of the fibrinogen in blood plasma correlates with plasma viscosity^[20]. The drastic changes in mechanical properties occur with the onset of the fibrin clot formation (gelation), which could be traced by a change of turbidity^[21] and an increase in the elastic or shear modulus in rheological measurements^[22-24]. *In vitro*, gelation time which can take from several seconds to several minutes is mostly controlled by the concentration of thrombin and temperature^[21,25].

The resulted fibrin gel has a set of remarkable and unique viscoelastic properties among polymers which are related to its molecular structure with complex multi-scale hierarchy^[7]. Fibrin fibers might constitute <1% of the gel volume, yet it will have measurable elastic modulus and strength. The gel also has a high water-uptake ratio of 30 – 50^[21]. The fibrin fibers of the gel can have different length, thickness, and density and type of branching points, which generally made up of three fibers at a junction^[17,23]. These parameters are strongly

dependent on the polymerization conditions, including a concentration of fibrinogen, thrombin, additional factors such as Factor XIII and CaCl₂, and physical factors such as temperature and external tension or compression forces. Several models for fibrin mechanics have been suggested that take into account its filamentous nature and interactions between the fibers at different hierarchy levels^[7,8,17].

The storage modulus of the gel only weakly depends on frequency, while the loss modulus increases with frequency^[23]. Thus, at low frequencies (<10 – 100 Hz), the behavior is mostly elastic and could be efficiently characterized by elastic modulus only, but the viscous component is pronounced at high frequencies. The shear and elastic moduli show non-linear behavior with relation to strains, the so-called strain hardening or stiffening^[23]. Shear modulus increases up to a factor of twenty-fold at large strains^[18]. The elastic modulus initially decreases (up to strain = 0.5), but then dramatically increases by a factor of 100 (compressive strains >0.8)^[26]. Strain hardening might be of biological importance since it allows fibrin clots to sustain larger deformations without significant integrity loss.

Table 1. Mechanical properties of pure fibrinogen and fibrin.

Components concentrations					Viscosity (cP)	E(Pa)	G' (Pa)	Comments	Ref
Fibrin (mg/ml)	Thrombin (U/ml)	Ca+ (mM)	Factor XIII (µg/ml)	Buffer					
10–150	–	–	–	PBS	2–43	n/a	n/a	–	[19]
25	100	–	–	PBS	n/a	580-640	–	–	[27]
1, 2, 4, 8	0.1–6.4	–	–	–	n/a	n/a	3.1-247.5	–	[28]
6, 7, 8, 9	–	–	–	–	n/a	n/a	4-147	PEGylated fibrinogen, polymerized by photo-initiator using a UV light	[29]
2–50	2–100	40	–	–	n/a	0.058–4000	n/a	–	[39]
2	1	2	0–20	HEPES 23 mM NaCl 175 mM pH 7.4	n/a	n/a	33-150	–	[6]

Ref.: References; E: Young's modulus; n/a: Not available; PBS: Phosphate buffer saline; HEPES: 4-(2-hydroxyethyl)-1-piperazineethanesulfonic acid

The main parameter that controls the gel stiffness appears to be fibrinogen concentration. By varying it in a range from 1 to 50 mg/mL, the elastic modulus of the resulted gel from several Pa to several hundred Pa might be achieved^[27-29]. Another important modulator is Factor XIII, its addition substantially increases the elastic modulus of the gel by incorporating fibrin covalent crosslinking and compacting fibers^[6]. The cell embedded into the gel might also induce its stiffening through myosin-driven cell contraction^[30].

The low viscosity of pure fibrinogen solution makes it suitable for inkjet bioprinting methods^[31]. However, shape fidelity and mechanical properties of such gels are relatively poor. Due to irreversible and fast fibrin gelation at physiological temperatures, bioprinting with fibrinogen/thrombin mixture might be performed at low temperatures, or thrombin can be added to the construct after bioprinting^[32]. The gelated fibrin cannot be printed with standard extrusion-based techniques without damaging its structure. To improve or modify the mechanical properties of the gel construct, the composite bioinks of fibrin with other components were used. Combinations with gelatin^[33], alginate^[34], collagen^[35], hyaluronic acid^[36], or more complex formulations^[37] were used for different applications. Some biochemical modifications were also introduced to the fibrinogen to modulate the structural and mechanical properties of the gel^[27,29,38].

3 Biological properties and their tuning

3.1 Wound healing

The formation of fibrin which is known as fibrinogenesis is associated with hemostasis, one of the main stages in wound healing. By forming an interconnected porous network, fibrin fibers act as a temporary scaffold for migrating and proliferating cells. Fibrin provides an angiogenic environment that enables the growth of capillaries' sprouts. Together with fibroblasts and macrophages, they form the mature granulation tissue, essential for the following re-epithelialization. Hence, its angiogenic (will be discussed in the next section) and healing

potential are physiologically determined, and it is not surprising that fibrin is widely applied in vascular tissue engineering and improvement of wound healing.

Due to its tunable properties that can guide cells and determine substance release kinetics, fibrin is commonly used in skin equivalent design or cell/bioactive substance delivery for the defect site treatment^[40]. Even only by adjusting, for example, its mechanical properties, one can tailor its biological properties. For instance, Murphy *et al.*^[41] varied the component concentrations to reveal their correlation with gel stiffness, degradation rate, and vascular endothelial growth factor (VEGF), and prostaglandin (PGE2) secretion by encapsulated mesenchymal stromal cell (MSC) spheroids. They showed that the secretion of both factors was the highest in hydrogels with medium values of compressive and storage moduli.

To improve its innate healing potential, fibrin can be combined with cells, functionalized particles, or bioactive compounds (**Table 2**). In the first case, various cell types, for example, keratinocytes^[42], fibroblasts^[43], bone-marrow derived,^[44] and adipose-derived^[45] MSC, have already been tested. In the second case, for instance, platelet-like particles prepared from functionalized ultralow crosslinked poly (N-isopropylacrylamide-co-acrylic acid) microgels were offered to improve wound healing. In the third case, growth factors are usually applied, which can be physically entrapped within a fibrin mesh or affinely or covalently bonded. For instance, fibrin can be mixed with growth factor-loaded nanoparticles that promoted wound healing. Losi *et al.*^[46] tested poly(lactic-co-glycolic acid) (PLGA) nanoparticles loaded with VEGF and bFGF and showed that they can significantly promote wound closure and facilitate the re-epithelialization and granulation tissue formation. Growth factors can be linked to fibrin, for example, by transglutaminase-assisted binding of their recombinant modifications that ensures their prolonged release. Mittermayr *et al.*^[47] showed the efficacy of such approach. In their study, they achieved a controllable release of platelet-derived growth factor AB (PDGF-AB) from fibrin that enabled the acceleration and

Table 2. Possible fibrin modifications to tune its biological properties.

Modifying agent	Type of IM	Type of experiments	Outcomes	Ref.
PLGA nanoparticles loaded with VEGF and bFGF	Physical	<i>In vivo</i> (diabetic mice)	Promoted wound closure Accelerated re-epithelialization Increased formation of granulation tissue Enhanced collagen synthesis	[46]
Platelet-like particles	Physical	<i>In vitro</i> <i>In vivo</i> (mice)	Promoted cell migration Improved wound healing	[55]
TG-PDGF.AB	Covalent	<i>In vivo</i> (pigs)	Enhanced wound healing	[47]
KGF	Covalent	<i>In vitro</i> <i>In vivo</i> (mice)	Increased cell migration Improved wound healing	[48]
RGD, IKVAV, YIGSR, and RNIAEIIKDI	Cocrosslinking	<i>In vitro</i> (dorsal root ganglia dissected from chicken embryos) <i>In vivo</i> (rats)	Enhanced neurite outgrowth Improved axons regeneration	[56]
Bifunctional carboxylated N-hydroxysulfosuccinimide-active ester PEG	Covalent	<i>In vitro</i> <i>In vivo</i> (nude mice)	Maintained cell proliferation Increased ALP activity Up-regulated osteoblast-specific genes Formation of soft vascularized connective tissue	[57]
O,O'-bis[2-(N-succinimidylsuccinylamino)ethyl]PEG	Covalent	<i>In vitro</i> (MSC spheroids)	Promoted better sprouting	[58]
TG-VEGF121	Covalent	<i>In vivo</i> (VEGFR2-luc mice)	Enhanced vessel formation SMC stabilization	[59]
Fusion proteins LN-TGF- β 1 and LNG-TGF- β 1	Covalent	<i>In vitro</i>	Enhanced contractile function of vascular constructs	[60]
T1 peptide sequence from CCN1	Covalent	<i>In vitro</i> <i>In vivo</i> (CAM)	Improved cellular sprouting without adding VEGF Increased effects when VEGF is added Stimulated formation of new vessels	[61]
Anti-VEGF aptamer and anti-PDGF-BB aptamer	Covalent Affinity	<i>In vivo</i> (mice)	Enhanced blood vessel growth	[62]
TG-PDGF.AB	Covalent	<i>In vivo</i> (rats)	Decreased flap tissue necrosis Enhanced perfusion Maturation of new vessels	[63]
Vector containing the VEGF-A cDNA	Physical	<i>In vivo</i> (rats)	Prolonged flap survival for 7 days after surgery Increased perfusion of tissues Higher VEGF-A expression	[64]

Abbreviations. Ref: References; ALP: Alkaline phosphatase activity; bFGF: Basic fibroblast growth factor; CAM: Chorioallantoic membrane; IM: Immobilization; KGF: Keratinocyte growth factor; MSC: Mesenchymal stromal cells; PDGF: Platelet-derived growth factor; PEG: Polyethylene glycol; PLGA: Poly(lactic-co-glycolic acid); SMC: Smooth muscle cells; TG: Transglutaminase; TGF- β : Transforming growth factor beta; VEGF: Vascular endothelial growth factor

improvement of wound healing in severe burns^[47]. Muhamed *et al.*^[48] fabricated fibrin nanoparticles, which were modified with keratinocyte growth factor (KGF) by its coupling using carbodiimide derivative and N-hydroxysulfosuccinimide. These particles had higher healing potential than those from non-loaded ones.

Except pure fibrin and the mentioned above modifications, there is also platelet-rich fibrin (PRF) that is so-called the “second-generation platelet concentrate”^[49]. This review does not go into details regarding this type of fibrin-based products. The reader can learn more about it from the following publications^[49-54].

3.2 Angiogenesis

As mentioned above, fibrin has intrinsic angiogenic properties and provides relevant microenvironment determined by structure-dependent chemical, physical, and biochemical cues. Its fibrillar structure serves as a scaffold for invading cells which bind to its fibers through cellular receptors and form capillaries. It was showed that the fiber network morphology can be significantly influenced by fibrinogen and thrombin concentrations^[65-67], pH^[68], buffers^[5], incorporation of extra molecules^[27], etc.

On invading cells, receptors bind to specific sites on fibrin fibers that not only ensures cell adhesion but also triggers various intracellular pathways due to their biochemical interaction and formed tensional forces. Such cues determine position-assisted cell response to the external stimulation by cytokines and growth factors. The cell adhesion to fibrin is mainly ensured by two arginylglycylaspartic acid (RGD) sites located on the α -chain through integrins ($\alpha v\beta 3$, $\alpha 5\beta 1$, etc.). Integrin $\alpha v\beta 3$ and integrin $\alpha 5\beta 1$ were proven to control vacuolation and lumen formation by endothelial cells^[69]. Interestingly, the insertion of additional selective binding sites for $\alpha v\beta 3$ integrin (the sixth immunoglobulin-like (Ig-like) domain of the cell adhesion molecule L1 (L1Ig6)) provided the increase in vessel formation by them^[68]. Except RGD sites, endothelial cells interact with $\beta 15-42$ sequence of fibrin where VE-cadherin serves as a specific cell receptor^[70]. The adhesion of MSC used to stabilize the newly forming vessels and induce their formation is ensured through the interaction with another type of integrins – $\alpha 6\beta 1$ – to fibrin fibers^[71].

However, in angiogenesis, fibrin is not a stable scaffold for migrating cells; it is a highly responsive system that remodels providing the required environment for forming vessels. Its degradation and remodeling are critical in the new vessel formation and mainly orchestrated by matrix metalloproteinases (MMP), including membrane-type MMP (MT-MMP). When cells migrate within a fibrin network, they degrade it facilitating their invasion and making space for lumenogenesis

that causes the heterogeneity in local ECM stiffness and changes in its bulk structure^[72]. Among the MMP variety, the MMP2, MMP9, and MT1-MMP are considered to play the most important role. In endothelial cells, VEGF, well-known angiogenic factor, is proven to induce the MMP9 and MT1-MMP expression through Notch signaling that regulates cell morphogenesis^[73]. It was observed that initial stages of capillarogenesis by endothelial cells corresponds with the rise of proenzyme proMMP-2 and drop of proMMP-9; however, MMP-2 was not revealed and MMP-9 was low^[74]. MT1-MMP was proven to regulate vessel formation by both EC and MSC and more strongly affected it than MMP-2 and MMP-9^[75,76]. Interestingly, compared to fibroblast-assisted one, MSC-induced vessel formation is totally controlled by MT-MMP^[77]. Hence, by tuning fibrin gel properties through its modification that changes its mechanical properties and degradability the tissue engineers can significantly influence angiogenesis *in vitro*^[78]. Moreover, fibrin ensures the synthesis of extracellular matrix (ECM) proteins such as laminin, and collagen type IV^[66,79,80] that stabilizes the formed microvasculature.

Angiogenesis can be also promoted by fibrin degradation products. It was showed that fibrin fragment E undergone thrombin-assisted proteolytic cleavage led to the increase in the endothelial cell proliferation, migration and differentiation *in vitro*^[81] and in the vessel number while applied on the chorioallantoic membrane (CAM) model^[82].

To increase its angiogenic properties, several structural modifications which can be divided into two main groups: Inert or active substance loading/binding were offered. For instance, it was showed that the PEGylation of fibrin can ensure the enhanced endothelial and mesenchymal stromal cells' migration and spreading followed with the formation of cell extensions and intercellular junctions and expression of specific MMP^[66,79]. Moreover, compared to the native fibrin gel, the PEGylated fibrin promoted the increased growth rate, branching, and length of tubules formed by encapsulated spheroids from adipose-derived MSC^[58] (**Figure 1**). However, the most trivial

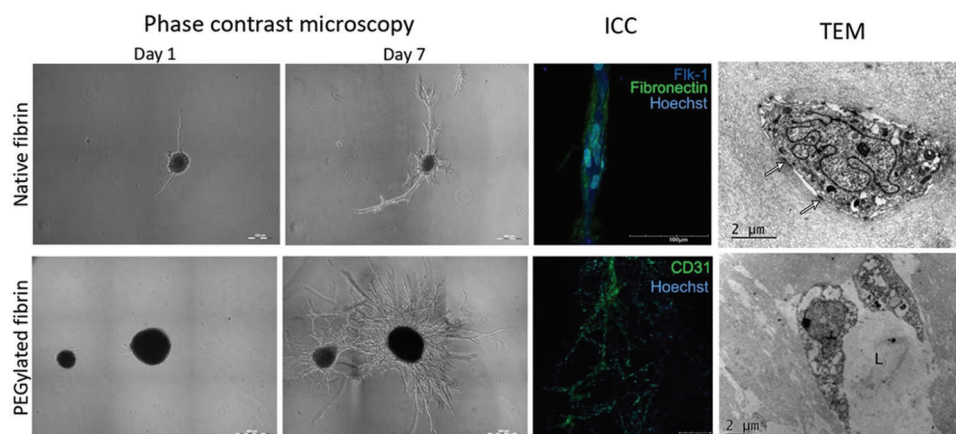


Figure 1. Tubulogenesis within native and PEGylated fibrin gels ICC – immunocytochemical staining; L – lumen; TEM – transmission electron microscopy. Copyright permission provided by IOP Publishing^[58].

approach to improve fibrin angiogenic properties is to use single or multiple pro-angiogenic factors such as VEGF or bFGF. They can be entrapped within a fiber network or immobilized using release systems (e.g. nanoparticles) or through affinity or covalent binding (**Table 2**). Moreover, the binding of some peptides such as RGD, LN-TGF- β 1, or T1 peptide sequence from CCN1 can significantly promote vessel formation. The efficiency of plasmids delivered by fibrin to improve angiogenesis is questionable and requires further investigation. On the one hand, Michlits *et al.*^[64] showed that VEGF plasmid-laden fibrin gel increased skin flap survival. On the other hand, Jozkowitz *et al.*^[83] revealed that all carrier types used for the VEGF plasmid delivery (water, phosphate buffer saline, and fibrin glue) stimulated similar effects on capillaries growth.

3.3 Application

Fibrin is a commonly used biomaterial and widely applied in medicine from the 70 to 80s as a surgical sealant (fibrin glue). Due to its flexible properties, fibrin has become a versatile tool in engineering of various tissues, for example, skin, blood vessels, and bone.^[84-86] Fibrin and its blends with other biomaterials, such as collagen, alginate, and hyaluronic acid, are applied in both scaffold and scaffold-free technologies.

Since the advent of bioprinting and its influence started to take hold of the field of tissue engineering, fibrin (fibrinogen) has become a biomaterial

of choice due to its good biocompatibility, biodegradability, and other described biological properties in **Table 3**. The experience gained in cell encapsulation was transferred and adapted to bioprinting.

Fibrin-based bioinks were successfully applied to print skin, heart, and neural constructs. Particularly, Cubo *et al.*^[87] fabricated a bioprinted skin substitute from plasma-derived fibrin and primary fibroblasts and keratinocytes that were tested *in vivo* and showed to be similar to the native skin. Fibrin-collagen bioinks provided favorable environment for cells bioprinted using a mobile skin bioprinting system.^[88] Hence, the *in situ* fabricated constructs accelerated wound closure and re-epithelialization. Moreover, Kumar *et al.*^[89] revealed that cardiomyocytes printed using a fibrin-based bioink not only were viable and proliferating but also expressed a specific cardiac marker and coupled with cardiac fibroblasts. Wang *et al.*^[90] also successfully applied a fibrin-based bioink to fabricate functional cardiac tissue constructs that contracted synchronously and responded to epinephrine and carbachol. Being the same complex as cardiac one, neural tissue was achieved using fibrin which structure ensured cell alignment and guided Schwann cells' growth.

Bioprinting tumors is a novel interesting direction in not only fibrin application but also in bioprinting in general.^[91] The fabricated tumor models are positioned mostly to be used as a more relevant platform for drug screening and

Table 3. Bioprinting with fibrin-based bioinks.

Components			Bioprinting	Origin	Cells	Outcomes	Ref
Fibrinogen	Cross-linking agents	Additives					
60 mg/ml	Thrombin 50 U/ml CaCl ₂ 80 mM	Furfuril-gelatin 155 mg/ml RB	Extrusion-based	n/a	iPSC-derived cardiomyocytes	Printed structures were porous and showed good stability Cells remained viable, proliferated, and expressed cardiac marker (troponin I)	[89]
30 mg/ml	Thrombin n/a	Gelatin 35 mg/ml Hyaluronic acid 3 mg/ml	Extrusion-based	n/a	bladder urothelial cells, bladder smooth muscle cells	Cells maintained high viability for a week after printing, actively proliferated and expressed specific biomarkers	[94]
50 mg/ml	NaCl 150 mM CaCl ₂ 5 mM PVA 1.4%w/v Thrombin 50 U/ml	Hyaluronic acid 4 mg/ml Factor XIII 1 U/ml Aprotinin 0.5 mg/ml	Extrusion-based	Bovine	primary Schwann cells	Cells were viable and proliferated Directed cell alignment was observed	[36]
10 % w/v	Thrombin 100 U	Gelatin 5 % w/v	Extrusion-based	Bovine	HUVECs, MSCs	EC-MSC distance defining cell-cell communication regulates angiogenesis	[93]
20 mg/ml	Thrombin 50 U/ml	Gelatin 30 mg/ml Aprotinin 20 µg/ml Hyaluronic acid 3 mg/ml Glycerol 10%	Extrusion-based	n/a	neonatal rat ventricular cardiomyocytes	Bioprinted constructs contracted, were formed by aligned and electromechanically coupled cells and responsive to drugs	[90]
20 mg/ml	Thrombin 2000 U/ml	Gelatin 7.5 % w/v	Extrusion-based, rotary	Bovine	primary neonatal human dermal fibroblast	Heat-treated gelatin increased fibrinogen-based bioink printability Tensile mechanical properties of printed constructs induced the rise in circumferential and axial elastic moduli	[95]

(Contd...)

Table 3. (Continued)

Components			Bioprinting	Origin	Cells	Outcomes	Ref
Fibrinogen	Cross-linking agents	Additives					
20 mg/ml	Thrombin U/ml	4 Hyaluronic acid 1% w/v	Laser- assisted	Human	iPSCs	Cells were sensitive to biomaterials used as a bioink base (not printing) Hyaluronic-based blends ensured better cell survivability without pluripotency loss	[96]
20 mg/ml	Thrombin 40 U/ml CaCl2 50 mM	Hyaluronic acid 1% w/v	Laser- assisted	Human	ASCs, ECFCs	Cell-cell contacts regulate the formation of vessel networks	[97]

Ref: References; n/a: Not available; RB: Rose bengal; PVA: Polyvinyl alcohol; iPSC: Induced pluripotent cells; HUVEC: Human umbilical vein endothelial cells; MSC: Mesenchymal stromal cells; ASC: Adipose-derived stromal cells; ECFC: Endothelial colony-forming cells

personalized patient's therapy. For instance, Lee *et al.*^[92] printed an *in vitro* glioblastoma model using a fibrin-based bioink. Cells remained viable for more than 1 week after printing and formed spheres expressing cancer stem cells and metastatic invasiveness markers. Moreover, the printed constructs treated with a novel method were shown to be more *in vivo* relevant than a monolayer culture. Using a fibrin blend, Zhao *et al.*^[32] described a method to print a 3D cervical tumor model that also was more resistant to chemotherapy than two-dimensional culture.

Despite the biofabrication of tissues and organs, fibrin-based bioinks are demanded to study cell-cell interactions, mainly for deeper understanding of cell biology features related to vascularization, innervation, etc. For instance, by regulating the distance between ECs and MSCs with bioprinting, Piard *et al.*^[93] showed that angiogenesis can be significantly modulated: When endothelial cells were placed closer to stromal ones ($\leq 200 \mu\text{m}$), the better angiogenesis promotion was observed.

3.4 Trends

As it is clear from above, the use of fibrin as a bioink base is only growing that corresponds with an increasing trend to bioprinting in general.

Undoubtedly, the development of bioprinting is strongly connected with the development of new bioinks, particularly fibrin-based ones; and widening its applications will be the applications of bioinks. Therefore, fibrin as one of biomaterials of choice will be used to print not only tissues and organs but also tumor models, organ-on-a-chip, etc.

To improve fibrin (fibrinogen) mechanical properties, shape fidelity, etc., for bioprinting, the main strategy is blending with other biomaterials such as gelatin, collagen, and alginate. Despite its simplicity, it will be further used because it does not need strong structural changes in protein molecule requiring deep knowledge of biomaterial chemistry and a bioink can be easier roughly tuned to a particular protocol.

However, blending consumes too much time and labor when fine tuning both mechanical and biological properties is required. Therefore, the number of modifications has been already offered that were described above. Moreover, such biomaterials give a birth to a new class of bioink – “smart bioinks.” These bioinks with finely tuned mechanical and biological properties provide not only a favorable microenvironment supporting cell survivability, proliferation, and differentiation but also the information on cell functioning, for

example, oxygen consumption, and changes in pH level. This approach was previously realized using scaffolds, but no study regarding bioinks, particularly fibrin-based bioinks, has been performed. For instance, O'Donnell fabricated pH-sensitive cellulose-based scaffolds labeled through cellulose-binding domain with enhanced cyan fluorescent protein^[98]. Such scaffolds ensured the analysis of extracellular acidification combined with probe-based monitoring of cell oxygenation. Moreover, being “smart,” such bioinks may adapt to meet cell requirements that include not only matrix re-modeling but also bioactive substance release. Hence, researchers will have a unique *in vitro* platform for organ and tissue fabrication.

Compared to the majority of biomaterials, fibrin can be autologously derived that is a significant advantage for further clinical translation of the bioprinted constructs. However, the fibrinogen concentration in blood is relatively low in comparison with the used one for bioink preparation (2 mg/ml^[99] vs. 20 mg/ml^[95]). Therefore, in recent papers^[87,100], such bioinks were prepared not from pure fibrinogen, but blood plasma.

4 Conclusions

The development of bioprinting has inspired new applications of fibrin as a bioink. Compared to other biomaterials, fibrin can be autologously derived that facilitates its clinical translation and has significant intrinsic properties such as induction of wound healing and angiogenesis that are highly valuable in tissue engineering. It also provides a possibility for fine tuning both mechanical and biological properties. Fibrin and its blends can be pioneering in the development of smart bionks that provide not only an adaptable cell-friendly microenvironment but also the information on cell functioning.

Authors' contributions

AS, VM, and PS outlined the manuscript. DO contributed to “Fibrin overview,” YE – “Mechanical properties,” PB, EB, and NK – “Wound healing,” AS and ASo - “Trends”, and RS, ML, and MV – “Angiogenesis.” AS drafted the manuscript with primary editing and

revision support from PS, RS, and EB. PS and VM coordinated the manuscript preparation. All authors read and approved the final manuscript.

Acknowledgments

This work was supported by the Russian Science Foundation (18-15-00407, general information, applications, biological properties and their tuning) and Russian academic excellence project 5–100 (trends).

Conflicts of interest

The authors declare that they have no conflicts of interest.

References

1. Antoshin AA, Churbanov SN, Minaev NV, *et al.*, 2019, LIFT-bioprinting, is it Worth it? *Bioprinting*, 15:e00052. DOI: 10.1016/j.bprint.2019.e00052.
2. Jiang T, Munguia-Lopez JG, Flores-Torres S, *et al.*, 2019, Extrusion Bioprinting of Soft Materials: An Emerging Technique for Biological Model Fabrication. *Appl Phys Rev*, 6:011310. DOI: 10.1063/1.5059393.
3. Gudapati H, Dey M, Ozbolat I, 2016, A Comprehensive Review on Droplet-based Bioprinting: Past, Present and Future. *Biomaterials*, 102:20–42. DOI: 10.1016/j.biomaterials.2016.06.012.
4. Unagolla JM, Jayasuriya AC, 2020, Hydrogel-based 3D Bioprinting: A Comprehensive Review on Cell-laden Hydrogels, Bioink Formulations, and Future Perspectives. *Appl Mater Today*, 18:100479. DOI: 10.1016/j.apmt.2019.100479.
5. Kurniawan NA, Van Kempen TH, Sonneveld S, *et al.*, 2017, Buffers Strongly Modulate Fibrin Self-Assembly into Fibrous Networks. *Langmuir*, 33:6342–52. DOI: 10.1021/acs.langmuir.7b00527.
6. Kurniawan NA, Grimbergen J, Koopman J, *et al.*, 2014, Factor XIII Stiffens Fibrin Clots by Causing Fiber Compaction. *J Thromb Haemost*, 12:1687–96. DOI: 10.1111/jth.12705.
7. Weisel JW, Litvinov RI, 2017, Fibrin Formation, Structure and Properties. *Subcell Biochem*, 82:405–56.
8. Kim E, Kim OV, Machlus KR, *et al.*, 2011, Correlation between Fibrin Network Structure and Mechanical Properties: An Experimental and Computational Analysis. *Soft Matter*, 7:4983–92. DOI: 10.1039/c0sm01528h.

9. Brown AE, Litvinov RI, Discher DE, *et al.*, 2009, Multiscale Mechanics of Fibrin Polymer: Gel Stretching with Protein Unfolding and Loss of Water. *Science*, 325:741–4. DOI: 10.4016/12254.01
10. Mosesson MW, 2005, Fibrinogen and Fibrin Structure and Functions. *J Thromb Haemost*, 3:1894–904.
11. Fuss C, Palmaz JC, Sprague EA, 2001, Fibrinogen: Structure, Function, and Surface Interactions. *J Vasc Interv Radiol*, 12:677–82.
12. Kattula S, Byrnes JR, Wolberg AS, 2017, Fibrinogen and Fibrin in Hemostasis and Thrombosis. *Arterioscler Thromb Vasc Biol*, 37:e13–e21. DOI: 10.1161/atvbaha.117.308564.
13. Fish RJ, Neerman-Arbez M, 2012, Fibrinogen Gene Regulation. *Thromb Haemost*, 108:419–26. DOI: 10.1160/th12-04-0273.
14. Yang Z, Mochalkin I, Doolittle RF, 2000, A Model of Fibrin Formation Based on Crystal Structures of Fibrinogen and Fibrin Fragments Complexed with Synthetic Peptides. *Proc Natl Acad Sci U S A*, 97:14156–61. DOI: 10.1073/pnas.97.26.14156.
15. Chapin JC, Hajjar KA, 2015, Fibrinolysis and the Control of Blood Coagulation. *Blood Rev*, 29:17–24. DOI: 10.1016/j.blre.2014.09.003.
16. Cesarman-Maus G, Hajjar KA, 2005, Molecular Mechanisms of Fibrinolysis. *Br J Haematol*, 129:307–21. DOI: 10.1111/j.1365-2141.2005.05444.x.
17. Litvinov RI, Weisel JW, 2017, Fibrin Mechanical Properties and their Structural Origins. *Matrix Biol*, 60–61:110–23. DOI: 10.1016/j.matbio.2016.08.003.
18. Janmey PA, Amis EJ, Ferry JD, 1983, Rheology of Fibrin Clots. VI. Stress Relaxation, Creep, and Differential Dynamic Modulus of Fine Clots in Large Shearing Deformations. *J Rheol*, 27:135–53. DOI: 10.1122/1.549722.
19. Martens TP, Godier AF, Parks JJ, *et al.*, 2009, Percutaneous Cell Delivery into the Heart Using Hydrogels Polymerizing *In Situ*. *Cell Transplant*, 18:297–304. DOI: 10.3727/096368909788534915.
20. Metry G, Adhikarla R, Schneditz D, *et al.*, 2011, Effect of Changes in the Intravascular Volume during Hemodialysis on Blood Viscoelasticity. *Indian J Nephrol*, 21:95. DOI: 10.4103/0971-4065.82139.
21. Zhao H, Ma L, Zhou J, *et al.*, 2008, Fabrication and Physical and Biological Properties of Fibrin gel Derived from Human Plasma. *Biomed Mater*, 3:1–10. DOI: 10.1088/1748-6041/3/1/015001.
22. Roberts WW, Lorand L, Mockros LF, 1973, Viscoelastic Properties of Fibrin Clots. *Biorheology*, 10:29–42. DOI: 10.3233/bir-1973-10105.
23. Weisel JW, 2004, The Mechanical Properties of Fibrin for Basic Scientists and Clinicians. *Biophys Chem*, 112:267–76.
24. Carr ME, Shen LL, Hermans J, 1976, A Physical Standard of Fibrinogen: Measurement of the Elastic Modulus of Dilute Fibrin Gels with a New Elastometer. *Anal Biochem*, 72:202–11. DOI: 10.1016/0003-2697(76)90522-4.
25. Kaibara M, 1973, Dynamic Viscoelastic Study of the Formation of Fibrin Networks in Fibrinogen-Thrombin Systems and Plasma. *Biorheology*, 10:61–73. DOI: 10.3233/bir-1973-10109.
26. Kim OV, Litvinov RI, Weisel JW, *et al.*, 2014, Structural Basis for the Nonlinear Mechanics of Fibrin Networks under Compression. *Biomaterials*, 35:6739–49. DOI: 10.1016/j.biomaterials.2014.04.056.
27. Shpichka AI, Konarev PV, Efremov YM, *et al.*, 2020, Digging Deeper: Structural Background of PEGylated Fibrin Gels in Cell Migration and Lumenogenesis. *RSC Adv*, 10:4190–200. DOI: 10.1039/c9ra08169k.
28. Jaramillo M, Singh SS, Velankar S, *et al.*, 2015, Inducing Endoderm Differentiation by Modulating Mechanical Properties of Soft Substrates. *J Tissue Eng Regen Med*, 9:1–12. DOI: 10.1002/term.1602.
29. Shapira-Schweitzer K, Seliktar D, 2007, Matrix Stiffness Affects Spontaneous Contraction of Cardiomyocytes Cultured within a PEGylated Fibrinogen Biomaterial. *Acta Biomater*, 3:33–41. DOI: 10.1016/j.actbio.2006.09.003.
30. Jansen KA, Bacabac RG, Piechocka IK, *et al.*, 2013, Cells Actively Stiffen Fibrin Networks by Generating Contractile Stress. *Biophys J*, 105:2240–51. DOI: 10.1016/j.bpj.2013.10.008.
31. Panwar A, Tan LP, 2016, Current Status of Bioinks for Micro-extrusion-based 3D Bioprinting. *Molecules*, 21:685. DOI: 10.3390/molecules21060685.
32. Zhao Y, Yao R, Ouyang L, *et al.*, 2014, Three-Dimensional Printing of Hela Cells for Cervical Tumor Model *In Vitro*. *Biofabrication*, 6:035001. DOI: 10.1088/1758-5082/6/3/035001.
33. Xu W, Wang X, Yan Y, *et al.*, 2007, Rapid Prototyping Three-Dimensional Cell/Gelatin/Fibrinogen Constructs for Medical Regeneration. *J Bioact Compat Polym*, 22:363–77.
34. Shikanov A, Xu M, Woodruff TK, *et al.*, 2009, Interpenetrating Fibrin Alginate Matrices for *In Vitro* Ovarian Follicle Development. *Biomaterials*, 30:5476–85. DOI: 10.1016/j.biomaterials.2009.06.054.
35. Lai VK, Lake SP, Frey CR, *et al.*, 2012, Mechanical Behavior of Collagen-Fibrin Co-Gels Reflects Transition From Series

- to Parallel Interactions With Increasing Collagen Content. *J Biomech Eng*, 134:011004. DOI: 10.1115/1.4005544.
36. England S, Rajaram A, Schreyer DJ, *et al.*, 2017, Bioprinted Fibrin-factor XIII-Hyaluronate Hydrogel Scaffolds with Encapsulated Schwann Cells and their *In Vitro* Characterization for use in Nerve Regeneration. *Bioprinting*, 5:1–9. DOI:10.1016/j.bprint.2016.12.001.
 37. Han J, Kim DS, Jang H, *et al.*, 2019, Bioprinting of Three-dimensional Dentin Pulp Complex with Local Differentiation of Human Dental Pulp Stem Cells. *J Tissue Eng*, 10:2041731419845849. DOI: 10.1177/2041731419845849.
 38. Weigandt KM, White N, Chung D, *et al.*, 2012, Fibrin Clot Structure and Mechanics Associated with Specific Oxidation of Methionine Residues in Fibrinogen. *Biophys J*, 103:2399–407. DOI: 10.1016/j.bpj.2012.10.036.
 39. Duong H, Wu B, Tawil B, 2009, Modulation of 3D Fibrin Matrix Stiffness by Intrinsic Fibrinogen-thrombin Compositions and by Extrinsic Cellular Activity. *Tissue Eng Part A*, 15:1865–76. DOI: 10.1089/ten.tea.2008.0319.
 40. Shpichka A, Butnaru D, Bezrukov EA, *et al.*, 2019, Skin Tissue Regeneration for Burn Injury. *Stem Cell Res Ther*, 10:1–16. DOI: 10.1186/s13287-019-1203-3.
 41. Murphy KC, Whitehead J, Zhou D, *et al.*, 2017, Engineering Fibrin Hydrogels to Promote the Wound Healing Potential of Mesenchymal Stem Cell Spheroids. *Acta Biomater*, 64:176–86. DOI: 10.1016/j.actbio.2017.10.007.
 42. Krasna M, Planinsek F, Knezevic M, *et al.*, 2005, Evaluation of a Fibrin-based Skin Substitute Prepared in a Defined Keratinocyte Medium. *Int J Pharm*, 291:31–7. DOI: 10.1016/j.ijpharm.2004.07.040.
 43. Idrus RB, Rameli MA, Low KC, *et al.*, 2014, Full-thickness Skin wound Healing Using Autologous Keratinocytes and Dermal Fibroblasts with Fibrin: Bilayered Versus Single-Layered Substitute. *Adv Ski Wound Care*, 27:171–80. DOI: 10.1097/01.asw.0000445199.26874.9d.
 44. Falanga V, Iwamoto S, Chartier M, *et al.*, 2007, Autologous Bone Marrow-derived Cultured Mesenchymal Stem Cells Delivered in a Fibrin Spray Accelerate Healing in Murine and Human Cutaneous Wounds. *Tissue Eng*, 13:1299–312. DOI: 10.1089/ten.2006.0278.
 45. Mendez JJ, Ghaedi M, Sivarapatna A, *et al.*, 2015, Mesenchymal Stromal Cells form Vascular Tubes when Placed in Fibrin Sealant and Accelerate wound Healing *In Vivo*. *Biomaterials*, 40:61–71. DOI: 10.1016/j.biomaterials.2014.11.011.
 46. Losi P, Briganti E, Errico C, *et al.*, 2013, Fibrin-based Scaffold Incorporating VEGF and bFGF-Loaded Nanoparticles Stimulates wound Healing in Diabetic Mice. *Acta Biomater*, 9:7814–21. DOI: 10.1016/j.actbio.2013.04.019.
 47. Mittermayr R, Branski L, Moritz M, *et al.*, 2016, Fibrin Biomatrix-conjugated Platelet-derived Growth Factor AB Accelerates wound Healing in Severe Thermal Injury. *J Tissue Eng Regen Med*, 10:E275–85. DOI: 10.1002/term.1749.
 48. Muhamed I, Sproul EP, Ligler FS, *et al.*, 2019, Fibrin Nanoparticles Coupled with Keratinocyte Growth Factor Enhance the Dermal Wound-Healing Rate. *ACS Appl Mater Interfaces*, 11:3771–80. DOI: 10.1021/acsami.8b21056.
 49. Dohan DM, Choukroun J, Diss A, *et al.*, 2006, Platelet-rich Fibrin (PRF): A Second-generation Platelet Concentrate. Part I: Technological Concepts and Evolution. *Oral Surg Oral Med Oral Pathol Oral Radiol Endod*, 101:37–44. DOI: 10.1016/j.tripleo.2005.07.008.
 50. Choukroun J, Diss A, Simonpieri A, *et al.*, 2006, Platelet-rich Fibrin (PRF): A Second-generation Platelet Concentrate. Part IV: Clinical Effects on Tissue Healing. *Oral Surg Oral Med Oral Pathol Oral Radiol Endodontol*, 101:56–60. DOI: 10.1016/j.tripleo.2005.07.011.
 51. Dohan DM, Choukroun J, Diss A, *et al.*, 2006, Platelet-rich Fibrin (PRF): A Second-generation Platelet Concentrate. Part II: Platelet-related Biologic Features. *Oral Surg Oral Med Oral Pathol Oral Radiol Endodontol*, 101:45–50. DOI: 10.1016/j.tripleo.2005.07.009.
 52. Dohan DM, Choukroun J, Diss A, *et al.*, 2006, Platelet-rich Fibrin (PRF): A Second-generation Platelet Concentrate. Part III: Leucocyte Activation: A New Feature for Platelet Concentrates? *Oral Surg Oral Med Oral Pathol Oral Radiol Endodontol*, 101:51–5. DOI: 10.1016/j.tripleo.2005.07.010.
 53. Miron RJ, Fujioka-Kobayashi M, Bishara M, *et al.*, 2017, Platelet-Rich Fibrin and Soft Tissue Wound Healing: A Systematic Review. *Tissue Eng Part B Rev*, 23:83–99. DOI: 10.1089/ten.teb.2016.0233.
 54. Anitua E, Nurden P, Prado R, *et al.*, 2019, Autologous Fibrin Scaffolds: When Platelet and Plasma-derived Biomolecules Meet Fibrin. *Biomaterials*, 192:440–60. DOI: 10.1016/j.biomaterials.2018.11.029.
 55. Nandi S, Sproul EP, Nellenbach K, *et al.*, 2019, Platelet-like Particles Dynamically Stiffen Fibrin Matrices and Improve Wound Healing Outcomes. *Biomater Sci*, 7:669–82. DOI: 10.1039/c8bm01201f.
 56. Schense JC, Bloch J, Aebischer P, *et al.*, 2000, Enzymatic Incorporation of Bioactive Peptides into Fibrin Matrices Enhances Neurite Extension. *Nat Biotechnol*, 18:415–9. DOI: 10.1038/74473.
 57. Galler KM, Cavender AC, Koeklue U, *et al.*, 2011,

- Bioengineering of Dental Stem Cells in a PEGylated Fibrin Gel. *Regen Med*, 6:191–200. DOI: 10.2217/rme.11.3.
58. Gorkun AA, Shpichka AI, Zurina IM, et al., 2018, Angiogenic Potential of Spheroids from Umbilical Cord and Adipose-derived Multipotent Mesenchymal Stromal Cells within Fibrin Gel. *Biomed Mater*, 13(4):44108. DOI: 10.1088/1748-605x/aac22d.
 59. Ehrbar M, Zeisberger SM, Raeber GP, et al., 2008, The Role of Actively Released Fibrin-Conjugated VEGF for VEGF Receptor 2 Gene Activation and the Enhancement of Angiogenesis. *Biomaterials*, 29:1720–9. DOI: 10.1016/j.biomaterials.2007.12.002.
 60. Liang MS, Andreadis ST, 2011, Engineering Fibrin-binding TGF- β 1 for Sustained Signaling and Contractile Function of MSC Based Vascular Constructs. *Biomaterials*, 32:8684–93. DOI: 10.1016/j.biomaterials.2011.07.079.
 61. Loureiro J, Torres AL, Neto T, et al., 2019, Conjugation of the T1 Sequence from CCN1 to Fibrin Hydrogels for Therapeutic Vascularization. *Mater Sci Eng C*, 104:109847. DOI: 10.1016/j.msec.2019.110514.
 62. Zhao N, Suzuki A, Zhang X, et al., 2019, Dual Aptamer-Functionalized *In Situ* Injectable Fibrin Hydrogel for Promotion of Angiogenesis via Codelivery of Vascular Endothelial Growth Factor and Platelet-Derived Growth Factor-BB. *ACS Appl Mater Interfaces*, 11:18123–32. DOI: 10.1021/acsami.9b02462.
 63. Mittermayr R, Slezak P, Haffner N, et al., 2016, Controlled Release of Fibrin Matrix-Conjugated Platelet Derived Growth Factor Improves Ischemic Tissue Regeneration by Functional Angiogenesis. *Acta Biomater*, 29:11–20. DOI: 10.1016/j.actbio.2015.10.028.
 64. Michlits W, Mittermayr R, Schäfer R, et al., 2007, Fibrin-embedded Administration of VEGF Plasmid Enhances Skin Flap Survival. *Wound Repair Regen*, 15:360–7. DOI: 10.1111/j.1524-475x.2007.00238.x.
 65. Mooney R, Tawil B, Mahoney M, 2010, Specific Fibrinogen and Thrombin Concentrations Promote Neuronal Rather than Glial Growth when Primary Neural Cells are Seeded within Plasma-derived Fibrin Gels. *Tissue Eng Part A*, 16:1607–19. DOI: 10.1089/ten.tea.2009.0372.
 66. Shpichka AI, Koroleva AV, Deiwick A, et al., 2017, Evaluation of the Vasculogenic Potential of Hydrogels Based on Modified Fibrin. *Cell Tissue Biol*, 11:81–7. DOI: 10.1134/s1990519x17010126.
 67. Shpichka AI, Revkova VA, Aksenova NA, et al., 2018, Transparent PEG-fibrin Gel as a Flexible Tool for Cell Encapsulation. *Sovrem Tehnol Med*, 10:64–9. DOI: 10.17691/stm2018.10.1.08.
 68. Hall H, Baechi T, Hubbell JA, 2001, Molecular Properties of Fibrin-based Matrices for Promotion of Angiogenesis *In Vitro*. *Microvasc Res*, 62:315–26. DOI: 10.1006/mvre.2001.2348.
 69. Bayless KJ, Salazar R, Davis GE, 2000, RGD-dependent Vacuolation and Lumen Formation Observed During Endothelial Cell Morphogenesis in Three-dimensional Fibrin Matrices Involves the Alpha(v) Beta(3) and Alpha(5)beta(1) Integrins. *Am J Pathol*, 156:1673–83. DOI: 10.1016/s0002-9440(10)65038-9.
 70. Bach TL, Barsigian C, Yaen CH, et al., 1998, Endothelial Cell VE-cadherin Functions as a Receptor for the β 15-42 Sequence of Fibrin. *J Biol Chem*, 273:30719–28. DOI: 10.1074/jbc.273.46.30719.
 71. Carrion B, Kong YP, Kaigler D, et al., 2013, Bone Marrow-derived Mesenchymal Stem Cells Enhance Angiogenesis via their α 6 β 1 Integrin Receptor. *Exp Cell Res*, 319:2964–76. DOI: 10.1016/j.yexcr.2013.09.007.
 72. Juliar BA, Keating MT, Kong YP, et al., 2018, Sprouting Angiogenesis Induces Significant Mechanical Heterogeneities and ECM Stiffening Across Length Scales in Fibrin Hydrogels. *Biomaterials*, 162:99–108. DOI: 10.1016/j.biomaterials.2018.02.012.
 73. Funahashi Y, Shawber CJ, Sharma A, et al., 2011, Notch Modulates VEGF Action in Endothelial Cells by Inducing Matrix Metalloprotease Activity. *Vasc Cell*, 3:2. DOI: 10.1186/2045-824x-3-2.
 74. Thi MU, Trocmé C, Montmasson MP, et al., 2012, Investigating Metalloproteinases MMP-2 and MMP-9 Mechanosensitivity to Feedback Loops Involved in the Regulation of *In Vitro* Angiogenesis by Endogenous Mechanical Stresses. *Acta Biotheor*, 60:21–40. DOI: 10.1007/s10441-012-9147-3.
 75. Lafleur MA, Handsley MM, Knäuper V, et al., 2002, EC tubulogenesis in fibrin requires MT-MMPs. *J Cell Sci*, 115:3427–38.
 76. Kachgal S, Carrion B, Janson IA, et al., 2012, Bone Marrow Stromal Cells Stimulate an Angiogenic Program that Requires Endothelial MT1-MMP. *J Cell Physiol*, 227:3546–55. DOI: 10.1002/jcp.24056.
 77. Ghajar CM, Kachgal S, Kniazeva E, et al., 2010, Mesenchymal Cells Stimulate Capillary Morphogenesis via Distinct Proteolytic Mechanisms. *Exp Cell Res*, 316:813–25. DOI: 10.1016/j.yexcr.2010.01.013.
 78. Urech L, Bittermann AG, Hubbell JA, et al., 2005, Mechanical Properties, Proteolytic Degradability and Biological Modifications Affect Angiogenic Process Extension Into Native and Modified Fibrin Matrices *In Vitro*. *Biomaterials*,

- 26:1369–79. DOI: 10.1016/j.biomaterials.2004.04.045.
79. Koroleva A, Deiwick A, Nguyen A, *et al.*, 2016, Hydrogel-based Microfluidics for Vascular Tissue Engineering. *BioNanoMaterials*, 17:19–32. DOI: 10.1515/bnm-2015-0026.
 80. Morin KT, Smith AO, Davis GE, *et al.*, 2013, Aligned Human Microvessels Formed in 3D Fibrin Gel by Constraint of Gel Contraction. *Microvasc Res*, 90:12–22. DOI: 10.1016/j.mvr.2013.07.010.
 81. Bootle-Wilbraham CA, Tazzyman S, Thompson WD, *et al.*, 2001, Fibrin Fragment E Stimulates the Proliferation, Migration and Differentiation of Human Microvascular Endothelial Cells *In Vitro*. *Angiogenesis*, 4:269–75. DOI: 10.1023/a:1016076121918.
 82. Thompson WD, Smith EB, Stirk CM, *et al.*, 1992, Angiogenic Activity of Fibrin Degradation Products is Located in Fibrin Fragment E. *J Pathol*, 168:47–53. DOI: 10.1002/path.1711680109.
 83. Jozkowicz A, Fügl A, Nanobashvili J, *et al.*, 2003, Delivery of High dose VEGF Plasmid Using Fibrin Carrier does Not Influence its Angiogenic Potency. *Int J Artif Organs*, 26(2):161–9. DOI: 10.1177/039139880302600211.
 84. Noori A, Ashrafi SJ, Vaez-Ghaemi R, *et al.*, 2017, A Review of Fibrin and Fibrin Composites for Bone Tissue Engineering. *Int J Nanomed*, 12:4937–61. DOI: 10.2147/ijn.s124671.
 85. Blache U, Ehrbar M, 2018, Inspired by Nature: Hydrogels as Versatile Tools for Vascular Engineering. *Adv Wound Care*, 7:232–46. DOI: 10.1089/wound.2017.0760.
 86. Li Y, Meng H, Liu Y, *et al.*, 2015, Fibrin Gel as an Injectable Biodegradable Scaffold and Cell Carrier for Tissue Engineering. *Sci World J*, 2015:685690. DOI: 10.1155/2015/685690.
 87. Cubo N, Garcia M, Del Cañizo JF, *et al.*, 2017, 3D Bioprinting of Functional Human Skin: Production and *In Vivo* Analysis. *Biofabrication*, 9:15006. DOI: 10.1088/1758-5090/9/1/015006.
 88. Albanna M, Binder KW, Murphy SV, *et al.*, 2019, *In Situ* Bioprinting of Autologous Skin Cells Accelerates Wound Healing of Extensive Excisional Full-Thickness Wounds. *Sci Rep*, 9:1–15. DOI: 10.1038/s41598-018-38366-w.
 89. Kumar SA, Alonzo M, Allen SC, *et al.*, 2019, A Visible Light-Cross-Linkable, Fibrin-Gelatin-Based Bioprinted Construct with Human Cardiomyocytes and Fibroblasts. *ACS Biomater Sci Eng*, 5:4551–63. DOI: 10.1021/acsbomaterials.9b00505.
 90. Wang Z, Lee SJ, Cheng H, *et al.*, 2018, 3D Bioprinted Functional and Contractile Cardiac Tissue Constructs. *Acta Biomater*, 70:48–56. DOI: 10.1016/j.actbio.2018.02.007.
 91. Oztan YC, Nawafleh N, Zhou Y, *et al.*, 2020, Recent Advances on Utilization of Bioprinting for Tumor Modeling. *Bioprinting*, 18:e00079. DOI: 10.1016/j.bprint.2020.e00079.
 92. Lee C, Abelseh E, de la Vega L, *et al.*, 2019, Bioprinting a Novel Glioblastoma Tumor Model Using a Fibrin-based Bioink for Drug Screening. *Mater Today Chem*, 12:78–84. DOI: 10.1016/j.mtchem.2018.12.005.
 93. Piard C, Jeyaram A, Liu Y, *et al.*, 2019, 3D Printed HUVECs/MSCs Cocultures Impact Cellular Interactions and Angiogenesis Depending on Cell-cell Distance. *Biomaterials*, 222:119423. DOI: 10.1016/j.biomaterials.2019.119423.
 94. Zhang K, Fu Q, Yoo J, *et al.*, 2017, 3D Bioprinting of Urethra with PCL/PLCL Blend and Dual Autologous Cells in Fibrin Hydrogel: An *In Vitro* Evaluation of Biomimetic Mechanical Property and Cell Growth Environment. *Acta Biomater*, 50:154–64. DOI: 10.1016/j.actbio.2016.12.008.
 95. Freeman S, Ramos R, Chando PA, *et al.*, 2019, A Bioink Blend for Rotary 3D Bioprinting Tissue Engineered Small-diameter Vascular Constructs. *Acta Biomater*, 95:152–64. DOI: 10.1016/j.actbio.2019.06.052.
 96. Koch L, Deiwick A, Franke A, *et al.*, 2018, Laser Bioprinting of Human Induced Pluripotent Stem Cells the Effect of Printing and Biomaterials on Cell Survival, Pluripotency, and Differentiation. *Biofabrication*, 10:35005. DOI: 10.1088/1758-5090/aab981.
 97. Gruene M, Pflaum M, Hess C, *et al.*, 2011, Laser Printing of Three-dimensional Multicellular Arrays for Studies of Cell-cell and Cell-environment Interactions. *Tissue Eng Part C Methods*, 17:973–82. DOI: 10.1089/ten.tec.2011.0185.
 98. O'Donnell N, Okkelman IA, Timashev P, *et al.*, 2018, Cellulose-based Scaffolds for Fluorescence Lifetime Imaging-assisted Tissue Engineering. *Acta Biomater*, 80:85–96. DOI: 10.1016/j.actbio.2018.09.034.
 99. McQuilten ZK, Bailey M, Cameron PA, *et al.*, 2017, Fibrinogen Concentration and Use of Fibrinogen Supplementation with Cryoprecipitate in Patients with Critical Bleeding Receiving Massive Transfusion: A Bi-national Cohort Study. *Br J Haematol*, 179:131–41. DOI: 10.1111/bjh.14804.
 100. Ahlfeld T, Cubo-Mateo N, Cometta S, *et al.*, 2020, A Novel Plasma-based Bioink Stimulates Cell Proliferation and Differentiation in Bioprinted, Mineralized Constructs. *ACS Appl Mater Interfaces*, 12:12557-72. DOI: 10.1021/acscami.0c00710.

Software for Bioprinting

Catherine Pakhomova^{1,2*}, Dmitry Popov¹, Eugenio Maltsev¹, Iskander Akhatov¹,
Alexander Pasko^{1,3}

¹Center for Design, Manufacturing and Materials, Skolkovo Institute of Science and Technology, Moscow

²Institute of Engineering Physics for Biomedicine, NRNU Mephi, Moscow

³The National Centre for Computer Animation, Bournemouth University, UK

Abstract: The bioprinting of heterogeneous organs is a crucial issue. To reach the complexity of such organs, there is a need for highly specialized software that will meet all requirements such as accuracy, complexity, and others. The primary objective of this review is to consider various software tools that are used in bioprinting and to reveal their capabilities. The sub-objective was to consider different approaches for the model creation using these software tools. Related articles on this topic were analyzed. Software tools are classified based on control tools, general computer-aided design (CAD) tools, tools to convert medical data to CAD formats, and a few highly specialized research-project tools. Different geometry representations are considered, and their advantages and disadvantages are considered applicable to heterogeneous volume modeling and bioprinting. The primary factor for the analysis is suitability of the software for heterogeneous volume modeling and bioprinting or multimaterial three-dimensional printing due to the commonality of these technologies. A shortage of specialized suitable software tools is revealed. There is a need to develop a new application area such as computer science for bioprinting which can contribute significantly in future research work.

Keywords: Bioprinting, Computer and mathematical modeling, Computer science for bioprinting, Digital biofabrication, Function representation approach, Software

*Corresponding Author: Catherine Pakhomova, Skolkovo Institute of Science and Technology, Moscow; catherine.pakhomova@skoltech.ru

Received: March 21, 2020; **Accepted:** April 24, 2020; **Published Online:** June 05, 2020

(This article belongs to the *Special Section: Bioprinting in Russia*)

Citation: Pakhomova C, Popov D, Maltsev E, *et al.*, 2020, Software for Bioprinting, *Int J Bioprint*, 6(3): 279. DOI: 10.18063/ijb.v6i3.279.

1 Introduction

There are two research fields of bioprinting in a broad sense: Printing of living cells and printing for purposes of a living organism. Printing of living cells includes printing of tissues or whole organs for purposes of medicine, for example, for surgery, pharmaceutical research and tests, transplantation, and others. The printing of multi-material or heterogeneous structures is the main issue in bioprinting nowadays. In the application of living cells printing, the main issue is that the structure of the majority of

human organs is often vascularized and consists of different tissues.

A full description of research and manufacturing fields of bioprinting is illustrated in **Figure 1**^[1-26]. In the field of bioprinting, the printing of living cells, including vascularized tissues, skin, bones, and cartilages is the most widespread. There is also bioprinting of physiologically relevant tissues for pharmaceutical research and development therapy of cancer treatment. Furthermore, there is also bioprinting of complete living organs which is the subject of active research and elaboration nowadays. While another general field of

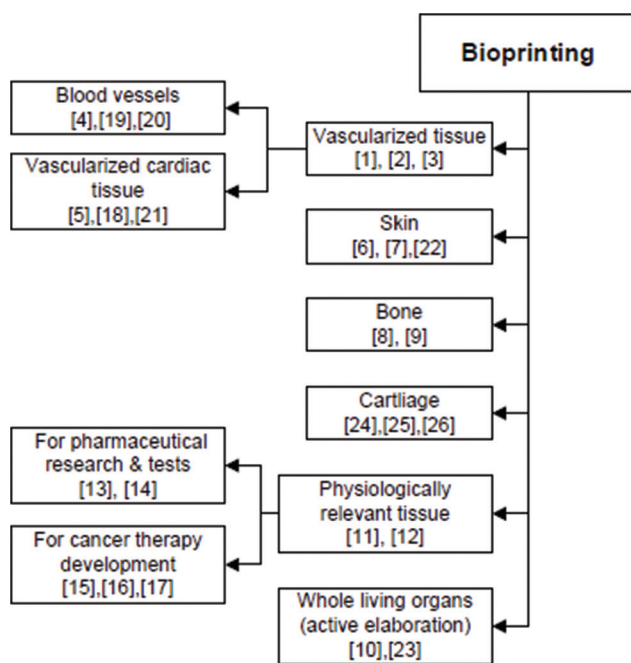


Figure 1. The schematic diagram of the research and manufacturing fields of the bioprinting ^[1-26].

manufacturing is the printing of multiple scaffolds for bioprinting and tissue engineering which may be both biodegradable and non-biodegradable, bioprinting of some critical parts for drug delivery systems and tissue reconstruction.

2 Living cells printing

There are several fields in the printing of living tissue. Physiologically, relevant tissues are often printed, in addition to other purposes, for pharmaceutical researches. For example, in Peng *et al.*^[12], the authors reported that three-dimensional (3D) tissue models could mimic native tissues quite closely. The authors had adopted scaffold-free and scaffold-based approaches to the creation of models and demonstrated that the 3D tissue models could simulate the physiological response of natural tissue to drug.

Scaffold-free 3D models can be generated from cells, often from stem cells which are self-assembled into neotissues through cadherin-mediated adhesion using exogenous scaffold support. Stem cells are suitable option and commonly used because of their pluripotency (opportunity to differentiate into many different

cell types). The ability of stem cells to produce a large number of cells is the second reason for using them^[27,28]. Scaffold-based 3D models can be generated by seeding cells or embedding cells in a hydrogel matrix or on a prefabricated scaffold. Widely used materials for scaffolds include decellularized extracellular matrix components and many synthetic and natural biomaterials. Bioprinting technologies can be potentially useful for the fabrication of a wide variety of tissues such as composite tissues, vascular tissues, lung, neural, pancreas, brain, bone, cancer, cardiac, cartilage, heart valve, liver, retinal, skin, and others^[1-5,7,8,15,25]. In addition, there are different goals of using bioprinting in pharmaceutical researches such as developing drugs against cancer and other diseases^[13-17].

Vascularization in 3D printed tissues is challenging and is the current subject of active research and it still remains as unsolved problem^[3,12]. Vascularization plays a crucial role in tissue viability for its survival and growth and for drug delivery. Bioprinting of vascular constructs, such as bioprinting of physiologically relevant tissues, can be performed using scaffold-based or scaffold-free approaches. These approaches produce the same results as in the case of the bioprinting of physiologically relevant tissues^[29].

There are two main approaches for arranging cells in 3D patterns: Top-down fabrication or bottom-up fabrication^[30]. Top-down fabrication means that cells co-arranged with biomimetic scaffolds with tissue maturation in a bioreactor. Bottom-up fabrication means secretion of a matrix by cells themselves instigated by temporary support^[31,32].

As an example of the early progress that can be considered, as bioprinting is the first bioprinted skin created in 2009 by Lee *et al.*^[6,30]. They presented a method of creating multi-layered engineered tissue composites that consist of human skin fibroblasts and keratinocytes, which mimic skin layers. It could be useful for drug testing and modeling of diseases. Another opportunity of using skin in bioprinting is wound healing with the 3D bioprinting of skin^[33].

3 Scaffolds and bioimplants printing

In the field of biomedicine, there are many important purposes for each component of the created device. The task of finding a material that will satisfy all these needs is a complicated issue. Therefore, creating biomedical devices must be heterogeneous in most cases. According to Shi and Wang^[34], current researches on 3D printing technology for biomedical applications in the field of printing of non-living objects can be classified into two main areas: Personalized manufacturing of permanent non-invasive implants and fabrication of local scaffolds, which could be biodegradable or bioactive. The advantage of 3D printing of implants over traditional machine technology is that 3D printing can achieve personalized real-time manufacturing of any sophisticated implant with high-dimensional accuracy and short production cycles. Multi-material 3D printing is a widespread technology in the field of implants manufacturing. For example, in Yan *et al.*^[35], a bone prosthesis of 3D hydroxyapatite (HA)-coated porous titanium with osteoconductivity composed of an osteoinductive composite material was successfully created. The new bone successfully grew through it after 24 weeks. The porous Ti, which also acted as an osteoinductor, provided the required mechanical strength.

3D printing technologies could be used for the manufacturing of various scaffolds for the bioprinting of living tissues or whole organs. Scaffolds must satisfy such requirements as biophysicochemical properties, structural features, mechanical properties, and other necessary characteristics. According to Mogali *et al.*^[36], these essential characteristics could be a 3D porous interconnected network for cell growth, flow transport of nutrients and metabolic waste; suitable surface chemistry for cell adhesion, proliferation and differentiation; biocompatibility, and matching with the controlled degradation and absorption rate of cell or tissue growth; and properties that match the tissues to be implanted. Scaffolds with high water content, excellent biocompatibility, and controllable biodegradation can be manufactured using different technique such as extrusion-based, inkjet-based, microvalve-based, or laser-assisted

bioprinting. The selected method should be based on the properties of the tissue, for which the scaffold is created. The mechanical properties of scaffolds can be enhanced using various crosslinking technologies.

Ionic crosslinking can be used to deplete mechanical energy. Personalized scaffolds should provide an environment with micro-stress that is equal to the natural habitat for cells. It should maintain structural stability and integrity. It must possess mechanical strength, which matches those of the subchondral bone and adjacent cartilage of the implant location to provide an immediate and long-term load-bearing function^[37]. Crosslinking technologies were adopted to improve the mechanical properties of widely used gel materials due to their disadvantages such as poor mechanical properties, natural shrinking, and others^[38]. Considering Hutmacher, Wu *et al.*^[37,38], 3D printed bioactive glass scaffolds were manufactured with a hierarchical pore architecture and well-ordered mesopores in various shapes. Then, polyvinyl alcohol as a thermo-crosslinking agent was used to improve the mechanical properties. A combination of materials can be used to resist cracking and fatigue, to obtain desired physicochemical properties, to avoid extra cost, and for antibacterial purposes which is crucial in health care^[39].

3D printing technologies can be useful for the creation of high-fidelity clinical organ models for clinical treatments and medical education. Thanks to 3D printing technologies, these models could be created at a lower cost and taking into account of the individual differences among patients. Advantages of 3D printed models are physical dimension and durability, as well as the opportunity to be color- or material-coded by tissue type. Future materials with different elasticity, color, and composition to simulate the appearance of human tissues and organs can be developed^[40].

To achieve different functions, scaffolds should integrate different materials, for example, metal with ceramic and polymer can be used to fabricate a porous scaffold to satisfy the implant requirements^[33,41]. 3D printed smart materials, which can switch their shape or properties under the specific external stimulus, can show high

potential for therapy in clinical application that will be minimally invasive.

Multiple materials usually are integrated into medical biomaterials that are used in 3D printing to achieve complex functions in printed objects. New equipment to guarantee high porosity, dimensional precision, and other useful properties could be developed in the future. There is also a need to study high-performance materials for various medical-oriented 3D printing techniques.

For all applications in the field of 3D bioprinting described above, multi-component compatible materials must be used. A combination of materials should lead to maximum fitness according to specified parameters.

A number of issues in the field of bioprinting are similar to problems that are already solvable by additive technologies and manufacturing. Therefore, it would be a perspective solution to use the experience that was previously gained in the field of multi-material 3D printing with necessary adaptation for the bioprinting. Summarizing all the above, studying multi-material 3D printing and developing new approaches in this research field represent one of the critical elements that will make progress in the field of bioprinting.

Bioprinting research field could be subdivided into the biology, materials, and computer engineering. We will focus our attention on the third subdivision.

In the field of multimaterial printing for both bioprinting and additive technologies, the creation of the mathematical and computational model represents one of the critical tasks. To produce a perfect model in this field, it is necessary to choose or create software that meets all model requirements.

4 Software for bioprinting

The computational model is a crucial point in bioprinting technology. It is the first issue that must be solved when there is a task in creating some living tissue or whole organ using bioprinting. Nonetheless, the software development still lags behind than the advancement of bioprinting^[42].

4.1 Printer control software

Most of the current existing software are for the bioprinting process controlling such as graphical user interfaces (GUI)-based control software like Bioscaffolder from GeSim company^[43]. This software works with StereoLithography (STL) files representing object surface. It has two modules: Scaffold-generator and STL-interface. The Organovo company for their NovoGen MMX Bioprinter developed a general software that only includes essential functions. It has a graphical interface for designing various 3D constructs. It allows a user to choose parameters such as materials, cell types, printing speed, and write and load pre-defined commands for realizing specific movements of the robot and deposition heads. Now, Organovo collaborates with Autodesk to develop controlling software for bioprinters^[44]. EnvisionTEC company has developed a computer-aided design and computer-aided manufacturing (CAD-CAM) software with a user-friendly graphical interface for its 3D-Biplotter system. This software has been designed to monitor and control the printing process until it is completed. Fujifilm Holdings Corporation Ltd. developed a GUI application software for its Dimatix Materials Printer. This software works with bitmap files by importing them as CAD models and allows the conversion to bitmap format.

CELLINK designed their own software package named HeartOS, DNA Cloud, and DNA Studio to control the bioprinting process. It is for fast droplet layer-by-layer printing, where the model in the G-code or the STL format could be loaded. The software package is user-friendly and does not force users to spend their time on learning the process. The software allows the user to simply adjust parameters such as flow and speed^[45]. The software enables the user to preview a model before printing, to perform slicing preview to see how each layer setting will affect the results and to use active tools for printing infill.

Allevi developed the Allevi BioPrint Pro control software for bioprinting^[46]. It runs online, which allows user to work with it from any computer. Allevi BioPrint Pro has built-in-model generation,

project-based workflow, and integrated slicing. Besides, the software supplies cutting-edge visualization features and interface to allow users to view and fix potential problems in their projects before printing.

RegenHU Ltd. is an innovative biomedical company that developed three specialized software for bioprinting which represents as a “bioprinting software suite”^[43,44]. BIOCAD serves as a user-friendly drawing suite to design scaffolds or tissues within minutes from scratch. BIOCAM is the user-friendly toolpath generator and slicer of STL files for 3D models for RegenHu’s bioprinters. This software allows the user to create multimaterial tissues that are based on digital 3D models obtained from 3D scanners or CAD systems or medical images. BIOCUT is a user-friendly Digital Imaging and Communications in Medicine (DICOM) viewer with analyzation tools integrated into RegenHu’s bioprinting digital workflow. Using this software, complex tissue structures can be created from medical images in the DICOM file format into multi-tissue modeling and multimaterial interface for bioprinting. This software suite had been developed to explore the comprehensive potential of the 3DDiscover Evolution RegenHU’s bioprinter. In summary, the RegenHU’s software suite for bioprinting can works with STL and DICOM file formats and allows user to slice 3D models that are generated in STL. This software suite acts as a bridge between medical and bioprinting field. However, it still works with STL which is time-consuming and difficult approach for complicated multimaterial objects such as heterogeneous living organs. In addition, they had developed two instruments for the bioprinting: BioFactory and 3D Discovery, and the Windows-based Human Machine interface software to control it.

Digilab company has developed CellJet printer and Windows-based control software for the printer. The software is named Axsys, and automates low volume liquid handling applications^[43]. It is user-friendly and provides a user to program protocols for printing with a graphical format. The nScript company developed printers equipped with the computer-aided biology technology that

was created based on the CAD environment. This software, as many described above, is produced for the fabrication process control. In this software, parameters such as deposition linear speed, toolpath deposition, syringe plunger rate in the displacement heads, and air pressure can be altered flexibly.

4.2 Software for pre-processing

4.2.1 Software for operations with G-code

According to Gulyas *et al.*^[42], specialized software tools to control bioprinter hardware that fulfilled the bioprinting requirements was developed. Typically, it represents a package of open-source software tools that allow the users to specify the machine movements precisely with the help of high-level programming languages. Besides, it enables us to distribute the machine movements easily across the batch of dishes of tissue culture. The software is useful in applications for printing of living cells and printing of extracellular matrices. The software can represent movements of the machine or elements of the gCode with simple functions of a high-level programming language such as C# or Python. It includes gCodeAPI.NET, gCode Editor, and PetriPrintes as a graphic user interface. PetriPrinter allows a user to distribute printer movements into several culture dishes that organized in a grid pattern, which is defined programmatically. As for bath printing, PetriPrinter distributes gCode objects into several dishes of the culture. PetriPrinter represents a gCode generator and provides collision-safe and optimized entry, movement between the dishes, and exit. Furthermore, this application can be adjusted to different hardware platforms using settings such as start height, printing temperature, row, or column distance. Besides PetriPrinter, there is second graphic interface known as gCode Editor. It was developed to visualize gCode from third-party slicer applications such as Cura or Slic3r and allows for manual modification and optimization for utilization in the cell culture. Unlike general slicers that do not offer detailed control over the tool movements, gCode Editor

allows us to identify and to replace the problematic head movements, to insert new control points, and to relocate existing points with just a few clicks. Output files of the gCode Editor are compatible with PetriPrinter. The first and the most critical part of these software tools are the gCode API, which can encapsulate gCode commands into high-level programming language functions such as C# or Python^[42]. GCodeAPI.NET includes such commands as temperature, speed, extrude, line, arc, relative, and absolute position. The scheme of using the gCodeAPI.NET is presented in **Figure 2**. Collectively, these software tools represent a useful and user-friendly software to make gCode analysis easier and less time-consuming. It is a control software for the bioprinting process which can help to make research processes more effective because of the accurate and straightforward prescribing of the machine movements and fast and easy finding some problematic machine movements in the raw gCode.

4.2.2 CAD-based software

The most general approach in model creation for bioprinting is CAD-based software and the STL file format. The most popular commercial software is based on the Boundary Representation modeling principles and Constructive Solid Geometry. Such software are computer-aided 3D interactive application (CATIA) (Dassault Systems), NX (Siemens PLM Software), SolidWorks (Dassault Systems), and Pro/Engineer (PTC)^[43]. CATIA is a

multi-platform software suite that was developed for CAD. It works with the STL file format and specialized CATIA model formats. NX is a software for design, engineering analysis, and manufacturing. It works with STL, CATIA, STEP, Parasolid, DXF, DWG, 3MF, Initial Graphics Exchange Specification (IGES), ACIS formats, or image, or Virtual Reality Modeling Language data for the import. For the export, it works with all these formats and also PLY, portable document format (PDF), or CSG files. SolidWorks is a CAD and computer-aided engineering (CAE) software that works with the STL file format and widely-used neutral solid modeling formats such as IGES, DXF, DWG, STEP, and ACIS. Pro/Engineer is a software for solid modeling or CAD, CAE, and CAM. It is used to import and export file formats such as ACIS, IGES, and Parasolid formats, which are specialized widely-used general file formats for solid modeling but not for bioprinting. The platform for the CAD system for tissue scaffolds (CASTS) has been developed later based on Pro/Engineer^[47,48]. For the input model, CASTS uses imaging software such as materialize interactive medical image control system (MIMICS) to convert the patient data from magnetic resonance imaging (MRI) or computer tomography (CT) to the IGES, neutral CAD file format. An output model in this software is saves in the STL file format.

The use of CAD-based software in bioprinting is discussed in detail with concrete CAD systems in this section. The first one is TinkerCAD (AutoDesk, Inc., San Rafael, CA, USA), it is a simple online Web 3D modeling system that does not require any specific and in-depth knowledge from users. Due to its simplicity, experts in bioprinting could exploit it for modeling of basic geometric primitives. Cylindrical primitives modeled in TinkerCAD were used for shape definition of bioprinted samples in works^[49,50]. The authors of Jeon *et al.*^[51] printed a cuboid. More complex primitives of TinkerCAD were used in works Lehner *et al.*^[52] and Jeon *et al.*^[53]. In the mentioned articles, the authors used letters. More sophisticated models printed from organic materials can be seen in Markstedt *et al.*^[54], in which

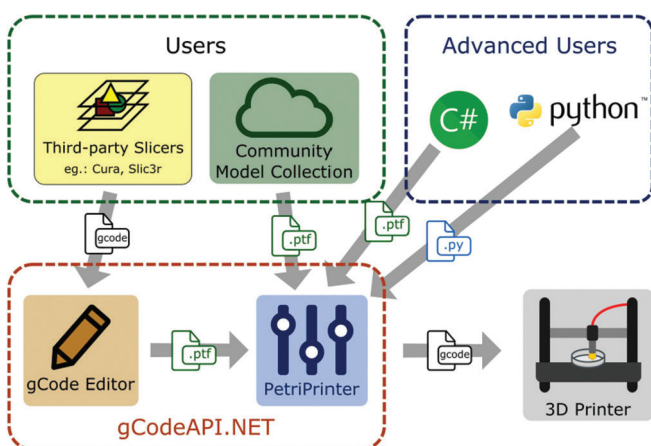


Figure 2. The schematic diagram of using the gCode API^[42].

a lattice structure was designed and manufactured. Another example of the printed cellular structures can be found in Faramarzi *et al.*^[55], which bioinks were used in this study.

Some researchers used TinkerCAD to print for the printing of necessary equipment needed for biofabrication. For example, it was used for modeling of inserts in papers^[56,57]. In Ivanov and Grabowska^[58], the design of the mold maker was provided with TinkerCAD, the authors of Yang *et al.*^[59] used it to create a model of a special extruder. Another example of the TinkerCAD application is the modeling of microfluidic chips^[60,61].

TinkerCAD is mostly used for modeling of simple geometry or for manipulation with existing meshes. Moreover, in some cases, more advanced specialized software tools like Meshmixer has to be used to postprocess meshes created with TinkerCAD. Meshmixer as a software tool will be considered further.

More sophisticated software can be used for the same purposes. There are few examples of using Blender software for modeling purposes. Blender allows producing more complex geometry based on the skills of the user. In one study, it had demonstrated the use of Blender (Blender Foundation, The Netherlands) for cryogenic 3D printing^[62]. Built-in Blender primitives also can be used for bioprinting of simple shapes^[63]. In the study conducted by Mussi *et al.*^[64], it was used to prepare an ear model. Some other studies also show the use of Blender's for scaffold generation^[65,66]. Some papers had also proposed Blender as a tool for vascular modeling^[67-70].

However, software tools that were used for modeling the STL format are usually used as a 3D printing standard. An STL file contains triangular mesh, therefore it is necessary to have a powerful tool for mesh processing when working with STL file. Meshmixer (Autodesk, San Rafael, USA) is one of such software tools. Autodesk Meshmixer is the software for editing and modification of the STL mesh. It also allows us to do in filling to build microstructure inside the 3D model. It was used in some above-mentioned researches, such as one study that involves an artery fabrication has applied Meshmixer in their

work^[71]. Its functionality becomes pretty helpful, when the manufactured geometry is obtained from medical scanning data and mimics natural structures^[72]. More details on this topic will be discussed further at the software to translate medical data to CAD section.

It should be noted that a short overview above does not mean that the three mentioned software are the most wide spread tools in modeling for bioprinting. Researchers use many other modeling packages. There are others Autodesk products such as Maya, Fusion 360, Inventor Netfabb; SketchUp (Trimble Inc, United States), Rhinoceros (Robert McNeel & Associates, United States), and Voxelizer (ZMorph, Poland).

CAD-based software have a number of lacks for the bioprinting. Some errors of CAD systems acceptable for its direct purposes can lead to serious problems in the development of bioprinting industry. Computer software characterizes commonly as a service, not a product, and its failure leads to legal issues. Clarifying the industry standards could help in the early identification of potential coding defects. However, it could be challenging to predict scenarios that may require legal attention in 3D bioprinting. Therefore, there will be a need to determine what are the essential quality of the 3D bioprinted organ or tissue, including the type of models, biomaterials, methods, or all of these combined. Besides, in software development, there is a need to pay more attention not only to its efficiency but also to the safety of the software. Requirements of the software validation should meet the patient requirements. Hence, there is a need for various validation methods due to the fact that a number of software tools cannot be comprehensively tested only through the source code^[73].

There is also another problem arises with using CAD-based software. The software is usually used for modeling of simple shapes or for operating with reconstructed 3D models of organs. In the last case, the interaction is performed under meshes in common such representation lacks functionality essential for bioprinting. For example, it is quite difficult or sometimes impossible to model natural structures with multiple materials. Another problem is difficulties with modeling of multiscale structures.

4.2.3 Software for translates medical data to CAD

A standard method for living tissue modeling is using medical scans obtained by CT, optical microscopy, and MRI, ultrasound (US) 3D to create a model based on these images. One of the suitable software for this method is the MIMICS Innovation Suite (MIS) from Materialize^[74]. It is the specialized software working with medical scans in the DICOM file format and designing 3D models based on the STL file format. Created models could be sliced and exported for 3D printing or 3D bioprinting. Besides, this software suite allows users to analyze the anatomy segments, to make finite elements and other types of 3D analysis. MIS offers a wide range of tools for various clinical applications such as orthopedic, respiratory, and others. Another software for such tasks is BioCAD by Biomedical Modeling Inc.^[75]. This software was developed for anatomical 3D printing and CAD models for the design of medical devices. It translates medical images obtained by CT and MRI to SolidWorks files. BioCAD allows users to work with mesh and CAD models and to fabricate models for 3D printing. This software is useful to create anatomical models such as bones, blood vessels, heart, and some other internal organs. Developing minimally invasive surgical devices is another purpose for this software usage. There are other options for this purpose in the form of open-source license use such as InVesalius^[76,77], a multilingual cross-platform, and 3D Slicer^[78]. InVesalius is an open-source software tool for visualization and analysis of medical images that works with the DICOM file format. It allows user image segmentation, triangular mesh creation, manual or semiautomatic image segmentation, and volume rendering based on initial medical data obtained by scanning. This software is useful for the reconstruction of a CAD model based on medical scanning data obtained by CT or MRI. InVesalius allows us to import files in the DICOM or analyze format, and to export to the STL, OBJ, and PLY. Besides, InVesalius provides a capability of execution in different operating

systems. 3D Slicer enables user to perform medical image informatics, image processing, and 3D visualization. 3D Slicer is an open-source platform for analysis and visualization of medical images obtained by CT, MRI, US, microscopy, and nuclear medicine. It can be used for analysis and visualization of data includes interactive segmentation and volume rendering.

However, making organ blueprints just based on CT or MRI data is not a comprehensive approach. This approach could be convenient for considering the anatomy of an organ in a big scale. Nevertheless, to avoid errors or to preserve the anatomy of the printed organ as similar to the diseased organ, some small details of the organ such as alveoli in lung or nephrons in the kidney should be reverse engineered. Besides, the creation of a comprehensive functional organ is rather crucial than imitation of organ histology and anatomy^[79]. The complex structure of organs that include nerves and complex vascular systems makes the task of organ model designing more challenging. According to Dernowsek *et al.*^[79,80], tissue composition and cell redistribution cannot be absolutely identified yet by clinical bioimaging because the technology has not reached the cellular and histological level. Therefore, one of the best ways to produce organ blueprint using medical data is to combine bioimaging, CAD modeling or reverse engineering, and mathematical modeling and simulation^[80,81].

4.3 Software for slicing

There are various software tools for the slicing of the model, which are commercial and open-source. A commercial software simplify 3D is a software that provides model setup, slicing and print file creation, pre-print simulations, customizable support structures, mesh analysis and repair, machine control, and monitoring^[82]. Simplify 3D supports hundreds of different printers, provides easy switching between multiple machines, has incredibly realistic simulations, identifies issues in advance, and allows access to industry learning resources to improve print quality. In Sahai and Gogoi^[83], the 3D printer Tarantula 3D was modified

with syringe paste extruder for the printing of chitosan composite scaffolds. It allows us to use simplify 3D as slicing and preprocessing software for bioprinting. Other professional software such as additive manufacturing “Magics” (Materialize) was used for the preparation and slicing of the 3D model of the biocompatible implant for the patient’s cranial^[84]. The 3D model was reconstructed from computed tomography and fabricated from titanium. According to Naghieh *et al.*^[85], Magics is used for the design and preprocessing of the 3D model of scaffolds, followed by fabrication of the scaffolds from gelatin using 3D bioplotter (EnvisionTEC, Germany). There are also open-source projects for slicing and preprocessing of polygonal 3D models, such as CuraEngine and Slic3r. CuraEngine is a part of a large open-source project Cura. It represents as a console application and provides prepared G-code for a wide range of fused filament fabrication printers^[86,87]. Cura is an engine for slicing. CAD integration and other powerful features had been developed for 3D printing and could be useful to resolve 3D bioprinting issues.

According to Ariffin *et al.*^[88], CuraEngine is the better solution for application that requires increase accuracy using lesser filament. For the production of parts with a hanging structure, the best solution is Slic3r due to excessive material that can act as a support. The Cura software is popular slicing software for the prototyping of 3D bioprinters. It has many features of 3D model preprocessing and supports various motherboards to control the device that is under development. For example, in projects Mielczarek *et al.*^[89] and Datta *et al.*^[90], the Cura software plays a role in the graphical interface with G-code preparation for a prototype of a 3D bioprinter constructed by the authors. These prototypes of 3D bioprinters use syringe pump extruders with different inks. The gelatin methacrylate doped with a photoinitiator as the printing substance was used in the first study and alginate with honey was used in the second study. In other work, Cura and Slic3r are mentioned as “slicer” software and also used for extrusion-based bioprinters^[91].

4.4 Software for scaffold generation (pre-processing)

4.4.1 Software for automatic scaffold generation

Scaffold generation is a crucial task for bioprinting, and there are specific requirements for tissue scaffolds. For the research tasks in the tissue scaffolds engineering, the following parameters are required: Generation of a uniform and non-uniform lattice, changing the size of pores and porosity of the whole construction, setting up of a volume of material to be used for scaffold fabrication, and opportunity to create the continuous tool paths inside and between layers and others.

The uniform lattices with regular continuous patterns can be generated using BioScaffolds PG. It is a specific software for scaffold generation for bioprinting^[92]. It has the necessary parameters for modeling of a customizable uniform scaffold and the opportunity to export the models for the Fab@Home platform^[93]. Successful tests with polycaprolactone scaffolds fabrication proven the usability of this software.

The function representation approach (FRep) based on using real continuous functions can be used for the parametrized non-uniform scaffold modeling^[94]. It gives a certain freedom in the modeling of lattices and microstructures with complicated forms. It allows us to apply any functions, space-mappings, and transformations for the space coordinates to obtain the sophisticated geometrical shapes. The software which implements such an approach are HyperFun^[95], Uformia software^[96], and FRepCAM^[97].

For the scaffolds fabrication for clinical purposes, triply periodic minimal surfaces (TPMS) structures were studied. In some research works, such structures showed good properties of permeability^[98-100]. The first researcher working on TPMS structures is Schwarz^[101], followed by Schoen^[102] and Karcher^[103]. An open-source software based on the generation of the TPMS structures around any surface was developed, which is known as POMES (Porous and Modifications for Engineering Surfaces)^[104]. It allows generation

of different porous and roughness morphology on surfaces using such structures as Schwartz P, Schwartz D, Gyroid, Neovius and others. Such modification of surfaces increases cells migration inside the implants and improves osteoblast adhesion.

nTopology (nTop) is the software for the lattice generation and microstructures using the method of the implicit surfaces^[105]. This software is also based on the FRep approach.

The Voronoi tessellation is a generative algorithms used for 3D modeling of the bone microstructure^[106]. The Grasshopper^[107] is the software with a visual programming language that allows us to build generative algorithms, including Voronoi tessellation

Autodesk Netfabb^[108] has a module for the lattice generation, which is called “Lattice Commander.” It allows the user to generate microstructures using the unit cell repetition. It has a wide range of the unit cell patterns, including TPMS structures and a variety of beams intersection.

4.4.2 Software for post-processing issues

Developing the software for bioprinting is the most anticipated subject of research currently. SIMMMC is the specialized application for predicting post-printing structure formation in bioprinted construct, generating 3D models of various types of bioprinted constructs, and simulating its evolution. The application has been extended for bioprinting purposes, such as modeling and simulation of the evolution of bioprinted tissue constructs composed of living cells, hydrogels, and cell culture medium^[109]. The metropolis Monte Carlo algorithm (MMC) is the base of this development. Besides, the specialized module that can generate 3D models of fabricated tissue constructs automatically after loading an XYZ file has been created. The XYZ files are used for the purposes of biological systems graphical visualization using visual molecular dynamics^[110]. According to Robu *et al.*^[109], many architectures of bioprinted tissue constructs could be integrated into this platform. SIMMMC for bioprinting was implemented in the Visual Studio.Net 2015 using the Visual C#.Net language. SIMMMC for

scaffold-based approach allows user to create the 3D model of a particular type of biological system that includes living cells and biomaterials and simulates the evolution of the multicellular system in the vicinity of biomaterials using the MMC algorithm^[111]. SIMMMC for bioprinting as an extension of the initial SIMMMC which allows a user to load different geometry of tissue construct that was obtained by post-printing. Besides, it enables user to simulate shape changes of the uploaded bioprinted construct that includes living cells, biomaterial, hydrogel, and cellular medium with the help of the MMC algorithm. SIMMMC for bioprinting had been validated by procedural bioprinting of the vessel^[109]. Collectively, SIMMMC for bioprinting represents an useful software tool to produce computer simulations of a large variety of 3D models for predicting post-printing structure formation.

At present, the software tool CompuCell3D is used for *in silico* tissue engineering^[112-114]. It is based on the Glazier-Graner-Hogeweg model and is an open-source software that was developed especially for simulating the evolution of bioprinted constructs^[112]. The Surface Evolver software has been invented to predict simulation of directed self-assembly in multicellular systems which considering each single cell as a bubble^[115,116]. It is based on the Finite Element Method. In the field of bioprinting, Surface Evolver could be used for modeling fusion of vascular tissue spheroids in bioprinted segment of a vascular tree^[117]. This approach allows us an estimation of the quantity of tissue spheroids concentric layers. These layers must be printed in sequential vascular segments to keep accuracy of each diameter of the vascular section of vascular wall^[117,118]. However, the software tools that are provided in the Surface Evolver could not allow the comprehensive modeling and simulation in the field of bioprinting, because they can only solve highly-specialized issues. Besides, these software tools are meant for biological simulation, not primarily for bioprinting. There is currently no available software to simulate all aspects of bioprinting or formation of the bioprinted tissue structures with 10^6 – 10^9 cells. However, developing

of control software tools for bioprinting is more widespread nowadays, in comparison with software tools for providing the information of shape changes during the process. In the future, new bioprinters are preferred to have an integrated computational framework that should include software modules for modeling and simulation of pre-printing and post-printing stages, and are compatible with medical image data^[118]. Therefore, to prevent existing bioprinting software becoming hurdles in their research field, it is necessary to develop new software tools that are specialized and able to meet all bioprinting requirements.

The next step after printing of the organ is a crucial stage where maturation of the organs takes place in bioreactor. At this step, the growth and maturation of the bioproduct occurs. Bioreactors are necessary for the acceleration of the tissue maturation which controls the mechanical, electrical, and biochemical conditions^[119]. Bioreactors act as a crucial environment in maintaining of the viability of the engineered tissue. Besides, bioreactors are useful for experiments and cells maturation processes monitoring. Although the bioprinting and bioproduct maturation steps are separated steps, it is worth mentioning some of the bioreactors control software. In the future, bioprinting and bioreactor may be able to integrate as one complicated device, but it still remains a task for future development^[79].

According to the Burdge and Libourel^[120], there is an open-source software based on LabVIEW that was developed for the sophisticated control of environments of the culture. This software uses Python for protocols and allows user to control parameters of the process. LabVIEW also provides an interface for monitoring the process, logging of data, and creating a protocol to execute user-defined protocols. ILS automation provides a bioreactor control system that includes specialized bioreactors integrated with control systems for cell culture systems, fermentation systems, biofuel systems, and two separate software tools as system integration and control software tools^[121].

Ignition Scada Integrator is a system integration software tool. It is an all-in-one software solution that provides user with unparalleled data

integration, analysis, control, and visualization. The general control software tools are represented as Real-time Web-based SCADA Software: Batch Expert+. It allows user to manage all bioreactors in one place to get intelligent alarming, store live and historical data together in history, and improve process, yield, and production.

LAMBDA laboratory provides two control software tools, FNet and SIAM, for the control of cell cultures and fermentation in MINIFOR fermentor and bioreactor^[122,123]. FNet can control common cultures and up to 6 MINIFOR bioreactors with limited options. SIAM has better functions, including able to control up to 99 bioreactors and offers extended functions. Both software tools provide graphical visualization.

BioProcess by Eppendorf Inc provides three BioCommand software packages for fermentors and bioreactors^[124]. BioCommand provides tools needed for research, optimization, and security trials. BioCommand Track and Trend is useful for essential laboratory management and offers full monitoring and historical record-keeping capabilities with control of set-points and trends visualization. BioCommand Batch Control includes all features of the previous one but also allows us to perform equipment lock-out, programming capability, and has a customize synoptic display. It is useful for optimization and control for the process. BioCommand Batch Control Plus adds three levels of security, including operator, supervisor, and administrator. It provides event logs, audit trails, and a database structure. Besides, this software allows user to have powerful control capabilities.

According to Dernowsek *et al.*^[79], omics technologies in integration with data science, machine learning, and other intelligent tools will contribute to a new field known as “computational biology in the 4.0 industry.” Integration platforms that consist of these fields are known as biofabrication lines. Biofabrication line consists of a set of devices that could produce all necessary types of models: mathematical, physical, and biological, keeping the necessary spatial distribution. It is presumed that biofabrication lines will be common in the future^[79]. The current computational biology

includes analysis of biological data such as cell populations, genetic sequences, or others to make new prediction. There are researches about genome data analysis and computational biology algorithms^[125], development of some pattern-based system prototypes^[90], and also hierarchical modeling with supporting composite modeling^[126]. The progress in computation biology could be also accelerated by integrating with machine learning and other research fields, which are traditionally related to data science^[127]. As for computational approaches for biofabrication, computational fluid dynamics software packages are widely used to calculate flow fields, shear stresses, and mass transport with and around 3D bioconstructs and bioreactor environments^[119].

Nonetheless, the most crucial tools in the field of computational biology for the 3D bioprinting are computational methods such as analytical methods, mathematical modeling, and simulation on all 3D bioprinting stages such as pre-processing, processing, and post-processing.

4.5 Approaches for future development

According to Robu *et al.*^[109], the software that controls the bioprinter and, in general, includes of CAD or CAM software now should include a module for simulation to predict the evolution of the printed construct. However, nowadays, bioprinting software usually can offer either only control or only simulation. Besides, the software for simulation in bioprinting is not so widespread. The solution of this problem could be developing such software that will include ability to work on all necessary stages. It should be able to provide control of the bioprinting process. Besides, it should have a module for simulation, and a slicer that can work with model file formats that are suitable for heterogeneous volume modeling in bioprinting. FRep has shown appropriate method to solve this issue^[128-130]. FRep can define an object by a continuous function

$$f(x_1, x_2, \dots, x_n) \quad (1)$$

where f is a real continuous function defined on n -dimensional Euclidean space E^n that must have positive values inside the object, negative values outside, and zero on the surface^[130,131]. In the 3D

space, the object boundary is named “implicit surface.” Any algorithm or function can be used until it can return a real value. Functions in the FRep approach form a system where different materials and other parameters can be described. The FRep approach is a suitable method to provide a heterogeneous representation of objects with any complexity. Besides, a mammalian cell colony was simulated using the FRep approach^[132]. The colony was modeled as a set of deformable particles, which are contacting with each other. A new particles pair, which models the process of cell division, can substitute an existed before particle. This simulation has specific features such as real functions that define arbitrary shapes of particles and particular rules of particles’ behavior. A collision detection algorithm was used to define communication between particles. To solve of the packing problem, a genetic algorithm was used. Changing the particle shape, size, and orientation was used for the simulation of a deformable particle. One of the figures of the simulation is presented in **Figure 3**^[132].

Therefore, the FRep approach represents a method that could help to solve such crucial issues in bioprinting as the heterogeneous volume modeling of living tissues and whole organs. Besides in the living objects modeling, the FRep approach allows us to model various cellular structures that are very important for implants modeling. The example of the cellular structure, developed with the FRep approach, is presented in

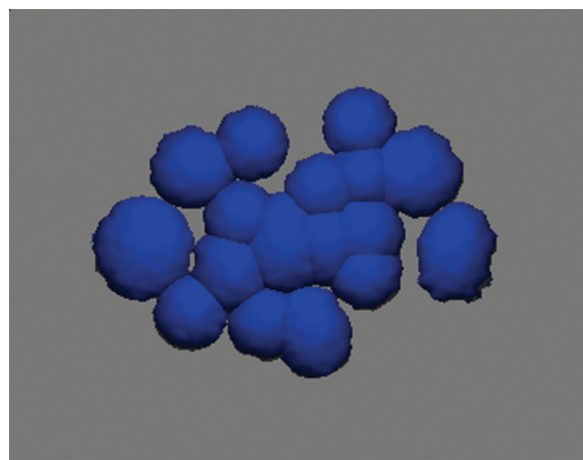


Figure 3. Simulated with the help of function representation approach mammalian cell colony^[132].

Figure 4^[128]. Software tools utilizes this approach are Hyperfun, FRepCAM, nTop, and Uformia that were mentioned above. There is also software such as Curv^[133] and libfive^[134], but not noticeable in the field of bioprinting and biofabrication yet.

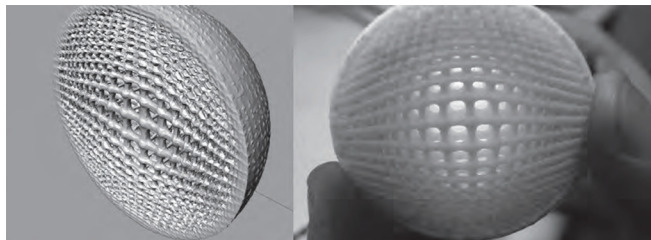


Figure 4. Digitally fabricated non-uniform microstructure developed with the help of the function representation approach^[128].

Summarizing all the above, the overview of properties of the leading software tools and applications are listed in **Table 1**. The current most popular software for the model generation in the field of bioprinting is CAD-based software. Usually, in this kind of software, users can generate STL-file models only and then slice them. This approach is the most common approach, but it is slightly outdated. STL files allow us to work exclusively with surfaces that are good for homogeneous models but are not suitable for heterogeneous models. In addition, using the STL file format leads to some problems. This file format does not allow us to use any colors and textures because these options are not a part of the STL standard.

Table 1. An overview of the software tools and applications for bioprinting.

The software name	Supported file formats	Distribution	Purpose	References
GeSim	STL	Commercial	Control	[43]
Novogen	STL	Commercial	Control	[43]
BIOCAD (RegenHU)	STL	Commercial	3D models design	[44]
BIOCUT	DICOM, STL	Commercial	Convert DICOM data to STL, make slices	[44]
BIOCAM	STL	Commercial	Generate the STL and slice it	[44]
No name software from Fujifilm Holdings Corporation Ltd.	Bitmap	Commercial	Control	[43]
Axsys	Graphical formats	Commercial	Allows a user to program printing protocols	[43]
CATIA	IGES, DXF, DWG, STEP, STL, CATPart, CATProduct, CATDrawing, cgr, 3dxml	Commercial	CAD-based	[43]
NX	STL, CATIA, STEP, Parasolid, DXF, DWG, 3MF, IGES, ACIS formats, PLY (export only), image, VRML data	Commercial	CAD-based	[43]
SolidWorks	STL and general solid modeling formats	Commercial	CAD-based	[43]
Pro/Engineer	STL and neutral formats	Commercial	CAD-based	[43]
CASTS	DICOM to IGES to STL	Commercial	Based on Pro/Engineer for tissue scaffolds	[46,48]
MIMICS	DICOM to STL	Commercial	Translate medical data from MRI and CT output files to SolidWorks files + slicer	[43,74]
Biocad (Biomedical Modeling Inc.)	DICOM, SolidWorks files	Commercial	Translate DICOM to SolidWorks files, allows a user to work with the mesh and generates CAD models	[75]

(Contd...)

Table 1. (Continued)

The software name	Supported file formats	Distribution	Purpose	References
CELLINK software	GCode, STL	Commercial	Control, preview, slicing	[45]
Allevi BioPrint Pro	-	Commercial	Control from any place (runs online)	[46]
SIMMMC	Visual C#, XYZ	Research project, by request	Simulation	[109-111]
GCodeAPI.NET (PetriPrinter)	GCode, C#, Python	Research project, by request	Convert gCode to functions on C# or Python	[42]
CompuCell3D	XML	Research project, by request	Simulation of the shape changes	[113,114]
Surface Evolver	C	Research project, by request	Simulation of the shape changes considering each cell as a bubble	[116,117]
In Vesalius	Import: DICOM, Analyze Export: STL, PLY, OBJ	Open-source, free	Reconstruction of volume models based of medical scanning data	[76,77]
3D Slicer	DICOM	Open-source, free	Analysis and visualization of medical data	[78]
Simplify 3D	STL, OBJ, PLY, AMF, OFF, 3MF, MIX	Commercial	Pre-processing of the 3D model, slicing, G-code generation	[82]
Materialize Magics	STL, OBJ, PLY, AMF, OFF, 3MF, MIX	Commercial	Pre-processing of the 3D model, slicing, G-code generation	[74,135]
Cura, CuraEngine	STL, OBJ, PLY, AMF, OFF, 3MF, MIX	Open-source, free	Pre-processing of the 3D model, slicing, G-code generation	[86,87]
TinkerCAD	STL, OBJ	Free	CAD	[136]
Autodesk Meshmixer	STL, OBJ, PLY, AMF, OFF, 3MF, MIX	Free	Mesh editing and repair	[137]
Blender	OBJ, FBX, 3DS, PLY, STL	Free	CAD	[138]
BioScaffolds PG	-	Research project, by request	Scaffolds generation	[92]
HyperFun	HF, TXT	Open-source, free	Modeling by Function Representation (FRep)	[95]
Uformia	OBJ, STL	Comercial	FRep modeling	[96]
FRepCAM	C++	Research project, by request	FRep modeling	[97]
POMES	-	Research project, open-source, free	Scaffold generation	[104,139]
nTopology	STL, OBJ, PLY, OFF, X_B, STEP, CAT PART, SLDPRT, etc	Commercial	Building models and slicing (CLI)	[140]
Grasshopper	-	Commercial	Scaffold generation	[107]
Autodesk Netfabb	3DM, CATPART, CGR, FBX, IGES, IGS, JT, MODEL, NEU, PRT, XPR, CLI, SLI, STL, OBJ, PLY, AMF, 3MF, etc.	Commercial	CAM	[141]

(Contd...)

Table 1. (Continued)

The software name	Supported file formats	Distribution	Purpose	References
SCADA	-	Commercial	Bioreactor control software, also provides analysis and visualization	[121]
LabVIEW	-	Commercial	Bioreactor control software, allows a user to load Python protocols	[120]
FNet	-	Commercial	Bioreactor control software and graphical visualization	[122,123]
SIAM	-	Commercial	Bioreactor control software and graphical visualization	[122,123]
BioCommand	-	Commercial	Bioreactor control software, visualization	[124]
Curv	Export meshes to STL, OBJ, and X3	Open-source, free	FRep modeling	[133]
libfive	-	Open-source, free	FRep modeling	[134]

CAD: Computer-aided design, 3D: Three-dimensional, STL: StereoLithography, DICOM: Digital imaging and communications in medicine, CATIA: Computer-aided three-dimensional interactive application, PDF: Portable document format, VRML: Virtual reality modeling language

Only one-material surfaces are available. There is no material definition in the STL, thus complex geometry may have given errors. Typical types of errors with the STL standard are missing facets and redundant data, such as unremoved coincident surfaces or traversals, which are not crossed by coincident surfaces that will lead to weakness in the creation. Microstructures such as porosity must be in geometry thus will lead to substantial model files. Communication with build setup is an issue which may leads to issue in the orientation in printer also. Besides all the disadvantages described above, cracks and self-intersections can occur in STL files, and editing in this standard is difficult. Hence, there is a need to develop a specialized software for the heterogeneous modeling in bioprinting based on the FRep approach, which will allow us to work with suitable model file formats for this bioprinting.

5 Conclusions

Modeling for biomedicine purposes, especially for bioprinting, needs to transmit and convert biological and medical data as accurately as possible. Such a model must meet a number of special requirements, not only about the accuracy of data converting, but also others, depending on the model and printer specifics.

There are printing of vascularized tissue, skin, bones, cartilage, physiologically relevant tissue and whole living organs. Printer control drivers exist and can process a correctly created model.

Therefore, the created software must be highly specialized. A number of various widespread nowadays software tools, in the focus of using for bioprinting technologies, were reviewed and analyzed. Properties that act as advantages and disadvantages of these software tools were considered applicable to issues of digital bioprinting, especially of the bioprinting of heterogeneous tissues and organs. The authors' approach to systematization and generalization is proposed taking into account the complexity of such a process as creating a model of a complex heterogeneous structure. This paper identifies the main, most important components, through the prism of which the review of studies is conducted. It seems that our review can be regarded as a road map and have an impact on the further development of science in this field of knowledge. It should be noted that the authors have not found such a review, which claims to be comprehensive, either in domestic or foreign literature, which emphasizes its relevance and scientific novelty. The authors reviewed a number of properties of existing software tools for different issues

in the field of digital bioprinting. The direction of development of software tools that will meet critical requirements comprehensively in this field was revealed. A shortage of specialized suitable software tools was revealed with the classification as control tools, general CAD tools, tools to convert medical data to CAD formats, and a few highly specialized research-project tools. All considered software tools were sub-divided on three groups: software tools for pre-processing, for processing, and for post-processing. A number of existing software tools, especially modeling software tools, were considered in the focus of requirements of bioprinting process that they meet and stages of the bioprinting process that they allow us to describe. Comparative analysis of these software tools was carried out, and, based on it, the direction to the future development in this field was obtained. Every kind of bioprinting have specific requirements for modeling software. Programs developed for another applications are widely used. Software for operations with G-code can be used for printing of models with simple geometry. It allows us to print with very high accuracy. But it is difficult to operate with huge and complex geometry on G-code level. The accepted solution is to use standard CAD systems and software that can process meshes in STL-like format. On the other hand, these systems bring their problems strongly linked with boundary representation: cracks, holes, self-intersection in the geometry. Moreover, the size of models that were reconstructed from scans are extremely huge. Some cases of complex geometry can be captured by specific software like the software for scaffold generation. Nevertheless, a general solution for robust modeling in different scales doesn't exist. Recommendations for using of suitable software is given in Table 1.

On the authors opinion the most promising modeling systems for bioprinting are FRep based systems. They allow to operate with compact and accurate models applicable for bioprinting.

To reach progress in modeling methods, the FRep approach represents a suitable method to solve the heterogeneous volume modeling for the digital bioprinting issue. Hence, the possible

solution to the crucial problems in bioprinting is to adapt the FRep approach to the bioprinting problems and to develop a new application area such as computer science for bioprinting that represents a significant future work.

Conflicts of interest

The authors declare no conflict of interest.

References

1. Fleming PA, Argraves WS, Gentile C, *et al.*, 2010, Fusion of Uniluminal Vascular Spheroids: A Model for Assembly of Blood Vessels. *Dev Dyn*, 239:398–406. DOI: 10.1002/dvdy.22161.
2. Inamori M, Hiroshi M, Toshihisa K, 2009, An Approach for Formation of Vascularized Liver Tissue by Endothelial Cell-covered Hepatocyte Spheroid Integration. *Tissue Eng Part A*, 15:2029–2037. DOI: 10.1089/ten.tea.2008.0403.
3. Rouwkema J, Khademhosseini A, 2016, Vascularization and Angiogenesis in Tissue Engineering: Beyond Creating Static Networks. *Trends Biotechnol*, 34:733–45. DOI: 10.1016/j.tibtech.2016.03.002.
4. Hoch E, Tovar GE, Borchers K, 2014, Bioprinting of Artificial Blood Vessels: Current Approaches Towards a Demanding Goal. *Eur J Cardiothorac Surg*, 46:767–78. DOI: 10.1093/ejcts/ezu242.
5. Alonzo M, AnilKumar S, Roman B, *et al.*, 2019, 3D Bioprinting of Cardiac Tissue and Cardiac Stem Cell Therapy. *Transl Res*, 211:64–83. DOI: 10.1016/j.trsl.2019.04.004.
6. Lee W, Debasitis JC, Lee VK, *et al.*, 2009, Multi-layered Culture of Human Skin Fibroblasts and Keratinocytes Through Three-dimensional Freeform Fabrication. *Biomaterials*, 30:1587–95. DOI: 10.1016/j.biomaterials.2008.12.009.
7. Vijayavenkataraman S, Lu WF, Fuh JY. 2016, 3D Bioprinting of Skin: A State-of-the-art Review on Modelling, Materials, and Processes. *Biofabrication*, 8:032001. DOI: 10.1088/1758-5090/8/3/032001.
8. Midha S, Patra P, Mohanty S, 2019, Advances in 3D Bioprinting of Bone: Progress and Challenges. *J Tissue Eng Regen Med*, 13:925–45. DOI: 10.1002/term.2847.
9. Adepu S, Dhiman N, Laha A, *et al.*, 2017, Three-dimensional Bioprinting for Bone Tissue Regeneration. *Curr Opin Biomed Eng*, 42:22–8. DOI: 10.1016/j.cobme.2017.03.005.
10. Bulanova EA, Koudan EV, Degosserie J, *et al.*, 2017, Bioprinting of a Functional Vascularized Mouse Thyroid Gland Construct. *Biofabrication*, 9:034105. DOI:

- 10.1088/1758-5090/aa7fdd.
11. Ma X, Liu J, Zhu W, *et al.*, 2018, 3D Bioprinting of Functional Tissue Models for Personalized Drug Screening and *In Vitro* Disease Modeling. *Adv Drug Deliv Rev*, 132:235–51. DOI: 10.1016/j.addr.2018.06.011.
 12. Peng W, Unutmaz D, Ozbolat IT, 2016, Bioprinting Towards Physiologically Relevant Tissue Models for Pharmaceuticals. *Trends Biotechnol*, 34:722–32. DOI: 10.1016/j.tibtech.2016.05.013.
 13. Peng W, Datta P, Ayan B, *et al.*, 2017, 3D Bioprinting for Drug Discovery and Development in Pharmaceuticals. *Acta Biomater*, 57:26–46. DOI: 10.1016/j.actbio.2017.05.025
 14. Knowlton S, Onal S, Yu CH, *et al.*, 2015, Bioprinting for Cancer Research. *Trends Biotechnol*, 33:504–13.
 15. King SM, Presnell SC, Nguyen DG, *et al.*, 2013, Development of 3D Bioprinted Human Breast Cancer for *In Vitro* Screening of Therapeutics Targeted Against Cancer Progression. American Society of Biology, New Orleans, LA. DOI: 10.1158/1538-7445.am2014-2034.
 16. Knowlton S, Joshi A, Yenilmez B, *et al.*, 2016, Advancing Cancer Research Using Bioprinting for Tumor-on-a-chip Platforms. *Int J Bioprinting*, 2:3–8. DOI: 10.18063/ijb.2016.02.003
 17. Larsen M, Mishra R, Miller M., *et al.*, 2015, Bioprinting of Bone. In: *Essentials of 3D Biofabrication and Translation*. Academic Press, Cambridge, Massachusetts. pp. 293–308. doi.org/10.1016/b978-0-12-800972-7.00017-7.
 18. Duan B, 2017, State-of-the-art Review of 3D Bioprinting for Cardiovascular Tissue Engineering. *Ann Biomed Eng*, 45:195–209. DOI:10.1007/s10439-016-1607-5.
 19. Gao Q, Liu Z, Lin Z, *et al.*, 2017, 3D Bioprinting of Vessel-like Structures with Multilevel Fluidic Channels. *ACS Biomater Sci Eng*, 3:399–408. DOI: 10.1021/acsbomaterials.6b00643.
 20. Moldovan L, Babbey CM, Murphy MP, *et al.*, 2017, Comparison of Biomaterial-dependent and-Independent Bioprinting Methods for Cardiovascular Medicine. *Curr Opin Biomed Eng*, 2:124–31. DOI: 10.1016/j.cobme.2017.05.009
 21. Beyersdorf F, 2014, Three-dimensional Bioprinting: New Horizon for Cardiac Surgery. 46:339–41.
 22. Pourchet LJ, Thepot A, Albouy M, *et al.*, 2017, Human Skin 3D Bioprinting Using Scaffold-free Approach. *Adv Healthc Mater*, 6:1601101. DOI: 10.1002/adhm.201601101.
 23. Murphy SV, Atala A, 2014, 3D Bioprinting of Tissues and Organs. *Nat Biotechnol*, 32:773–5. DOI: 10.1038/nbt.2958.
 24. Müller M, Öztürk E, Arlov Ø, *et al.*, 2017, Alginate Sulfate-nanocellulose Bioinks for Cartilage Bioprinting Applications. *Ann Biomed Eng*, 45:210–23. DOI: 10.1007/s10439-016-1704-5.
 25. Mouser VH, Melchels FP, Visser J, *et al.*, 2016, Yield Stress Determines Bioprintability of Hydrogels Based on Gelatin-methacryloyl and Gellan Gum for Cartilage Bioprinting. *Biofabrication*, 8:035003. DOI: 10.1088/1758-5090/8/3/035003.
 26. Di Bella C, Fosang A, Donati DM, *et al.*, 2015, 3D Bioprinting of Cartilage for Orthopedic Surgeons: Reading between the Lines. *Front Surg*, 2:39. DOI: 10.3389/fsurg.2015.00039.
 27. Nam KH, Smith AS, Lone S, *et al.*, 2015, Biomimetic 3D Tissue Models for Advanced High-throughput Drug Screening. *J Lab Autom*, 20:201–15. DOI: 10.1177/2211068214557813.
 28. Takahashi K, Tanabe K, Ohnuki M, *et al.*, 2007, Induction of Pluripotent Stem Cells from Adult Human Fibroblasts by Defined Factors. *Cell*, 132:861–72. DOI: 10.1016/j.cell.2007.11.019.
 29. Datta P, Ayan B, Ozbolat IT, 2017, Bioprinting for Vascular and Vascularized Tissue Biofabrication. *Acta Biomater*, 51:1–20. DOI: 10.1016/j.actbio.2017.01.035.
 30. Sabater AL, Guarnieri A, Espana EM, *et al.*, 2013, Strategies of Human Corneal Endothelial Tissue Regeneration. *Regen Med*, 8:183–95.
 31. Tarassoli SP, Jessop ZM, Al-Sabah A, *et al.*, 2018, Skin Tissue Engineering Using 3D Bioprinting: An Evolving Research Field. *J Plastic Reconstr Aesthet Surg*, 71:615–23. DOI: 10.1016/j.bjps.2017.12.006.
 32. Katakam P, Dey B, Assaleh FH, *et al.*, 2015, Top-down and Bottom-up Approaches in 3D Printing Technologies for Drug Delivery Challenges. *Crit Rev Ther Drug Carrier Syst*, 32:61–87. DOI: 10.1615/critrevtherdrugcarriersyst.2014011157.
 33. Binder K, 2011, *In Situ* Bioprinting of the Skin. Wake Forest University, North Carolina.
 34. Shi Y, Wang W, 2019, 3D Inkjet Printing of the Zirconia Ceramic Implanted Teeth. *Mater Lett*, 261:127131. DOI: 10.1016/j.matlet.2019.127131.
 35. Yan Q, Dong H, Su J, *et al.*, 2018, A Review of 3D Printing Technology for Medical Applications. *Engineering*, 4:729–42.
 36. Mogali SR, Yeong WY, Tan H, *et al.*, 2018, Evaluation by Medical Students of the Educational Value of Multi-material and Multi-colored Three-dimensional Printed Models of the Upper Limb for Anatomical Education. *Anat Sci Educ*, 11:54–64. DOI: 10.1002/ase.1703.
 37. Hutmacher DW, 2000, Scaffolds in Tissue Engineering Bone and Cartilage. *Biomaterials*, 21:2529–43. DOI: 10.1016/s0142-9612(00)00121-6.
 38. Wu C, Luo Y, Cuniberti G, *et al.*, 2011, Three-dimensional Printing of Hierarchical and Tough Mesoporous Bioactive

- Glass Scaffolds with a Controllable Pore Architecture, Excellent Mechanical Strength and Mineralization Ability. *Acta Biomater*, 7:2644–50. DOI: 10.1016/j.actbio.2011.03.009.
39. Gratson GM, Xu M, Lewis JA, 2004, Microperiodic Structures: Direct Writing of Threedimensional Webs. *Nature*, 428:386. DOI: 10.1038/428386a.
 40. Bian WG, Lei P, Liang FH, *et al.*, 2007, Morphogenetic Protein-2 and Gel Complex on Hydroxyapatite-coated Porous Titanium to Repair Defects of Distalfemur in Rabbits. *Chin J Orthop Trauma*, 9:550–4.
 41. Pati F, Jang J, Ha DH, *et al.*, 2014, Printing Three-dimensional Tissue Analogues with Decellularized Extracellular Matrix Bioink. *Nat Commun*, 5:3935. DOI: 10.1038/ncomms4935.
 42. Gulyas M, Csiszer M, Mehes E, *et al.*, 2018, Software Tools for Cell Culture-related 3D Printed Structures. *PLoS One*, 13:e0203203. DOI: 10.1371/journal.pone.0203203.
 43. Chua CK, Wai YY, 2014, *Bioprinting: Principles and Applications*. Vol. 1. World Scientific Publishing Co., Inc., New Jersey.
 44. Available from: <https://www.regenhu.com/3d-bioprinters/software>. [Last accessed on 2020 Feb 17].
 45. Available from: <https://www.cellink.com/software>. [Last accessed on 2020 Feb 17].
 46. Available from: <https://www.3dnatives.com/en/allevi-software-bioprinting-050920195>. [Last accessed on 2020 Feb 17].
 47. Naing MW, Chua CK, Leong KF, *et al.*, 2005, Fabrication of Customised Scaffolds Using Computer-aided Design and Rapid Prototyping Techniques. *Rapid Prototyp J*, 11:249–59. DOI: 10.1108/13552540510612938.
 48. Sudarmadji N, Chua CK, Leong KF, 2012, The Development of Computer-Aided System for Tissue Scaffolds (CASTS) System for Functionally Graded Tissue-Engineering Scaffolds. In: *Computer-Aided Tissue Engineering*. Springer, Berlin. pp. 111–123. DOI: 10.1007/978-1-61779-764-4_7.
 49. Sil BC, Patel A, Crowther JM, *et al.*, 2019, A Preliminary Investigation of Additive Manufacture to Fabricate Human Nail Plate Surrogates for Pharmaceutical Testing. *Pharmaceutics*, 11:250. DOI: 10.3390/pharmaceutics11060250.
 50. Van der Valk DC, van der Ven CF, Blaser MC, *et al.*, 2018, Engineering a 3D-Bioprinted Model of Human Heart Valve Disease Using Nanoindentation-based Biomechanics. *Nanomaterials*, 8:296. DOI: 10.3390/nano8050296.
 51. Jeon O, Lee YB, Jeong H, *et al.*, 2019, Living Cell-only Bioink and Photocurable Supporting Medium for Printing and Generation of Engineered Tissues with Complex Geometries. *bioRxiv*, 1:611525. DOI: 10.1101/611525.
 52. Lehner BA, Schmieden DT, Meyer AS., 2017, A Straightforward Approach for 3D Bacterial Printing. *ACS Synth Biol*, 6:1124–30. DOI: 10.1021/acssynbio.6b00395.
 53. Jeon O, Leea YB, Hinton TJ, *et al.*, 2019, Cryopreserved Cell-laden Alginate Microgel Bioink for 3D Bioprinting of Living Tissues. *Mater Today Chem*, 12:61–70. DOI: 10.1016/j.mtchem.2018.11.009.
 54. Markstedt K, Håkanssonabd K, Toriz G, *et al.*, 2019, Materials from Trees Assembled by 3D Printing Wood Tissue Beyond Nature Limits. *Appl Mater Today*, 15:280–5. DOI: 10.1016/j.apmt.2019.02.005.
 55. Faramarzi N, Yazdi IK, Nabavinia M, *et al.*, 2018, Patient-specific Bioinks for 3D Bioprinting of Tissue Engineering Scaffolds. *Adv Healthc Mater*, 7:1701347. DOI: 10.1002/adhm.201701347.
 56. Boyer CJ, Ballard DH, Yun JW, *et al.*, 2018, Three-dimensional Printing of Cell Exclusion Spacers (CES) for Use in Motility Assays. *Pharm Res*, 35:155. DOI: 10.1007/s11095-018-2431-4.
 57. Boyer CJ, Ballard DH, Barzegar M, *et al.*, 2018, High-throughput Scaffold-free Microtissues through 3D Printing. *3D Print Med*, 4:1–6. DOI: 10.1186/s41205-018-0029-4.
 58. Ivanov DP, Grabowska AM, 2018, *In Vitro* Tissue Microarrays for Quick and Efficient Spheroid Characterization. *SLAS Discov*, 23:211–7.
 59. Yang F, Tadepalli V, Wiley BJ, 2017, 3D Printing of a Double Network Hydrogel with a Compression Strength and Elastic Modulus Greater than those of Cartilage. *ACS Biomater Sci Eng*, 3:863–9. DOI: 10.1021/acsbomaterials.7b00094.
 60. Ferraz MA, Henning HH, Costa PF, *et al.*, 2017, Improved Bovine Embryo Production in an Oviduct-on-a-Chip System: Prevention of Poly-spermic Fertilization and Parthenogenic Activation. *Lab Chip*, 17:905–16. DOI: 10.1039/c6lc01566b.
 61. Knowlton S, Yu CH, Ersoy F, *et al.*, 2016, 3D-printed Microfluidic Chips with Patterned, Cell-laden Hydrogel Constructs. *Biofabrication*, 8:025019. DOI: 10.1088/1758-5090/8/2/025019.
 62. Adamkiewicz M, Rubinsky B., 2015, Cryogenic 3D Printing for Tissue Engineering. *Cryobiology*, 71:518–21. DOI: 10.1016/j.cryobiol.2015.10.152.
 63. Cristovão AF, Sousa D, Silvestre F, *et al.*, 2019, Customized Tracheal Design Using 3D Printing of a Polymer Hydrogel: Influence of UV Laser Cross-linking on Mechanical Properties. *3D Print Med*, 5:12. DOI: 10.1186/s41205-019-0049-8.
 64. Mussi E, Furferi R, Volpe Y, *et al.*, 2019, Ear Reconstruction Simulation: From Handcrafting to 3D Printing.

- Bioengineering*, 6:14. DOI: 10.3390/bioengineering6010014.
65. Germain L, Fuentesc CA, van Vuure AW, *et al.*, 2018, 3D-printed Biodegradable Gyroid Scaffolds for Tissue Engineering Applications. *Mater Des*, 151:113–22. DOI: 10.1016/j.matdes.2018.04.037.
 66. Gu Q, Tomaskovic-Crook E, Lozano R, *et al.*, 2016, Functional 3D Neural Mini-tissues from Printed Gel-based Bioink and Human Neural Stem Cells. *Adv Healthc Mater*, 5:1429–38. DOI: 10.1002/adhm.201670060.
 67. Grigoryan B, Paulsen SJ, Corbett DC, *et al.*, 2019, Multivascular Networks and Functional Intravascular Topologies within Biocompatible Hydrogels. *Science*, 364:458–64.
 68. Costa PF, Albers HJ, Linssen JE, *et al.*, 2017, Mimicking Arterial Thrombosis in a 3D-printed Microfluidic *In Vitro* Vascular Model Based on Computed Tomography Angiography Data. *Lab Chip*, 17:2785–92. DOI: 10.1039/c7lc00202e.
 69. Liberski AR, 2016, Three-dimensional Printing of Alginate: From Seaweeds to Heart Valve Scaffolds. *QSci Connect*, 2:3. DOI: 10.5339/connect.2016.3.
 70. Miller JS, Stevens KR, Yang MT, *et al.*, 2012, Rapid Casting of Patterned Vascular Networks for Perfusable Engineered Three-dimensional Tissues. *Nat Mater*, 11:768–74. DOI: 10.1038/nmat3357.
 71. Tomov ML, Cetnar A, Do K, 2019, Patient-Specific 3-Dimensional-Bioprinted Model for *In Vitro* Analysis and Treatment Planning of Pulmonary Artery Atresia in Tetralogy of Fallot and Major Aortopulmonary Collateral Arteries. *J Am Heart Assoc*, 8:e014490. DOI: 10.1161/jaha.119.014490.
 72. McCracken JM, Rauzan BM, Kjellman JC, *et al.*, 2019, Ionic Hydrogels with Biomimetic 4D-Printed Mechanical Gradients: Models for Soft-Bodied Aquatic Organisms. *Adv Funct Mater*, 29:1806723. DOI: 10.1002/adfm.201806723.
 73. Ammar J, 2019, Defective Computer-Aided Design Software Liability in 3d Bioprinted Human Organ Equivalents. *Santa Clara High Tech Law J*. 35:37–67. Available from: <https://www.digitalcommons.law.scu.edu/chtj/vol35/iss3/2>. [Last accessed on 2020 Feb 16].
 74. Available from: <https://www.materialise.com/en/medical/mimics-innovation-suite>. [Last accessed on 2020 Feb 16].
 75. Available from: <https://www.solidworks.com/partner-product/biocard>. [Last accessed on 2020 Feb 16].
 76. Available from: <https://www.cti.gov.br/en/invesalius>. [Last accessed on 2020 Feb 16].
 77. Amorim P, de Moraes TF, Pedrini H, *et al.*, 2015, In Vesalius: An Interactive Rendering Framework for Health Care Support. International Symposium on Visual Computing. Springer, Cham.
 78. Available from: <https://www.slicer.org>. [Last accessed on 2020 Feb 16].
 79. Dernowsek A, Janaina D, Alvarenga RR, *et al.*, 2017, The Role of Information Technology in the Future of 3D Biofabrication. *J 3D Print Med*, 1:63–74.
 80. Rodrigo AR, Vladimir K, Vladimir M, *et al.*, 2015, Organ Printing as an Information Technology. *Proc Eng*, 110:151–8.
 81. Rezende RA, Mironov V, da Silva JV, 2016, Bioprinting Tissues and Organs. In: Reference Module in Materials Science and Materials Engineering. 1st ed., Vol. 1. Elsevier, Amsterdam, Netherlands, pp. 1-14. DOI: 10.1016/b978-0-12-803581-8.04139-4.
 82. Available from: <https://www.simplify3d.com>. [Last accessed on 2020 Feb 15].
 83. Sahai N, Gogoi M, 2020, 3D Tissue Scaffold Library Development from Medical Images for Bioprinting Application. *Mater Today Proc*. DOI: 10.1016/j.matpr.2019.12.063.
 84. Jardini AL, Larosa MA, Filho RM, *et al.*, 2014, Cranial Reconstruction: 3D Biomodel and Custom-built Implant Created Using Additive Manufacturing. *J Craniomaxillofac Surg*, 42:1877–84. DOI: 10.1016/j.jcms.2014.07.006.
 85. Naghieh S, Sarker MD, Abelseth E, *et al.*, 2019, Indirect 3D Bioprinting and Characterization of Alginate Scaffolds for Potential Nerve Tissue Engineering Applications. *J Mech Behav Biomed Mater*, 93:183–93. DOI: 10.31224/osf.io/pyq29.
 86. Available from: <https://www.ultimaker.com/software/ultimaker-cura>. [Last accessed on 2020 Feb 15].
 87. Available from: <https://www.github.com/ultimaker/curaengine>. [Last accessed on 2020 Feb 15].
 88. Ariffin MK, Sukindar NA, Baharudin HT, *et al.*, 2018, Slicer Method Comparison Using Open-source 3D Printer. IOP Conference Series: Earth and Environmental Science. Vol. 114. IOP Publishing, Bristol, United Kingdom. DOI: 10.1088/1755-1315/114/1/012018.
 89. Mielczarek J, Gazdowicz G, Kramarz J, *et al.*, 2015, A Prototype of a 3D Bioprinter. Solid State Phenomena. Vol. 237. Trans Tech Publications Ltd. DOI: 10.4028/www.scientific.net/ssp.237.221.
 90. Datta S, Sarkar R, Vyas V, *et al.*, 2018, Alginate-honey Bioinks with Improved Cell Responses for Applications as Bioprinted Tissue Engineered Constructs. *J Mater Res*, 33:2029–39. DOI: 10.1557/jmr.2018.202.
 91. Jessop ZM, Al-Sabah A, Gardiner MD, *et al.*, 2017,

- 3D Bioprinting for Reconstructive Surgery: Principles, Applications and Challenges. *J Plas Reconstr Aesthetic Surg*, 70:1155–70. DOI: 10.1016/j.bjps.2017.06.001.
92. Dávila JL, Freitas MS, Neto P, 2015, Software to Generate 3D Continuous Printing Paths for the Fabrication of Tissue Engineering Scaffolds. *Int J Adv Manuf Technol*, 84:1671–7. DOI: 10.1007/s00170-015-7866-8.
93. Malone E, Lipson H, 2007, Fab@ Home: The Personal Desktop Fabricator Kit. *Rapid Prototyp J*, 13:245–55. DOI: 10.1108/13552540710776197.
94. Fryazinov O, Vilbrandt T, Pasko A, 2013, Multi-scale Space-variant FRep Cellular Structures. *Comput Aided Des*, 45:26–34. DOI: 10.1016/j.cad.2011.09.007.
95. Available from: <http://www.hyperfun.org>. [Last accessed on 2020 Feb 03].
96. Available from: <http://www.uformia.com>. [Last accessed on 2020 Feb 03].
97. Popov D, Sajfert V, Pop N, et al., 2020, Efficient Contouring of Functionally Represented Objects for Additive Manufacturing. *Comput Aided Des*. Available from: <http://github.com/Torrero/FRepCAM>. [Last accessed on 2020 Jun 02].
98. Zhang XY, Yan XC, Fang G, et al., 2020, Biomechanical Influence of Structural Variation Strategies on Functionally Graded Scaffolds Constructed with Triply Periodic Minimal Surface. *Addit Manuf*, 32:101015. DOI: 10.1016/j.addma.2019.101015.
99. Tikhonov AA, Evdokimov PV, Putlyayev VI, et al., 2019, On the Choice of the Architecture of Osteoconductive Bioceramic Implants. *Inorg Mater*, 10:242–7.
100. Kapfer SC, Hyde ST, Mecke K, et al., 2011, Minimal Surface Scaffold Designs for Tissue Engineering. *Biomaterials*, 32:6875–82. DOI: 10.1016/j.biomaterials.2011.06.012.
101. Schwarz HA, 1972, *Gesammelte Mathematische Abhandlungen*. Vol. 260. American Mathematical Society, Providence, Rhode Island.
102. Schoen AH, 1970, Infinite Periodic Minimal Surfaces without Self-intersections. National Aeronautics and Space Administration, Washington, DC.
103. Karcher H, 1989, The Triply Periodic Minimal Surfaces of Alan Schoen and their Constant Mean Curvature Companions. *Manuscr Math*, 64:291–357. DOI: 10.1007/bf01165824.
104. Dinis JC, Moraes TF, Amorim HJ, et al., 2016, POMES: An Open-source Software Tool to Generate Porous/Roughness on Surface. *Proced CIRP*, 49:178–82. DOI: 10.1016/j.procir.2015.07.085.
105. Available from: <https://www.ntopology.com>. [Last accessed on 2020 Feb 05].
106. Li H, Li K, Kim T, et al., 2012, Spatial Modeling of Bone Microarchitecture. *Proc SPIE*, 8290:23.
107. Available from: <https://www.grasshopper3d.com>. [Last accessed on 2020 Feb 05].
108. Available from: <https://www.autodesk.com>. [Last accessed on 2020 Feb 05].
109. Robu A, Robu N, Neagu A, 2018, New Software Tools for Hydrogel-based Bioprinting. 2018 IEEE 12th International Symposium on Applied Computational Intelligence and Informatics (SACI). IEEE, Piscataway, New Jersey. DOI: 10.1109/saci.2018.8440971.
110. Robu A, Stoicu-Tivadar L, 2016, SIMMMC an Informatics Application for Modeling and Simulating the Evolution of Multicellular Systems in the Vicinity of Biomaterials. *Rom J Biophys*, 26:145–62.
111. Neagu A, 2017, Role of Computer Simulation to Predict the Outcome of 3D Bioprinting. *J 3D Print Med*, 1:103–21.
112. Glazier JA, Balter A, Poplawski NJ, Anderson AR, Chaplain MA, Rejniak KA, 2007, Magnetization to Morphogenesis: A Brief History of the Glazier Graner Hogeweg Model. In: Anderson AR, Chaplain MA, Rejniak KA, editors. *Single-Cell-Based Models in Biology and Medicine*, Birkhäuser, Basel, Switzerland, pp. 79–106. DOI: 10.1007/978-3-7643-8123-3_4.
113. Izaguirre JA, Chaturvedi R, Huang C, et al., 2004, CompuCell, a Multi-model Framework for Simulation of Morphogenesis. *Bioinformatics*, 20:1129–37.
114. Swat MH, Hester SD, Balter AI, et al., 2009, Multicell Simulations of Development and Disease Using the CompuCell3D Simulation Environment. In: Maly IV, editor. *Systems Biology*. Humana Press, New York, USA, pp. 361–428. DOI: 10.1007/978-1-59745-525-1_13.
115. Hoehme S, Drasdo D, 2010, A Cell-based Simulation Software for Multi-cellular Systems. *Bioinformatics*, 26:2641–2. DOI: 10.1093/bioinformatics/btq437.
116. Brakke KA, 1992, The Surface Evolver. *Exp Math*, 1:141–65.
117. Rezende R. A., V. Mironov, and J. V. L. da Silva. 2016, Bioprinting Tissues and Organs. In: *Reference Module in Materials Science and Materials Engineering*. Elsevier Amsterdam, Netherlands, pp. 1–14. DOI: 10.1016/b978-0-12-803581-8.04139-4.
118. Rezende RA, Vladimir K, Vladimir M, Lopes Da JV, 2015, Organ Printing as an Information Technology. *Proc Eng*, 110:151–8.
119. Rezende R, Laureti CA, da Silva JV, et al., 2011, Towards Simulation of a Bioreactor Environment for Biofabricated Tissue Maturation. In: Bártolo PJ, editor. *Innovative*

- Developments in Virtual and Physical Prototyping. CRC Press, Boca Raton, Florida. DOI: 10.1201/b11341-110.
120. Burdge DA, Libourel IG, 2014, Open-source Software to Control Bioflo Bioreactors. *PLoS One*, 9:e92108. DOI: 10.1371/journal.pone.0092108.
121. Available from: <http://www.ils-automation.com>. [Last accessed on 2020 Feb 06].
122. Available from: <https://www.lambda-instruments.com/fnet-fermentor-control-software>. [Last accessed on 2020 Feb 06].
123. Available from: <http://www.fermentor.net/feature/fermentation-control-software>. [Last accessed on 2020 Feb 06].
124. Available from: <https://www.bioprocessonline.com/doc/biocommand-software-0002>. [Last accessed on 2020 Feb 06].
125. Weiguo L, Schmidt B, 2006, Parallel Pattern-based Systems for Computational Biology: A Case Study. *IEEE Trans Parallel Distrib Syst*, 17:750–63. DOI: 10.1109/tpds.2006.109.
126. Carsten M, John M, Röhl M, *et al.*, 2008, Hierarchical Modeling for Computational Biology. In: International School on Formal Methods for the Design of Computer, Communication and Software Systems. Springer, Berlin, Heidelberg.
127. Davide C, 2017, Ten Quick Tips for Machine Learning in Computational Biology. *BioData Min*, 10:35.
128. Turlif V, Pasko A, Vilbrandt C, 2009, Fabricating Nature. *Technoetic Arts*, 7:165–73. DOI: 10.1386/tear.7.2.165/1.
129. Alexander P, Fryazinov O, Vilbrandt T, *et al.*, 2011, Procedural Function-based Modelling of Volumetric Microstructures. *Graph Models*, 73:165–81. DOI: 10.1016/j.gmod.2011.03.001
130. Alexander P, Adzhiev V, Sourin A, *et al.*, 1995, Function Representation in Geometric Modeling: Concepts, Implementation and Applications. *Vis Comput*, 11:429–46. DOI: 10.1007/s003710050034
131. Alexander P, Adzhiev V, Schmitt B, *et al.*, 2001, Constructive Hypervolume Modeling. *Graph Models*, 63:413–42. DOI: 10.1006/gmod.2001.0560.
132. Savchenko VV, Basnakian AG, Pasko AA, *et al.*, 1995, Simulation of a Growing Mammalian Cell Colony: Collision-Based Packing Algorithm for Deformable Particles. In: Computer Graphics. Academic Press, United States, pp. 437–447.
133. Available from: <https://www.github.com/curv3d/curv>. [Last accessed on 2020 Feb 19].
134. Available from: <https://libfive.com>. [Last accessed on 2020 Feb 19].
135. Available from: <https://www.materialise.com>. [Last accessed on 2020 Feb 19].
136. Available from: <https://www.tinkercad.com>. [Last accessed on 2020 Feb 19].
137. Available from: <http://www.meshmixer.com>. [Last accessed on 2020 Feb 19].
138. Available from: <https://www.blender.org>. [Last accessed on 2020 Feb 19].
139. Available from: <https://www.github.com/jcdinis/POMES>. [Last accessed on 2020 Feb 19].
140. Available from: <https://www.ntopology.com/ntop-platform>. [Last accessed on 2020 Feb 19].
141. Available from: <https://www.autodesk.com/products/netfabb/overview>. [Last accessed on 2020 Feb 19].

3D Bioprinting: The Roller Coaster Ride to Commercialization

Anton Elemoso^{1*}, Grigoriy Shalunov^{1*}, Yakov M. Balakhovsky², Alexander Yu. Ostrovskiy^{2,3}, Yusef D. Khesuani^{1,2}

¹Laboratory of Biotechnical Research 3D Bioprinting Solutions, Moscow, Russian Federation

²Vivax Bio, LLC, New York, NY, USA

³Independent Laboratory *IN VITRO*, Moscow, Russian Federation

Abstract: Three-dimensional (3D) bioprinting as a technology is being researched and applied since 2003. It is actually several technologies (inkjet, extrusion, laser, magnetic bioprinting, etc.) under an umbrella term “3D bioprinting.” The versatility of this technology allows widespread applications in several; however, after almost 20 years of research, there is still a limited number of cases of commercialized applications. This article discusses the potential for 3D bioprinting in regenerative medicine, drug discovery, and food industry, as well as the existing cases of companies that create commercialized products and services in the aforementioned areas and even in fashion, including their go-to-market route and financing received. We also address the main barriers to creating practical applications of 3D bioprinting within each sphere the technology that is being studied for.

Keywords: 3D bioprinting, Commercialization, Regenerative medicine, Drug discovery, Food

***Corresponding Authors:** Anton Elemoso, Laboratory of Biotechnical Research 3D Bioprinting Solutions, Moscow, Russian Federation; Anton.elemoso@gmail.com/Grigoriy Shalunov, Laboratory of Biotechnical Research 3D Bioprinting Solutions, Moscow, Russian Federation; gregshalunov@bioprinting.ru

Received: June 10, 2020; **Accepted:** June 23, 2020; **Published Online:** July 30, 2020

(This article belongs to the *Special Section: Bioprinting in Russia*)

Citation: Elemoso A, Shalunov G, Balakhovsky YM, *et al.*, 2020, 3D Bioprinting: The Roller Coaster Ride to Commercialization. *Int J Bioprint*, 6(3): 301. DOI: 10.18063/ijb.v6i3.301.

1 From 3D printing to 3D bioprinting

Three-dimensional (3D) printing is the technology of fast prototyping and additive manufacturing used to create the complex architecture of high accuracy through stage process of product construction according to the specified digital mode^[1]. Hull has received the patent for photopolymerization-based stereolithography (SLA) technology in 1986. This work was the first in the area of 3D printing techniques. Nowadays, several technologies are united by the term “3D printing:” Fused deposition modeling; SLA, digital light processing; ColorJet printing; multiple jet modeling; selective laser

sintering; selective laser melting; and direct metal laser sintering. Boland has suggested the bioprinting method based on traditional two-dimensional (2D) inkjet technology in 2003^[2]. In the same year, Mironov *et al.* have proposed the method of extrusion 3D bioprinting with the use of tissue spheroids as “building blocks”^[3].

The implementation of an automated additive process eases the fabrication of 3D products on the basis of high-precision control of their architecture, external shape, inner geometry of pores, and the correlation between high reproducibility and repeatability^[4-6]. Due to these features, 3D bioprinting technology appears

to be an extremely promising approach in the fabrication of cell material-containing biomimetic scaffolds (substrates) that serves as the basis for the creation of living and functional 3D constructs for the benefit of regenerative medicine.

Thus, 3D bioprinting is the technology of layer-by-layer fabrication of 3D tissue and organ constructs according to the assumed digital model using living cells as printing material.

For now, however, the lack of cell material is one of the limiting factors for bioprinting technology development. With advances in cell technology, this situation is going to change, but today, the bioprinting technology depends on development; it has niche implementation. It is like having Google or Baidu web search engines without the development of the internet. Therefore, the technology comes into use in new areas, such as food arrangement, fashion industry, and space science. We have also noticed the development of bioprinting technology itself; the new technologies for cell materials positioning in 3D space are emerging in addition to the “golden triad” (inkjet, extrusion, and laser bioprinting). Some of them will be discussed in more detail later on.

2 *In situ* bioprinting

One of the new approaches developed in 3D bioprinting is *in situ* bioprinting that is the replacement of tissues and organ defects using bioprinters directly during surgery. This method is considered advantageous in view of the possible “physiological” solution to the vascularization problem due to progenitor cell migration in the printed tissue-engineered construct and vascularization process that starts in surrounding recipient tissues. The idea of *in situ* bioprinting was first proposed by Weiss *et al.* in 2007^[7]. However, there were only few experiments on *in situ* bioprinting since then due to the difficulties with forming of the construct directly in the wound (on non-horizontal surfaces). As a consequence, it is necessary to have interactive software for analyzing the shape and depth of the tissue defect with the immediate consideration of this information for bioprinting. Moreover, there are special requirements for extrusion biomaterials

that particularly have to be polymerized instantly in the wound without any influence from additional factors such as ultraviolet radiation or chemical cross-linking agents. Nevertheless, *in situ* bioprinting has several significant advantages over other bioprinting techniques. Thus, applying direct bioprinting in tissue defect excludes the need to prepare the substrate that minimizes the risks of *in vitro* contamination. Furthermore, *in situ* bioprinting can exclude the need of stem and progenitor cell differentiation *in vitro* for critical or large defects, and reducing fabrication time and costs. The stem cells are immediately placed in the natural, growth-factor-rich environment that ensures organotypic differentiation when printed by stem or progenitor cells *in situ*. More importantly, *in situ* bioprinting can achieve the needed hierarchy of different cells’ placement and orientation in the defect, while in technologies of prepared scaffolds transplantation the substrate can change its shape due to swelling compression or any other deformations.

There are few experiments on *in situ* bioprinting but they confirm its advantages as stated above. Skardal *et al.* have demonstrated the possibility of inkjet *in situ* bioprinting using fibroblasts and keratinocytes for burns restoration^[8]. Kerikel *et al.* have published the results of successful experiments on bone defect restoration using laser *in situ* bioprinting^[9]. This technology seems particularly advantageous in terms of using it in hospitals to restore lost functions.

At present, we can find the presence of bioprinters in hospitals. For example, a bioprinting center has opened in Brisbane, Australia (Institute of Health and Biomedical Innovation 2017). These developments lead to the appearance of a business model which allows the printing of constructs in specialized labs, and the direct application of *in situ* bioprinting at the patient’s hospital bed.

Poietis, a French-based company, has entered into a clinical research collaboration with the Assistance Publique – Hôpitaux de Marseille (AP-HM) to pursue a clinical trial for bioprinted skin tissue. Through the partnership, Poietis and AP-HM aim to carry out a Phase I clinical trial for an Innovative Advanced Therapeutic Medicinal Product for skin healing issues. The timeline for this phase is 2 years^[10].

Such technical solutions could be used for chronic wounds such as diabetic, venous, and pressure ulcers and burn wounds that affect over 7 million patients in the United States with an annual treatment expenditure of US\$ 25 billion^[11]. Globally, this statistic increases to 11 million injuries per year. Chronic, large or non-healing wounds are especially costly because they often require multiple treatments; for example, a single diabetic foot ulcer can cost approximately US\$ 50,000 to treat. Full-thickness skin injuries are a major source of mortality and morbidity for civilians, with an estimated 500,000 civilians who were treated for these injuries in the United States each year^[12-15].

Bioprinting technology could also be used for military purposes. For example, for military personnel, burn injuries account for 10 – 30% of combat casualties in conventional warfare. US company nScrypt partnered with the U.S. Military in the Uniformed Services University 4D Bio3 Program to develop a special bioprinter for point-of-care bioprinting in unexposed conditions^[16]. It is possible that this program will bioprint meniscus from live cells and hydrogel-based scaffolds.

Economic impact on potential markets of *in situ* bioprinting could be considered as following:

The global wound care market is estimated to reach US\$ 25 billion by 2024 (Wound Care Market by Product, Research and Markets, 2019).

We are targeting the following segments:

- Skin grafts for patients with post-operative defects after removal of skin tumors or diabetic ulcers
- Plastic surgery applications
- Orthopedic surgeries
- Military and civilian field surgery for burn victims.

We estimate that the skin bioprinting market will reach around US\$ 1 billion by 2024 (3D Bioprinting Market Report, Roots Analysis, 2014).

A further US\$ 130 million is the estimated size of the cartilage bioprinting market by 2024.

Since *in situ*, bioprinting has a lot of advantages as automatization of the application process that allows to create multi-layered constructs (of complex geometrical shapes) made of configurable hydrogel solution with autologous patient cells.

The bioprinting process is carried out with high precision and can be conducted from various angles. Moreover, the computer vision system brings adaptability to the system, allowing us to use it on various wounds and defects without additional reconfiguration of the software, while IR proximity sensors ensure trajectory adjustment for breathing and other physiological processes. *In situ* bioprinting will allow to print structures with small (300 µm) pores, which help maintain optimal temperature and humidity inside the healing wound, thereby speeding up the healing process and lowering the incidence of complications.

However, it also has some disadvantages (not only technological ones) such as bioprinters, cell material and biomaterials of substrates (scaffolds) registration for their use in clinical practice, clinical and pre-clinical trials, and intellectual property registration. Nevertheless, we see positive changes in approaching the idea of printing tissues and organs, not just scientific publications.

3 Space bioprinting

As we divined in our previous review, commercial companies started to provide B2S (business-to-science) services of conducting experiments for research institutions on the international space station (ISS)^[17]. Commercial companies, such as 3D Bioprinting Solutions, Techshot, and nScrypt, have set series of experiments in space. Interestingly, for these experiments, bioprinting technology was used not only for regenerative medicine purposes but also for other research purposes, such as:

- Bacteria behavior in space study
Conventionally, genetic antibiotic resistance research is carried out on 2D cultures on earth. However, such experiment design ignores the fact that bacteria in living organisms tend to form 3D biofilms, which have the unique phenotypic antibiotic resistance, due to the fact that antibiotic molecules do not diffuse into the full volume of a biofilm.
- Protein structure modeling in space
There is a lot of interest in structure prediction as a screening process for proteins that are

not tenable for experimental determination. Structure prediction depends on protein crystallography, which allows us to create a mathematical model of the protein in question.

- Biomaterial research

The calcium phosphate particles can be used for bone defect regeneration. Microgravity allows obtaining biocompatible octocalcium phosphate phase rapidly in the final product. Thus, magnetic levitation of calcium phosphate particles is a promising approach for rapid 3D fabrication in the field of bone tissue engineering.

More companies plan to participate in space experiments. Cellink, a Swedish 3D bioprinter manufacturer, has announced a strategic collaboration with Made In Space, a microgravity manufacturing specialist, to identify bioprinting opportunities for the ISS (<https://cellink.com/cellink-partners-with-made-in-space-for-microgravity-bioprinting/>). US companies such as Allevi and Made In Space are also developing 3D bioprinter for space^[18].

In space, companies try to use two main approaches: (i) Using classical extrusion bioprinting technology (main challenge to overcome microgravity, and especially using hydrogels for scaffold material printing) and magnetic/acoustic approach, and (ii) using novel technology that applies microgravity as an additional trigger for biofabrication (main challenge to design 3D model of the printed construct).

These technologies are compared in **Figure 1**.

Here, we would like to discuss in detail the acoustic and magnetic bioprinting technologies as the new directions of bioprinting.

The use of magnetic forces in tissue engineering has begun with a series of studies by Ito *et al.*^[19]. The developed approach was defined as “magnetic force-driven tissue engineering.” Magnets and magnetic fields were used to place cells with magnetic nanoparticles on various scaffolds in initial series of experiments. The next step in the development of this approach was the use of magnetic forces to control the movement of tissue spheroids containing magnetic nanoparticles in 2D space^[20,21]. Recent works have shown that superparamagnetic nanoparticles of iron oxide

in moderate concentrations are not toxic and are recovered by binding iron ions in the body^[22].

Demirci *et al.* were the first who have used the method of magnetic levitation of cells without its saturation with magnetic nanoparticle^[23]. Diamagnetic objects ranging in size from several millimeters to centimeters were used in these experiments. Their final equilibrium configuration depended on the balance of magnetic and gravitational forces (in special paramagnetic environment, in the gradient magnetic field created by special magnets, and in the absence of direct contacts between its components). Such approach allows to manage building blocks in paramagnetic environments to fabricate 3D construct^[24]. Gadolinium salts were added as the additional agent to enhance the medium paramagnetic properties in their experiments^[25,26]. Gadolinium salts can be included in some contrast mediums used in magnetic resonance imaging (e.g., Omniscan), so they are allowed for clinical use. Nevertheless, gadolinium salts in high concentrations can cause toxic effect on cells and tissue spheroids. This approach also creates certain risk of osmotic pressure imbalance due to excessive ion concentration in the paramagnetic medium.

Another approach in the development of “scaffold-free” technology is the management of cell material (including tissue spheroids) using ultrasonic waves or so-called acoustic bioprinting^[27]. One of the approaches in acoustic bioprinting is to control cells using so-called “acoustic tweezers.”

The mode of action of “acoustic tweezers” is as follows: Piezoelectric substrate and two transversely-spaced pairs of interdigital transducers generate standing acoustic-surface waves that capture and move cells. The change of the cell position occurs due to the change in acoustic amplitude and transducers pair phase. Since phase and amplitude can be set and changed easily, the accuracy of cell movement will be limited only by the equipment resolution. Whereby, the cell movement speed can reach 5 $\mu\text{m/s}$ ^[28]. Some studies have illustrated that such manipulation with cell material does not affect its viability, functionality, and genes expression^[29,30]. Moreover, it has variety of advantages in comparison with approaches

	Additive printing	Formative printing
Scaffold	Required	Not required
Printing speed	Medium	High
Printing area	Limited by axes of the bioprinter	Limited by cuvette volume
Viability of cells	Might decrease, due to the extrusion process	Might decrease, due to the concentration of magnetic/paramagnetic supplements
Biosafety	Sealing of the whole bioprinting system is required	Biosafety is inherent, cuvette is a hermetic medium

Figure 1. Comparison of additive and formative bioprinting.

described above, such as: (i) Ability to control cells in closed systems that significantly reduces the risk of possible microbial and fungal contamination; (ii) allows not to use any cell material labeling for manipulation; and (iii) allows to avoid any physical impact on the cells. At the same time, “acoustic tweezers” have the capacity that is 106-fold lower than optical tweezers^[31]. Thus, “acoustic tweezers” work in the frequency range similar to the one that is used in medical ultrasound equipment (like ultrasound diagnostic apparatus for the imaging of the fetus in the womb)^[32]. The platform consisting of “acoustic tweezers” can be built in the unified software and hardware complex without the use of nozzles and other expensive elements of classic bioprinters necessary for biomaterial management (nozzle-free approach).

The simultaneous use of magnetic and acoustic fields for cell material control using an inhomogeneous magnetic-acoustic field is possible. The principle of this method involves fast levitation fabrication of construct in inhomogeneous magnetic field from cells and/or tissue spheroids chaotically distributed in the active volume of liquid medium. The construct is fabricated in the area where there is the “magnetic-acoustic trap” (area of gravitational, magnetic, and acoustic fields crossing). The gravitational forces are compensated, and tissue spheroids experience forces pulling them together. The final construct can have spherical, annular, ellipsoidal, or other shapes defined by the specific configuration of the

magnetic-acoustic field^[33]. The described approach involves the development of complex acoustic and magnetic waves design and requires special skills and competencies in experimental physics as well as the availability of specialized equipment. That is why this bioprinting method is not widely applied as it is still on the engineering development stage. Using this method, we create not only the construct model but also field (or several fields) configuration that will determine the object’s shape.

Thus, whichever method of bioprinting in microgravity could be used, the main purposes for tissue engineering in space are:

3.1 Investigation of gravity-free effect on human tissues

Tissue engineering constructions are used to study the gravity-free effect on human tissues on earth and in space. First tissue construction (cartilage)^[34] was created in zero-gravity in space on the Russian space station “MIR” by the team of the Massachusetts Institute of Technology (MIT) under the supervision of Professor Robert Langer using rotation bioreactor Synthecon developed by NASA. Cell suspension forms tissue aggregates (tissue spheroids) in this rotation-type bioreactor.

3.2 Drug discovery and disease modeling (including possible diseases during long space flights)

During the great voyages of discovery through world oceans, seamen suffered from an awful

disease—scurvy that was caused by chronic vitamin C deficiency as a result of the lack of fresh fruit and vegetables. This condition happened when the seafaring people were at sea continuously for probably more than 3 months, at some stage in the voyaging and the price was more than 2 million lives^[35]. This case shows that humans have to prepare for investigating not only new deep space but also possible risks and dangers during these flights.

3.3 Investigation of space radiation effect on human tissues

Another separate, essential branch of space biological science is space radiation studies. Recently, the possibility of creating permanent bases on the Moon, sending manned spacecraft to Mars, and establishing planetary settlements on the planet has been in discussion more frequently according to the vast experience of habitability of space. Space radiation is known to have a negative effect on the human body, especially in space flights outside the earth's protective magnetosphere. Bioprinting technology allows to create radiation-sensitive organs, so-called sentinel organs, as models for further studies of radiation effects.

4 Drug discovery

The pharmaceutical industry could strongly benefit from having means of early detection of negative side effects of potential drugs. This allows pharmacologists to save time and money on formulations as well as cases when a side effect was only discovered when the drug is already in the market but needs to be recalled, with obvious legal and financial ramifications.

2D-based assays are currently the main technology being used for pre-clinical studies. The problem with this technology is that in two dimensions, the cells have a limited amount of contacts between themselves. Most of their contacts are with the culture medium or the surface they are on. This in turn leads to limited modeling of real human tissue interactions (signaling, biomarkers, etc.) This is the reason why the drugs

tested in 2D fail when tested *in vivo*. Finally, a new alternative has become available – tests 3D tissue and organ constructs. They can also be used for testing cosmetic formulations as an alternative to animal tests which are getting banned in different jurisdictions (like the EU since 2013).

The increased effectiveness of 3D cultures comparing to 2D analogs is widely accepted. However, the question on how to obtain standardized fabrication methods that allow reproducibility of constructs, rapidness, and cost-effectiveness required for drug testing remains. 3D bioprinting with its automation capabilities and possibility to form complex structures seems the most likely candidate for providing the answer. Other advantages of 3D bioprinting in comparison to other fabrication methods include the ability to create channels for vascularization inside the constructs as well as allowing coculture to form heterotypic constructs under the conditions similar to a typical tissue environment. This increases interest in applying 3D bioprinting to various stages drug discovery (**Figure 2**)^[36-38].

Biofabrication strategies that are being used include rotating flask methods, liquid overlay, hanging drop, and magnetic levitation. Manual cell seeding or fabrication of a mold are typically used for these methods^[39]. Bioprinting offers higher precision, resolution, and accuracy in comparison to the methods listed above^[40]. Other advantages of bioprinting include easier fabrication of spatially-patterned coculture models, low risk of cross-contamination while handling different cell types (in a limited physical space), precise control over delivery of growth factors and genes, and controlled architecture with high-throughput. Bioprinting also enables fabrication of constructs with desired pore sizes associated with a specific type of tissue as well as a controlled architecture. A crucial advantage of bioprinting is that it can be utilized under physiologically-amenable conditions (e.g., pH, humidity, and temperature), while adding genes and proteins that help modulate the behavior of cells. Moreover, using magnetic levitation for bioprinting of tissue spheroids improves the throughput and resolution of bioprinted constructs^[41].

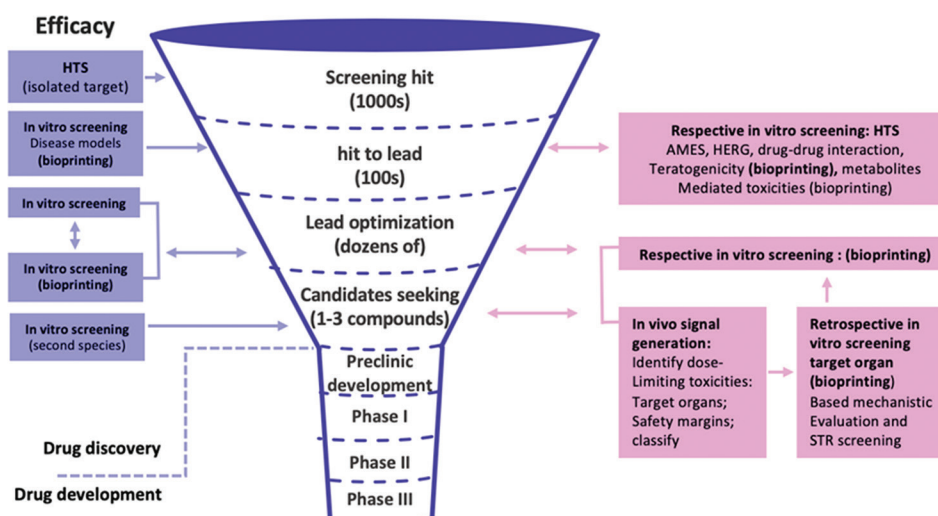


Figure 2. The role of bioprinting in different stages of drug discovery.

In comparison to other fabrication methods, 3D bioprinting offers increased ability to position multiple cell types precisely mimicking the native tissue design. Another opportunity provided by bioprinting is creating a 3D construct considering coculture and vascularization possibilities by depositing multiple cell types (**Figure 3**). The ability to process several materials, complex spatial positioning and make bioprinting a very adaptive technology and increased cell-matrix interactions improves the viability of cells for longer periods. Recent studies have demonstrated that bioprinting allows high-throughput fabrication in generating^[42,43].

Drug testing requires perfusion, which is relatively easy for bioprinted constructs. There is increased demand for patient-specific diseased models for personalized drug discovery and therapeutic planning, for which bioprinting has already demonstrated undoubted potential, especially in the application of induced pluripotent stem cells (iPSCs)^[44,45]. It is necessary to note, however, that there have not been cases of completely functional tissue made of bioprinted iPSCs^[45]. Considering all of the advantages detailed above, there are multiple *in vitro* models for drug testing that has already been created (detailed in **Table 1**)^[46].

3D bioprinting technology has provided major advantages in the fabrication of 3D tissue and

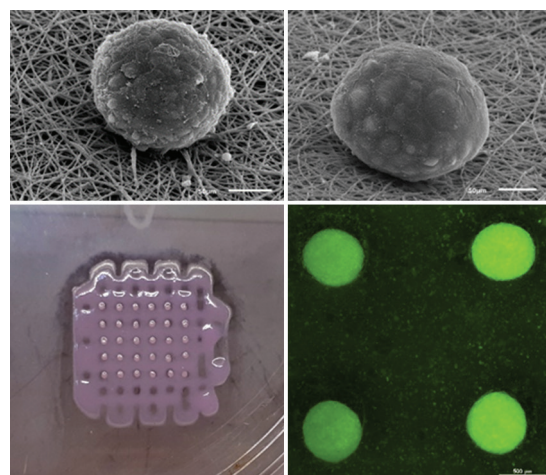


Figure 3. Type-specific 3D spheroids robotically inserted into the collagen grid represent *in vitro* model of human tissue.

organ models in comparison to other fabrication methods. Its unique properties make bioprinting a prime candidate for high-throughput industrial applications, even though vascularization remains a challenge. An interesting approach with a lot of promise for fabrication of *in vitro* tissue and organ models is combining bioreactors with on-chip perfusion. Naturally, bioprinters will need to increase their user-friendliness and lower the costs to become commercially viable on a large scale. In summary, bioprinted 3D models will likely soon be adopted by pharmaceutical companies for drug discovery.

Table 1. *In vitro* organ models for drug testing manufactured through bioprinting.

Organ/Tissue model	Bioprinting modality	Bioink	Cell types	Drugs tested	References
Liver	Sacrificial bioprinting	GelMA	-HepG2/C3A cells, HUVECs	-Acetaminophen, Trovafloxacin,	[47,48]
	DBB	Alginate	-HepG2 and human epithelial cells	-Levofloxacin -Amifostine	[49,50]
Vascular network	Indirect bioprinting	Gelatin/Pluronic	MSCs	Rho-kinase inhibitors	[51-53]
Alveolar model	Valve-based printing	Matrigel™	Type-II alveolar epithelial cells and endothelial cells		[54]
Cornea	EBB	Collagen/ alginate	keratinocytes	-	[55]
Intestine	EBB	Scaffold-free	Epithelial cells of human intestinal origin and myofibroblasts	Indomethacin	[56]
Kidney	EBB	Gelatin/fibrin as ECM and Pluronic as sacrificial ink	Proximal tubule epithelial cells	Cyclosporine A, cisplatin, resazurin	[57]
Muscle	EBB	Alginate/Pluronic	C2C12 cells	Cardiotoxin	[58,59]
Heart	EBB	Fibrin	Rat heart origin primary cardiomyocytes	Epinephrine and carbachol	[60]
Glioma	EBB	Alginate/gelatin/ fibrinogen	Breast cancer cells	Temozolomide	[61]
	DBB	Matrigel	OVCAR-5 cells and MRC-5 fibroblasts	Prolactin, estrodine	[62]
3D neoplastic tissues	EBB	Alginate/gelatin/ fibrinogen	HeLa cells	Paclitaxel	[63]
Skin	LBB	Collagen/ Matrigel™	HaCaT keratinocytes/ NIH3T3 fibroblasts	All-trans retinoic acid, dexamethasone, doxorubicin, S ² -fluorouracil, and forskolin	[64,65]

The legal aspect of 3D bioprinting is becoming increasingly important with the growing usage of this technology. There are concerns that while bioprinting is regulated by existing laws that govern medicine and medical research, this current framework does not allow us to mitigate risks to patients, as well as address the requirements of health-care providers and manufacturers. At the very least, that is the situation in the US and EU^[66]. There is no specific regulatory framework or even strategy toward 3D bioprinting developed in countries that lead the way in biofabrication research and industry applications. This is further complicated by the fact that 3D bioprinting is a truly unique technology in the sense that it combines 3D printing techniques, materials science and cell biology, and meaning this technology combines

the challenges of all possible applications (organ transplantation, medical devices, and cell therapy)^[67,68]. Separate regulation does not account for the combined use of the technologies and applications listed above. There is also a question of multiple actors involved in the production chain.

There is also the issue of informed consent, which is not clearly regulated when it comes to novel medical technologies. Ideally, a consent form should inform about all potential risks and adverse effects as well as list a detailed composition of a bioprinted product and fully describe the implantation process. Donors should be better informed of how their cells, tissues, or organs can be utilized now or in the future and this information should be made available with strict access guidelines through specialized databases.

This brings on another issue of data protection on a global scale which requires specialized infrastructure for storing encrypted files with data about cells, tissues, and organs received by patients. This information should also be in a unified format, accessible by commercially used bioprinters, with measures to protect intellectual property also in place. Clearer guidance would also assist innovators, who had to be able to better understand how their products are to be classified once released into the market. One suggested approach to licensing in bioprinting is placing responsibility on companies to share benefits and at the same time emphasizing the role of public research.

A draft version of guidelines was released in May 2016 by the US Food and Drug Administration (FDA) for manufacturers of medical devices that work with additive manufacturing^[69]. While it was meant to provide manufacturers with the agency's initial outlook on manufacturing 3D printed devices, it does not address the use or incorporation of biological, cellular, or tissue-based products in additive manufacturing. Products that contain living human cells/tissues (including specific medical devices) and are intended for transplantation in human patients are qualified by the FDA as human cells, tissues, and cellular and tissue-based products (or combination products). Similar classification criteria exist in the EU, but without a general definition or specific regulation for combination products. They are currently regulated as medicinal products or medical devices^[70,71].

In summary, international cooperation is required to create clear legal guidelines regulating 3D bioprinting while ensuring that intellectual property, safety, and bioethics are addressed on a global scale. Hopefully, together with educating medical professionals and general population, this will enable future innovations and active medical applications of 3D bioprinting.

5 Financing

3D bioprinting industry is not currently being widely used in healthcare, and its large

commercial success is likely to be at least 15 – 20 years away, when bioprinted human organs will become available for transplantation at the costs comparable to the current market. However, a few companies have already launched products into the market and have raised investments through various available means.

There is an important distinction between investments in bioprinting companies focused on regenerative medicine and companies that are working toward creating a cultured meat product. While the former has produced a couple of notable initial public offerings (IPOs) (Organovo, Cellink), the latter have also recently begun to attract investor interest, which led to some major investment rounds. In this chapter, we are covering regenerative medicine companies, and you can read about cultured meat investments in chapter 9.

The first bioprinting company that raised significant amounts of capital is Organovo which had set to create tissue models for drug discovery. Organovo went public in 2012 using a reverse IPO and over the next few years raised about US\$ 128 million in several installments^[72]. This was a crucial breakthrough for the whole bioprinting industry not to mention the company itself. In December 2019, Organovo and Tarveda Therapeutics announced a merger agreement under which Tarveda would execute a merger with a subsidiary of Organovo; the joint company would use the name Tarveda Therapeutics, Inc. and trade on Nasdaq.

CELLINK decided to pursue their IPO just several months after the company was created. However, that was not without reason, as at the time, their bioprinter (priced at US\$ 10,000) was sold in 25 countries, mostly to research institutions. CELLINK listed on Nasdaq First North, and notably their IPO was oversubscribed by 1070%. Cellink's current market cap is at US\$ 400 million^[73].

Cyfuse Biomedical K.K., a manufacturer of 3D bioprinters from Japan, closed its Series B private placement funding in 2015. Cyfuse raised about US\$ 12.5 million, bringing the total amount of investments to about US\$ 17.8 million^[74].

Poietis, a bioprinting company that was one of the first to create a commercially available

bioprinted tissue has raised €5 million in their Series A round in 2018. Poietis has established partnerships with companies such as Badische Anilin und Soda Fabrik and. The contributors to this round included Nouvelle Aquitaine Co-investment Fund. This has provided the company with financial resources that will enable them to accelerate compatibility with regulations and good manufacturing practices requirements. The company has announced that it could produce the first bioprinted tissues for implantation into patients in 2021^[75].

In 2019, Aspect Biosystems, a Canadian biotech company, have raised US\$ 20 million during their Series A from Radical Ventures, a VC firm focused on companies that aim to solve global problems as well as Pangaea Ventures, Pallasite Ventures, and Rhino Ventures. The company specializes in microfluidic 3D bioprinting. Aspect Biosystems have created a bioprinting platform for production of human tissues^[76].

Allevi, formerly known as Biobots, creates desktop 3D bioprinters. The company's clients include companies such as AbbVie, GSK, and Johnson & Johnson. The company was founded in 2014 and has US\$ 3.6 million in funding raised up to date^[77].

We may expect the industry to start consolidating in the next few years through mergers of bioprinting companies with each other and with strategic partners through acquisitions, reflecting the general trend of the increased interest of industry leaders in regenerative medicine and drug discovery through testing on 3D models.

6 Food industry

Another emerging industry where bioprinting is widely used is alternative protein food technology. There are two major fields of alternative protein: Plant-based meat products and cultured meat products. Plant-based products use specific plant proteins and other supplements to imitate taste and texture of meat, while cell-based products aim to grow various cell types, which constitute natural meat tissues *in vitro* and then assemble these cells into a final product. Both fields use additive

manufacturing approaches as means to confer complex specific geometric shapes, organoleptic qualities, or nutritional characteristics to the final product.

While none of the cell-based meat startups have not rolled out their products on any market yet, plant-based alternatives have been growing by leaps and bounds over the recent years, culminating in the successful IPO of Beyond Meat, an American company, that produces a range of meat alternatives using a mix of various plant proteins, and achieved more than 200% growth^[78]. Spain-based Novameat^[79] and Israeli Redefine Meat^[80] now use 3D printing to create more sophisticated plant-based products; while the former focuses on exact material formulation and simulation of proper meat texture, the latter develops multi-layered plant-based steak structure.

Cell-based meat (also known as *in vitro* meat or IVM) is another approach to production of alternative protein. Despite not being present on the market, cultured meat products still attract attention from potential consumers (**Figure 4**), some studies show that as many as 66% of US adults would try meat grown from animal cells^[81].

Cultured meat startups vary widely in their approach to product development (**Table 2**). Since one of the major barriers, serum-free medium formulation, was overcome in November 2019 by Mosa Meats that was the first to introduce a cell-based burger patty^[82], several companies now focus on using bioprinting to create unique products.

Since the cost of final product is still expected to be prohibitive during early stages, there are various possible applications, for example, production of cultured meat in space^[83]. Space launches incur high costs and constant resupply is not a viable solution for long-term manned missions. Therefore, creation of sustainable food production systems is a high priority for multiple space agencies.

Keeping crewmembers fed during such expeditions will face several challenges, and cultured meat products can potentially solve most of them. Using water recovery system in combination with serum-free medium produced

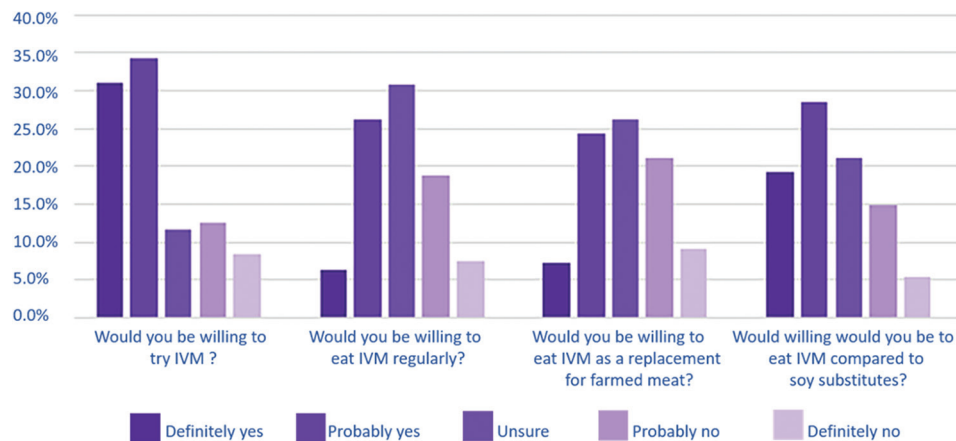


Figure 4. Consumer survey on *in vitro* meat.

Table 2. Cell-based meat companies.

Cell source species	Bioprinting	Non-bioprinting companies	
Mammals	Meal Source Technologies Aleph Farms Fork and Goode Meatech	Wild Earth LabFarm Mosa Meat Biftek. Co. Higher Steaks Cell Farm	Bio. Tech. Foods New Age Meats Meatable MiraiFoods Biofood
Seafood	BlueNalu	Avant Finless Foods Future Fields Clean research	Wild Type Seafuture Shiok Meats
Poultry		JUST Bond Pet Foods Clear Meat Integriculture	Gourmet SuperMeat Peace of Meat Vital Meat
Multi-species	Future Meat Technologies	Memphis meats VOW Foods	Cellular Agriculture Mission Barns

by algae will create self-sustaining systems, which would in turn eliminate any need for resupply runs. Moreover, the self-sustaining systems allow astronauts to directly control and adjust their diet to combat specific medical conditions such as muscle atrophy and osteopenia, which arise during prolonged space travel. In addition to meeting specific medical and nutrition requirements, these systems also allow crewmembers to select palatability preferences as bioprinting can be used to create distinct texture and palatability characteristics in the food that can help crewmembers to endure all the various psychological hardships of long-duration space travel.

Early prototypes of this technology were produced in joint experiments by 3D Bioprinting Solutions^[84] and Aleph Farms^[85,86]. In these experiments aboard the ISS, magnetic bioprinting was used to assemble spherical constructs out of spheroids, made from animal and fish cells. Both 3D Bioprinting Solutions and Aleph Farms carried out extensive research in tissue engineering, developed originally for regenerative medicine purposes, to create food products from multiple tissue types (e.g., myoblasts, fibroblasts, adipocytes, and blood vessels). Multiple companies across the world embrace this approach, transferring bioprinting advances from tissue engineering to food tech.

BlueNalu, which employs several former members of Organovo, plans to print thin slices of layered fish tissues that consist of muscle cells, connective tissue, and fat cells, and combine it with industrial-scale bioreactor system^[87]. Meatech and Future Meat Technologies, two startups from Israel, also plan to use bioprinting as a method to combine multiple tissue types to create a final product which would resemble natural meat cut texture. However, beyond bioprinting, they use different technologies; Meatech plans to use umbilical cord samples as the prime source of cells, while future meat technologies, according to their patents, plans to focus on bioreactor system development^[88]. Fork and Goode, an American company led by Gabor Forgacs which is one of the bioprinting pioneers, has not unveiled any product plans, but they have multiple patents relevant to the printing of food products which were filed by Organovo several years ago^[89].

However, the application of bioprinting in consumer goods is not limited to the food industry only. Cellular agriculture in textile production also uses its techniques. BioLogic, based in MIT, uses bioprinting to create responsive biomaterial for sportswear^[90,91], while Modern Meadows employs bioprinting to create artificial leather textiles. This novel approach has the potential to solve the issue of animal abuse in fashion industry, but there is more – technologies used by this two companies, BioLogic's approach in particular, allow us to create smart fabrics that could potentially revolutionize a wide range of industries. Sensors and actuators on nanoscale will transform everything, from fashion to military applications, since they can adjust the properties of a wide range of materials in real time^[92].

7 Conclusion

The practical applications described in this article demonstrate the evident potential of 3D bioprinting for a number of industries. There is undoubtedly increasing interest from both private investors and governments as bioprinting can be applied to solving crucial and fundamental problems such as the lack of donor organs or the environmental impact of meat industry. This should propel both the

science and the opportunities for commercialization forward. Once the limiting factors such as the lack of adequate cell material are successfully addressed, we shall no doubt see more commercial products and services in regenerative medicine, space science, drug discovery, food industry, and perhaps even beyond that.

Conflict of interest

The authors declare no conflict of interest.

References

1. O'Brien CM, Holmes B, Faucett S, *et al.*, 2015, Three-Dimensional Printing of Nanomaterial Scaffolds for Complex Tissue Regeneration. *Tissue Eng*, 21:103–14. DOI: 10.1089/ten.teb.2014.0168.
2. Wilson WC, Boland T, 2003, Cell and Organ Printing 1: Protein and Cell Printers. *Anat Rec*, 272a:491–6. DOI: 10.1002/ar.a.10057.
3. Mironov V, Boland T, Trusk T, 2003, Organ Printing: Computer-aided Jet-based 3D Tissue Engineering. *Trends Biotechnol*, 21:157–61. DOI: 10.1016/s0167-7799(03)00033-7.
4. Dababneh AB, Ozbolat IT, 2014, Bioprinting Technology: A Current State-of-the-Art Review. *J Manuf Sci Eng*, 136:61.
5. Duan B, Hockaday LA, Kang KH, Butcher JT, 2013, Bioprinting of Heterogeneous Aortic Valve Conduits with Alginate/Gelatin Hydrogels. *J Biomed Mater Res*, 101A:1255–64. DOI: 10.1002/jbm.a.34420.
6. Wang S, Lee JM, Yeong WY, 2007, Smart Hydrogels for 3D Bioprinting. *J Bioprinting*, 1:3–14. DOI: 10.18063/ijb.2015.01.005.
7. Campbell PG, Weiss LE, 2007, Tissue Engineering with the Aid of Inkjet Printers. *Expert Opin Biol Ther*, 7:1123–7.
8. Skardal A, Mack D, Kapetanovic E, 2012, Bioprinted Amniotic Fluid-Derived Stem Cells Accelerate Healing of Large Skin Wounds. *Stem Cells Transl Med*, 1:792–802. DOI: 10.5966/sctm.2012-0088.
9. Keriquel V, Guillemot F, Arnault I, 2010, *In Vivo* Bioprinting for Computer and Robotic-assisted Medical Intervention: Preliminary Study in Mice. *Biofabrication*, 2:14. DOI: 10.1088/1758-5082/2/1/014101.
10. Poietis Signs a Clinical Research Collaboration Contract with the Assistance Publique Hôpitaux de Marseille (AP-HM) to Prepare the First Clinical Trial of a Bioprinted Skin. Available from: <https://www.poietis.com/poietis-signs-a-clinical-research-collaboration-contract-with-the-assistance->

- publique-hopitaux-de-marseille-ap-hm-to-prepare-the-first-clinical-trial-of-a-bioprinted-skin. DOI: 10.1016/j.traccli.2009.12.003.
11. Sen CK, Gordillo GM, Roy S, 2017, Human skin wounds: A major and snowballing threat to public health and the economy. *Wound Repair Regen*, 17:763–71. DOI: 10.1111/j.1524-475x.2009.00543.x.
 12. Albanna M, Binder KM, Murphy S, *et al.*, 2019, *In Situ* Bioprinting of Autologous Skin Cells Accelerates Wound Healing of Extensive Excisional Full Thickness Wounds. *Sci Rep*, 9:1856. DOI: 10.1038/s41598-018-38366-w.
 13. Beckrich K, Aronovitch SA, 1999, Hospital-Acquired Pressure Ulcers: A Comparison of Costs in Medical vs. Surgical Patients. *Nurs Econ*, 17:263–71.
 14. Miller SF, Bessey P, Lentz CW, *et al.*, 2008, National Burn Repository 2007 Report: A Synopsis of the 2007 Call for Data. *J Burn Care Res*, 29:862–70. DOI: 10.1097/bcr.0b013e31818cb046.
 15. Thomas SJ, Kramer GC, Herndon DN, 2003, Burns: Military Options and Tactical Solutions. *J Trauma*, 54:207–18.
 16. nScript and Taking Bioprinting to the Field. Available from: <https://www.3dprintingmedia.network/bioprinting-today-series-nscript>. [Last accessed on 2020 Jul 27].
 17. Balakhovskiy Y, Ostrovskiy A, Khesuani Y, 2017, Emerging business models toward commercialization of bioprinting technology. In: 3D Printing and Biofabrication. Springer, Berlin, pp. 1–22. DOI: 10.1007/978-3-319-40498-1_25-1.
 18. Available from: <https://www.allevi3d.com/allevi-bioprinting-in-space>. [Last accessed on 2020 Jul 27].
 19. Ito A, Ino K, Hayashida M, 2005, Novel Methodology for Fabrication of Tissue-Engineered Tubular Constructs Using Magnetite Nanoparticles and Magnetic Force. *Tissue Eng*, 11:1553–61. DOI: 10.1089/ten.2005.11.1553.
 20. Luciani N, Du V, Gazeau F, *et al.*, 2016, Successful Chondrogenesis within Scaffolds, Using Magnetic Stem Cell Confinement and Bioreactor Maturation. *Acta Biomater*, 37:101–10. DOI: 10.1016/j.actbio.2016.04.009.
 21. Whatley BR, Li X, Zhang N, *et al.*, 2014, Magnetic-Directed Patterning of Cell Spheroids. *J Biomed Mater Res A*, 102:1537–47. DOI: 10.1002/jbm.a.34797.
 22. Mazuel F, Espinosa A, Luciani N, 2016, Massive Intracellular Biodegradation of Iron Oxide Nanoparticles Evidenced Magnetically at Single-Endosome and Tissue Levels. *ACS Nano*, 8:7627–38. DOI: 10.1021/acsnano.6b02876.
 23. Tasoglu S, Yu CH, Liaudanskaya V, *et al.*, 2015, Magnetic Levitational Assembly for Living Material Fabrication. *Adv Healthc Mater*, 4:1469–76. DOI: 10.1002/adhm.201500092.
 24. Durmus NG, Tekin HC, Guven S, 2015, Magnetic Levitation of Single Cells. *Proc Natl Acad Sci*, 112:3661–8. DOI: 10.1073/pnas.1509250112.
 25. Mirica KA, Ilievski F, Ellerbee AK, *et al.*, 2011, Using Magnetic Levitation for Three Dimensional Self-Assembly. *Adv Mater*, 23:4134–40. DOI: 10.1002/adma.201101917.
 26. Subramaniam AB, Yang D, Yu HD, *et al.*, 2014, Noncontact Orientation of Objects in Three-dimensional Space Using Magnetic Levitation. *Proc Natl Acad Sci*, 111:12980–85. DOI: 10.1073/pnas.1408705111.
 27. Guo F, Mao Z, Chen Y, *et al.*, 2016, Three-Dimensional Manipulation of Single Cells Using Surface Acoustic Waves. *Proc Natl Acad Sci*, 113:1522–7. DOI: 10.1073/pnas.1524813113.
 28. Guo F, Li P, French JB, *et al.*, 2015, Controlling Cell-Cell Interactions Using Surface Acoustic Waves. *Proc Natl Acad Sci*, 112:43–8. DOI: 10.1073/pnas.1422068112.
 29. Ding X, Li P, Lin SC, *et al.*, 2013, Surface Acoustic Wave Microfluidics. *Lab Chip*, 18:3626–49.
 30. Li P, Mao Z, Peng Z, *et al.*, 2015, Acoustic Separation of Circulating Tumor Cells. *Proc Natl Acad Sci*, 112:4970–5. DOI: 10.1073/pnas.1504484112.
 31. Sapozhnikov OA, Bailey MR, 2013, Radiation Force of an Arbitrary Acoustic Beam on an Elastic Sphere in a Fluid. *J Acoust Soc Am*, 133:661–76. DOI: 10.1121/1.4773924.
 32. Friend J, Yeo LY, 2011, Microscale Acoustofluidics: Microfluidics Driven via Acoustics and Ultrasonics. *Rev Mod Phys*, 83:647–704. DOI: 10.1103/revmodphys.83.647.
 33. Zhou Y, 2016, The Application of Ultrasound in 3D Bio-Printing. *Molecules*, 21:590.
 34. Freed LA, Langer R, Martin I, *et al.*, 1997, Tissue Engineering of Cartilage in Space. *Natl Acad Sci USA*, 94:13885–90. DOI: 10.1073/pnas.94.25.13885.
 35. Lamb J, 2016, Scurvy: The Disease of Discovery.
 36. Peng W, Unutmaz D, Ozbolat IT, 2016, Bioprinting towards Physiologically Relevant Tissue Models for Pharmaceuticals. *Trends Biotechnol*, 34:722–32. DOI: 10.1016/j.tibtech.2016.05.013.
 37. Ozbolat IT, Peng W, Ozbolat V, 2016, Application Areas of 3D Bioprinting. *Drug Discov Today*, 21:1257–71. DOI: 10.1016/j.drudis.2016.04.006.
 38. Peng W, Datta P, Ayan B, *et al.*, 2017, 3D Bioprinting for Drug Discovery and Development in Pharmaceuticals. *Acta Biomater*, 57:26–46.
 39. Peng W, Datta P, Wu Y, *et al.*, 2018, Challenges in Bio-fabrication of Organoid Cultures. *Adv Exp Med Biol*, 1107:53–71.
 40. Ozbolat IT, Yin Y, 2013, Bioprinting toward Organ

- Fabrication: Challenges and Future Trends. *IEEE Trans Biomed Eng*, 60:691–9. DOI: 10.1109/tbme.2013.2243912.
41. Haisler WL, Timm DM, Gage JA, *et al.*, 2013, Three-Dimensional Cell Culturing by Magnetic Levitation. *Nat Protoc*, 8:1940–9. DOI: 10.1038/nprot.2013.125.
 42. De Moor L, Merovci I, Baetens S, *et al.*, 2018, High-throughput Fabrication of Vascularized Spheroids for Bioprinting. *Biofabrication*, 10:035009. DOI: 10.1088/1758-5090/aac7e6.
 43. Ling K, Huang G, Liu J, *et al.*, 2015, Bioprinting-Based High-Throughput Fabrication of Three-Dimensional MCF-7 Human Breast Cancer Cellular Spheroids. *Engineering*, 1:269–74. DOI: 10.15302/j-eng-2015062.
 44. Mordwinkin NM, Lee AS, Wu JC, 2013, Patient-Specific Stem Cells and Cardiovascular Drug Discovery. *JAMA*, 310:39–40. DOI: 10.1001/jama.2013.282409.
 45. Ma X, Liu J, Zhu W, *et al.*, 2018, 3D Bioprinting of Functional Tissue Models for Personalized Drug Screening and *In Vitro* Disease Modeling. *Adv Drug Deliv Rev*, 132:235–51.
 46. Satpathy A, Datta P, Wu Y, *et al.*, 2018, Developments with 3D Bioprinting for Novel Drug Discovery. *Expert Opin Drug Discov*, 13:1115–29. DOI: 10.1080/17460441.2018.1542427.
 47. Nguyen DG, Funk J, Robbins JB, *et al.*, 2016, Bioprinted 3D Primary Liver Tissues Allow Assessment of Organ-Level Response to Clinical Drug Induced Toxicity *In Vitro*. *PLoS One*, 11:e0158674. DOI: 10.1371/journal.pone.0158674.
 48. Massa S, Sakr MA, Seo J, *et al.*, 2017, Bioprinted 3D Vascularized Tissue Model for Drug Toxicity Analysis. *Biomicrofluidics*, 11:044109.
 49. Chang R, Emami K, Wu H, *et al.*, 2010, Biofabrication of a Three-Dimensional Liver Micro-Organ as an *In Vitro* Drug Metabolism Model. *Biofabrication*, 2:045004. DOI: 10.1088/1758-5082/2/4/045004.
 50. Snyder JE, Hamid Q, Wang C, *et al.*, 2011, Bioprinting Cell-laden Matrigel for Radioprotection Study of Liver by Pro-drug Conversion in a Dual-tissue Microfluidic Chip. *Biofabrication*, 3:034112. DOI: 10.1088/1758-5082/3/3/034112.
 51. Ji S, Guvendiren M, 2017, Recent Advances in Bioink Design for 3D Bioprinting of Tissues and Organs. *Front Bioeng Biotechnol*, 5:23. DOI: 10.3389/fbioe.2017.00023.
 52. Hong S, Lee JY, Hwang C, *et al.*, 2016, Inhibition of Rho-Associated Protein Kinase Increases the Angiogenic Potential of Mesenchymal Stem Cell Aggregates via Paracrine Effects. *Tissue Eng Part A*, 22:233–43. DOI: 10.1089/ten.tea.2015.0289.
 53. Hong S, Song SJ, Lee JY, *et al.*, 2013, Cellular Behavior in Micropatterned Hydrogels by Bioprinting System Depended on the Cell Types and Cellular Interaction. *J Biosci Bioeng*, 116:224–30. DOI: 10.1016/j.jbiosc.2013.02.011.
 54. Horvath L, Umehara Y, Jud C, *et al.*, 2015, Engineering an *In Vitro* Air-Blood Barrier by 3D Bioprinting. *Sci Rep*, 5:7974. DOI: 10.1038/srep07974.
 55. Isaacson A, Swioklo S, Connon CJ, 2018, 3D Bioprinting of a Corneal Stroma Equivalent. *Exp Eye Res*, 173:188–93. DOI: 10.1016/j.exer.2018.05.010.
 56. Madden LR, Nguyen TV, Garcia-Mojica S, *et al.*, 2018, Bioprinted 3D Primary Human Intestinal Tissues Model Aspects of Native Physiology and ADME/Tox Functions. *iScience*, 2:156–67. DOI: 10.1016/j.exer.2018.05.010.
 57. Homan KA, Kolesky DB, Skylar-Scott MA, *et al.*, 2016, Bioprinting of 3D Convulated Renal Proximal Tubules on Perfusible Chips. *Sci Rep*, 6:34845. DOI: 10.1038/srep34845.
 58. Mozetic P, Giannitelli SM, Gori M, *et al.*, 2017, Engineering Muscle Cell Alignment through 3D Bioprinting. *J Biomed Mater Res A*, 105:2582–8. DOI: 10.1002/jbm.a.36117.
 59. Agrawal G, Aung A, Varghese S, 2017, Skeletal Muscle-on-a-Chip: An *In Vitro* Model to Evaluate Tissue Formation and Injury. *Lab Chip*, 17:3447–61. DOI: 10.1039/c7lc00512a.
 60. Wang Z, Lee SJ, Cheng HJ, *et al.*, 2018, 3D Bioprinted Functional and Contractile Cardiac Tissue Constructs. *Acta Biomater*, 70:48–56.
 61. Dai X, Ma C, Lan Q, *et al.*, 2016, 3D Bioprinted Glioma Stem Cells for Brain Tumor Model and Applications of Drug Susceptibility. *Biofabrication*, 8:045005. DOI: 10.1088/1758-5090/8/4/045005.
 62. Xu F, Celli J, Rizvi I, *et al.*, 2011, A Three-Dimensional *In Vitro* Ovarian Cancer Coculture Model Using a High-throughput Cell Patterning Platform. *Biotechnol J*, 6:204–12. DOI: 10.1002/biot.201000340.
 63. Zhao Y, Yao R, Ouyang L, *et al.*, 2014, Three-Dimensional Printing of Hela Cells for Cervical Tumor Model *In Vitro*. *Biofabrication*, 6:035001. DOI: 10.1088/1758-5082/6/3/035001.
 64. Koch L, Deiwick A, Schlie S, *et al.*, 2012, Skin Tissue Generation by Laser Cell Printing. *Biotechnol Bioeng*, 109:1855–63.
 65. Tseng H, Gage JA, Shen T, *et al.*, 2015, A Spheroid Toxicity Assay Using Magnetic 3D Bioprinting and Real Time Mobile Device-Based Imaging. *Sci Rep*, 5:13987. DOI: 10.1038/srep13987.
 66. Tran JL, 2015, To Bioprint or Not to Bioprint. *N C J Law Tech*, 15:123–78.
 67. Murphy SV, Atala A, 2014, 3D Bioprinting of Tissues and

- Organs. *Nat Biotechnol*, 32:773–85. DOI: 10.1038/nbt.2958.
68. Groll J, Boland T, Blunk T, *et al.*, 2016, Biofabrication: Reappraising the Definition of an Evolving Field. *Biofabrication*, 8:013001. Doi: 10.1088/1758-5090/8/1/013001.
 69. Lamb J, 2018, FDA Code of Federal Regulations 21CFR1271. In: *Scurvy: The Disease of Discovery*. Princeton University Press, Princeton, New Jersey. pp. 15–20.
 70. Di Prima M, Coburn J, Hwang D, *et al.*, 2016, Additively Manufactured Medical Products the FDA Perspective. *3D Print Med*, 2:1. DOI: 10.1186/s41205-016-0005-9.
 71. Hourd P, Medcalf N, Segal J, *et al.*, 2015, A 3D Bioprinting Exemplar of the Consequences of the Regulatory Requirements on Customized Processes. *Regen Med*, 10:863–83.
 72. Available from: <https://www.nasdaq.com/articles/depth-look-organovo>. [Last accessed on 2012 Aug 20].
 73. Available from: <https://www.cellink.com/exclusive-with-cellink-co-founders-erik-gatenholm-and-dr-hector-martinez-in-medgadget>. [Last accessed on 2020 Jul 27].
 74. Available from: <https://www.engineering.com/3DPrinting/3DPrintingArticles/ArticleID/9713/Japanese-BioPrinting-Firm-Closes-12M-Series-B-Funding.aspx>. [Last accessed on 2020 Jul 27].
 75. Available from: <https://www.poietis.com/poietis-closes-a-5me-financing-round-to-accelerate-the-development-of-its-bio-printing-platform-for-tissue-therapy-manufacturing>. [Last accessed on 2020 Jul 27].
 76. Available from: <https://www.betakit.com/aspect-biosystems-raises-26-million-cad-in-series-a-for-3d-printing-of-human-tissues>. [Last accessed on 2020 Jul 27].
 77. Available from: <https://www.3dprintingindustry.com/news/allevi-launches-bioink-kit-for-3d-printing-multi-layered-skin-cells-151813>. [Last accessed on 2020 Jul 27].
 78. Available from: <https://www.marketwatch.com/story/beyond-meat-soars-163-in-biggest-popping-us-ipo-since-2000>. [Last accessed on 2019 Apr 02].
 79. Available from: <https://www.techcrunch.com/2019/09/05/novameat-has-a-platform-for-3d-printing-steaks-and-has-new-money-to-take-it-to-market>. [Last accessed on 2020 Jul 27].
 80. Available from: <https://www.forbes.com/sites/jimvinoski/2019/09/25/with-food-grade-3-d-printing-redefine-meat-is-out-to-well-redefine-meat/#2971f42a75c7>. [Last accessed on 2020 Jul 27].
 81. Wilks M, Phillips CJ, 2017, Attitudes to *In Vitro* Meat: A Survey of Potential Consumers in the United States. *PLoS One*, 12:e0171904. DOI: 10.1371/journal.pone.0171904.
 82. Available from: <https://www.mosameat.com/blog/2019/11/15/mosa-meat-on-netflixs-explained>. [Last accessed on 2020 Jul 27].
 83. Available from: <https://www.wired.com/story/the-high-cost-of-lab-to-table-meat>. [Last accessed on 2020 Jul 27].
 84. Available from: <https://www.bloomberg.com/news/articles/2019-10-07/startup-aleph-farms-hitches-ride-on-iss-to-make-space-meat?srnd=premium-europe>. [Last accessed on 2020 Jul 27].
 85. Available from: <https://www.bloomberg.com/news/articles/2019-10-07/startup-aleph-farms-hitches-ride-on-iss-to-make-space-meat>. [Last accessed on 2020 Jul 27].
 86. Ben-Arye T, Shulamit L, 2019, Tissue Engineering for Clean Meat Production. *Front Sustain Food Syst*, 3:46. Doi: 10.3389/fsufs.2019.00046.
 87. Available from: <https://www.foodnavigator-usa.com/Article/2019/02/11/From-edible-scaffolding-to-bio-printing-What-would-an-industrial-scale-cell-based-meat-plant-look-like>. [Last accessed on 2020 Jul 27].
 88. Novik E, Yarmush ML, Freedman RB, *et al.*, 2016, Compositions and Methods of Functionally Enhanced *In Vitro* Cell Culture System. Patent No. 20120129207A1 US.
 89. JAKAB, 2014, Gabor Forgacs Françoise MargaKaroly Robert. Engineered Comestible Meat. Patent No. 8703216B2 US.
 90. Yao L, Ou J, Wang G, *et al.*, 2013, bioPrint: A Liquid Deposition Printing System. *3D Print Addit Manuf*, 2:168–79. DOI: 10.1089/3dp.2015.0033.
 91. Wang W, Yao L, Cheng CY, *et al.*, 2017, Harnessing the Hygroscopic and Biofluorescent. *Sci Adv*, 3:e1601984.
 92. Karoly J, Françoise M, Ryan K, *et al.*, 2019, Non-medical Applications of Tissue Engineering: Biofabrication of a Leather-like Material. *Mater Today Sustain*, 5:100018. DOI: 10.1016/j.mtsust.2019.100018.

Laser-induced Forward Transfer Hydrogel Printing: A Defined Route for Highly Controlled Process

Vladimir Yusupov¹, Semyon Churbanov^{1,2}, Ekaterina Churbanova¹, Ksenia Bardakova^{1,2}, Artem Antoshin^{1,2}, Stanislav Evlashin³, Peter Timashev^{1,2,4,5}, Nikita Minaev^{1*}

¹Institute of Photon Technologies, Federal Scientific Research Centre “Crystallography and Photonics,” Russian Academy of Sciences, Pionerskaya 2, Troitsk, Moscow, 108840, Russia

²Institute for Regenerative Medicine, Sechenov First Moscow State Medical University, 8-2 Trubetskaya st., Moscow, 119991, Russia

³Center for Design Manufacturing and Materials, Skolkovo Institute of Science and Technology, Bolshoy Boulevard 30, Bld. 1, Moscow, 121205, Russia

⁴Department of Polymers and Composites, N.N.Semenov Institute of Chemical Physics, 4 Kosygin St., Moscow, 119991, Russia

⁵Department of Chemistry, Lomonosov Moscow State University, Leninskiye Gory 1-3, Moscow 119991, Russia

Abstract: Laser-induced forward transfer is a versatile, non-contact, and nozzle-free printing technique which has demonstrated high potential for different printing applications with high resolution. In this article, three most widely used hydrogels in bioprinting (2% hyaluronic acid sodium salt, 1% methylcellulose, and 1% sodium alginate) were used to study laser printing processes. For this purpose, the authors applied a laser system based on a pulsed infrared laser (1064 nm wavelength, 8 ns pulse duration, 1 – 5 J/cm² laser fluence, and 30 μm laser spot size). A high-speed shooting showed that the increase in fluence caused a sequential change in the transfer regimes: No transfer regime, optimal jetting regime with a single droplet transfer, high speed regime, turbulent regime, and plume regime. It was demonstrated that in the optimal jetting regime, which led to printing with single droplets, the size and volume of droplets transferred to the acceptor slide increased almost linearly with the increase of laser fluence. It was also shown that the maintenance of a stable temperature (±2°C) allowed for neglecting the temperature-induced viscosity change of hydrogels. It was determined that under room conditions (20°C, humidity 50%), the hydrogel layer, due to drying processes, decreased with a speed of about 8 μm/min, which could lead to a temporal variation of the transfer process parameters. The authors developed a practical algorithm that allowed quick configuration of the laser printing process on an applied experimental setup. The configuration is provided by the change of the easily tunable parameters: Laser pulse energy, laser spot size, the distance between the donor ribbon and acceptor plate, as well as the thickness of the hydrogel layer on the donor ribbon slide.

Keywords: LIFT, Laser-induced forward transfer, Hydrogel parameters, Optimal jetting regime, Jet and droplets parameters

*Corresponding Author: Nikita Minaev, Institute of Photonic Technologies, Federal Scientific Research Centre “Crystallography and Photonics,” Russian Academy of Sciences, Pionerskaya 2, Troitsk, Moscow, 108840, Russia; minaevn@gmail.com

Received: February 20, 2020; **Accepted:** March 16, 2020; **Published Online:** April 23, 2020

(This article belongs to the *Special Section: Bioprinting in Russia*)

Citation: Yusupov V, Churbanov S, Churbanova E, *et al.*, 2020, Laser-induced Forward Transfer hydrogel printing: A defined route for highly controlled process, *Int J Bioprint*, 6(3): 271. DOI: 10.18063/ijb.v6i3.271.

1 Introduction and background

Laser-induced forward transfer (LIFT) is a digital printing technique that allows for the nozzle-free

direct transfer of matter. This technology has been used (1) to print a wide range of biological materials, such as proteins^[1,2] and DNA^[3,4]; (2) to separate microorganisms^[5]; (3) to print various types of cells

© 2020 Yusupov, *et al.* This is an Open Access article distributed under the terms of the Creative Commons Attribution-NonCommercial 4.0 International License (<http://creativecommons.org/licenses/by-nc/4.0/>), permitting all non-commercial use, distribution, and reproduction in any medium, provided the original work is properly cited.

to create three-dimensional (3D) bioequivalents of natural tissues^[6-10]; and (4) to transfer stimulatory factors for cell differentiation^[6-10].

For the printing process, one should prepare the ribbon (target, donor, or a source film). The ribbon usually consists of a glass slide on the surface, of which a nanolayer of laser-absorbing material (Au, Ti, etc.) is applied^[8,11,12], which is then covered with a hydrogel-containing transferred objects.

Laser pulses pass through the uncoated transparent side of the ribbon and then focus on a layer that absorbs laser radiation. The partial absorption of the laser pulse energy by the absorbing layer leads to the rapid heating of its local area and of the adjacent thin layer of hydrogel, which leads to the formation of the high-pressure and high-temperature vapor bubble^[13]. The rapid expansion of this vaped region leads to the formation of jets of various types^[14] with the subsequent separation of one or more droplets and their transfer to the acceptor surface^[15]. Finally, according to a predetermined design and with a high productivity of the process^[16], a two-dimensional (2D)^[17] and, if necessary, 3D^[18] structure with the necessary concentration of transferred objects is fabricated from these microdroplets.

To become a truly universal method, laser bioprinting applying the LIFT technique must be an accurate technology that can guarantee the transfer of a strictly specified volume of hydrogel with minimal negative effects on living objects in the gel. The main difficulty in the work with this technology is the accurate selection of factors that significantly affect the process of laser transfer.

The characteristics of the laser printing process depend (**Figure 1**) on the (1) parameters of the laser impact (wavelength, laser pulse duration, focusing parameters, and energy); (2) ribbon factors (absorbing layer material, type of transferred objects, hydrogel parameters, and hydrogel layer thickness); and (3) external factors (experiment configuration, environmental factors, and transfer distance).

Red parameters, as a rule, are set by an experimental setup, and most often stay unchanged. Yellow parameters change, as a rule, when printed objects are changed. Green

parameters are configured each time according to a particular experimental condition.

To implement the LIFT printing process, a laser system with a set of basic optomechanical components (3D stages and focusing optics) is required. The main component of the system is a laser source, which determines the main characteristics of the laser pulse. The most common, commercially available, and studied^[19,20], laser sources have nanosecond pulse length^[21-24] and a wavelength of $\lambda = 1064$ nm (near infrared range). Near-IR radiation is well absorbed by the metal absorbing layer, while remaining transparent to living tissues and cells^[25,26]. It is also important that IR radiation, due to the low energy of quanta, practically does not affect the physicochemical characteristics of hydrogels^[27] and does not damage cells^[25]. It is worth noting that several studies Zhang *et al.*^[28,29] used laser sources of the ultraviolet spectrum, and their radiation is well absorbed by the hydrogel material, which makes it possible to avoid using the absorbing layer. On the other hand, such short-wavelength laser radiation can change the physicochemical characteristics of hydrogels, and moreover, this radiation is well absorbed by living tissues and cells, which can be detrimental to them.

When choosing a laser source and an radiation optical focusing scheme, the following laser factors should be considered (**Figure 1**): Pulse duration, laser pulse energy, and laser spot size, since these parameters directly determine the energy density (fluence)^[16,21,30,31], and peak laser power. However, the vapor bubble growth dynamics and all LIFT laser transfer process^[19,21] depend on the pulse duration and absorbed fluence, which is, in turn, determined by the laser radiation absorption coefficient of the energy absorbing layer. The choice of material and thickness of the ribbon absorbing layer are associated with the need to provide the most efficient conversion of a laser pulse with a given wavelength λ into heat, while minimizing transmitted radiation, which can adversely affect biological objects contained in the hydrogel layer. It is also necessary to consider that, from a metal absorbing layer, laser irradiation can produce nanoparticles which are then transferred

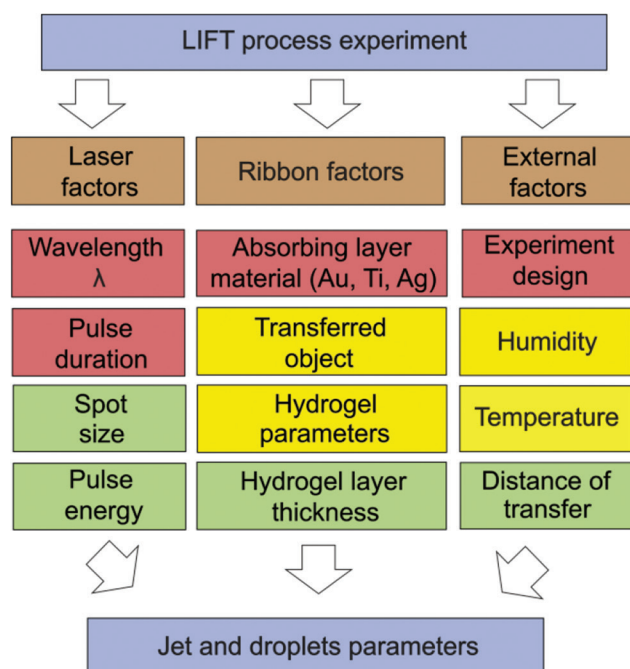


Figure 1. Factors affecting the laser-induced forward transfer printing process.

together with the hydrogel causing a negative effect on the transferred objects^[13,32].

In addition to the parameters of laser exposure, the transfer process is also affected by the hydrogel parameters (viscosity, density, and surface tension)^[16,33] and its thickness on the ribbon. The variation of these parameters allows changing the jetting dynamics and droplet formation^[15] and achieving the optimal transfer regime with the formation of a stable jet without spraying^[14], the formation of hydrogel droplets of the required volume^[15], and the absence of unnecessary shock stresses on the transferred objects^[13,34].

When transferring living objects using the LIFT technique, a major role is played by the controlled optimal “external factors” (Figure 1), such as: Temperature, humidity, and the composition of the gaseous medium ensuring the vital activity of the transferred objects, for example, various cell populations^[6,23,35] or bacterial cultures^[36]. During the printing process, it is necessary to provide “comfortable” conditions for the transferred objects, as well as to prevent changes in the parameters of ribbon and acceptor surfaces over time (for example, due to the drying of hydrogels).

For transferred objects, it is important to select the physicochemical characteristics of the hydrogel medium: The viscosity, surface tension, and the nature (polymer or inorganic). Furthermore, the presence of the additives (growth factors, proteins, etc.) in the gel helps to create the most favorable conditions for the metabolism of the transferred objects. In some cases, an important factor is also the geometric arrangement of droplets on the acceptor surface, which provides, in particular, the optimal overlap and droplet spacing of individual non-merging drops^[37,38].

At present, a number of laser systems have been described in the scientific literature where LIFT printing is feasible^[24,31]. However, it is worth noting that the selection of optimal parameters for a specific combination of laser-hydrogel microobjects actually represents a separate study. This is explained by the fact that the final result (high-quality pattern with the droplets of a given size) is determined by a combination of many interdependent factors (Figure 1). A change in one parameter may not lead to the desired effect due to the mutual influence of the parameters on each other. From this point of view, one of the actual challenges for LIFT technique is the development of the algorithm allowing for the selection of the optimal parameters for high-quality laser printing for each given laser system.

The purpose of this article is to develop an algorithm based on the determination of the operating ranges for laser fluence to achieve the optimal regime with the transfer of single microdroplets. The performed studies were carried out on the most common hydrogel materials for laser printing, such as hyaluronic acid sodium salt^[39,40], methylcellulose^[41], and sodium alginate^[8,42,43].

2 Experiment

The main input parameters and working stages are presented in Figure 2. We studied the influence of various parameters on the printing process, as well as ways to optimize the experimental conditions to obtain the most stable and repeatable printing results.

2.1 Laser printing setup

The experimental setup used a pulsed fiber laser YLPM-1-4x200-20-20 (NTO “IRE-Polus,” Russia) with a wavelength of 1064 nm, with an approximate Gaussian intensity profile in the beam ($M^2 < 1.3$). Laser radiation was focused on an absorbing layer of the ribbon using a LscanH-10-1064 galvo scanning head (AtekoTM, Russia) with a F-theta SL-1064-110-160 lens (Ronar-Smith, Singapore) with a focal length of 160 mm. The system (**Figure 3**) formed a laser spot with diameter of 30 μm positioning it with an accuracy of several microns in the X-Y plane. The range of laser energies in the experiments ranged from 7 to 35 μJ with a pulse duration of 8 ns.

The glass slides, the donor (ribbon) and acceptor, were mounted on the precision optical translators with the distance of 0.5 – 2 mm and were placed in the working plane parallel to the lens. Using a

galvo scanning system, laser radiation was moved along the surface of the donor ribbon according to a predetermined pattern.

2.2 Ribbon preparation

For all printing presented experiments, 1-mm thick glass slides (25×75 mm) were purified by sequential exposure to isopropanol, deionized water, and acetone in an ultrasonic treatment for 30 s for each liquid, followed by purging with purified air. The slides were coated with a 50-nm thick gold layer by magnetron sputtering. The thickness of the deposited layers was controlled by a microinterferometer (Lomo Mii4, AO Lomo, Russia). A hydrogel layer 200 ± 20 μm thick was applied to the absorbing layer using blade-coater.

Importantly, we used a gel layer of relatively large thickness based on the following. The use of hydrogel layers with a thickness of more than 100 μm allows (1) a significant reduction of the effect of drying-induced hydrogel layer thickness change of the ribbon; (2) avoidance from strong shock stresses associated with the action of shock waves and a reduction of dynamic stresses during transfer^[34]; (3) minimization of the negative effect of high temperature and nanoparticles produced by the absorbing layer^[13,32,44]; and (4) an increase in system performance and the ability to transfer quite large objects, for example, cell spheroids.

2.3 Hydrogel viscosity and evaporation determination

For the experiments, the hydrogels were obtained by dissolving the powder of methylcellulose (Sigma-Aldrich – M0262), hyaluronic acid sodium salt (Contipro - HySilk), and sodium alginate (Sigma-Aldrich – A-2033) in deionized water overnight with mass concentrations of 1%, 2%, and 1%, respectively.

The viscosity of the studied hydrogels was measured using a Kyoto Electronics Manufacturing EMS-1000 electromagnetically spinning viscometer. The measurements were carried out in the temperature range of 20 – 37°C, with exposure at each temperature point for 5 min. The drying

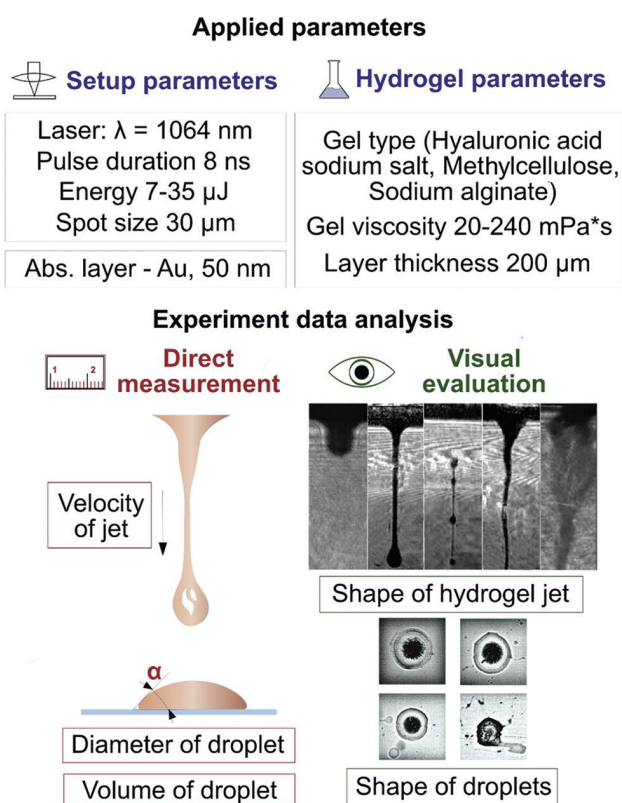


Figure 2. The main input parameters of the experiments and the scheme for evaluating the results.

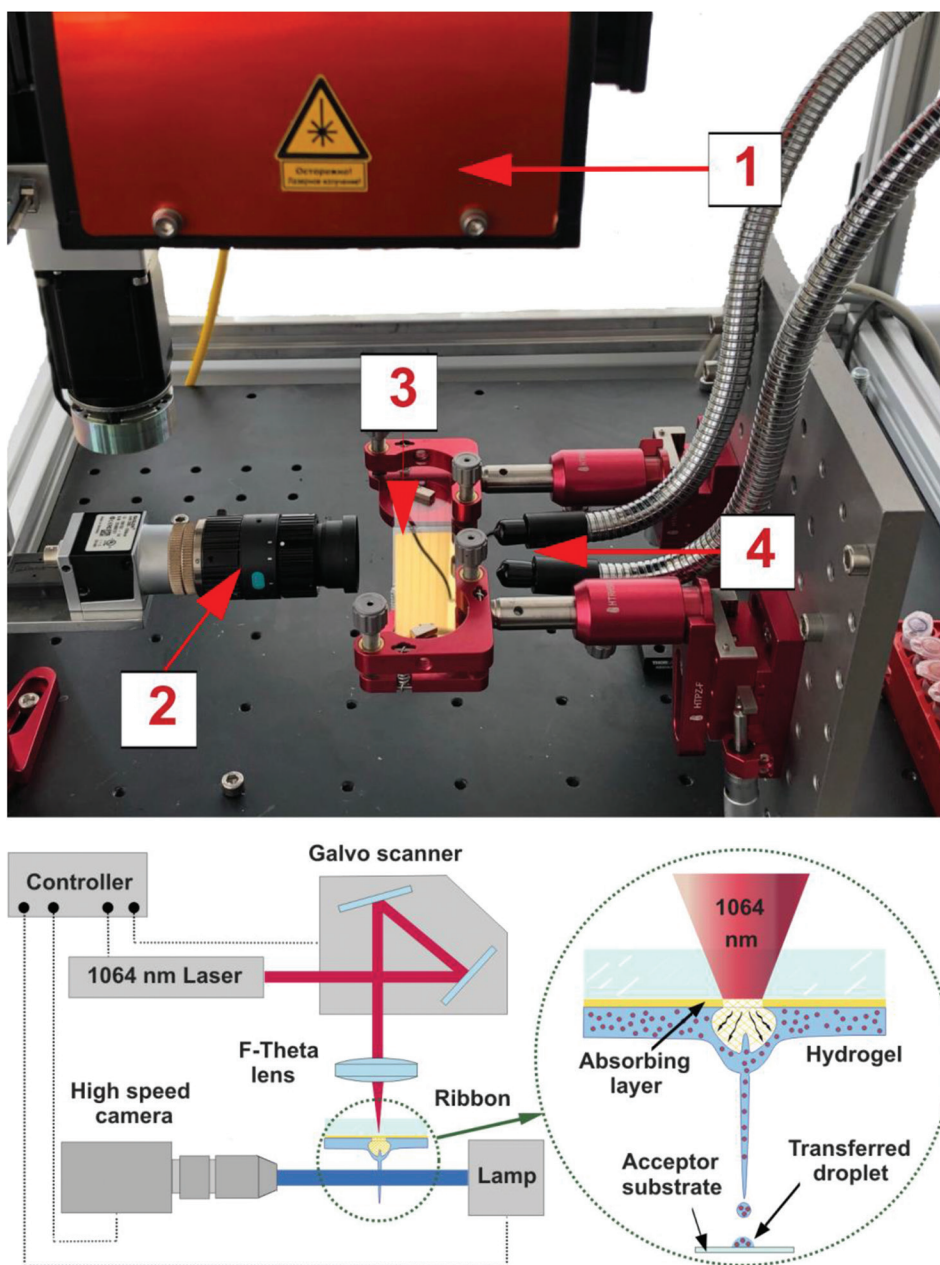


Figure 3. The image and scheme of the part of the experimental laser-induced forward transfer (LIFT) setup. On the top panel, (1) galvo scanner with F-theta lens, (2) digital camera, (3) ribbon, and (4) light source. The scheme of LIFT setup is shown on the bottom panel. The scheme of printing process is depicted in the circle.

intensity of the hydrogel layer on ribbon was estimated gravimetrically using Adventurer Pro AV114C (Ohaus, USA).

2.4 Measuring droplet sizes

The size of the transferred hydrogel microdroplets was measured using a direct optical microscope

(Huvtz HRM-300). The volume of transferred droplets was calculated according to the contact angles and droplet diameter on the acceptor plate (Figure 2). The static contact angles of hydrogels were determined by the method of a sessile drop using an ACAM D-3 goniometer (APEX Instruments, India).

2.5 Visualization of jetting and measurement of jetting velocity

The printing and transfer processes of the material were visualized and investigated using a high-speed Fastcam SA-3 camera (Photron, Japan) (shutter 1/60000, FPS 10000-60000) with a long-focus microscopic lens providing a shooting field of up to 5×3.5 mm. The illumination was performed using a K150 Laboratory Illuminator (Optics Co, China).

3 Results and discussion

3.1 General observations

The LIFT process is based on local heating occurring during the interaction of a laser pulse with an absorbing layer, which leads to explosive boiling of water in a gel^[13], while more intensive heating can lead to explosive boiling of the absorbing layer material^[45]. As a result, a high-pressure bubble is formed^[46-48], the expansion of which leads, depending on the initial parameters^[15], to the formation of various types of jets^[49], and the separation of one or more droplets and their

subsequent transfer to an acceptor plate^[15]. The processes associated with the formation and collapse of a gas bubble, as well as possible regimes of jet formation are represented in **Figure 4**.

At the first stage of the LIFT process ($t = 0.01$ a.u.), the metal energy absorbing layer, the nearest thin layers of the glass slide, and the hydrogel are heated to high temperatures due to the partial absorption of the laser pulse energy by the energy absorbing layer. In the applied laser printing regimes, the achieved temperature significantly exceeds the melting temperature of the material of the absorbing layer (for Au $T \approx 1337$ K)^[13]. On reaching a temperature of ~ 0.95 from the critical temperature (for water $T_c = 647$ K), the water contained in the gel boils explosively^[34], which converts the water into steam compressed to a high (around critical) pressure ($P_c \sim 22.5$ MPa). As a result, a rapidly expanding vapor bubble forms in the gel in the area of laser exposure.

At $t = 1$, the size of this bubble already exceeds the thickness of the gel. Due to the hydrogel viscosity, the presence of a solid surface of the donor plate and the limited thickness of the gel, this

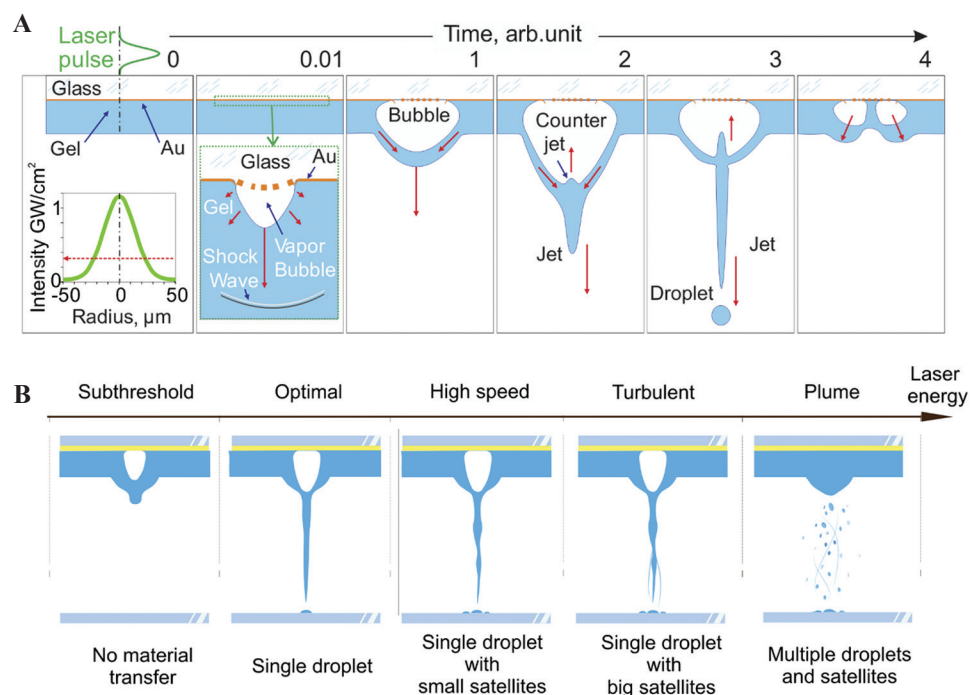


Figure 4. (A) The main stages of the jet and droplet formation during laser printing. Red arrows indicate the direction of fluid movement (B) changes in jetting regimes with the increase of laser energy.

bubble becomes easier to expand along the optical axis, but not across it. All these factors generate a pressure gradient along the bubble wall leading to the gel flows from the periphery to the optical axis center of the bubble top. The interaction of these flows leads at $t = 2$ to the appearance of a jet and a counter jet.

As the bubble expands, the pressure inside it drops monotonically and its expansion at the stages $t = 1$ and $t = 2$ occurs by inertia. When the bubble reaches its maximum size, the pressure inside it decreases almost to zero and the bubble begins to compress ($t = 3$) due to the pressure difference outside ($\approx 10^5$ Pa)^[48] and inside it. The bubble apex serves as the base of an elongated jet, from which a microdroplet detaches due to Rayleigh–Plateau instability. Depending on the selected regime, the jet can move back and be completely absorbed by the gel layer or it can separate and continue the independent movement toward the acceptor plate or it can break up into several fragments.

At stage $t = 4$, the microdroplet (not shown in the figure) continues to move toward the acceptor plate or has already reached its surface. Having collapsed, the bubble begins to expand again. Moreover, since its center is substituted with by fragments of the counter jet, its shape looks like a donut. The maximum speeds of the outer walls of this “donut” are directed at a certain angle to the optical axis. At sufficiently high laser energies, hydrogel splashing can occur in these directions.

3.2 Regimes of jet formation

In this part, we will discuss the regimes of jet formation in more detail. The energy of a laser pulse directly sets the amount of transferred energy which leads to the formation of a gas bubble^[47]. The effect of the kinetic energy transferred to the jet/droplet on the printing process is well studied in the literature^[14,15]. **Figure 4B** shows five basic laser transfer regimes that determine the amount of transferred material and printing quality^[14,15,45]. At low values of laser energy (subthreshold regime) a small jet forms and does not transfer the material. When a certain energy threshold is overpassed (optimal regime), a part of the jet begins to separate and transfer in the form of a single droplet

onto an acceptor plate. With a further increase in the laser pulse energy, the length and velocity of the transferring jet increase, which lead to the transfer, besides the main droplet, of small satellite droplets (high speed regime). On reaching the energies leading to turbulent jets or the formation of several jets simultaneously (turbulent regime), large satellite drops are transferred along with the main droplet. With a further increase in laser energy, the energy stored in the expanding bubble becomes so large that a rupture of the outer wall of the bubble (plume regime) occurs, leading to a chaotic transfer of hydrogel both in shape and volume.

The best printing quality achievable in laser transferring can only be realized in a relatively narrow range of laser energies corresponding to the optimal regime and leading to the transfer of a single droplet. It is worth noting that usually for describing the LIFT process, instead of the parameter “laser pulse energy,” the parameter “laser fluence” is used, which is determined by the ratio of laser pulse energy to laser spot size and measured in J/cm². Laser fluence is a more universal parameter, since the main role in the transfer processes is played by the radiation energy density. In our experiments, when the energy changed from 7 to 25 μ J while maintaining a spot size of 30 μ m, the fluence range was 1 – 5 J/cm².

To assess the effect of laser fluence on the jetting regime and jetting velocity, we used a high-speed shooting of the printing process. The LIFT occurred between the donor ribbon and acceptor plate located at a distance of 1 mm.

Figure 5 shows that using hyaluronic acid sodium salt (2%) as an example, with small fluence (up to 1.7 J/cm²), the transfer process did not occur. With an increase in laser fluence, there was a transition to the optimal jetting regime with single droplet transferring (2.0 J/cm²), then to the high-speed regime (2.5 J/cm²), and, finally, to the turbulent regime (3.7 J/cm²).

During the process of laser printing, the living objects transferred inside the jet practically do not experience any mechanical and thermal stresses. They experience significant dynamic stresses only at the initial moment of bubble and jet

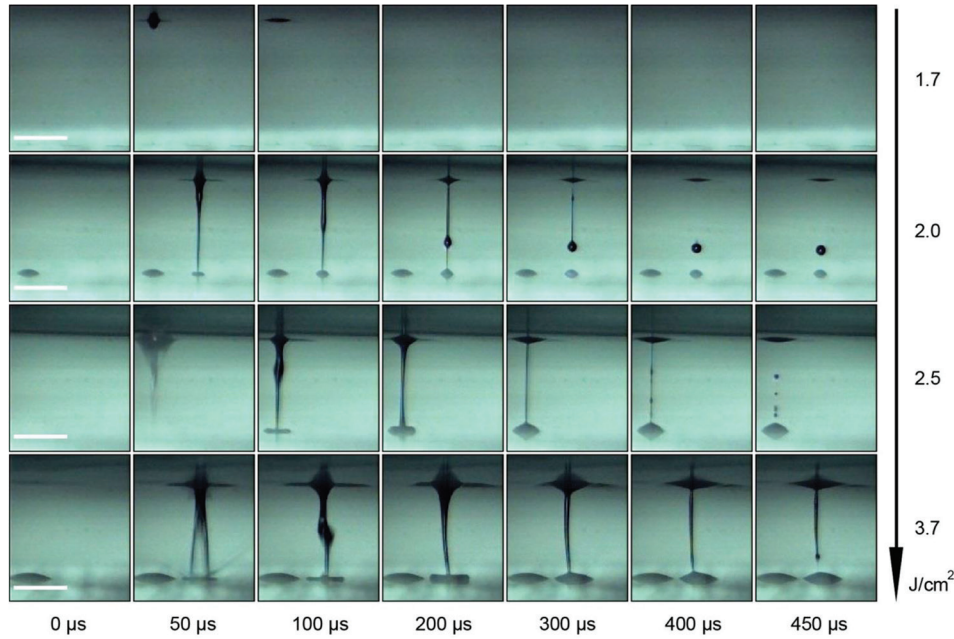


Figure 5. Time resolved images of the hyaluronic acid sodium salt (2%) transferring process for various laser fluences. Scale bar: 400 μ .

formation, as well as at the final moment during the impingement of a gel microdroplet with an acceptor plate (or landing)^[50]. Hence, according to the calculations, at a jet speed of 50 m/s, the accelerations can reach 7×10^8 m/s² at the initial moment and 6×10^9 m/s² during the landing process. Caused by dramatic accelerations and fluid dynamics, mechanical stress can have a negative effect on transferred objects, for example, it can lead to severe deformation of cells, rupture of their membranes and subsequent cell deaths^[50]. As shown in Wang and Chrisey^[50], the acceleration at the final stage can be reduced by almost an order of magnitude to 7×10^8 m/s² when the acceptor plate is coated with a 40- μ m thick acceptor gel layer. Such a coating during landing significantly reduces dynamic stress, which leads to a decrease in mechanical damage of the cells and increases post-transfer cell viability up to 95%^[51]. It is worth noting that with an increase in the thickness of the gel on the acceptor plate, dynamic stress will decrease. However, with a large thickness of the gel, negative effects associated with immersion of cells at a great depth can be observed, which are explained by a decrease in cell metabolism due to diffusion limitations^[52].

The whole process, ending with droplet transfer, begins with the absorption of the laser pulse and rapid heating to high temperatures of the area of the absorbing layer and nearby thin layers of the donor glass plate and gel. In the case of short (nanosecond) pulses, when it can be assumed that heat spreads only in the direction of the optical axis, the increase in temperature under laser irradiation with fluence F_0 will be:

$$\Delta T \approx a \cdot F_0 / (\rho_{Eff} \cdot C_{PEff} \cdot h_{Eff}) \quad (1)$$

where a is the absorption coefficient of laser radiation by a metal energy absorbing layer; ρ_{Eff} , C_{PEff} and h_{Eff} are the effective density, heat capacity, and thickness of a thin heated gel/metal / glass layer. The h_{Eff} value is determined by the thermal diffusion length of the donor plate materials (fused silica) and gel: where τ is the time, at which the temperature reaches its maximum, which in most cases are equal to the laser pulse duration, D – is the thermal diffusivity^[53]. Taking into account $D_{silica} = 5.8 \times 10^{-7}$ m²/s and $D_{water} = 1.4 \times 10^{-7}$ m²/s, at $\tau = 8$ ns we get: $h_{Eff} = 68$ nm + 34 nm = 102 nm. Thus, all the main processes of heat transfer are associated with the heating of this thin layer.

3.3 Effect of laser pulse fluence on printed droplets

It is known that the key role in controlling the LIFT process is played by laser fluence^[19,30]. Changing the laser fluence allows for controlling the diameter and volume of the transferred droplets, which determine the resolution and throughput of printing as well as the ability to transfer objects of various sizes from single cells to cell spheroids. **Figure 6** shows the influence of laser fluence on the diameter and volume of droplets for different hydrogels.

The volumes of transferred droplets were calculated by measuring their contact angles on the acceptor plate, particularly, for the applied hydrogels the contact angles were: 2% hyaluronic acid sodium salt $-21.5^\circ \pm 0.4$, 1% sodium alginate $-17.4^\circ \pm 0.3$, and 1% methylcellulose $-22.4^\circ \pm 0.6$. From the data obtained, it follows that for the optimal jetting regime, the increase in the diameter and volume of the transferred droplets has linear-like relationship with laser fluence. In this case, the smallest droplets are obtained for hyaluronic acid-based hydrogel. For other two hydrogels, the obtained values of the diameter and volume of the transferred droplets are practically the same for most of the fluences applied.

For all the gels used in this work, various transfer regimes were defined depending on the change in laser pulse energy. It was realized by conducting a series of experiments with a high-speed shooting of transfer processes, where we the

measured the resulting jet velocities, the diameters and volumes of the droplets formed on the acceptor plate. The measurement results for the all gel types are represented in **Figure 7**.

From **Figure 7**, it follows that for all the gels used in the experiment, the optimal laser fluence range for the formation of a single jet and stable transfer of hydrogel droplets is between 2 and 3 J/cm². For optimal transfer regime, the widest fluence range is observed for hyaluronic acid sodium salt, while the narrowest fluence range is observed for methylcellulose. That is, the use of 2% solution of hyaluronic acid sodium salt provides the most stable transfer of gel droplets. In this case, small changes in the parameters of the hydrogel, the laser fluence, and the parameters of the absorbing layer of the plate will not approve the transition to other non-optimal printing regimes.

3.4 The environment-dependent parameters of the hydrogel

This section discusses the influence of external factors (experiment temperature and experiment time) on the viscosity of the hydrogel layer and its drying on the donor ribbon. The vast majority of articles pay insufficient attention to the drying-induced change of the hydrogel layer parameters during the experiment. When the hydrogel layer dries, the changes in its viscosity and thickness can significantly impact the process of laser transfer.

The viscosity of the hydrogel layer directly determines (1) the required laser fluence to provide

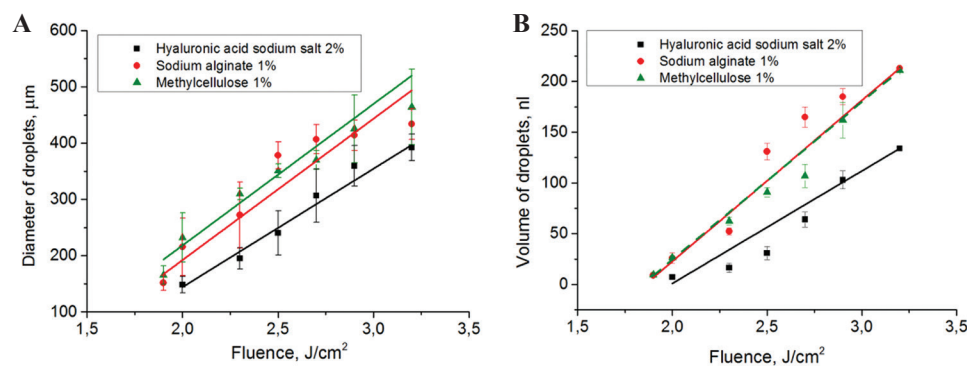


Figure 6. Relationship between laser fluence, diameter, and volume of transferred droplets. (A) Droplet diameters (inserted image illustrates the transferred droplets of 2% hyaluronic acid sodium salt, scale bar: 100 μm); (B) droplet volumes. For all relationships, linear trends are plotted with the error considered. The measurements were carried out in the optimal transfer regime.

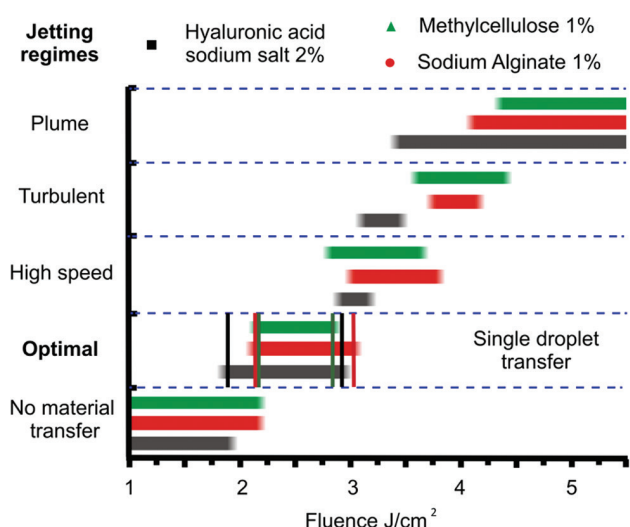


Figure 7. Relationship between laser-induced forward transfer regimes and laser fluences for three gel types. Vertical lines indicate the corresponding boundaries of the optimal range.

the optimal transfer regime, (2) the shape and size of the jet^[54,55], as well as (3) the resulting droplet volume on the acceptor plate.

In our experiments, the viscosities of hydrogels were determined at temperatures ranging from 20 to 37 °C. These temperatures were chosen deliberately, since they covered the range from standard (room) temperature to standard cell culture temperatures. A temperature change had a similar effect on the viscosity of hydrogels based on sodium alginate and hyaluronic acid sodium salt: An increase in temperature by 4°C led to a decrease in viscosity by an average of 9%. In the case of methylcellulose, the viscosity of the solutions also decreased with an increase in temperature for every 4°C by approximately 14% (Table 1). Importantly, all the obtained viscosity values are suitable for LIFT: According to Hözl *et al.*^[56], LIFT technology utilizes hydrogels with a viscosity ranging from 1 to 300 mPa*s.

Table 1 shows that with a change in temperature in the range of 20–37° C, the viscosity of hydrogels can reduce by almost 2 times, which must be considered in experiments.

In addition to controlling the ambient temperature during the experiment, one should also monitor the drying of the hydrogel layer on

the donor ribbon and printed drops on the acceptor plate, which is largely dependent on, besides the temperature, the air humidity. The high drying rate of the gel layer covered on the donor ribbon can lead to a change in its thickness and viscosity during the experiment, which will directly affect the printing regimes and landed droplet sizes. The rapid drying of the gel on an acceptor plate, in particular, leads to the change of gel droplet shapes resulting in the “coffee-ring” effect^[21] observed within few minutes after printing.

In our experiments, at a relative humidity of 50%, an ambient temperature of 20°C, and with the use of relatively thick hydrogel layers (200 ± 20 µm) within 30 min after applying the gel layer to ribbon, a mass loss of more than 60% was observed (Table 2).

However, glycerol can be added to prevent the hydrogel from drying; for example, in one study^[21] introduced 10% (v/v) of glycerol into all printing solutions. Nevertheless, it should be borne in mind that an increase in glycerol concentration above 10% (v/v) is detrimental for cell survival^[21]. Furthermore, glycerol should be added to protein-containing solutions with caution, since glycerin is considered to be a denaturing agent^[57]. Alternatively, in another study^[58], the authors added methylcellulose to reduce the drying rate of the hydrogel layer.

Thus, to ensure they stable controlled laser printing, it is necessary to maintain a constant ambient temperature and consider the high drying rate of hydrogels (~ 8 µm/min) under standard conditions during the experiment (Table 2). For example, within 5 min, the mass of the hydrogel (and, therefore, its thickness on the donor ribbon) decreases by 20%, which is beyond the measurement error (10%). Therefore, to obtain droplets of the same size within the experiment, one should finish it in few minutes, or organize additional donor ribbon moisturizing, or introduce the drying-preventing agents into the hydrogel.

4 Decision tree for controlled hydrogel transfer

For more than 15 years, various printing methods for the transfer of biomaterials have been

Table 1. The relationship between the hydrogel viscosity and ambient temperature.

Hydrogel	Viscosity (mPa*s)				
	20	24	28	32	37
Temperature, °C	20	24	28	32	37
Methylcellulose 1% w/v	231±12	194±11	170±12	133±11	104±13
Sodium alginate 1% w/v	76±3	68±2	61±3	56±4	50±5
Hyaluronic acid sodium salt 2% w/v	20±2	18±2	16±1	15±1	13±1

Table 2. The time-dependent hydrogel mass changes.

Hydrogel	Hydrogel layer weight (% of the initial)				
	0	2	5	10	30
Time, min	0	2	5	10	30
Methylcellulose 1% w/v	100	92.2±0.4	82±2	67±4	35±4
Sodium alginate 1% w/v	100	91.6±0.4	81±2	68±3	32±4
Hyaluronic acid sodium salt 2% w/v	100	92.1±0.4	82±2	68±3	27±5

studied^[56,59]. Regarding laser printing methods, they have the best resolution as well as provide cell survival during the transfer at the level of 95% or more^[10,56]. One of the main difficulties in applying the LIFT technique for biological applications is the need for individual selection of a large number of parameters for the combination “hydrogel-transferred object”^[59]. For example, two studies^[14,15] on LIFT printing establish the detailed relationships between printing parameters, the regimes of hydrogel jet and droplet formation using sodium alginate in various concentrations as a model. Moreover, the authors of several research articles^[15,60] mainly operate with the (1) Weber Number (We), which characterizes the ratio between inertial force and surface tension, and the (2) Ohnesorge number (Oh), which describes the process of droplet formation. These dimensionless quantities comprehensively characterize printing regimes:

$$We = \frac{\rho LV^2}{\sigma}, \quad Oh = \frac{\eta}{\sqrt{\rho \sigma L}},$$

where ρ , hydrogel density; L , characteristic length which in many cases is determined by the spot size^[14,60,61]; V , fluid gel speed; σ , surface tension; η , the shear viscosity of the gel.

In one study,^[61] the authors suggested using the inverse number $J = 1/Oh$. It is shown that jets form well in the range of $0.86 \leq J \leq 2.49$ at $F = 717 \pm 45 \text{ mJ/cm}^2$. With an increase in fluence, jet formation occurs well at a slightly higher viscosity (lower J).

Hydrogel parameters are very important for the jet formation. The characteristic time $\Delta\tau$ for the destruction of a cylindrical jet of radius (R) with the density (ρ) and surface tension σ as a result of Plateau–Rayleigh instability is^[62]:

$$\Delta\tau \cong 2.91 \cdot \sqrt{\rho \cdot R^3 / \sigma} \quad (2)$$

In the case of $R=50 \mu\text{m}$, with $\sigma=73 \times 10^{-3} \text{ N/m}$, we obtain $\Delta\tau = 120 \mu\text{s}$ with a radius of microdroplets of $\sim 9 R$ ^[62]. It was established^[54] that at a low gel viscosity, the gas bubble does not form and breaks at the initial stage. In this case, the lower working value of the viscosity at which the formation of the gel jet occurs decreases with decreasing spot size.

The We and Oh ranges for optimal printing regimes have already been described in the literature. The works^[15,59] present an algorithm in the form of a decision tree that helps to find the optimal printing regimes for specific gels in terms of the We and Oh values. However, in practice, usually there is a task of transferring certain bioink with unique physicochemical characteristics at an already-made laser system. Moreover, there is also sometimes no possibility of a significant change in the viscosity and surface tension of the hydrogel and adapting them to the parameters known in the literature. The task of identifying the optimal regime for a given bioink is quite complicated, and it may require a separate study using high-speed shooting for the selection of We and Oh values^[14,15,60] to ensure the optimal transfer regime. Therefore, we want to suggest a simplified decision tree based on our results. Following this

decision tree, you can get a successful printing, changing the most accessible parameters and analyzing the results without using additional expensive equipment such as high-speed shooting.

From a practical point of view, the most optimal algorithm for producing “quality” droplets of a given size is based on the variation of easily changeable parameters of the laser, such as energy per pulse (E) and spot size (SS), as well as at the distance between the donor and acceptor (D). In some cases (for example, if very large or very small droplets are needed), the thickness of the hydrogel layer (T) on the donor ribbon can also be varied.

Figure 8 shows a decision tree, which allows for achieving an optimal printing regime by

sequential selection of easily variable parameters for a particular experiment.

The scheme shows an algorithm that allows for quick configuration of the laser printing process to achieve the optimal regime, which forms “quality” droplets from the bioink with the given parameters. Based on the technical specifications for the formation of 2D or 3D structures, the optimal diameter of hydrogel droplets is determined. Subsequently, the parameters of the experiment, namely, Energy (E), Distance (D), Thickness (T), and Spot size (SS) are set and a trial transfer is performed. Based on the results of our works^[13,32,44,63,64] and the results of other authors^[14,15,54], for a wide variety of hydrogels^[24,65,66], the threshold fluence is 2 – 3 J/

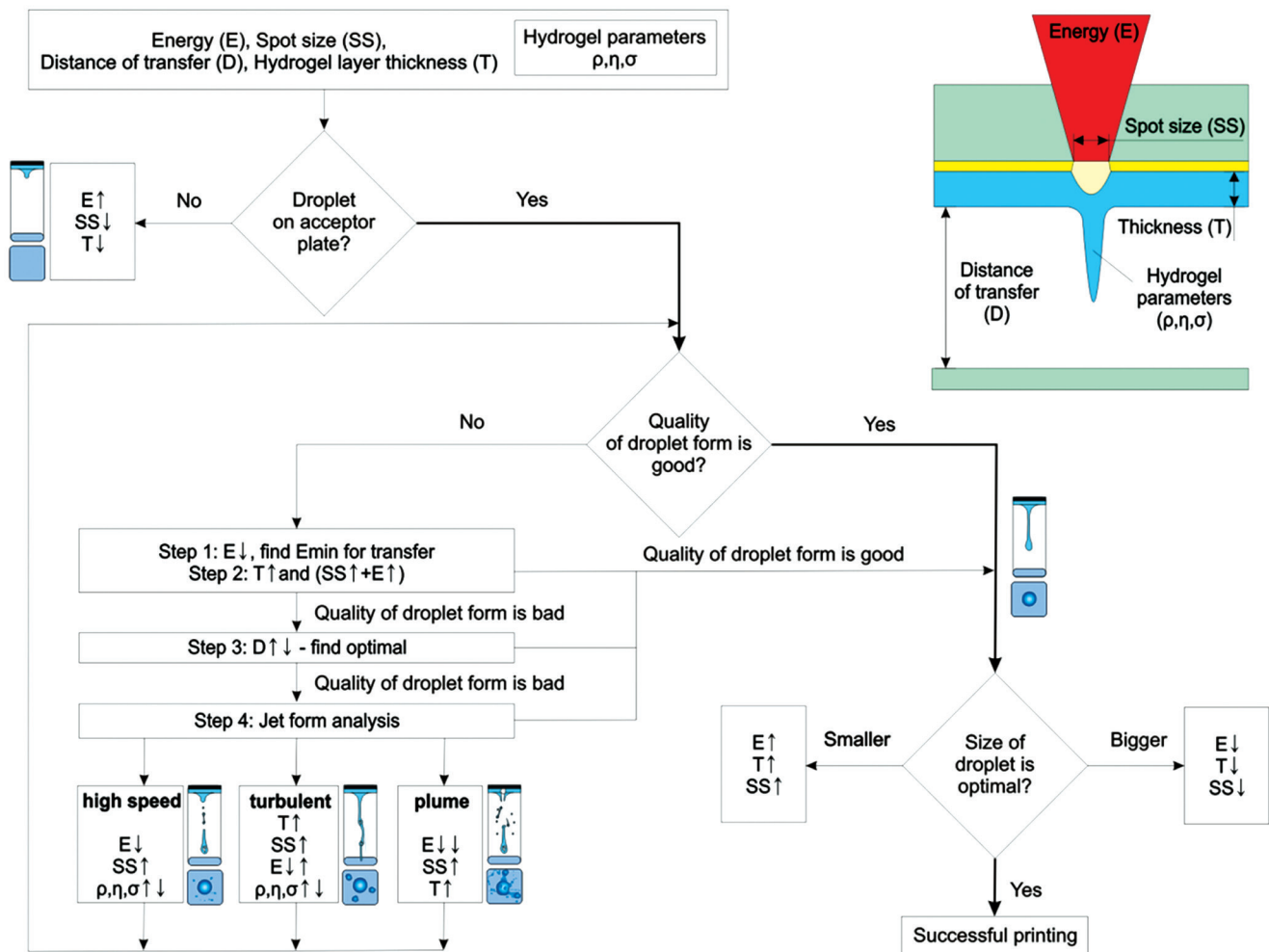


Figure 8. Decision tree for achieving a success story with laser-induced forward transfer. The symbol “↓” represents a decrease, “↑” an increase, and “↓ ↑” a variation.

cm² (nanosecond laser and Au absorbing layer). In practice, the starting values for the experiments can be: $E = 15 - 20 \mu\text{J}$ and $SS = 30 \mu\text{m}$ for a laser with a wavelength of 1064 nm and a pulse duration of ~ 10 ns. Such values allow successful realization of laser transfer process with most hydrogel types.

If no hydrogel transfer toward acceptor plate occurs, one should gradually increase the laser pulse energy and reduce the spot diameter and gel layer thickness to initiate the transfer process. When the gel transfer is achieved, the next step assesses the “quality” of the droplet shape by its appearance. If the transfer is carried out with a droplet of an irregular shape or with several droplets (splashing), then it is necessary to gradually adjust the experimental parameters. First, it is necessary to find the minimum laser pulse energy (Step 1, **Figure 8**) sufficient for droplet transfer. Second, it is advisable to increase the thickness of the gel (Step 2, **Figure 8**), while raising the energy of the laser pulse and spot diameter to achieve the required droplet size.

If after the implementation of these steps the quality of the droplet is still poor, then this is probably due to suboptimal distance between the donor and acceptor slides. Usually, it occurs if instead of a single droplet, the acceptor plate is reached by the forming jet, which leads to its splashing. Therefore, in the next step, it is advisable to increase the distance between the donor and acceptor slides. However, it will be wrong to conclude that for the implementation of high-quality printing, a long distance is always necessary, since with its increase, the printing quality will deteriorate. This deterioration is associated with the horizontal velocity component of transferred droplets, which emerges due to hydrogel heterogeneity and no axial symmetry in absorbing layer heating. In some cases, one can encounter a regime when the jet breaks up into several droplets landing on the acceptor plate. In this case, as the distance increases, the shape of the resulting droplet may distort thus demonstrating a spraying effect^[15]. Therefore, we believe that it is necessary to vary the entire range of distances between the donor and acceptor plates to detect the optimal transfer regime (Step 3, **Figure 8**). If

the change of the distance D still does not yield a “quality” droplet shape, then it is necessary to analyze the operating regimes of jet formation. It can be performed using high-speed shooting or, if it is unavailable, by the analysis of the landed droplet images (Step 4, **Figure 8**). Further, depending on the registered transfer regimes (high-speed, turbulent, and plume), it is necessary to select parameters according to the mentioned algorithm. In addition, high-speed shooting can help determine the optimal distance D between the donor and acceptor slides.

On reaching the regime resulting in “quality” droplets, further it may be necessary to adjust their size to the required parameters of the experiment. At the first stage, for small adjustments, it will be sufficient to change the laser pulse energy. However, for significant adjustments, one should simultaneously change several parameters, since otherwise, optimal transfer regime will be lost.

5 Conclusion

We investigated laser printing processes using three most widely used hydrogels in bioprinting: 2% hyaluronic acid sodium salt, 1% methylcellulose, and 1% sodium alginate. For all gels, various transfer regimes (no transfer mode, optimal jetting mode with single droplet transfer, high speed mode, turbulent mode, and plume mode) were determined depending on the change in laser pulse energy. It was shown that in the optimal jetting regime, for all hydrogels, the size and volume of droplets increased almost linearly with increasing laser fluence. The effect of ambient temperature on the viscosity of hydrogels was also evaluated. It was shown that at room temperature ($22 \pm 2^\circ\text{C}$), this change can be neglected. For the experiments where no additional methods used for preventing ribbon hydrogel drying, we determined the time periods which provide a stable controlled laser printing and which allow for neglecting the drying-induced hydrogel thickness change. Moreover, we suggested a simple practical algorithm for quick setting up of the LIFT printing process to obtain “quality” bioink droplets with the required parameters on a given experimental

setup. Furthermore, this setting is mainly provided by easily changing variable parameters, such as laser pulse energy, laser spot size, the distance between the donor ribbon and acceptor slide, as well as the thickness of the hydrogel layer on the donor ribbon.

Acknowledgments

This study was supported partially by the Russian Foundation Research (19-75-00108, 3D laser printing), Russian Foundation for Basic Research (18-32-20184, experimental setup and discussion of transfer mechanism) partially by the Ministry of Science and Higher Education within the State assignment FSRC “Crystallography and Photonics” RAS (lift process analysis), partially by the Russian academic excellence project ‘5-100’ (hydrogel support and analysis).

Conflict of interest

The authors declare no conflict of interest.

References

- Serra P, Fernández-Pradas JM, Berthet FX, *et al.*, 2004, Laser Direct Writing of Biomolecule Microarrays. *Appl Phys A Mater Sci Process*, 79:949–952. DOI: 10.1007/s00339-004-2577-2.
- Zergioti I, Karaiskou A, Papazoglou DG, *et al.*, 2005, Femtosecond Laser Microprinting of Biomaterials. *Appl Phys Lett*, 86:1–3. DOI: 10.1063/1.1906325.
- Colina M, Serra P, Fernández-Pradas JM, *et al.*, 2005, DNA Deposition through Laser Induced Forward Transfer. *Biosens. Bioelectron.*, 20(8):1638–1642. DOI: 10.1016/j.bios.2004.08.047.
- Serra P, Colina M, Fernández-Pradas JM, *et al.*, 2004, Preparation of Functional DNA Microarrays through Laser-induced Forward Transfer. *Appl Phys Lett*, 85:1639–1641. DOI: 10.1063/1.1787614.
- Cheptsov VS, Tsykina SI, Minaev NV, *et al.*, 2019, New Microorganism Isolation Techniques with Emphasis on Laser Printing. *Int J Bioprinting*, 5:1–12. DOI: 10.18063/ijb.v5i1.165.
- Koch L, Deiwick A, Schlie S, *et al.*, 2012, Skin Tissue Generation by Laser Cell Printing. *Biotechnol. Bioeng.*, 109:1855–1863. DOI: 10.1002/bit.24455.
- Gaebel R, Liu J, Koch, L, *et al.*, 2011, Patterning Human Stem Cells and Endothelial Cells with Laser Printing for Cardiac Regeneration. *Biomaterials*, 32:9218–9230. DOI: 10.1016/j.biomaterials.2011.08.071.
- Gaebel R, Kuhn S, Sorg H, *et al.*, 2009, Laser printing of skin cells and human stem cells. *Tissue Eng Part C Methods*, 16:847–854. DOI: 10.1089/ten.tec.2009.0397.
- Mandrycky C, Wang Z, Kim K, *et al.*, 2016, 3D Bioprinting for Engineering Complex Tissues. *Biotechnol. Adv.*, 34:422–434. DOI: 10.1016/j.biotechadv.2015.12.011.
- Koch L, Kuhn S, Sorg H, *et al.*, 2010, Laser Printing of Skin Cells and Human Stem Cells. *Tissue Eng Part C Methods*, 16:847–854. DOI: 10.1089/ten.tec.2009.0397.
- Catros S, Fricain JC, Guillotin B, *et al.*, 2011, Laser-assisted Bioprinting for Creating on-demand Patterns of Human Osteoprogenitor Cells and Nano-hydroxyapatite. *Biofabrication*, 3:025001. DOI: 10.1088/1758-5082/3/2/025001.
- Hopp B, Smausz T, Antal Z, *et al.*, 2004, Absorbing Film Assisted Laser Induced Forward Transfer of Fungi (*Trichoderma conidia*). *J Appl Phys*, 96:3478–3481. DOI: 10.1063/1.1782275.
- Yusupov VI, Zhigarkov VS, Churbanova ES, *et al.*, 2017, Laser-induced Transfer of Gel Microdroplets for Cell Printing. *Quantum Electron*, 47:1158–1165. DOI: 10.1070/qel16512.
- Zhang Z, Xiong R, Mei R, *et al.*, 2015, Time-Resolved Imaging Study of Jetting Dynamics during Laser Printing of Viscoelastic Alginate Solutions. *Langmuir*, 31:6447–6456. DOI: 10.1021/acs.langmuir.5b00919.
- Zhang Z, Xiong R, Corr DT, *et al.*, 2016, Study of Impingement Types and Printing Quality during Laser Printing of Viscoelastic Alginate Solutions. *Langmuir*, 32:3004–3014. DOI: 10.1021/acs.langmuir.6b00220.
- Guillotin B, Souquet A, Catros S, *et al.*, 2010, Laser Assisted Bioprinting of Engineered Tissue with High Cell Density and Microscale Organization. *Biomaterials*, 31:7250–7256. DOI: 10.1016/j.biomaterials.2010.05.055.
- Gaebel R, Ma N, Liu J, *et al.*, 2011, Patterning Human Stem Cells and Endothelial Cells with Laser Printing for Cardiac Regeneration. *Biomaterials*, 32:9218–9230. DOI: 10.1016/j.biomaterials.2011.08.071.
- Gruene M, Pflaum M, Hess C, *et al.*, 2011, Laser Printing of Three-dimensional Multicellular Arrays for Studies of Cell-cell and Cell-environment Interactions. *Tissue Eng Part C Methods*, 17:973–982. DOI: 10.1089/ten.tec.2011.0185.
- Koch L, Brandt O, Deiwick A, *et al.*, 2017, Laser-assisted Bioprinting at Different Wavelengths and Pulse Durations

- with a Metal Dynamic Release Layer: A Parametric Study. *Int J Bioprinting*, 3:42–53. DOI: 10.18063/ijb.2017.01.001.
20. Sorkio A, Koch L, Koivusalo L, *et al.*, 2018, Human Stem Cell Based Corneal Tissue Mimicking Structures Using Laser-assisted 3D Bioprinting and Functional Bioinks. *Biomaterials*, 171:57–71. DOI: 10.1016/j.biomaterials.2018.04.034.
 21. Guillemot F, Souquet A, Catros S, *et al.*, 2010, High-throughput Laser Printing of Cells and Biomaterials for Tissue Engineering. *Acta Biomater*, 6:2494–2500. DOI: 10.1016/j.actbio.2009.09.029.
 22. Catros S, Guillemot F, Nandakumar A, *et al.*, 2011, Layer-by-Layer Tissue Microfabrication Supports Cell Proliferation *In Vitro* and *In Vivo*. *Tissue Eng Part C Methods*, 18:62–70. DOI: 10.1089/ten.tec.2011.0382.
 23. Michael S, Sorg H, Peck CT, *et al.*, 2013, Tissue Engineered Skin Substitutes Created by Laser-Assisted Bioprinting form Skin-Like Structures in the Dorsal Skin Fold Chamber in Mice. *PLoS One*, 8:e57741. DOI: 10.1371/journal.pone.0057741.
 24. Antoshin AA, Churbanov SN, Minaev NV, *et al.*, 2019, LIFT-Bioprinting, is it Worth it? *Bioprinting*, 15:e00052. DOI: 10.1016/j.bprint.2019.e00052.
 25. Bashkatov AN, Genina EA, Kochubey VI, *et al.*, 2005, Optical Properties of Human Skin Subcutaneous and Mucous Tissues in the Wavelength Range from 400 to 2000 nm. *J Phys D Appl Physics*, 38:2543–2555. DOI: 10.1088/0022-3727/38/15/004.
 26. Carvalho S, Gueiral N, Nogueira E, *et al.*, 2017, Comparative Study of the Optical Properties of Colon Mucosa and Colon Precancerous Polyps between 400 and 1000 nm. *Dynamics and Fluctuations in Biomedical Photonics XIVXIV International Society for Optics and Photonics*, 10063:100631L. DOI: 10.1117/12.2253023.
 27. Pagès E, Rémy M, Kériquel V, *et al.*, 2015, Creation of Highly Defined Mesenchymal Stem Cell Patterns in Three Dimensions by Laser-Assisted Bioprinting. *J Nanotechnol Eng Med*, 6:021005. DOI: 10.1115/1.4031217.
 28. Zhang Z, Xu C, Xiong R, *et al.*, 2017, Effects of Living Cells on the Bioink Printability during Laser Printing. *Biomicrofluidics*, 11:034120. DOI: 10.1063/1.4985652.
 29. Zhang Z, Chai W, Xiong R, *et al.*, 2017, Printing-induced Cell Injury Evaluation during Laser Printing of 3T3 Mouse Fibroblasts. *Biofabrication*, 9:025038. DOI: 10.1088/1758-5090/aa6ed9.
 30. Unger C, Gruene M, Koch L, *et al.*, 2011, Time-resolved Imaging of Hydrogel Printing Via Laser-induced Forward Transfer. *Appl Phys A Mater Sci Process*, 103:271–277. DOI: 10.1007/s00339-010-6030-4.
 31. Desrus H, Chassagne B, Catros S, *et al.*, 2016, Laser Assisted Bioprinting using a Femtosecond Laser with and without a Gold Transductive Layer: A Parametric Study. *Proceedings Volume 9706, Optical Interactions with Tissue and Cells XXVII*. DOI: 10.1117/12.2209087.
 32. Cheptsov VS, Churbanova ES, Yusupov VI, *et al.*, 2018, Laser Printing of Microbial Systems: Effect of Absorbing Metal Film. *Lett Appl Microbiol*, 67:544–549. DOI: 10.1111/lam.13074.
 33. Riestler D, Budde J, Gach C, *et al.*, 2016, High Speed Photography of Laser Induced Forward Transfer (LIFT) of Single and Double-layered Transfer Layers for Single Cell Transfer. *J Laser Micro Nanoeng*, 11:199–203. DOI: 10.2961/jlmn.2016.02.0010.
 34. Zarubin VP, Zhigarkov VS, Yusupov VI, *et al.*, 2019, Physical Processes Affecting the Survival of Microbiological Systems in Laser Printing of Gel Droplets. *Quantum Electron*, 49:1068–1073. DOI: 10.1070/qel17081.
 35. Tomasina S, Bodet C, Mota T, *et al.*, 2019, Bioprinting Vasculature: Materials, Cells and Emergent Techniques. *Materials (Basel)*, 12:2701. DOI: 10.3390/ma12172701.
 36. Young HD, Modi R, Bucaro M, 2002, Generation of Mesoscopic Patterns of Viable *Escherichia coli* by Ambient Laser Transfer. *Biomaterials*, 23:161–166. DOI: 10.1016/s0142-9612(01)00091-6.
 37. Xiong R, Zhang Z, Huang Y, 2015, Identification of Optimal Printing Conditions for Laser Printing of Alginate Tubular Constructs. *J Manuf Process*, 20:450–455. DOI: 10.1016/j.jmapro.2015.06.023.
 38. Palla-Papavlu A, Córdoba C, Patrascioiu A, *et al.*, 2013, Deposition and Characterization of Lines Printed through Laser-induced Forward Transfer. *Appl Phys A Mater Sci Process*, 110:751–755. DOI: 10.1007/s00339-012-7279-6.
 39. Pescosolido L, Miatto S, Di Meo C, *et al.*, 2010, Injectable and *In Situ* Gelling Hydrogels for Modified Protein Release. *Eur Biophys J*, 39:903-9. DOI: 10.1007/s00249-009-0440-2.
 40. Ouyang L, Highley CB, Rodell CB, *et al.*, 2016, 3D Printing of Shear-Thinning Hyaluronic Acid Hydrogels with Secondary Cross-Linking. *ACS Biomater Sci Eng*, 2:1743–1751. DOI: 10.1021/acsbiomaterials.6b00158.
 41. Cochis A, Bonetti L, Sorrentino R, *et al.*, 2018, 3D Printing of Thermo-responsive Methylcellulose Hydrogels for Cell-sheet Engineering. *Materials (Basel)*, 11:1–14. DOI: 10.3390/ma11040579.
 42. Ovsianikov A, Gruene M, Pflaum M, *et al.*, 2010, Laser Printing of Cells into 3D Scaffolds. *Biofabrication*, 2:014104.

- DOI: 10.1088/1758-5082/2/1/014104.
43. Gruene M, Pflaum M, Deiwick A, *et al.*, 2011, Adipogenic Differentiation of Laser-printed 3D Tissue Grafts Consisting of Human Adipose-derived Stem Cells. *Biofabrication*, 3:015005. DOI: 10.1088/1758-5082/3/1/015005.
 44. Yusupov VI, Gorlenko MV, Cheptsov VS, *et al.*, 2018, Laser Engineering of Microbial Systems. *Laser Phys Lett*, 15:015604.
 45. Unger C, Koch J, Overmeyer L, *et al.*, 2012, Time-resolved Studies of Femtosecond-laser Induced Melt Dynamics. *Opt Express*, 20:24864. DOI: 10.1364/oe.20.024864.
 46. Hill C, 2016, Liquid-Phase Laser Induced Forward Transfer for Complex Organic Inks and Tissue Engineering. *Ann Biomed Eng*, 45:84–99. DOI: 10.1007/s10439-016-1617-3.
 47. Akhatov W, Lindau I, Topolnikov O, *et al.*, 2001, Collapse and Rebound of a Laser-induced Cavitation Bubble. *Phys Fluids*, 13:29–32. DOI: 10.1063/1.1401810.
 48. Mézel C, Hallo L, Souquet A, *et al.*, 2009, Self-consistent Modeling of Jet Formation Process in the Nanosecond Laser Pulse Regime. *Phys Plasmas*, 16:123112. DOI: 10.1063/1.3276101.
 49. Ali M, Pages E, Ducom A, *et al.*, 2014, Controlling Laser-induced Jet Formation for Bioprinting Mesenchymal Stem Cells with High Viability and High Resolution. *Biofabrication*, 6:045001. DOI: 10.1088/1758-5082/6/4/045001.
 50. Wang W, Chrisey DB, 2008, Study of Impact-Induced Mechanical Effects in Cell Direct. *J Manuf Sci Eng*, 130:1–10.
 51. Ringeisen BR, Pages E, Ducom A, *et al.*, 2004, Laser Printing of Pluripotent Embryonal Carcinoma Cells. *Tissue Eng*, 10:483–491.
 52. Kawecki F, Clafshenkel WP, Auger FA, *et al.*, 2018, Self-assembled Human Osseous Cell Sheets as Living Biopapers for the Laser-assisted Bioprinting of Human Endothelial Cells. *Biofabrication*, 10:035006. DOI: 10.1088/1758-5090/aabd5b.
 53. Vass C, Smausz T, Hopp B, 2004, Wet Etching of Fused Silica: A Multiplex Study. *J Phys D Appl Phys*, 37:2449–2454. DOI: 10.1088/0022-3727/37/17/018.
 54. Gruene M, Unger C, Koch L, *et al.*, 2011, Dispensing Pico to Nanolitre of a Natural Hydrogel by Laser-assisted Bioprinting. *Biomed Eng Online*, 10:9–12. DOI: 10.1186/1475-925x-10-19.
 55. Brown MS, Brasz CF, Ventikos Y, Arnold CB, 2012, Impulsively Actuated Jets from thin Liquid Films for High-resolution Printing Applications. *J Fluid Mech*, 709:341–370. DOI: 10.1017/jfm.2012.337.
 56. Hölzl K, Lin S, Tytgat L, *et al.*, 2016, Bioink Properties before, during and after 3D Bioprinting. *Biofabrication*, 8:032002. DOI: 10.1088/1758-5090/8/3/032002.
 57. Ringeisen BR, Spargo BJ, Wu PK, 2010, Cell and Organ Printing. Springer Science and Business Media, Berlin.
 58. Nasatto PL, Pignon F, Silveira JL, *et al.*, 2015, Methylcellulose, a Cellulose Derivative with Original Physical Properties and Extended Applications. *Polymers (Basel)*, 7:777–803. DOI: 10.3390/polym7050777.
 59. Shafiee A, Elham G, Ramesh H, *et al.*, 2019, Physics of Bioprinting. *Appl Phys Rev*, 6:021315.
 60. McKinley GH, Renardy M, 2011, Wolfgang von Ohnesorge. *Phys Fluids*, 23:127101. DOI: 10.1063/1.3663616.
 61. Yan J, Huang Y, Xu C, *et al.*, 2012, Effects of Fluid Properties and Laser Fluence on Jet Formation during Laser Direct Writing of Glycerol Solution. *J Appl Phys*, 112:083105. DOI: 10.1063/1.4759344.
 62. Bush JW, 2004, Rayleigh Instability. In: MIT Lecture Notes on Surface Tension, Lecture 5 (PDF) Massachusetts Institute of Technology.
 63. Gorlenko M, Chutko EA, Churbanova ES, *et al.*, 2018, Laser Microsampling of Soil Microbial Community. *J Biol Eng*, 12:1–11.
 64. Minaev NV, Chutko EA, Churbanova ES, *et al.*, 2018, Laser Printing of Gel Microdrops with Living Cells and Microorganisms. *KnE Energy Phys*, 2018:23–31. DOI: 10.18502/ken.v3i3.2010.
 65. Koch L, Deiwick A, Franke A, *et al.*, 2018, Laser Bioprinting of Human Induced Pluripotent Stem Cells the Effect of Printing and Biomaterials on Cell Survival, Pluripotency, and Differentiation. *Biofabrication*, 10:035005. DOI: 10.1088/1758-5090/aab981.
 66. Cheptsov VS, Tsykina SI, Minaev NV, *et al.*, 2019, New Microorganism Isolation Techniques With Emphasis On Laser Printing. *Int J Bioprint*, 5:165. DOI:10.18063/ijb.v5i1.165.

3D Printed Gene-activated Octacalcium Phosphate Implants for Large Bone Defects Engineering

Ilya Y. Bozo^{1,2}, Roman V. Deev^{2,3}, Igor V. Smirnov⁴, Alexander Yu. Fedotov⁴, Vladimir K. Popov⁵, Anton V. Mironov⁵, Olga A. Mironova⁵, Alexander Yu. Gerasimenko^{6,7}, Vladimir S. Komlev^{4,5*}

¹Department of Maxillofacial Surgery, A.I. Burnazyan Federal Medical Biophysical Center, FMBA of Russia, Moscow, Russia

²Research and Development Department, Human Stem Cells Institute, Moscow, Russia

³Department of Pathology, I.I. Mechnikov North-Western State Medical University, Saint-Petersburg, Russia

⁴A.A. Baikov Institute of Metallurgy and Materials Science, Russian Academy of Sciences, Moscow, Russia

⁵Institute of Photon Technologies of Federal Scientific Research Centre “Crystallography and Photonics,” Russian Academy of Sciences, Moscow, Russia

⁶Institute for Bionic Technologies and Engineering, I.M. Sechenov First Moscow State Medical University, Moscow, Russia

⁷Institute of Biomedical Systems, National Research University of Electronic Technology, Moscow, Russia

Abstract: The aim of the study was the development of three-dimensional (3D) printed gene-activated implants based on octacalcium phosphate (OCP) and plasmid DNA encoding *VEGFA*. The first objective of the present work involved design and fabrication of gene-activated bone substitutes based on the OCP and plasmid DNA with *VEGFA* gene using 3D printing approach of ceramic constructs, providing the control of its architectonics compliance to the initial digital models. X-ray diffraction, scanning electron microscopy (SEM), Fourier transform infrared spectroscopy, and compressive strength analyses were applied to investigate the chemical composition, microstructure, and mechanical properties of the experimental samples. The biodegradation rate and the efficacy of plasmid DNA delivery *in vivo* were assessed during standard tests with subcutaneous implantation to rodents in the next stage. The final part of the study involved substitution of segmental tibia and mandibular defects in adult pigs with 3D printed gene-activated implants. Biodegradation, osteointegration, and effectiveness of a reparative osteogenesis were evaluated with computerized tomography, SEM, and a histological examination. The combination of gene therapy and 3D printed implants manifested the significant clinical potential for effective bone regeneration in large/critical size defect cases.

Keywords: Three-dimensional printing, Bone tissue engineering, Calcium phosphate, Octacalcium phosphate, Gene, Plasmid DNA, Vascular endothelial growth factor.

*Corresponding Author: Vladimir S. Komlev, A.A. Baikov Institute of Metallurgy and Materials Science, Russian Academy of Sciences, Moscow, Russia; komlev@mail.ru

Received: March 10, 2020; **Accepted:** April 14, 2020; **Published Online:** June 03, 2020

(This article belongs to the *Special Section: Bioprinting in Russia*)

Citation: Bozo IY, Deev RV, Smirnov IV, *et al.*, 2020 3D Printed Gene-activated Octacalcium Phosphate Implants for Large Bone Defects Engineering. *Int J Bioprint*, 6(3): 275. DOI: 10.18063/ijb.v6i3.275.

1 Introduction

Skeletal bone disorder caused by traumas, inflammation, malignancies, intervertebral disk disease, as well as alveolar ridge atrophy following tooth loss is highly prevalent

and incrementally increasing^[1]. Despite the development of numerous ordinary and activated bone substitutes, the management of large bone defects is still challenging and usually demands the use of bone autografts that is associated with a certain complication rate, donor site morbidity,

contraindications, a considerable duration of the intervention, and post-surgery rehabilitation^[2]. This creates a strong need for acceptable alternative of bone autografts in clinical practice. Biodegradable implants possessing chemical composition, structure, osteoconductive and osteoinductive potential corresponding to native bone, with shape and sizes exactly conforming to the parameters of substitute for specific bone defect could become such an alternative. In addition, a personalized bone substitute should have optimal biomechanical properties allowing at least its stable fixation *in situ* with standard, for example, metal constructions.

Three-dimensional (3D) printing techniques that facilitate development of custom-made medical devices are the most promising approach to solve the problems in personalized bone reconstruction. However, in selecting the material for 3D printing, scientists frequently make their decision based on technical feasibility of additive manufacturing with a high spatial resolution rather than on the potential of a biomaterial to actually improve reparative osteogenesis. Therefore, some polymer materials such as polycaprolactone^[3] and polylactic-co-glycolic acid^[4], which are greatly suitable for 3D printing including that associated with addition of biologically active components (living cells, growth factors, etc.), but less effective for bone grafting^[5] are taken often. On the other hand, natural and synthetic analogues of bone matrix components with optimal biomechanical properties show that osteoconduction and biodegradable property through the release of components that cells can utilize to produce and mineralize the intercellular matrix are more appropriate for bone regeneration^[6]. For instance, octacalcium phosphate (OCP) has optimal osteoconductive properties and biodegradation rate. It is a precursor of natural mineral component of the bone matrix^[7], and it stimulates differentiation of multipotent mesenchymal stromal cells to osteogenic lineage^[8]. However, it is very difficult to achieve a high spatial resolution in 3D printing of ceramic implants, and the problem becomes even more irresistible if some biologically active components are needed to enhance osteoinductive

capacity required to restore large bone defects that are characterized by “osteogenic insufficiency”^[9].

Cells and growth factors are most actively employed osteoinducing factors for 3D printed scaffolds^[10]. However, cells require oxygenation that limits their possible use in creating personalized tissue engineering constructions or bioactive implants of large sizes, whereas growth factors are short-lived and short-distant^[9]. Gene-activated materials are devoid of these drawbacks, though the delivery of gene constructs in the safest, a non-viral, variant is “Achilles heel” of the approach^[9].

In this study, based on our previous experience in 3D printing of OCP bone substitutes^[11,12], considering the critical role of angiogenesis for reparative osteogenesis, we hypothesized that deposition of plasmid DNA carrying a gene of vascular endothelial growth factor (pDNA-*VEGFA*), as an active substance of the “Neovasculgen” drug (developed and certified for clinical applications by HSCI, Russia)^[13], into custom-made OCP-based 3D printed implants would make it effective in large bone defect substitution and guided bone regeneration.

2 Experimental method

2.1 Materials

Initial tricalcium phosphate (TCP) powder was produced in an aqueous medium by slowly adding diammonium phosphate ($(\text{NH}_4)_2\text{HPO}_4$) solution into calcium nitrate ($\text{Ca}(\text{NO}_3)_2 \cdot 4\text{H}_2\text{O}$) solution, containing NH_4OH . Fraction of TCP agglomerated particles with mean size in diameter 40 – 80 μm was selected as a raw material for all further experiments. 1.0% aqueous solution of salts of phosphoric acid (pH value equals 4.75) was utilized as “ink” for 3D printing^[11]. All used reagents were ordered and received from Sigma-Aldrich (USA).

2.2 3D printing

3D printed samples were made under a previously modified printing algorithm of ceramic constructions described elsewhere in details^[12].

Layer-by-layer printing process of 3D ceramics scaffolds was performed on custom-made 3D printer (shown in **Figure 1** and presented on Supplementary Video 1). The approach of 3D printing is based on a route, which allowed chemical reaction between TCP agglomerated particles and “ink” (diluted phosphoric acid). The schematic set up of the custom-made 3D printer is shown in **Figure 1A and B**.

There were several models prepared in our work: non-porous disks with diameter of 10-mm and thickness of 2-mm to assess baseline biodegradation and mechanical properties; disks with 10-mm diameter, 2-mm thickness, and a net-like structure to evaluate the efficacy of gene constructs delivery and custom-made

implants with a complex architectonics exactly corresponding to the planned defect substitution in adult pig mandibular (**Figure 1 C1**) and tibia (**Figure 1 C2**), followed by bone reconstruction.

3D models were made in the form of disks with standard tools in a Blender software (Blender Foundation, Germany). In the bone reconstruction experiment, multispiral medical computerized tomography (CT) of the skull and hindlimb of adult pig with a weight of 50 kg was done. Then, planned bone defects were mapped in computerized images using 3D slicer software (Brigham and Women’s Hospital, Inc., USA). These were a segmental “T-shaped” defect of the tibia diaphysis with a total length of 30 mm including 10 mm circular central part for complete

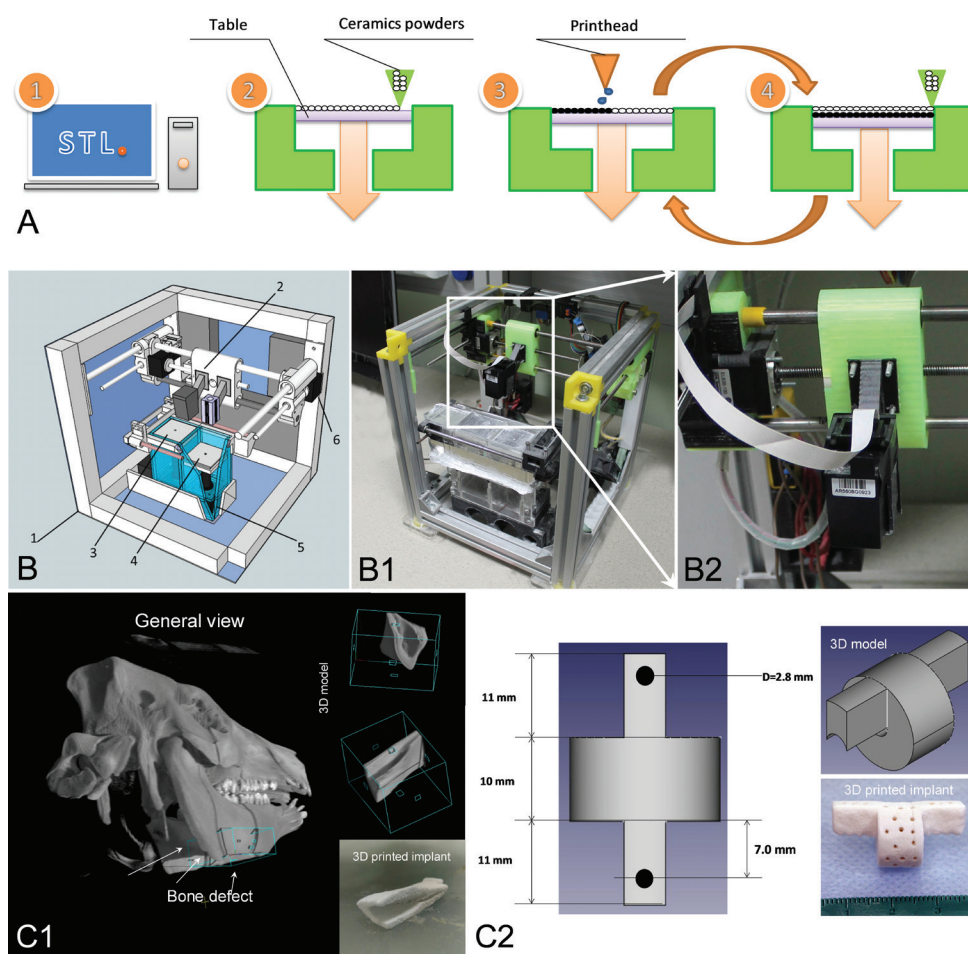


Figure 1. (A) Schematic overview of the three-dimensional (3D) printing approach; (B) Custom-made 3D printer: (1) 3D printer frame; (2) printing head; (3) stuffer with spreader; (4) Z-piston; (5) building box; (6) stepper motors. (B1, B2) Custom-made 3D printer and printing head; (C1, C2) 3D planned defects for mandibular and pig tibia.

disintegration and branching proximal and distal cortical defects of the diaphyseal anterior surface sized $10 \times 5 \times 5 \text{ mm}^3$ each; a full-layer defect of the mandible lower edge from the angle to the front sized $25 \times 15 \times 10 \text{ mm}^3$. The specified zones were segmented with the removal of surrounding tissues. 3D reconstructions of designated bone regions, corresponding to the planned bone defects were transferred into MeshLab (Visual Computing Lab, Italy), a mesh-object was generated, transferred into Blender and the implant structure was corrected, i.e. irregularities were removed, perforating canals with a diameter of 1 mm were added, a central opening with a diameter of 10 mm created in the circular implant part corresponding to the medullary canal for tibia reconstruction. The resulting STL-format models were loaded into the custom-made 3D printer software.

2.2 Post-treatment of 3D printed implants

3D printed samples were supplied for the post-treatment into biomimetic solution, which was produced by dissolving 115 g of monoammonium phosphate ($\text{NH}_4\text{H}_2\text{PO}_4$) in 500 mL of distilled water at room temperature and pH value 4.1 ± 0.1 . 3D printed samples were kept there at 40°C up to 168 h. After that, the samples were thoroughly washed in distilled water at least 10 times, dried in air at 37°C and placed in a second solution, which was prepared by dissolving 95.2 g of CH_3COONa in 700 mL of distilled water at 40°C and pH value 8.2 ± 0.2 . 3D printed samples were again kept at 40°C up to 168 h, then washed in distilled water for at least 10 times and dried in air at 37°C ^[11]. All used reagents were purchased from Sigma-Aldrich (USA).

2.3 Characterization of 3D printed implants

The porosity, intergranular size, and specific surface area were studied by mercury porosimeter (TriStar 3000, Micromeritics, USA). The phase composition was analyzed by conventional X-ray diffraction (XRD) (Shimadzu XRD-6000, Japan), with Ni-filtered $\text{CuK}\alpha 1$ target, $\lambda = 1.54183 \text{ \AA}$. The samples were scanned from $2\theta = 3^\circ$ to 60° with a step size of 0.02° and a preset time of 5 s. Scanning electron microscope (SEM) (Tescan

Vega II, Czech Republic) equipped with EDS analyzer, operating in secondary and backscattered electron modes, was used for investigation of surface morphology, microstructure, and chemical composition. For SEM analysis, all samples were sputter-coated before imaging with a 25 nm-thick gold layer to impart electrical conductivity to the specimen surfaces. Fourier transform infrared (FTIR) spectroscopy study was performed using an Infrared Spectroscopy microscope (Nicolet Avatar 330 FTIR spectrometer, UK) in transmission mode. FTIR data were recorded over the range of $4000 - 400 \text{ cm}^{-1}$ with 128 scans. The compressive strength of the samples was evaluated in accordance with the ISO standard 83.100: Cellular materials. At least five samples for each experimental point were tested. The compression test was carried out using an Instron 5581 (Bucks, UK) testing machine operating at a crosshead speed of $1 \text{ mm} \times \text{min}^{-1}$.

2.4 Plasmid DNA deposition on 3D printed implants

The supercoiled naked plasmid DNA encoding *VEGFA* gene, an active substance of “Neovasculgen,” the drug indicated for the treatment of patients with chronic lower limb ischemia (developed and certified for clinical applications by PJSC Institute of Human Stem Cells, Russia), was used to create personalized gene-activated implants^[13]. Plasmid DNA carrying the gene of luciferase (*Luc*) was also used in our experiments to evaluate the transfection efficacy *in vivo*. The combination of 3D printed bone substitute with plasmid DNA was performed under previously developed protocol^[14]. Briefly, 3D printed scaffolds were washed in a 0.5 M solution of sodium phosphate monobasic dihydrate ($\text{NaH}_2\text{PO}_4 \times 2\text{H}_2\text{O}$, Chimmed, Russia) at 37°C when constantly shaken for 10 h, washed in 1 ml of 10 mM $\text{NaH}_2\text{PO}_4 \times 2\text{H}_2\text{O}$ at 37°C when constantly shaken 4 times for 10 min, then were left at 37°C for 10 h until dried. After that, the samples were placed in a 10 mM $\text{NaH}_2\text{PO}_4 \times 2\text{H}_2\text{O}$ solution with plasmid DNA in the concentration of $1 \mu\text{g}/\mu\text{l}$ and incubated at 37°C and constant shaking for 10 h, and then a non-bound fraction of gene constructs was washed with 5 mM $\text{NaH}_2\text{PO}_4 \times 2\text{H}_2\text{O}$.

The binding of plasmid DNA with OCP surface was controlled visually by SEM and chemically when a bound plasmid DNA fraction was taken off with 0.5 M $\text{NaH}_2\text{PO}_4 \times 2\text{H}_2\text{O}$, and its concentration in a solution was measured with fluorometer Qubit 2.0 (Invitrogen, USA).

2.5 *In vivo* experiments

Animal trials were carried out in accordance with institutional guidelines/protocols in agreement with national laws and policies for animal care. The guidelines were approved by PJSC Institute of Human Stem Cells, Moscow, Russia.

2.5.1 Biodegradation assessment

Biodegradation assessment of 3D printed OCP based and gene-activated implants were studied in male rats with a body weight of 150 g ($n = 24$). A 15-mm median skin incision was done in the lower back under infiltration anesthesia with Sol. Lidocaini 1 – 2 ml and intramuscular sedation with Sol. Zoletili 100 – 10 mg/kg and 20 mm subcutaneous pockets were formed on both sides of the incision. The gene-activated bone substitutes were implanted into the right zone, but 3D printed scaffolds without plasmid DNA – into the left one. A post-operative wound was sutured by interrupted stitches with Polysorb 5/0. The animals were sacrificed in 15, 30, 90, 120, and 180 days by overdosage of Sol. Zoletili 100. The materials were extracted and fixed in 10% neutral formalin. Micro CT of the samples was performed by Brucker SKYSCAN 1174 (Belgium) and then the images were 3D-reconstructed using VG Studio Max software (Germany). A diameter, shape, and a surface area to implant volume ratio were determined. After decalcification in a Biodec-R solution (Bio-optica, Italy), histological slices were prepared under a standard procedure followed by hematoxylin and eosin staining.

2.5.2 Gene constructs delivery assessment *in vivo*

Balb/c mice with a body weight of 30 g ($n = 20$) were used in this experiment. 3D printed scaffolds (Control 1), 3D printed gene-activated

implants with *VEGFA*-carrying (Control 2) or *Luc*-carrying plasmid DNA (test group) were inserted subcutaneously to an animal. Sham-operated animals (Control 3) and those injected with a solution of plasmid DNA with *Luc* gene (Control 4) were used as additional controls. On days 1, 7, 14, and 28, D-luciferin sodium salt (Lumtec, Russia) was intraperitoneally injected to animals which had been preliminarily sedated with Sol. Zoletili 100 – 10 mg/kg. In 10 min, they were placed in a bioluminometer IVIS Spectrum chamber (PerkinElmer, Inc., USA), and a luminescent signal was recorded for 1 min.

2.5.3 Segmental bone defect reconstruction

Male pigs with an average body weight of 50 ± 2 kg ($n = 4$) were used in this study. Each animal underwent surgery on the right tibia and the mandible on both sides under combined endotracheal anesthesia. After the surgery, all animals received antibiotic therapy (Cefazolin-natrii 1.0) for 7 days and then were sacrificed by thiopental sodium overdose when sedated with Sol. Zoletili 100 in 3- and 6-months post-surgery. The bones with the previous surgery areas were resected. Reconstructive plates and screws were removed from the tibia; the metal constructions were left in the mandible to retain the regeneration integrity. The materials were fixed in 10% neutral formalin.

Tibia reconstruction: 10-cm straight incision was made through the skin along the anterior tibia surface, soft tissues were dissected, the diaphysis exposed subperiosteally and a T-shaped fragment corresponding to a planned bone defect with a total length of 30 mm was resected. 3D printed gene-activated implant was inserted into the defect, and osteosynthesis performed with the use of a 3.2 mm-thick reconstructive plate and screws with a diameter of 3.7 mm, some of them were fixed bicortically. Bone fragments were fixed stable on a surgical table. The post-operative wounds were closed in four layers with Polysorb 4/0, SurgiPro 4/0.

Mandible reconstruction: the intervention was carried out on both sides of the mandible under the same protocol. A skin linear incision was made

2 cm below and in parallel to the lower edge of the mandible from its angle by 4 cm forward, soft tissues were dissected, a surface of the mandibular body exposed subperiosteally. Osteotomy was performed by removing a lower edge fragment sized $25 \times 15 \times 10 \text{ mm}^3$ and retaining the mandible continuity. 3D printed gene-activated implant was fixed on the right side and plasmid-free 3D printed implant (as control) fixed on the left one within the defect using a straight titanium miniplate and miniscrews (a diameter of 2 mm, a length of 5 – 7 mm). The post-operative wounds were closed in four layers with Polysorb 4/0, SurgiPro 4/0.

CT: Having been fixed for 5 days, the materials were examined with medical CT in the same scanning mode and parameters, i.e. voxel size 0.08 mm, 80 kV, and 2 mA. The images were analyzed with standard tools in the Planmeca Romexis viewer software (Planmeca Oy, Finland). A quantitative assay of the images involved the determination of newly formed tissues density (in Hounsfield units (HU)) in three projections with apply of a region of interest tool and sizes of the remaining implants.

SEM: The bone fragments lengthwise through the central axis were cut. Several samples sized $5 \times 5 \times 5 \text{ mm}^3$ were resected from each part of every material from the border between the implant and a bone edge and from an implant central zone for SEM study. The remaining materials were used for a histologic examination. SEM study was performed after standard sampling with gold sputtering (section 2.3). Changes in the experimental samples' structure, chemical compositions, and the border between the implant and newly formed bone were evaluated.

Histological analysis: 5- μm thick slices were prepared from intact parts of every material without previous decalcification and stained with trichrome. The materials sampled for SEM were decalcified in a Biodec-R solution and used for histological specimens' preparation under the standard protocol with hematoxylin and eosin staining. All specimens were scanned in a Mirax Scanner (Carl Zeiss, Germany), and digital images were generated and evaluated qualitatively

and quantitatively in the Panoramic Viewer (3DHistech Ltd, USA).

2.6 Statistical analysis

All results are expressed as mean \pm SD. Mann–Whitney U-test was used to compare independent groups, with Wilcoxon signed-rank test used for intra-group comparisons for each time points. $P < 0.05$ was considered statistically significant.

3 Results

All initial implants were produced by our modified 3D printing technology^[11,12] of ceramic constructions from a synthesized TCP powder and 1.0% aqueous solution of phosphoric acid salt as described above. Experimental samples set reproduced a shape, sizes and the structure of CAD (computer assisted design) STL-models with a high (ca. $\pm 100 \mu\text{m}$) spatial accuracy and comprised: 1) non-porous disks to assess biodegradation; 2) porous disks to evaluate a level of plasmid DNA delivery; and 3) complex custom-made implants to reconstruct the tibia and mandible large defects in pigs.

3D printing fusing of TCP agglomerated particles and “ink” (diluted phosphoric acid) is based on a hydraulic setting reaction leading to formation of dicalcium phosphate dihydrate (DCPD), and thus, to layer-crossing bonding of the powder. Finally, 3D structure is formed. According to the XRD analysis, the 3D printed samples compose of unreacted TCP and certain amounts of DCPD (**Figure 2A**). FTIR and SEM data of the experimental samples confirmed the formation of DCPD (**Figure 2B and C**). SEM analysis of the 3D printed samples are shown in **Figure 2C**. Particles was about 5 – 20 μm in dimension. The DCPD crystals had a flower-like morphology. The width of the DCPD crystals was in the range of 1 – 50 μm , and their thickness was few microns.

Compressive strength of the 3D printed samples is presented on **Figure 2F** and was in the range of 1.5 – 4.5 MPa, depending on the number of micro-drops from printing head.

The post-treatment of the 3D printed samples lead to formation of OCP phase and the adhesive

effect between particles. The crystallization of TCP to DCPD was finished after 7 days (Figure 2A and B). 3D printed samples with DCPD phase composition were transformed into OCP of soaking in sodium acetate, according to XRD, FTIR and SEM (Figure 2A, B and D). XRD data of the OCP showed certain amounts of OCP phase with (100) reflection at $2\theta=4.9^\circ$. However, the post-treated samples contained some quantity of unreacted DCPD. High intensity of diffraction peaks indicates high crystallinity of OCP materials (Figure 2A). FTIR data of the OCP samples are presented on Figure 2B and are in agreement with those previously reported in Fowler *et al.*^[15]. The OH bending modes originating from the HPO_4 groups of OCP were observed at 1295 cm^{-1} . P–O in HPO_4 and PO_4 groups were assigned at 1118, 1029, and 960 cm^{-1} . The P–OH stretching mode of HPO_4 groups was at 870 cm^{-1} . OCP plates were needle-like 2 – 5 μm long and 1 – 2 μm wide (Figure 2D).

Compressive strength of 3D printed samples is presented in Figure 2F and G. The strength of the investigated samples increased from 1.5 to 4.5 MPa up to about 4.3 – 7.9 MPa after post treatment.

3D printed gene-activated implants were produced using the supercoiled naked plasmid DNA encoding *VEGFA* gene. Based on the SEM study, we identified some round structures on the surface of gene-activated bone substitutes, which corresponded to plasmid DNA macromolecules (Figure 3A and B). Fluorimetry results demonstrated an average concentration of 3D scaffold-bound plasmid DNA to be $52.74 \pm 1.76\text{ ng/mg}$.

A luminescent signal with intensity corresponding to the production level of luciferase encoded by pDNA-*Luc* was detected only locally – within a zone of localization of a pDNA-*Luc* solution or 3D printed gene-activated implants containing pDNA-*Luc*. No signal was detected in

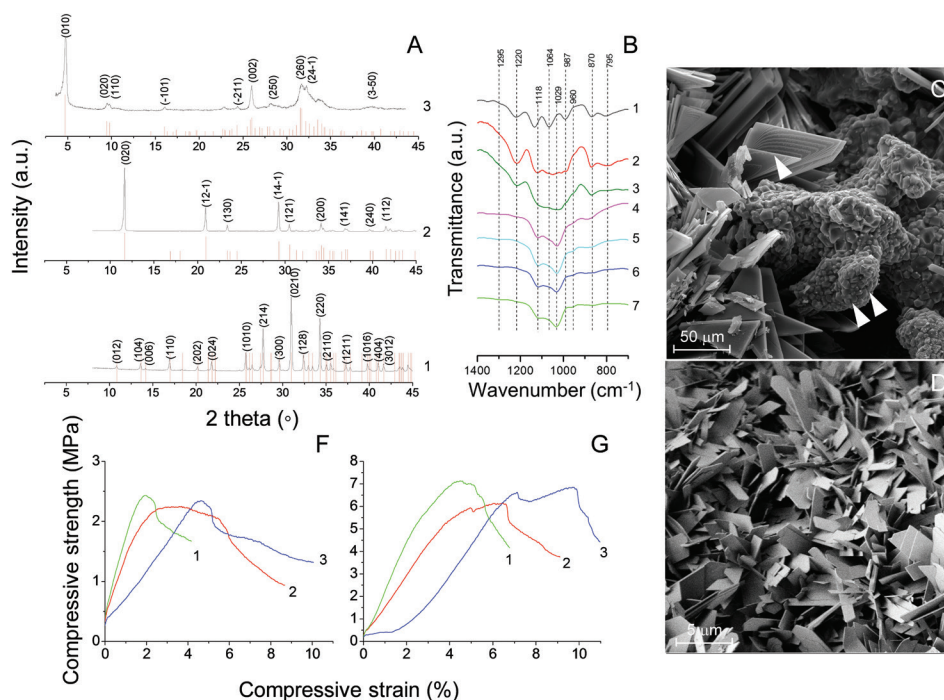


Figure 2. (A) XRD data of the formation of 3D printed TCP (1) to DCPD samples soaked in calcium nitrate solution during 7 days (2) and to OCP samples in sodium acetate during 7 days (3). (B) FTIR data of the formation of 3D printed samples soaked in calcium nitrate solution after 7 days (1) and samples in sodium acetate after 1 (2); 2 (3); 3 (4); 5 (5); 6 (6) and 7 (7) days. (C, D) SEM images of 3D printed samples. (F, G) Compressive strength of 3D printed samples before and after chemical treatment.

other animal body parts or groups. A luminescence level peaked on day 1 after a subcutaneous injection to mice in the control group 4, with its being the lowest intensity in the test group. Later on, the signal intensity gradually decreased in the control 4, while peaking on day 7 with a subsequent smooth reduction in the test group. Intergroup comparison showed the signal level to be significantly higher in the control 4 only 1 day

after surgery, with it being higher in the test group on days 7 – 28. The peak signal intensity value in the group with 3D printed gene-activated implants was 1.9-fold of a maximum value in the control group (**Figure 3C**). The others control groups (1-3) showed no luminescent signal.

The initial diameter, volume, and the “surface-to-volume” ratio of 3D printed disks was 10.1 ± 0.2 mm, 116.53 ± 8.16 mm³, and

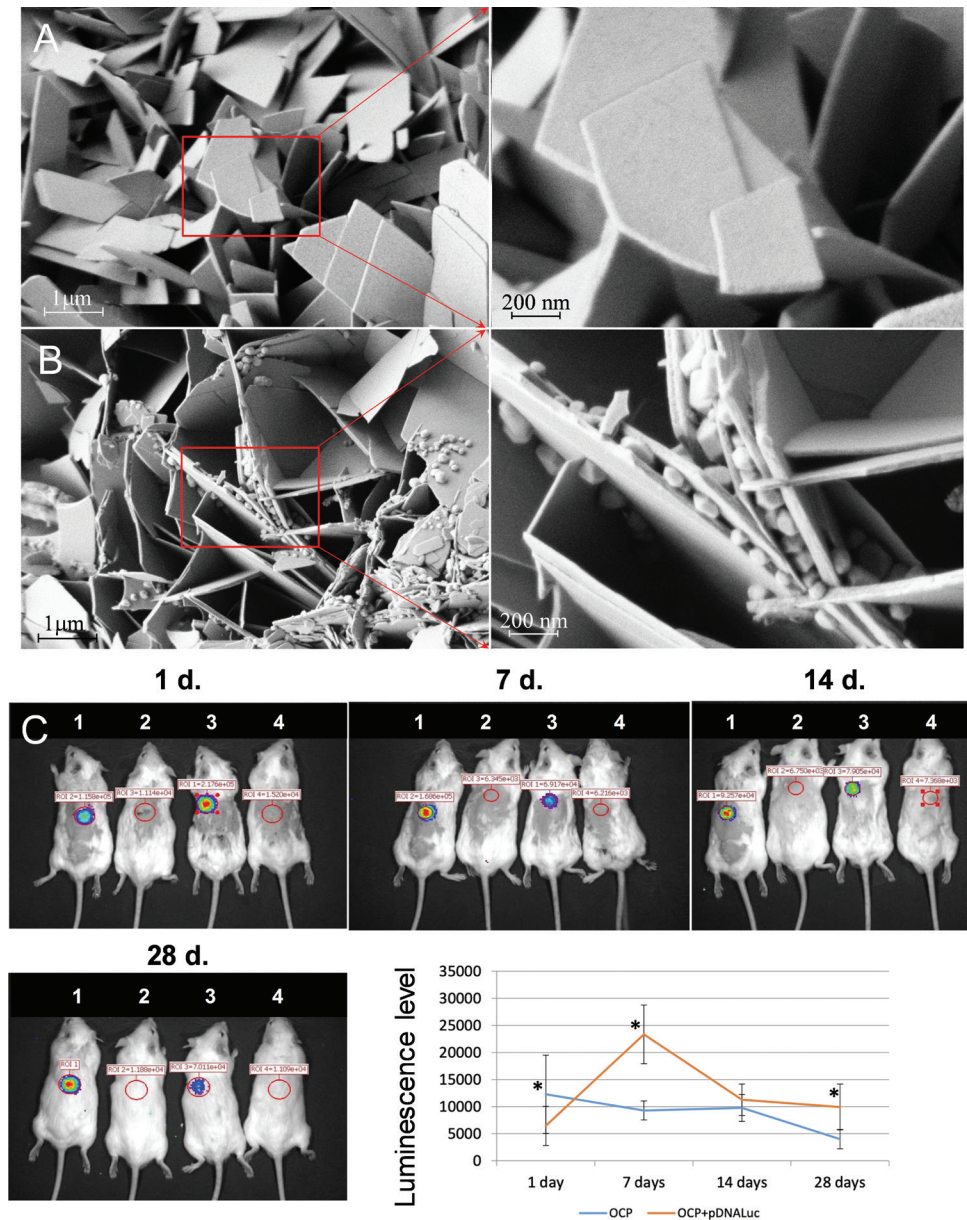


Figure 3. SEM images of 3D printed OCP implants (A) and gene-activated implants (B). (C) Plasmid DNA delivery from 3D printed OCP implants in subcutaneous *in vivo* test, bioluminescent study. (1) test group, (2) OCP implant without pDNA-*Luc*, (3) solution with pDNA-*Luc*, (4) OCP implant with pDNA-*VEGF*. *differences between the group are statistically significant, $P < 0.05$.

0.002, respectively. Materials resorbed from their surfaces and within a zone of the direct contact to soft tissues. The diameter and volume gradually reduced and the “surface-to-volume” ratio increased both in 3D printed scaffolds and gene-activated implants. An average diameter decreased more intensively with an abrupt drop by day 40 and a subsequent stabilization and a smooth decline in the test group, while its change being almost linear in the control group. There was a two-fold volume reduction by day 60 in both groups (Figure 4).

We found no histological signs of inflammation in the area of 3D printed OCP (control)

implantation. Since day 15, a highly vascularized connective tissue capsule with a thickness of 50 – 70 μm formed around implants. However, cellular and tissue elements did not penetrate into OCP structure. Starting from day 45, in some parts of the implants there were defects in the structure, their number and size gradually increased by day 180 by forming “cavities of dissolution” with a diameter of 30 – 50 μm and scalloped edges that indicated biodegradation. There were no multinucleated foreign bony giant cells. On day 180 after implantation, connective tissue grew inside the implants to 50 – 70 μm from a surface (Figure 4).

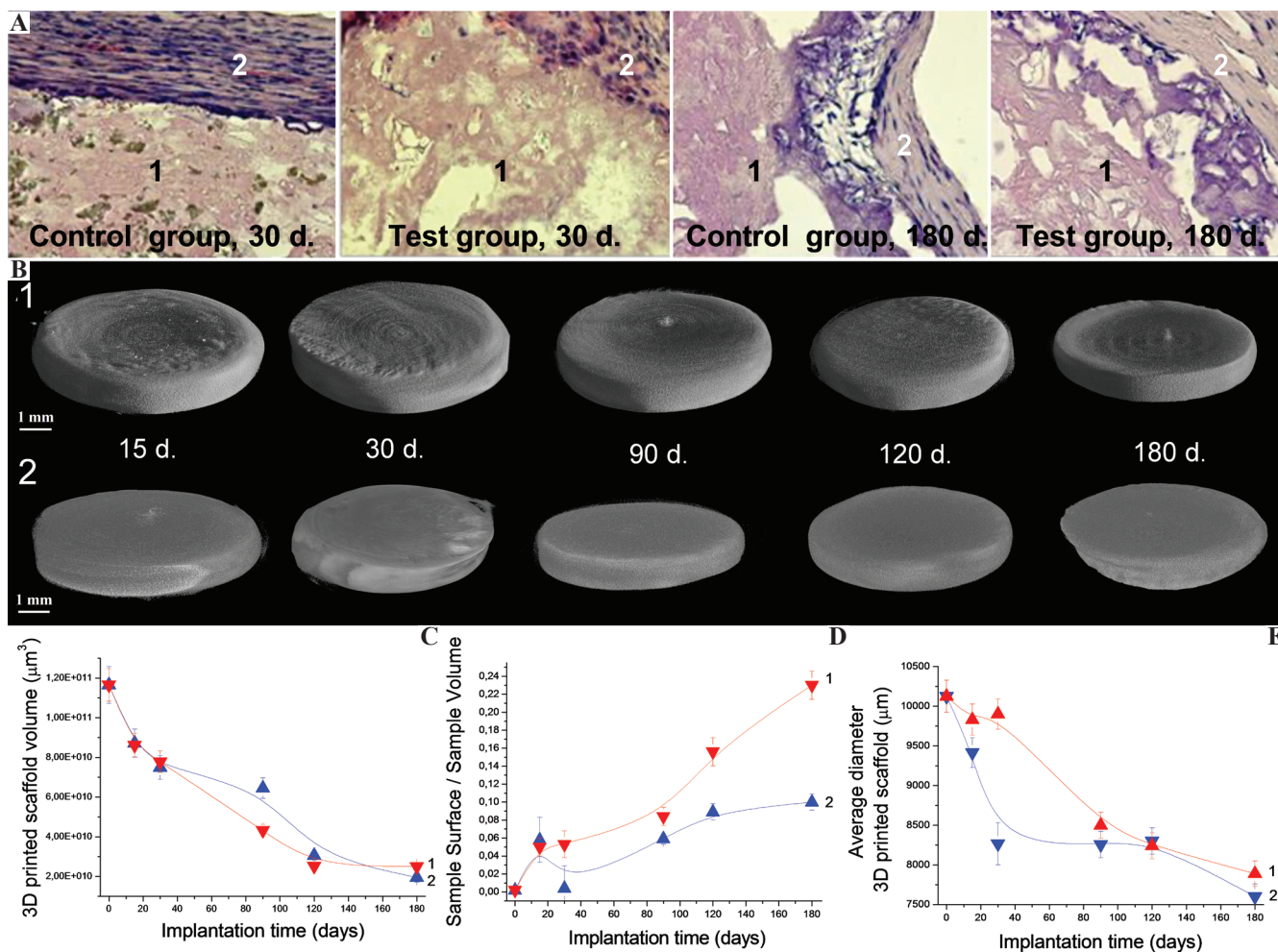


Figure 4. 3D printed OCP-based-(control group) and gene-activated (test group) implants in subcutaneous *in vivo* test, biodegradation study. (A) Histological analysis: (1) implants, (2) fibrous tissue; (B) 3D microCT images (1) (control (up) and (2) test (down) groups); (C, D, E) Kinetic of biodegradation parameters: red – control group (1); blue – test group (2). *differences between the group are statistically significant, $P < 0.05$.

The biodegradation study of personalized gene-activated constructs demonstrated implants structure disintegration and connective tissue growing into them from day 15 after implantation. A capsule covering the implants included active fibroblasts and was intensively vascularized with a larger number of blood vessels than in the control group ($P = 0.021$). In 45 – 120 days, we found a further structure disintegration and thinning of 3D printed gene-activated implant edges. Later on, all implants were highly porous: optically empty vacuoles occupied a significant volume (about 60%), their diameter achieved 200 – 250 μm . Connective tissue in-grew to a depth of 100 – 150 μm (**Figure 4**). As in the control, there were no signs of inflammation. In general, personalized gene-activated materials possessed a profile of more evident bioresorption and a slightly higher rate of biodegradation.

None of animals died during the experiment until a planned sacrifice. Wounds healed in three animals without abnormalities in 10 days after surgery. Since that time the animals started resting on the operated limb; one animal had a post-operative wound infection after tibia reconstruction.

Based on CT findings, the tibia integrity was restored in all cases, and implants integrated with bone fragments without forming a connective tissue capsule. Bone thickness increased within the area of intervention due to a pronounced periosteal callus; its diameter achieved 31.5 and 40.3 mm in the greatest dimension in 3 and 6 months after surgery, respectively, with an initial diameter of being <20 mm. The implants retained their initial shape with structure becoming heteromorphic. In addition to canals filled with newly formed tissues of bone density, we detected some cracks without fragment disintegration in the implant structure (**Figure 5**). The implants length reduced to 26 and 24 mm, whereas their diameter to 15 and 14 mm in 3 and 6 months after surgery, respectively. An average tissue density within a tibia reconstruction zone was 1362 ± 617.6 HU in 3 months and 1332 ± 572.2 HU in 6 months, with the initial implant density of more than 2000 HU.

Optimal osteointegration was confirmed by SEM and a histologic examination. SEM results showed that a crystal structure of OCP-based

scaffolds defused without a border between newly formed bone tissue and the implant. Calcium to phosphorus ratio (Ca/P) in the areas of 3D printed implants and newly formed bone tissue was 2.06 and 1.83 and 1.90 and 2.23 in 3 and 6 months after surgery, respectively.

Based on histological analysis, a gene-activated bone substitute surface contacted directly with a newly formed woven bone tissue without forming a connective tissue capsule in 3 months after surgery. There were both macropores corresponding to prefabricated canals and numerous micropores in the implant structure. Trabeculae of a newly formed bone tissue enlaced the implant, directly extending into macro- and micropores. Vascularized bone tissue had been growing from both periosteum and endosteum sides. Bone rods spread from the implant to a diaphysis wall in the form of bridges (**Figure 5**). Bone trabeculae arose directly from the implant both in the periphery and in its depth; newly formed trabeculae adhered to a rarefied implant surface, their side contacting with the material had irregular edge, an opposite side was characterized by a smooth surface with osteoblasts and bone lining cells involved. Fusing trabeculae of newly formed bone tissue constituted a mesh structure, neither evidence of woven bone remodeling into lamellar tissue, nor osteoclastic resorptions occurred at this time point. A fibrous tissue was detected only within inter-trabecular spaces. A newly formed diaphysis wall consisted of a spongy bone with bone marrow elements in inter-trabecular spaces. There was a pronounced periosteal response with woven bone tissue trabeculae formation within basal regions of the periosteum.

In 6 months after surgery, personalized gene-activated bone substitutes were completely integrated into the tibia proximal and distal fragments and significantly rarefied around initial perforations. Macro- and micropores as well as a peripheral implant surface were covered with trabeculae of a newly formed bone tissue. By this time point, the bone tissue directly in implant perforations as well as along its perimeter remodeled into lamellar forming osteons even in the implant macropores. There were no cells responsible for

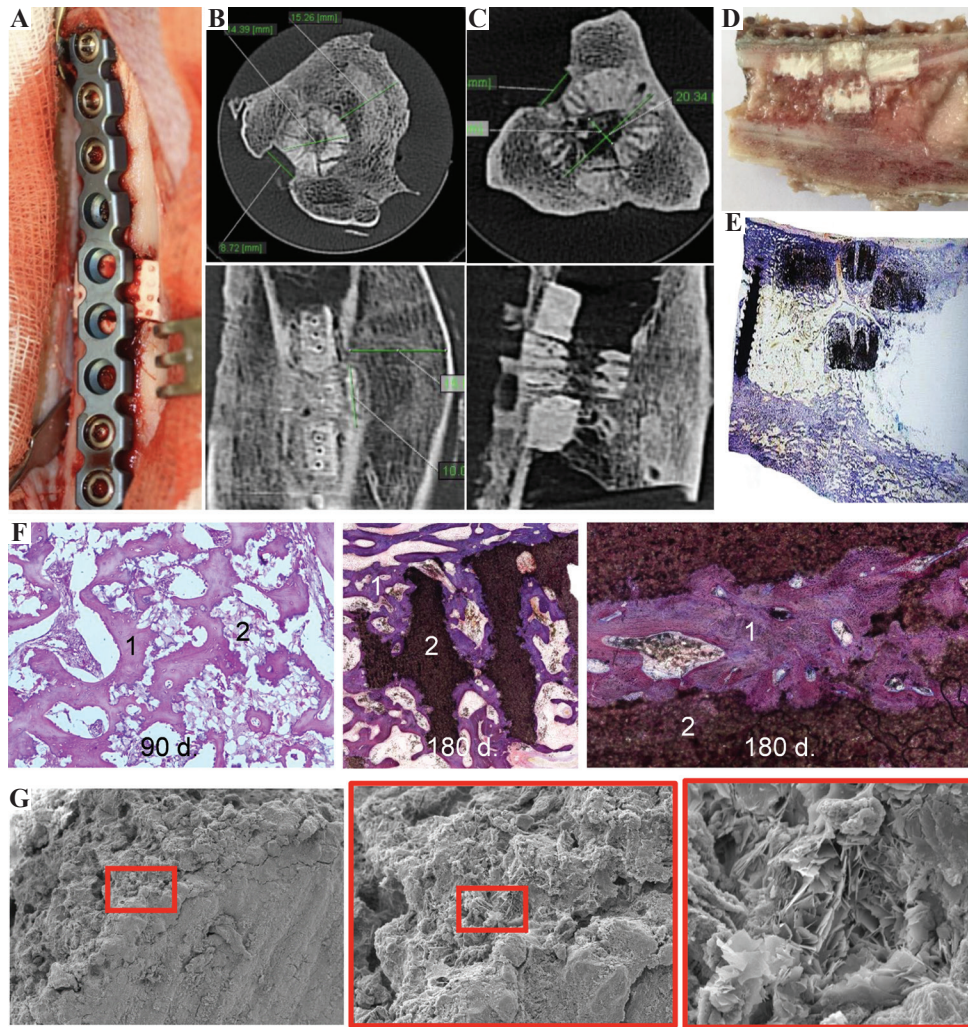


Figure 5. Tibia reconstructed with 3D printed gene-activated implants. (A) Intraoperation view; (B, C) CT scans in 3 and 6 months, respectively; (D) Longitudinal slice of the tibia with bone grafting zone; (E) Non-decalcified histological slice; (F) Histological analysis in 3 and 6 months after surgery: (1) newly formed bone tissue, (2) partially resorbed implant; (G) SEM images.

material resorption or bone tissue remodeling. Inter-trabecular spaces were filled with properly vascularized bone marrow (**Figure 5**).

As in case of long (tubular) bones the mandible integrity restored on both sides, the implants fully integrated with bone defect walls. There was no border between the implant and a bone defect wall in some regions, especially in 6 months after surgery. No hypertrophic periosteal callus formed. All sizes of both plasmid-free and gene-activated 3D printed implants reduced by, on average, 1 mm in 3 months and 2 mm in 6 months after surgery. Mean tissue densities within the zone of the

mandibular reconstruction in 3 and 6 months after surgery were 1972 ± 397.5 HU and 1974 ± 368.5 HU in the control group and 1925 ± 289.2 HU and 1986 ± 390.1 HU in the test group, respectively.

As in the tibia reconstruction, optimal osteointegration was confirmed by SEM. Ca/P ratios in the areas of 3D printed implants and newly formed bone tissue were: in the test group, 2.07 – 2.11 and 2.16 – 2.74 in 3 and 6 months after surgery, respectively; in the control group, 1.95 – 2.26 and 1.87 – 1.94 at 3 and 6 month time points.

According to the histological analysis, the gene-activated implants were integrated with

the mandible in 3 months after surgery; irregular implant surface was directly surrounded by a newly formed bone tissue of a mixed structure (woven and lamellar) without a connective tissue capsule. There was a typical tendency for osteon-like structures and circular trabeculae to be formed. There were no cells on the surface of bone trabeculae in contact with the bone substitute, while active osteoblasts detected on the opposite

side. There were evident signs of periosteal osteoblasts nearby the zone of implantation (**Figure 6**). A richly vascularized connective tissue was detected in inter-trabecular spaces. No cellular or tissue structures were identified in the implant central zones. There were single osteoclasts on a newly formed bone trabeculae surface on the side of connective tissue. A similar picture was observed in 3D printed OCP implants without gene

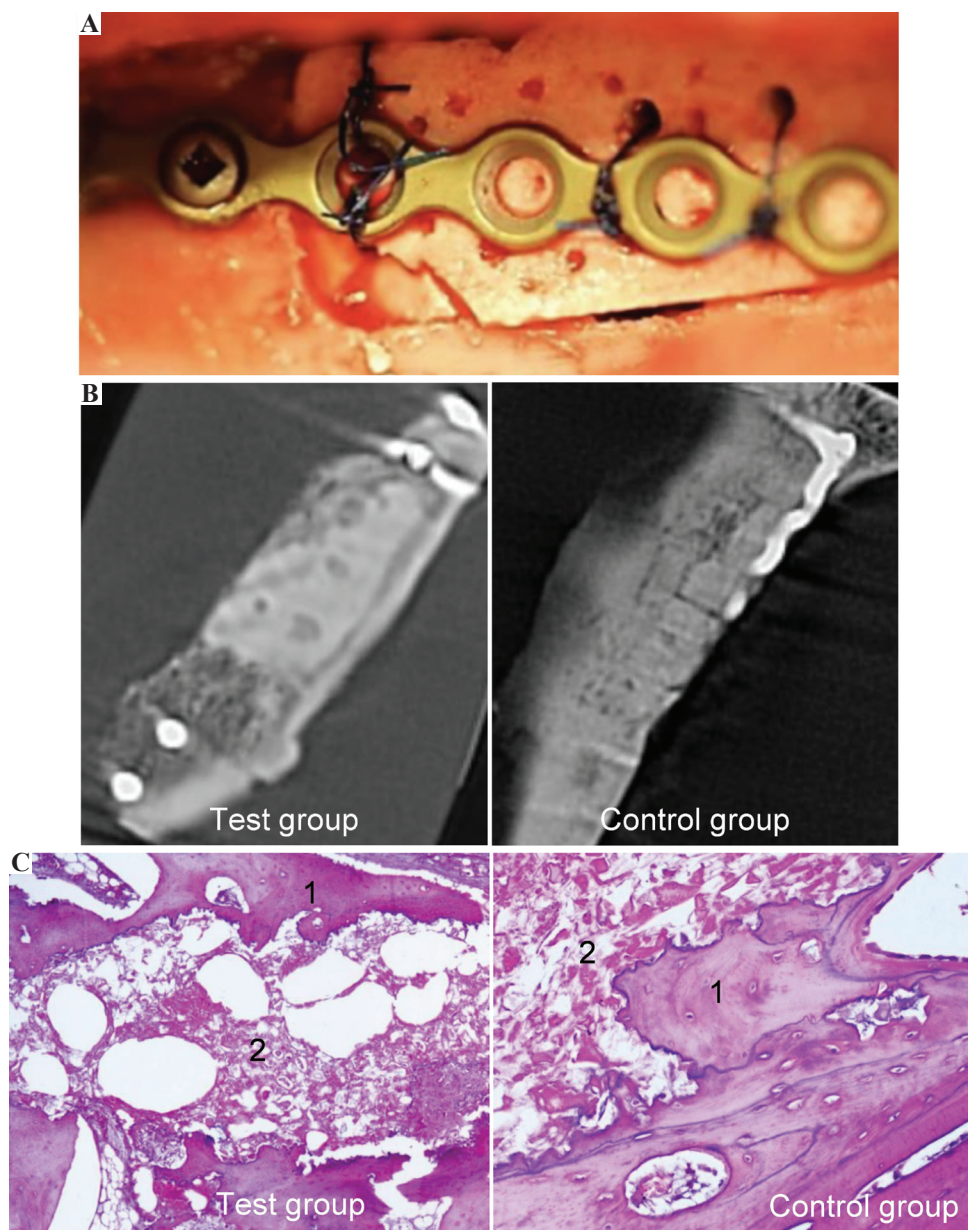


Figure 6. Mandible reconstructed with 3D printed OCP implants and gene-activated implants. (A) Intraoperation view; (B) CT scans in 6 months after surgery; (C) Histological analysis in 6 months after surgery: (1) newly formed bone tissue; (2) partially resorbed implant.

constructs; however, periosteal osteogenesis was less evident.

In 6 months after implantation, the peripheral part of gene-activated materials was actively substituted with bone tissue. A border with the implant along its entire length was composed of newly formed bone tissue trabeculae (**Figure 6**) without fibrous tissue. A woven bone tissue remodeled into lamellar tissue. The implant surface was rarefied and had a great number of optically empty cavities sized to 300 μm . Still, no cellular and tissue elements extended into the material. There were no cellular signs of osteoclastic resorption. Inter-trabecular spaces were in part colonized with hematopoietic bone marrow. There was an optimal osteointegration in 3D printed OCP implants with similar dynamics of bone tissue rearrangement into lamellar tissue; however, the colonization of inter-trabecular spaces with blood-forming (hematopoietic) bone marrow was less active.

4 Discussion

Bone reconstructive surgery in traumatology and orthopedics, neurosurgery, oral and maxillofacial surgery still remains challenging. Small defects can be managed with the use of osteoconductive bone substitutes, including a combination with “improvised” techniques for biologic activity enhancement such as mixing with autologous bone fragments, platelet-, or growth factor-enriched plasma, etc. However, large/critical size bone defects and alveolar ridge atrophy of significant size are characterized by “osteogenic insufficiency,” a loss of cambial cellular elements and/or factors, involved in bone regeneration, therefore intensive osteoinduction is required^[9].

Additive manufacturing or 3D printing techniques provide substantial opportunities for effective personalized treatment of patients with large bone defects. However, to overcome osteogenic insufficiency, custom-made implants should be combined with osteogenesis-stimulating factors such as living cells, growth factors, or gene constructs that encode them. 3D bioprinting of tissue-engineered constructs are most intensively

developed, probably due to the attractive idea to create a fully functional tissue or organ *ex vivo* for subsequent clinical transplantation^[6,10,16,17] or for usage as an *in vitro* model to study the disease pathogenesis and drugs development^[18]. However, in addition to well-known technological problems, tissue engineering is associated with high costs and considerable difficulties in clinical translation from a regulatory point of view^[9]. Furthermore, additive manufacturing is actively used to produce personalized bone implants with growth factors^[19,20]. However, protein molecules, being short-lived, and short-distant, cannot exhibit their full biological effect.

Although 3D bioprinting has become more complex in an attempt to combine different approaches^[21], there is a search for simpler alternatives that involves, for instance, the use of gene constructs for creating personalized bone substitutes. Despite significant advances in the research of standardized gene-activated matrices^[22-24] and additive manufacturing technologies for bone grafting, to date there are only a few studies related with personalized gene-activated tissue substitutes^[25,26], and none of them described calcium phosphate-based ceramic being used as a scaffold without any hydrogels or other materials that are easy to be printed.

Based on our previous results in OCP studies^[27], 3D printing of OCP-based implants^[11] and standardized gene-activated materials^[23,28], we have started the development of a personalized gene-activated bone substitute based on the OCP and plasmid DNA that delivers *VEGFA* gene, applicable for large bone defects substitution and guided bone regeneration. We expected the increased level of *VEGFA* to promote angiogenesis and reparative osteogenesis. Moreover, a direct stimulating effects of *VEGF* on proliferation and differentiation of bone cells^[29] and non-canonic intracrine effects specific for a VEGF gene transfer^[30] were described. Additional prerequisites to use this gene construct in the study were our previously obtained clinical data on a successful treatment of a patient with mandibular non-unions with the use of a gene-activated material, delivering *VEGFA*^[28].

First, in our work, we have realized a combination and further development of the processes involving chemical interaction between TCP agglomerated particles and “ink” based on diluted phosphoric acid, followed by chemical post-treatment of the printed DCPD structure at physiological temperatures^[11]. DCPD structure can be further transformed into OCP phase. **Figure 7** presents a schematic overview of the proposed mechanism of OCP-based 3D printed scaffolds production. It can be established: in the initial stage (3D printing), the pH value was low due to the presence of phosphoric acid, and the reaction between $\text{Ca}_3(\text{PO}_4)_2$ and H_3O^+ yielded Ca^{2+} ions. The Ca^{2+} ions reacted with HPO_4^{2-} ions, which formed $\text{CaHPO}_4 \times 2\text{H}_2\text{O}$. The further increase of the pH value of the solution during the post-treatment process leads to OCP nucleation and growth.

The next task of the present work involved the production of gene-activated implants based on the OCP and plasmid DNA with *VEGFA* gene. According to fluorimetry data, the concentration of plasmid DNA bound to 3D printed scaffolds was 52.74 ± 1.76 ng/mg that correlated with our previous findings related with OCP granule-based bone substitute^[32].

To evaluate intrinsic biodegradation rate of the material we have made non-porous OCP-based disk-shaped implants, since macro- and micropores unavoidably accelerate biodegradation of the scaffolds. Obtained data could be used as a reference value in the further studies of porous implants. At the same time, the presence of plasmid DNA almost did not affect the rate of this process.

A delivery of gene constructs, which does not exceed 1% in case of naked plasmid DNA,

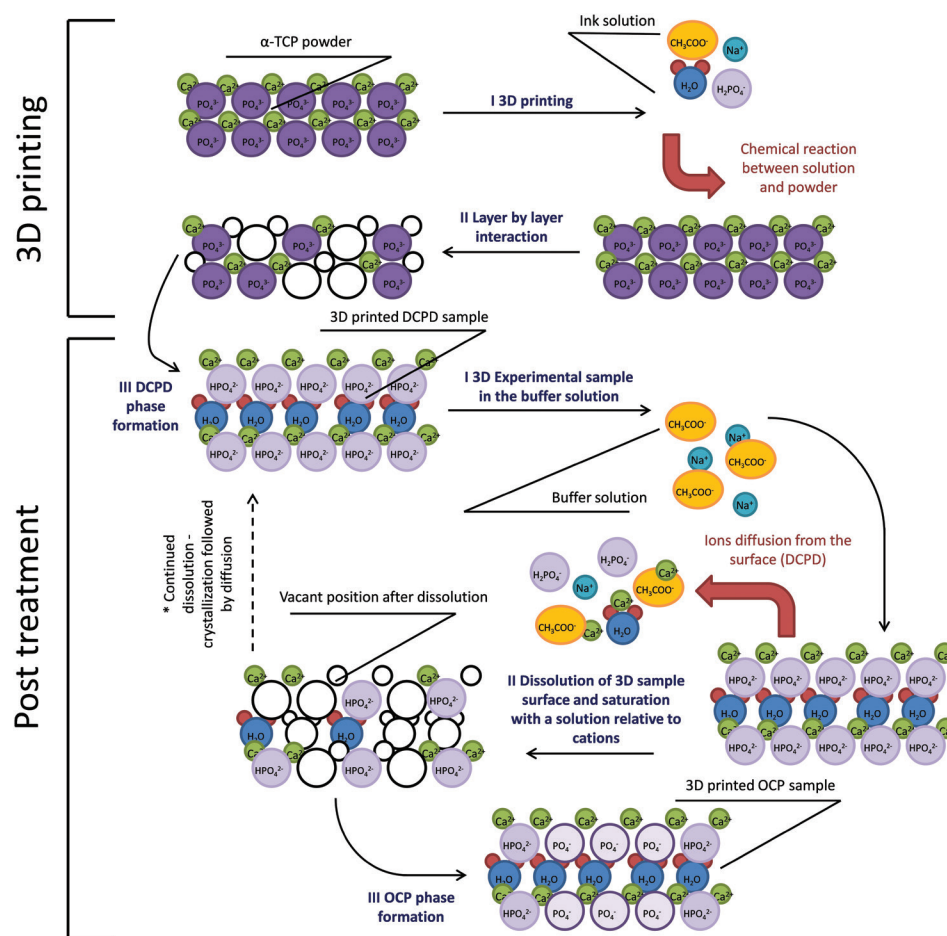


Figure 7. Schematic overview of the 3D printing and biomimetic post-treatment.

is the main challenge of gene-activated matrix approach^[32]. However, in our study, we have detected a high prolonged level of plasmid DNA delivery *in vivo* that might be caused by a positive effect of 3D printed OCP-based scaffold. Indeed, some authors suggested this effect for calcium phosphate matrixes^[33] that could be a peculiar extrapolation of well-known calcium phosphate method used to increase plasmid DNA transfection *in vitro*.

An osteoinductive effect of pDNA-*VEGFA* along with the osteoconductive effect of the OCP scaffold facilitated the restoration of bone integrity in pigs. Moreover, morphological and structural changes of 3D printed implants and their effects on adjacent tissues had similar features both in tibia and mandibular reconstruction. Materials from test and control groups were characterized by optimal osteointegration capability, since there was no fibrous tissue encapsulation of the scaffold. A newly formed bone tissue followed the implant topography filling in all irregularities and pores. One of the peculiarities was that rapid woven bone remodeled led into a lamellar tissue occupying almost the entire volume of the newly formed bone tissue in 6 months after surgery. At the latest time point, the 3D printed materials became more porous. However, a half-resorption period for OCP-based implants of that structure was not achieved in this study. In addition, sites of cartilaginous callus formation, which are specific for bones with enchondral ossification were not detected after tibia reconstruction that might be caused by osteoinductive effects mediated by angiogenesis stimulation. Increased angiogenesis could made the reparative process to bypass a cartilaginous callus stage at all or at least accelerate it with cartilaginous tissue replacement by bone before 3-month time point. Moreover, there was hematopoietic bone marrow formation within the inter-trabecular spaces at the 1st time point.

5 Conclusions

In our work, 3D personalized gene-activated bone substitutes, based on the OCP and pDNA-*VEGFA*, have been developed and produced with the use of 3D printing technology for the first time. The safety

of bioactive materials, a high level of plasmid DNA delivery in cells *in vivo* and the efficacy of large segmental bone defects substitution with and without pDNA-*VEGFA* loading have been confirmed experimentally. The results of our study demonstrated that combination of gene therapy and 3D printing with biomimetic post-treatment is an effective approach to overcome current limitations in production of personalized implants for critical size bone defect reconstruction.

Authors' contributions

Ilya Y. Bozo: Methodology, Investigation, Writing - Original Draft. Roman V. Deev: Study Design, Data Analysis. Igor V. Smirnov: Investigation, Visualization. Alexander Yu. Fedotov: Investigation. Vladimir K. Popov: 3D Printing Methodology Development, Original Draft Writing. Anton V. Mironov: Investigation. Olga A. Mironova: 3D Printing Software Development. Alexander Yu. Gerasimenko: Investigation. Vladimir S. Komlev: Conceptualization, Methodology, Writing - Reviewing and Editing, Visualization, Supervision. The manuscript was written through contributions of all authors. All authors have given approval to the final version of the manuscript.

Acknowledgment

This work was supported by the Ministry of Science and Higher Education within the State Assignment FSRC "Crystallography and Photonics" RAS in the part of 3D modeling of implants with predefined architecture and the Russian Foundation for Basic Research (grants no.18-29-11081 mk) in the part of the development of gene-activated materials. The authors acknowledge deep gratitude to M. Mavlikeev, A. Titova, A. Bilyalov, and M. Abyzova for their participation in the studies of gene construct delivery and to P.A. Makarevich for providing pDNA-*Luc* and to A.E. Baranchikov for high resolution SEM study.

Conflicts of Interest

The authors declare that they have no conflicts of interest.

References

1. Number of All-listed Procedures for Discharges from Shortly-stay Hospitals, 2010. Available from: http://www.cdc.gov/nchs/data/nhds/10Detaileddiagnosesprocedures/2010det10_alllistedprocedures.pdf. [Last accessed on 2020 March 01].
2. Rogers GF, Greene AK, 2017, Autogenous Bone Graft: Basic Science and Clinical Implications. *J Craniofac Surg*, 23:323–7.
3. Hernandez I, Kumar A, Joddar B, 2017, A Bioactive Hydrogel and 3D-Printed Polycaprolactone System for Bone Tissue Engineering. *Gels*, 3:26. DOI: 10.3390/gels3030026.
4. Ge Z, Tian X, Heng BC, *et al.*, 2009, Histological Evaluation of Osteogenesis of 3D-Printed Poly-lactic-co-glycolic Acid (PLGA) Scaffolds in a Rabbit Model. *Biomed Mater*, 4:021001. DOI: 10.1088/1748-6041/4/2/021001.
5. Shim JH, Kim SE, Park JY, *et al.*, 2014, Three-dimensional Printing of rhBMP-2-loaded Scaffolds with Long-term Delivery for Enhanced Bone Regeneration in a Rabbit Diaphyseal Defect. *Tissue Eng Part A*, 20:1980–92. DOI: 10.1089/ten.tea.2013.0513.
6. Ahlfeld T, Doberenz F, Kilian D, *et al.*, 2018, Bioprinting of Mineralized Constructs Utilizing Multichannel Plotting of a Self-setting Calcium Phosphate Cement and a Cell-laden Bioink. *Biofabrication*, 10:045002. DOI: 10.1088/1758-5090/aad36d.
7. Dorozhkin SV, 2009, Calcium Orthophosphates in Nature Biology and Medicine. *Materials*, 2:399–498. DOI: 10.3390/ma2020399.
8. Liu Y, Cooper PR, Barralet JE, *et al.*, 2007, Influence of Calcium Phosphate Crystal Assemblies on the Proliferation and Osteogenic Gene Expression of Rat Bone Marrow Stromal Cells. *Biomaterials*, 28:1393–1403. DOI: 10.1016/j.biomaterials.2006.11.019.
9. Deev RV, Drobyshev AY, Bozo IY, *et al.*, 2015, Ordinary and Activated Bone Grafts: Applied Classification and the Main Features. *Biomed Res Int*, 2015:365050. DOI: 10.1155/2015/365050.
10. Murphy SV, Atala A, 2014, 3D Bioprinting of Tissues and Organs. *Nat Biotechnol*, 32:773–85. DOI: 10.1038/nbt.2958.
11. Komlev VS, Popov VK, Mironov AV, *et al.*, 2015, 3D Printing of Octacalcium Phosphate Bone Substitutes. *Front Bioeng Biotechnol*, 3:81.
12. Barinov SM, Vakhrushev IV, Komlev VS, *et al.*, 2015, 3D Printing of Ceramic Matrices for Engineering of Bone Tissue. *Inorg Mater*, 6:316–322. DOI: 10.1177/1074248415574336.
13. Deev RV, Bozo IY, Mzhavanadze ND, *et al.*, 2015, pCMV-vegf165 Intramuscular Gene Transfer is an Effective Method of Treatment for Patients with Chronic Lower Limb Ischemia. *J Cardiovasc Pharmacol Ther*, 20:473–82.
14. Bozo IY, Komlev VS, Drobyshev AY, *et al.*, 2015, Method for Creating a Personalized Gene-activated Implant for Regenerating Bone Tissue. Patent No. EP3130342.
15. Fowler BO, Marković M, Brown WE, 1993, Octacalcium Phosphate. 3. Infrared and Raman Vibrational Spectra. *Chem Mater*, 5:1417–23. DOI: 10.1021/cm00034a009.
16. Kang HW, Lee SJ, Ko IK, *et al.*, 2016, A 3D Bioprinting System to Produce Human-scale Tissue Constructs with Structural Integrity. *Nat Biotechnol*, 34:312–9. DOI: 10.1038/nbt.3413.
17. Daly AC, Pitacco P, Nulty J, *et al.*, 2018, 3D-printed Microchannel Networks to Direct Vascularisation during Endochondral Bone Repair. *Biomaterials*, 162:34–46. DOI: 10.1016/j.biomaterials.2018.01.057.
18. Lal H, Patralekh MK, 2018, 3D-Printing and its Applications in Orthopaedic Trauma: A Technological Marvel. *J Clin Orthop Trauma*, 9:260–8. DOI: 10.1016/j.jcot.2018.07.022.
19. Huang KH, Lin YH, Shie MY, *et al.*, Effects of Bone Morphogenic Protein-2 Loaded on the 3D-Printed MesoCSScaffolds. *J Formos Med Assoc*, 117:879–87. DOI: 10.1016/j.jfma.2018.07.010.
20. Lee SJ, Lee D, Yoon TR, *et al.*, 2016, Surface Modification of 3D-Printed Porous Scaffolds via Mussel-inspired Polydopamine and Effective Immobilization of rhBMP-2 to Promote Osteogenic Differentiation for Bone Tissue Engineering. *Acta Biomater*, 40:182–191. DOI: 10.1016/j.actbio.2016.02.006.
21. Du M, Chen B, Meng Q, *et al.*, 2015, 3D Bioprinting of BMSC-laden Methacrylamide Gelatin Scaffolds with CBD-BMP2-collagen Microfibers. *Biofabrication*, 7:044104. DOI: 10.1088/1758-5090/7/4/044104.
22. Deev RV, Drobyshev RV, Bozo IY, *et al.*, 2013, Construction and Biological Effect Evaluation of Gene-activated Osteoplastic Material with Human VEGF Gene. *Cell Transplant Tissue Eng*, 8:78–85.
23. Feichtinger GA, Hofmann AT, Slezak P, *et al.*, 2014, Sonoporation Increases Therapeutic Efficacy of Inducible and Constitutive BMP2/7 *In Vivo* Gene Delivery. *Hum Gene Ther Methods*, 25:57–71. DOI: 10.1089/hgtb.2013.113.
24. Evans CH, Huard J, 2015, Gene Therapy Approaches to Regenerating the Musculoskeletal System. *Nat Rev Rheumatol*, 11:234–42. DOI: 10.1038/nrrheum.2015.28.
25. Cunniffe GM, Gonzalez-Fernandez T, Daly A, *et al.*, 2017, Three-dimensional Bioprinting of Polycaprolactone Reinforced Gene Activated Bioinks for Bone Tissue

- Engineering. *Tissue Eng Part A*, 23:891–900.DOI: 10.1089/ten.tea.2016.0498.
26. Gonzalez-Fernandez T, Rathan S, Hobbs C, 2019, Pore-forming Bioinksto Enable Spatio-temporally Defined Gene Delivery in Bioprinted Tissues. *J Control Release*, 301:13–27.DOI: 10.1016/j.jconrel.2019.03.006.
 27. Komlev VS, Barinov SM, Bozo IY, *et al.*, 2014, Bioceramics Composed of Octacalcium Phosphate Demonstrate Enhanced Biological Behaviour. *ACS Appl Mater Interfaces*, 6:16610–20.DOI: 10.1021/am502583p.
 28. Bozo IY, Deev RV, Drobyshev AY, *et al.*, 2016, World’s First Clinical Case of Gene-activated Bone Substitute Application. *Case Rep Dent*, 2016:8648949.DOI: 10.1155/2016/8648949.
 29. Yang YQ, Tan YY, Wong R, *et al.*, 2012, The Role of Vascular Endothelial Growth Factor in Ossification. *Int J Oral Sci*, 4:64–8.
 30. Liu Y, Berendsen AD, Jia S, *et al.*, 2012, Intracellular VEGF Regulates the Balance Between Osteoblast and Adipocyte Differentiation. *J Clin Invest*, 122:3101–13.DOI: 10.1172/jci61209.
 31. Bozo IY, Deev RV, Drobyshev AY, *et al.*, 2015, Efficacy of Gene-activated Osteoplastic Material Based on Octacalcium Phosphate and Plasmid DNA with VEGF Gene for Critical-sized Bone Defects Substitution. *N.N. Priorov Herald Traumatol Orthop*, 1:35–42.DOI: 10.32414/0869-8678-2015-1-35-42.
 32. Schertzer JD, Plant DR, Lynch GS, 2006, Optimizing Plasmid-based Gene Transfer for Investigating Skeletal Muscle Structure and Function. *Mol Ther*, 13:795–803.DOI: 10.1016/j.ymthe.2005.09.019.
 33. Keeney M, van den Beucken JJ, van der Kraan PM, *et al.*, 2010, The Ability of a Collagen/Calcium Phosphate Scaffold to Act as its Own Vector for Gene Delivery and to Promote Bone Formation Via Transfection with VEGF (165). *Biomaterials*, 31:2893–902.DOI: 10.1016/j.biomaterials.2009.12.041.

Scaffold-free, Label-free, and Nozzle-free Magnetic Levitational Bioassembler for Rapid Formative Biofabrication of 3D Tissues and Organs

Vladislav A. Parfenov^{1,2†*}, Stanislav V. Petrov^{1†}, Frederico D. A. S. Pereira¹, Aleksandr A. Levin¹, Elizaveta V. Koudan¹, Elizaveta K. Nezhurina³, Pavel A. Karalkin^{1,3}, Mikhail M. Vasiliev⁴, Oleg F. Petrov⁴, Vladimir S. Komlev², Yusef D. Khesuani^{1††}, Vladimir A. Mironov^{1,5††}

¹Laboratory for Biotechnological Research, “3D Bioprinting Solutions,” Moscow, Russia

²A.A. Baikov Institute of Metallurgy and Materials Science, Russian Academy of Sciences, Moscow, Russia

³P.A. Hertsen Moscow Oncology Research Center, National Medical Research Radiological Center, Moscow, Russia

⁴Joint Institute for High Temperatures, Russian Academy of Sciences, Moscow, Russia

⁵I.M. Sechenov First Moscow State Medical University of the Ministry of Health of the Russian Federation (Sechenov University), Moscow, Russia

†These authors contributed equally to this work

††Both researchers are senior authors in this paper

Abstract: Scaffolding is the conceptual framework of conventional tissue engineering. Over the past decade, scaffold-free approaches as a potential alternative to classic scaffold-based methods have emerged, and scaffold-free magnetic levitational tissue engineering (magnetic force-based tissue engineering [Mag-TE]) is a type of this novel tissue engineering strategy. However, Mag-TE is often based on the use of potentially toxic magnetic nanoparticles. Scaffold-free and label-free magnetic levitational bioassembly do not employ magnetic nanoparticles and thus, the potential toxicity of magnetic nanoparticles can be avoided. In this short review, we describe the conceptual foundation of scaffold-free, label-free, and nozzle-free formative biofabrication using magnetic fields as “scaffolds.” The design and implementation of “Organ.Aut,” the first commercial magnetic levitational bioassembler, and the potential applications of magnetic bioassembler are discussed as well.

Keywords: Magnetic levitation, Bioassembler, Formative biofabrication, Tissue spheroids, Scaffold

*Corresponding Authors: Vladislav A. Parfenov, Kashirskoye Shosse, 68-2, Moscow 115409, Russian Federation; vapar@mail.ru; Vladimir A. Mironov, Kashirskoye Shosse, 68-2, Moscow 115409, Russian Federation; vladimir.mironov54@gmail.com

Received: June 21, 2020; **Accepted:** July 14, 2020; **Published Online:** July 28, 2020

(This article belongs to the *Special Section: Bioprinting in Russia*)

Citation: Parfenov VA, Stanislav VP, Petrov SV, *et al.*, 2020, Scaffold-free, Label-free, and Nozzle-free Magnetic Levitational Bioassembler for Rapid Formative Biofabrication of Three-dimensional Tissues and Organs, *Int J Bioprint*, 6(3): 304. DOI: 10.18063/ijb.v6i3.304.

1 Introduction

The three-dimensional (3D) bioprinting could be defined as an automated, robotic, layer-by-layer additive biofabrication of 3D tissues, and organs

according to the digital model^[1-3]. 3D bioprinting promises to solve the shortage of human organs for transplantation, which is an urgent but still unsolved problem of clinical medicine. Today, there are three most common and well-established

types of 3D bioprinting technology: (i) Ink-jet bioprinting, (ii) extrusive bioprinting, and (iii) laser-based bioprinting such as laser-induced forward transfer (LIFT)^[4]. However, in recent reviews, especially in the market reports, new types of 3D bioprinting – magnetic and acoustic bioprinting were also mentioned^[5-8].

3D bioprinter is defined as a robotic device for additive (“layer-by-layer”) biofabrication of 3D tissue and organs in correspondence with digital models. Of note, a question is still under discussion – can magnetic and acoustic bioprinters be considered as real bioprinters, or must a new term “bioassemblers” be introduced to define the new type of equipment? There are still no commercially available magnetic or acoustic bioprinters. It is important to note that the development of scientific instrumentation is essential for technological progress and advances in the new research field. Thus, the focus of this paper is a presentation of a new custom-designed magnetic levitational bioassembler as a new type of device for rapid formative biofabrication of 3D tissue and organs. We also outline the conceptual framework for a new emerging biomedical field, which we call scaffold-free, label-free, and nozzle-free formative biofabrication. The scaffold-free and label-free magnetic levitational bioassembly are illustrative examples of emerging formative biofabrication. Finally, although many researchers^[5-8] and market analysts still prefer to use the more familiar term “magnetic bioprinter,” we hold a genuine belief that the name “magnetic levitational bioassembler” is more relevant to nozzle-free technology.

2 What does the “scaffold-free” approach mean?

Rapidly emerging scaffold-free tissue engineering is a potential alternative to traditional scaffold-based tissue engineering. There are several already published conceptual reviews on scaffold-free tissue engineering. The scaffold could be broadly defined as a temporal removable (sometimes biodegradable) support^[9,10]. In line

with this definition, it is easy to demonstrate that many so-called scaffold-free technologies are scaffold-based. For example, (i) based on the most cited paper by Gabor Forgacs’s group on scaffold-free tissue engineering, removable agarose hydrogel is not considered as a scaffold^[11]; (ii) the removable supporting metallic needles in the most popular and already automated and commercialized scaffold-free tissue engineering technology are not considered as temporal support or scaffold^[12]; and (iii) in the so-called scaffold-free bioprinting technology that is based on LIFT, fibrin hydrogel is not mentioned as a scaffold^[13]. The absence of a clear definition of scaffold-free technology leads to some semantic confusion when authors use some sort of materials as temporal and removable support, and claim their techniques as “scaffold-free.” Conceptually, if it is not a scaffold-free but still scaffold-based technology, then it automatically loses its desirable principal conceptual novelty. We are facing the situation when some researchers who try to show pseudo-novelty and attract attention are using certain semantic tricks. The logical question arises: Does any actual scaffold-free or material-free tissue engineering technology exist? For example, magnetic force-based tissue engineering (Mag-TE) could also be considered as a scaffold-free or material-free technology. However, in our opinion, nanoparticles be classified just as a new form of scaffold or at least temporal and removable supporting structure with both intracellular and extracellular localization. Thus, Mag-TE is not material-free and cannot be considered as scaffold-free technology.

3 Label-based magnetic tissue engineering

Mag-TE is a type of scaffold-free but label-based biofabrication that uses magnetic nanoparticles for enabling magnetic levitation. This technology was initially developed by Ito and Honda as an attempt to optimize cell sheet technology, which was initially developed by Prof. Okano’s group in Japan^[14]. The application of magnetic nanoparticles enables manipulation, handling, and rapid assembling of cell sheets into 3D tissue

constructs. There are already several published well-written reviews describing label-based Mag-TE^[15-17].

The main limitation of this promising technology is the employment of potentially toxic magnetic nanoparticles. There are two opposite opinions about the toxic effect of magnetic nanoparticles. One group of researchers, i.e., Claire Wilhelm's group, is trying to demonstrate that superparamagnetic iron oxide nanoparticle is practically not toxic and could be biodegraded to natural ferritin^[18]. Moreover, a type of magnetic nanoparticles-based contrast agent called "Feridex" has been used in clinical practice for the decades. From another point of view, there is a growing number of researchers who demonstrate the toxic effect of magnetic nanoparticles and claim that the accumulation of iron-based magnetic nanoparticles could lead to undesirable side effects such as liver and spleen hemosiderosis or the local accumulation of iron.

In a recently published review^[19], the authors defined three main challenges for tissue engineering based on removable physical fields (including Mag-TE): (i) Transition from academic-styled biofabrication of mini tissues to biofabrication of clinically relevant tissue fragments; (ii) the use of more advanced materials; and (iii) development of affordable instrumentation. The current paper is dealing with the third challenge – the production of bioassembler for magnetic levitational bioassembly^[18].

4 Concept of "scaffield" and "formative biofabrication"

There are three main ways of manufacturing: (i) Subtractive, (ii) additive, and (iii) formative manufacturing^[19]. During a long period from the early attempts until the end of the 20th century, subtractive manufacturing was the primary way of making things from wood, stones, and metals. At the end of the last century, additive manufacturing, initially known as the rapid prototyping technology, became a brilliant technology that formed the technological basis of the so-called third or fourth industrial revolution. Formative manufacturing

uses processes such as injection molding, die casting, pressing, and stamping to create materials into the desired shape. In traditional formative manufacturing, molds are applied to achieve the desired shape of used materials.

The term "formative biofabrication" was coined by Prof. Chua Chee Kai at the International Bioprinting Congress in Singapore to describe magnetic and acoustic levitational bioassembly using magnetic and acoustic fields as desirable shape forming scaffold (personal communication). Formative biofabrication comprises the technologies that uses magnetic, acoustic, electric, photonic, and other physical forces for levitational bioassembly of 3D tissue and organ constructs. A new word "scaffield" has been proposed to define magnetic and acoustic fields, which serve as some sort of temporal and removable support for levitating and assembling biological objects.

Thus, formative biofabrication is a scaffold-free and label-free levitational bioassembly of 3D tissues and organs that uses the combination of different physical fields as removable temporal support for levitating living building blocks which are capable of self-assembly. The device enabling magnetic levitational bioassembly of 3D tissue and organs should be called magnetic "bioassembler." Nowadays, there are no commercially available magnetic levitational bioassemblers. Here, we describe the first one of bioassemblers.

5 The main dilemma of label-free magnetic levitational bioassembly

Label-free magnetic levitational bioassembly does not employ potentially toxic magnetic nanoparticles, which are often used in magnetic tissue engineering. Hence, label-free magnetic levitational bioassembly may avoid the problem of toxicity and associated undesirable potential side effect. However, the label-free magnetic levitational bioassembly uses a paramagnetic medium, for example, a medium that contains gadolinium salts. Gadolinium salts have already been approved for clinical imaging as a contrast agent in computer tomography by the U.S. Food and Drug Administration and other

national regulatory agencies. In the meantime, there is a growing body of evidence indicates that gadolinium can induce kidney fibrosis in human patients. Moreover, it has been shown that gadolinium blocks calcium channels and causes toxicological effects on cells *in vitro* and *in vivo*^[20-23]. The reduction of gadolinium salts concentration practically enables the complete elimination of undesirable toxic effects, but it could compromise the magnetic levitation. In other words, cells are alive, but they could not levitate. From another point of view, the increasing concentration of gadolinium salts not only enables magnetic levitation but also induces a significant cytotoxic effect.

Thus, cells can levitate, but they are dying in a toxic concentration of gadolinium. There are three theoretically possible, potential strategies to solve this dilemma: (i) The development of non-toxic gadolinium salts; (ii) the use of a high magnetic field to achieve a significant reduction of gadolinium salt concentration; and (iii) performing label-free magnetic levitational bioassembly under the condition of microgravity in space to decrease gadolinium salt concentration. We systematically tried to address and explore all three strategies. First, we failed to find non-toxic gadolinium or its adequate paramagnetic media alternative. Second, we were able to perform label-free magnetic levitational bioassembly in the high magnetic field with significant (more than 100 times) reduction of paramagnetic gadolinium salts^[24]. We also successfully performed a label-free magnetic levitational bioassembly at the microgravity conditions in space^[25].

6 Design and construction of bioassembler

“Organ.Aut” is a magnetic bioassembler that was created to study the possibility of formative 3D biofabrication of tissue structures using the method of self-assembly of living tissues and organs in microgravity (**Figure 1A and B**). The central part of the magnetic bioassembler is the inner case, with six pairs of magnets placed inside (**Figure 2B**). The shape of the case (**Figure 2A**) made it possible to minimize the overall dimensions of the device

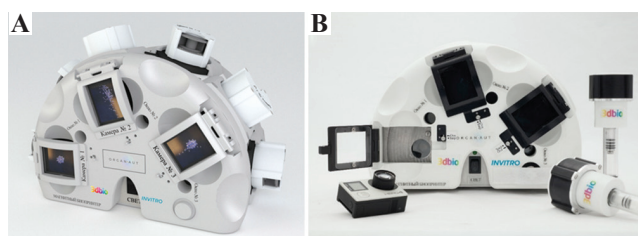


Figure 1. “Organ.Aut” is a magnetic levitational bioassembler. (A) Design of “Organ.Aut,” (B) the external view of “Organ.Aut.”

and conduct six experiments simultaneously. For the outer envelope, aluminum alloy D16-T was selected. Each pair of magnets (**Figure 2C**) was designed in such a way to form magnetic well in the center^[25].

The magnetic field was shielded to ensure the safe operation of the magnetic bioassembler on the International Space Station (ISS). Thus, individual screens were created (position 1, **Figure 2G**) from magnetically conductive stainless steel and connected to the inner case of the magnetic bioassembler. Furthermore, to ensure that various metal objects did not get into the magnetic bioprinter during its operation, unique covers with a diaphragm-based locking mechanism were added (**Figure 2E**). The material of these covers is magnetically conductive stainless steel.

Three cameras with special macro lenses were provided to visualize the biofabrication process. For this, Go Pro Hero 4 Silver (**Figure 2F**) having certificates for the use on ISS were used. Furthermore, a lighting unit which is powered by 6 A.A. batteries was provided for illumination during the process of video recording (**Figure 2D**).

A separate task was the development of special cuvettes for safe transportation of biological objects to the ISS, biological experiments, and fixing the fabricated constructs for further analysis (histological sections, etc.). Functionally, the cuvette is a system consisting of two V1 containers (the containers have the same volume but different contents) and the V2 biofabrication chamber. Between containers, there are valve assemblies that prevent fluid from moving from containers V1 to chamber V2 without pressing the pistons P (**Figure 3A**). The design of the cuvette was made of a transparent material

such as monolithic polycarbonate to provide airless filling of containers and the possibility of visual control of the biofabrication process. The inner parts of the cuvette are shown in **Figure 3B**. Since various fixatives, including paraformaldehyde, were used in the studies, the design of the cell requires three levels of biosafety. Accordingly, the layout of the cuvette that consists of three assembled cases was developed (**Figure 3C**). In addition to the three protection loops, the design of the cuvette includes a

locking mechanism that protects against accidental pressing of the piston systems (**Figure 3D**), which has a spring-loaded positioning mechanism in three positions (**Figure 3E**).

It should be noted that the use of the magnetic bioassembler “Organ.Aut” with cuvettes allows directed assembly of living biological constructs from tissue spheroids or various types of bacteria. Furthermore, it can be used to study the behavior of crystalline forms of chemical compounds

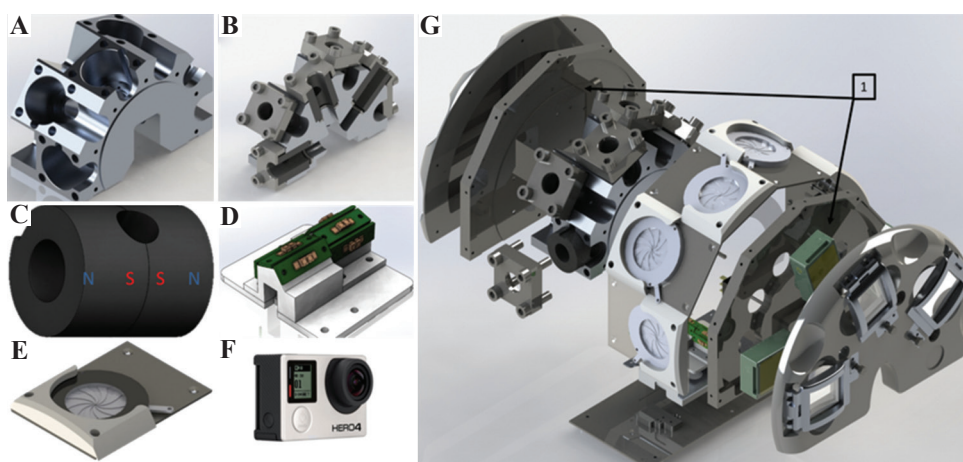


Figure 2. The basic design and construction of “Organ.Aut.” (A) The framework, (B) the framework with six pairs of cuvettes; (C) the assembly of two magnets; (D) the external view of illumination; (E) the external view of the cover shelf; (F) the external view of Go Pro Hero 4 Silver camera; (G) the blast-pattern of “Organ.Aut.”

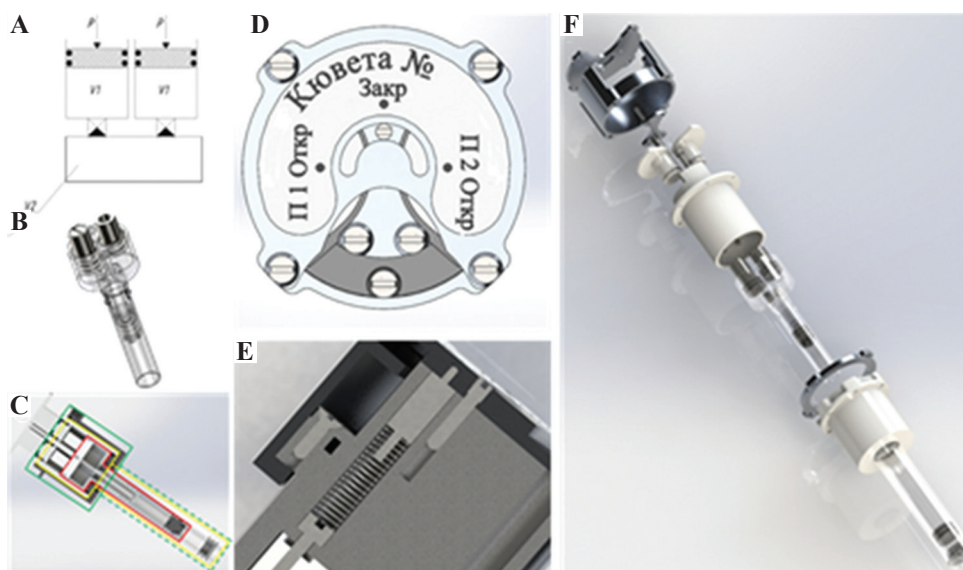


Figure 3. The design of cuvette. (A) The scheme of cuvette structure; (B) the inner parts of cuvette; (C) biosafety contours; (D) the protection from accidental hitting; (E) the fixation mechanism for protection from accidental hitting; (F) the assembly of the cuvette.

(inorganic components of the bone matrix, drugs, enzymes, hormones, etc.) placed in an inhomogeneous magnetic field with a high tension gradient. Thus, preliminary findings showed the unique capabilities of the magnetic fields used in the magnetic bioassembler “Organ.Aut” to induce faster recrystallization of synthetic calcium phosphates compared to traditional methods of inorganic synthesis, making it possible to obtain promising materials for bone grafting with high efficiency. Another area of research may be the assembly of 3D structures from bacteria in a magnetic field. Such conglomerates, otherwise called “bacterial biofilms,” are characterized by the ability to create or simulate volumetric living conditions under which bacterial cells exhibit different growth and synthetic activity compared to cultivation on flat surfaces.

7 Features and functionalities of magnetic bioassembler

Undeniably, our original magnetic levitational bioassembler has some unique advantages, which are outlined and emphasized in the following:

1. Magnetic bioassembler has a relatively small size, and it is not very heavy; therefore, it is compact, transportable, and space-saving.
2. Magnetic bioassembler is safe. It has three contours of defense for its chambers, and it has the necessary certification for use on the ISS.
3. Magnetic bioassembler has six chambers that allow multiple experiments to be run simultaneously; this may help with the generation of statistically sound experimental data.
4. Magnetic bioassembler has a video camera that assists experiment monitoring in real-time from long distance.
5. Magnetic bioassembler has a robust and durable design. This is evidenced by the sturdiness of the chambers as at least one from the six chambers survived the vigorous collisions as they fell with part of Russian spaceship from Space to the Earth. Now, the specimen is preserved in The Russian Museum of Space Research.

6. Magnetic bioassembler is very easy to operate. Russian cosmonauts have been trained on how to use bioassembler on the earth, and then they performed planned experiments in space without any technical problems.
7. Magnetic bioassembler could be optimized either by increasing its complexity (e.g., complete automation) or simplification (e.g., reduction of bioassembler size and number of its chambers).
8. Magnetic bioassembler has batteries. It is an autonomous device that does not need an external power supply.
9. Trained personnel are not required for the maintenance of magnetic bioassembler.
10. Magnetic bioassembler is commercially available, and it could serve as affordable instrumentation for performing magnetic levitational bioassembly in space.

8 Magnetic levitational bioassembly in microgravity in space

To perform the magnetic levitational bioassembly experiments under the condition of microgravity in space at The Russian Orbital Segment, three main steps have to be followed: (i) Delivering bioassembler and tissue spheroids in the thermo-reversible hydrogel to the space station; (ii) performing the actual magnetic levitational bioassembly experiments at the ISS; and (iii) fixing biofabricated 3D tissue constructs in space and delivering fixed specimen to the earth for sequential histological analysis (**Figure 4**).

The logistics of space experiments involving living cells and tissue are hugely complex and challenging. Getting official permission to perform operations on the ISS needs tremendous efforts and an unbelievable amount of paperwork. The certification of magnetic bioassembler is also not an easy task. Finally, the researchers are also running the risk of unable to perform the experiments due to unexpected technical problems with a spaceship. Despite the apparent limitations and restrictions associated with conducting space research, we were still able to get exciting results. We developed original cuvette with three levels

of defense or three contours of biosafety. We founded commercial thermo-reversible hydrogel, which allowed safe delivery of viable tissue spheroids without preliminary undesirable tissue fusion. Magnetic levitational bioassembly of 3D tissue constructs from chondrospheres (tissue spheroids prepared from a primary culture of human chondrocytes) using original magnetic levitational bioassembler have been successfully performed (**Figure 5**). After a short incubation, the bioassembled 3D tissue constructs were fixed in formalin and delivered to the earth for subsequent histological investigation. The correspondent article has been accepted for publication^[25].

9 Challenges and future perspectives: Biomaterials are forever

The main challenge in the development of magnetic levitational bioassembly as well as in the broader field – formative biofabrication is the potential employment of biomaterials. On the one hand, formative biofabrication is positioned as a

truly scaffold-free technology. On the other hand, it is becoming increasingly apparent that without biomaterials, this field could not evolve. How could these obvious contradictions be logically solved? How can one still use biomaterials and, at the same time, call magnetic biofabrication technology scaffold-free? At first, we must remember that any bioprinting or biofabrication technology has three main steps: (i) Pre-processing or design digital model and fabrication of building blocks; (ii) processing or actual biofabrication or bioassembly of 3D tissue and organs construct from building blocks; and (iii) post-processing. Second, to be precise, scaffold-free formative biofabrication refers to the second step or actual bioassembly, in which magnetic levitational bioassembly is indeed scaffold-free. However, using scaffold-free levitational bioassembly at the second step does not necessarily eliminate the need for using biomaterials for fabrication of building blocks at the first step and for accelerated tissue maturation at the third, post-processing step. Thus,

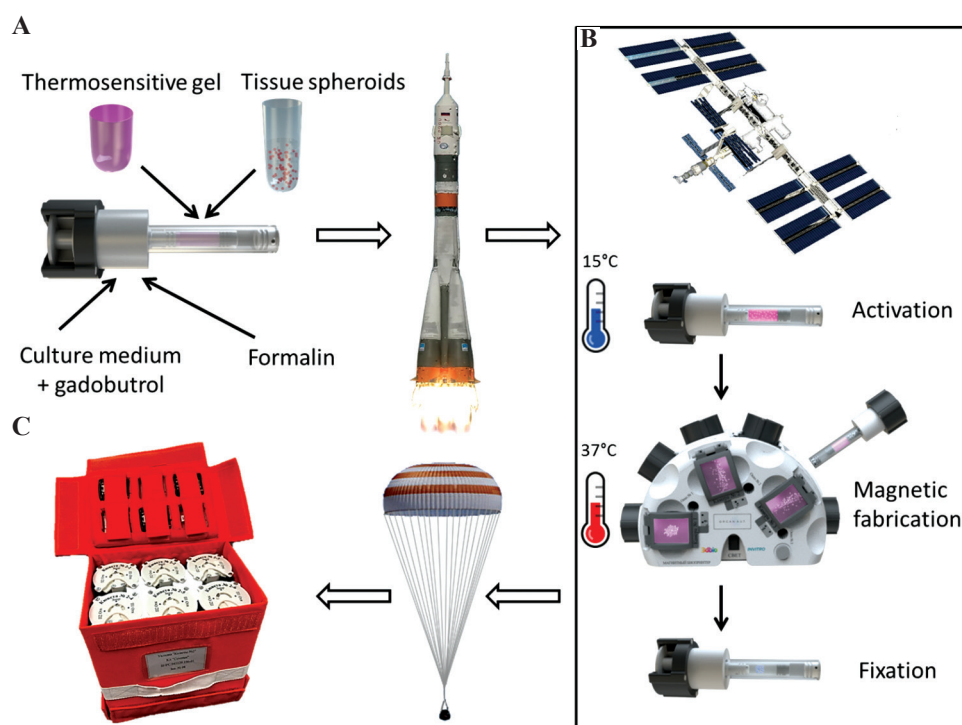


Figure 4. Schematic diagram of magnetic levitational bioassembly experiments at the Russian Orbital Segment (with permission from Science Advances)^[25]. (A) The filling of the cuvettes and their delivery to International Space Station (ISS); (B) the scheme of experiment on ISS; (C) the transportation of the cuvettes from ISS to earth.

such an approach not only solves the contradiction but also opens new avenues for chemists and material scientists to contribute to the development of formative biofabrication technology. The new types of synthetic and natural hydrogels could be used before bioassembly for sizing, shaping, and guided differentiation of organoids as potential new building blocks for scaffold-free formative biofabrication. Moreover, biomaterials and the special, thin fusogenic coating could be used for remote-controlled enhancements of tissue fusion process after initial bioassembly of 3D tissue and organ constructs. Finally, biomaterials could be used for directed tissue differentiation

and accelerated tissue maturation during post-processing. Hence, biomaterials are forever!

The development of magnetic levitational bioassembly is associated with another big challenge – toxicity of gadolinium salt. One of the potential ways to solve this problem is to develop novel bioassembler based on superconductive magnets. High magnetic fields generated by superconductive magnets reduce the concentration of gadolinium salts. To decrease power consumption, the superconductive magnets could be cooled by liquid nitrogen, which is a more affordable alternative compared to the expensive water perfusion-based cooling system.

The second potential strategy which could be employed for reducing concentration of gadolinium salts is the development of hybrid levitational bioassembly technology which is a combination of different physical forces and field. The hybrid magneto-acoustic bioassembler with built-in perfusion bioreactor allows switching from initial magnetic levitation to acoustic supporting levitation and complete removal of paramagnetic gadolinium salts through the nutrient flow.

The third perspective approach is the development of laser magneto-acoustic bioassembler. We already demonstrated that laser could rotate, elongate, and split 3D tissue

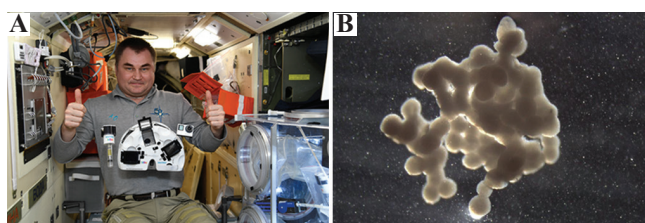


Figure 5. Space experiments. (A) “Organ. Aut” bioassembler at The Russian Orbital Segment, operated by Russian cosmonaut Alexey Ovchinin; (B) 3D tissue construct assembled with magnetic levitational from chondrospheres under microgravity in space on the International Space Station.

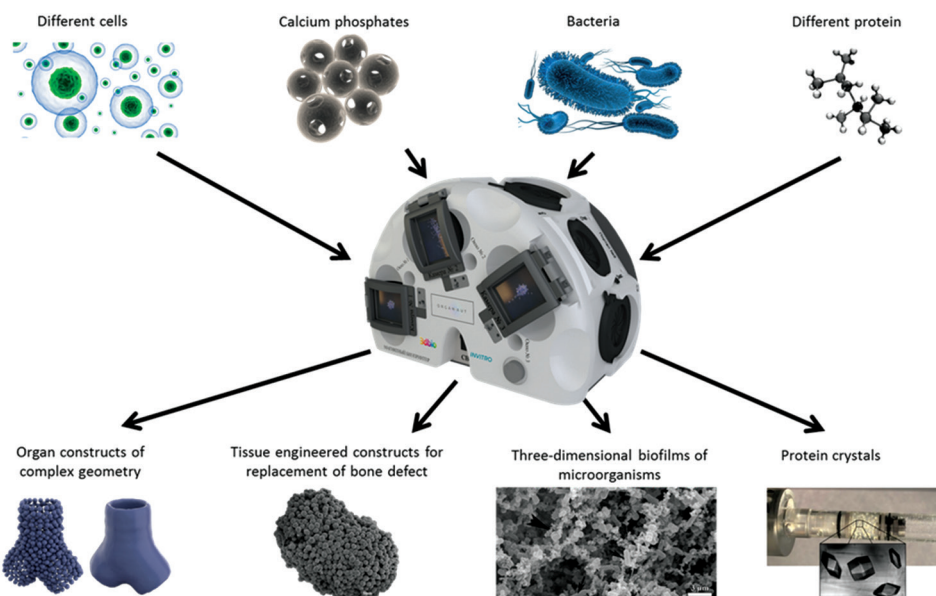


Figure 6. Potential applications of magnetic levitational bioassembler.

constructs. A laser could also be useful for the rapid fusion of tissue spheroids coated by a thin layer of photo-sensitive hydrogel after their magnetic levitation bioassembly in 3D tissue construct. The laser can be used for shaping more complex 3D tissue construct either by optogenetic apoptosis or laser-induced hyperthermia. A combination of magneto-acoustic levitational bioassembler with a laser could potentially improve the functionalities of bioassembler and enhances its capacities to form 3D tissue and organ constructs with complex geometry and structure. Incorporation of additional imaging facilities such as micro-computed tomography inside the bioassembler is also desirable, although it will significantly increase the cost of the instrument. Hence, there is also an unmet need for affordable bioassemblers.

10 Conclusion

The conceptual framework of scaffold-free, label-free, and nozzle-free magnetic levitational bioassembly has been described. Label-free magnetic levitational bioassembly is probably the most relevant example of the rapidly emerging, scaffold-free tissue engineering technology. The principal difference between label-free magnetic levitational bioassembly and the more traditional scaffold-based and label-based (using nanoparticles) magnetic tissue engineering are discussed. New terminology, including formative biofabrication, scaffold, and bioassembler, which represents the integral part of the novel conceptual framework, is also introduced.

Design, construction features, unique functionalities, and potential areas of applications of original magnetic levitational bioassembler have been described and illustrated. The most interesting example of using magnetic bioassembler for magnetic levitational bioassembly on the ISS under the condition of microgravity in space has been presented (**Figure 6**).

The challenges and perspectives of using magnetic bioassembler have been discussed. It is logical to assume that a combination of magnetic and acoustic levitation, as well as a combination of magnetic and acoustic levitation with laser or

photonic technology, will help develop a more functional magnetic bioassembler.

It is becoming evident that the development of affordable commercial bioassembler capable of rapid magnetic levitational bioassembly of clinically relevant tissue-engineered constructs in a non-toxic environment will become one of the main challenges.

As presented in this paper, original magnetic levitational bioassembler is the first commercial instrumentation specially designed for advancing scaffold-free tissue engineering and its clinical translation. While many researchers refer to their bioprinters as magnetic 3D bioprinters, we firmly believe that these instruments should be known as the “magnetic bioassembler for formative biofabrication.”

Acknowledgments

This work was supported by RFBR according to the research project № 18-29-11076. The authors are grateful to the Russian Space Agency (“ROSCOSMOS”) which grants us the permission to use some of illustrations taken at The Russian Orbital Segment.

Conflicts of interest

The authors declare no conflict of interest.

References

1. Derby B, 2012, Printing and Prototyping of Tissues and Scaffolds. *Science*, 338:921–6. DOI: 10.1126/science.1226340.
2. Murphy SV, Atala A, 2014, 3D Bioprinting of Tissues and Organs. *Nat Biotechnol*, 32:773–85. DOI: 10.1038/nbt.2958.
3. Mironov V, Kasyanov V, Drake C, *et al.*, 2008, Organ Printing: Promises and Challenges. *Regen Med*, 3:93–103. Doi: 10.2217/17460751.3.1.93.
4. Ng WL, Chua CK, Shen YF, 2019, Print Me An Organ! Why We Are Not There Yet. *Prog Polym Sci*, 97:101145. DOI: 10.1016/j.progpolymsci.2019.101145.
5. Adine C, Ng KK, Rungarunlert S, *et al.*, 2018, Engineering Innervated secretory Epithelial Organoids by Magnetic Three-dimensional Bioprinting for Stimulating Epithelial Growth in Salivary Glands. *Biomaterials*, 180:52–66. DOI:

- 10.1016/j.biomaterials.2018.06.011.
6. Souza GR, Tseng H, Gage JA, *et al.*, 2017, Magnetically Bioprinted Human Myometrial 3D Cell Rings as a Model for Uterine Contractility. *Int J Mol Sci*, 18:683. DOI: 10.3390/ijms18040683.
 7. Tseng H, Gage JA, Haisler WL, *et al.*, 2016, A High-throughput *In Vitro* Ring Assay for Vasoactivity Using Magnetic 3D Bioprinting. *Sci Rep*, 6:30640. DOI: 10.1038/srep30640.
 8. Tseng H, Gage JA, Shen T, *et al.*, 2015, A Spheroid Toxicity Assay Using Magnetic 3D Bioprinting and Real-Time Mobile Device-based Imaging. *Sci Rep*, 5:13987. DOI: 10.1038/srep13987.
 9. Hutmacher DW, 2000, Scaffolds in Tissue Engineering Bone and Cartilage. *Biomaterials*, 21:2529–43. DOI: 10.1016/s0142-9612(00)00121-6.
 10. Yang S, Leong KF, Du Z, *et al.*, 2001, The Design of Scaffolds for use in Tissue Engineering. Part I. Traditional Factors. *Tissue Eng*, 7:679–89. DOI: 10.1089/107632701753337645.
 11. Norotte C, Marga FS, Niklason LE, *et al.*, 2009, Scaffold-Free Vascular Tissue Engineering Using Bioprinting. *Biomaterials*, 30:5910–7. DOI: 10.1016/j.biomaterials.2009.06.034.
 12. Arai K, Murata D, Verissimo AR, *et al.*, 2018, Fabrication of Scaffold-free Tubular Cardiac Constructs Using a Bio-3D Printer. *PLoS One*, 13:e0209162. DOI: 10.1371/journal.pone.0209162.
 13. Gruene M, Deiwick A, Koch L, *et al.*, 2011, Laser Printing of Stem Cells for Biofabrication of Scaffold-Free Autologous Grafts. *Tissue Eng Part C Methods*, 17:79–87. DOI: 10.1089/ten.tec.2010.0359.
 14. Owaki T, Shimizu T, Yamato M, *et al.*, 2014, Cell Sheet Engineering for Regenerative Medicine: Current Challenges and Strategies. *Biotechnol J*, 9:904–14. DOI: 10.1002/biot.201300432.
 15. Dobson J, 2008, Remote Control of Cellular Behaviour with Magnetic Nanoparticles. *Nat Nanotechnol*, 3:139–43.
 16. Castro E, Mano JF, 2013, Magnetic Force-Based Tissue Engineering and Regenerative Medicine. *J Biomed Nanotechnol*, 9:1129–36.
 17. Armstrong JP, Stevens MM, 2020, Using Remote Fields for Complex Tissue Engineering. *Trends Biotechnol*, 38:254–63. DOI: 10.1016/j.tibtech.2019.07.005.
 18. Mazuel F, Espinosa A, Luciani N, *et al.*, 2016, Massive Intracellular Biodegradation of Iron Oxide Nanoparticles Evidenced Magnetically at Single-Endosome and Tissue Levels. *ACS Nano*, 10:7627–38. DOI: 10.1021/acsnano.6b02876.
 19. Chua CK, Leong KF, Lim CS, 2010, Rapid Prototyping: Principles and Applications. World Scientific Publishing Company, Singapore.
 20. Rogosnitzky M, Branch S, 2016, Gadolinium-Based Contrast Agent Toxicity: A Review of Known and Proposed Mechanisms. *Biometals*, 29:365–76. DOI: 10.1007/s10534-016-9931-7.
 21. Siew EL, Farris AF, Rashid N, *et al.*, 2020, Genes *In Vitro* Toxicological Assessment of Gadolinium (III) Chloride in V79-4 Fibroblasts. *Environ*, 42:22. DOI: 10.1186/s41021-020-00161-3.
 22. Ramalho J, Semelka RC, Ramalho M, *et al.*, 2016, Gadolinium-Based Contrast Agent Accumulation and Toxicity: An Update. *AJNR Am J Neuroradiol*, 37:1192–8. DOI: 10.3174/ajnr.a4615.
 23. Ramalho J, Ramalho M, 2017, Gadolinium Deposition and Chronic Toxicity. *Magn Reson Imaging Clin N Am*, 25:765–78. DOI: 10.1016/j.mric.2017.06.007.
 24. Parfenov VA, Mironov VA, van Kampen KA, *et al.*, 2020, Scaffold-free and Label-free Biofabrication Technology Using Levitational Assembly in High Magnetic Field. *Biofabrication*, 2020:7554. DOI: 10.1088/1758-5090/ab7554.
 25. Parfenov VA, Khesuanil YD, Petrov SV, *et al.*, 2020, Magnetic Levitational Bioassembly of 3D Tissue Construct in Space. *Sci Adv*, 6:eaba4174.

INTERNATIONAL JOURNAL OF BIOPRINTING

ISSN (print): 2424-7723

ABOUT THE JOURNAL

International Journal of Bioprinting is a biannual, double-blind peer-reviewed, open access journal. This journal focuses on the use of 3D printing technology with materials that incorporate viable living cells or biological elements to produce tissue or biotechnological products. Further discourses and technological advancements in bioprinting are the goals behind acceptance of high-quality basic and applied research: from concept creation to fabrication of the bioprinting process, associated clinical applications as well as social implications.



Whioce Publishing, official publisher for the journal welcomes researchers to submit their papers relevant to bioprinting for consideration via <http://ijb.whioce.com/>. For general enquiries and order for prints and reprints, please write in to IJB@whioce.com for a fast response.



SUBMIT YOUR
PAPERS HERE

ABOUT THE PUBLISHER

Whioce Publishing in Singapore is a registered publisher of excellent quality academic journals for an international readership. We deliver exceptional editorial support for the advancement and dissemination of scientific research by linking readers and researchers with networks and industries. We have ambitions to get our journals indexed in prominent databases such as EI, SCI, SSCI and AHCI, thereby aiming to be a first-class knowledge platform for researchers worldwide.

Whioce Publishing also engages in publishing e-books, organizing academic conferences and educational trainings, and providing translational services.



WHIOCE
PUBLISHING PTE. LTD.

International Journal of Bioprinting is an
independent open access journal published
by Whioce Publishing Pte.Ltd.



WHIOCE PUBLISHING PTE. LTD.
PROVIDING
FIRST-CLASS SCIENTIFIC INFORMATION
FOR TOP SCHOLARS

Whioce Publishing Pte.Ltd.

7030 Ang Mo Kio Avenue 5

#04-15 Northstar@AMK

Singapore 569880

Tel: +65 65702707/65702718

Fax: +65 65702803

See www.whioce.com/contact for a full list of offices and contact information.

Whioce Publishing Pte.Ltd. is a company registered in Singapore (No. 201427293E), whose registered office is at 7030 Ang Mo Kio Avenue 5 #04-15 Northstar@AMK Singapore 569880